ISSN 0003-2670

ANALYTICA CHIMICA ACTA

International monthly devoted to all branches of analytical chemistry
Revue mensuelle internationale consacrée à tous les domaines de la chimie analytique
Internationale Monatsschrift für alle Gebiete der analytischen Chemie

ELSEVIER SCIENTIFIC PUBLISHING COMPANY

AMSTERDAM

Anal. Chim. Acta, Vol. 92, 233–442, September 1977

Published monthly
Completing Volume 92

ANALYTICA CHIMICA ACTA

Publication Schedule for 1977

Vol. 88, No. 1	January 1977	
Vol. 88, No. 2	February 1977	(completing Vol. 88)
Vol. 89, No. 1	March 1977	
Vol. 89, No. 2	April 1977	(completing Vol. 89)
Vol. 90	May 1977	(complete in one issue)
Vol. 91, No. 1	June 1977	
Vol. 91, No. 2	July 1977	(completing Vol. 91)
Vol. 92, No. 1	August 1977	
Vol. 92, No. 2	September 1977	(completing Vol. 92)
Vol. 93	October 1977	(complete in one issue)
Vol. 94, No. 1	November 1977	
Vol. 94, No. 2	December 1977	(completing Vol. 94)

Subscription price for 1977 (Vols. 88–95): Dfl. 920.00 plus Dfl. 112.00 postage (approx. U.S.$421.22 inclusive of postage). Claims for issues not received should be made within three months of publication of the issues; if not, they cannot be honoured free of charge. Subscribers in the U.S.A. and Canada receive their copies by airmail. Additional charges for airmail to other countries are available on request. For advertising rates apply to the publishers.

Subscriptions should be sent to:
Elsevier Scientific Publishing Company, P.O. Box 211, Amsterdam, The Netherlands.

GENERAL INFORMATION

Languages

Papers will be published in English, French or German.

Detailed information

Authors should consult Vol. 73, p. 435 for detailed instructions. Reprints of this information are obtainable from Dr. Macdonald or from: Elsevier Editorial Services Ltd., Mayfield House, 256 Banbury Road, Oxford (Great Britain).

Submission of papers

Papers should be sent to:

Prof. Philip W. West,
Chemistry Department,
College of Chemistry and Physics,
Louisiana State University,
Baton Rouge,
La. 70803 (U.S.A.)

or to:

Dr. A. M. G. Macdonald,
Department of Chemistry,
The University,
P.O. Box 363
Birmingham B15 2TT (Great Britain)

Reprints

Fifty reprints will be supplied free of charge. Additional reprints (minimum 100) can be ordered at quoted prices. They must be ordered on order forms which are sent together with the proofs.

Reagents

MERCK

Merck HPTLC pre-coated plates for nano-TLC

Greater sharpness of separation

Higher number of samples per plate through smaller applied volumes

Shorter analysis times

Higher sensitivity

Achievement of hitherto unattainable reproducibilities

Please ask for our special brochure

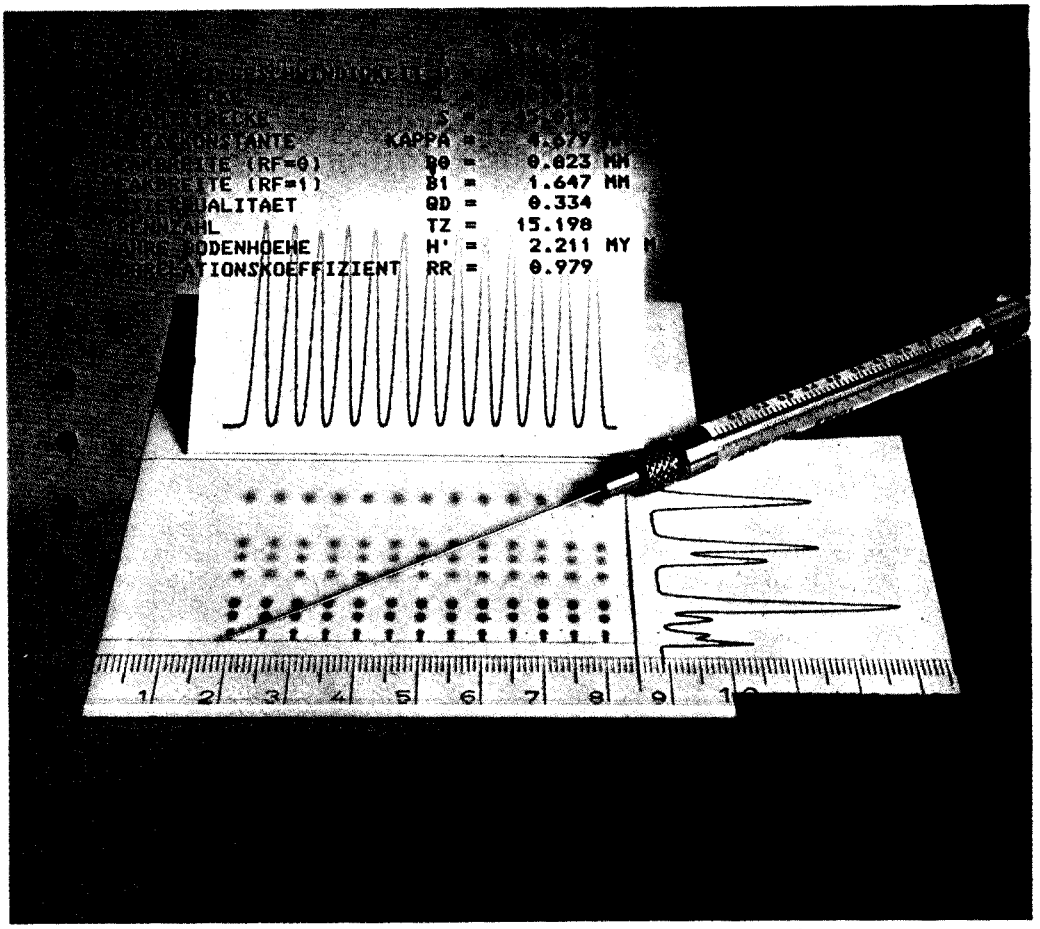

404-Eü

E. Merck, Darmstadt
Federal Republic of Germany

ref. no. 407

Analytica Chimica Acta, 92(1977) 233

PUBLISHER'S NOTE

It is with great regret that we announce the retirement of Professor Philip W. West as Joint Editor of *Analytica Chimica Acta.* This issue marks the end of his eighteen years of service. During Professor West's period of office, the journal has developed steadily in international status, and has expanded steadily from two volumes to eight volumes a year. We take this opportunity to express to him our sincere thanks for his devoted services over so many years.

EDITORIAL

The retiral of Professor Philip W. West from the Joint Editorship of *Analytica Chimica Acta* brings to an end an era in the development of the Journal which has been notable for its sustained growth. It is a very great pleasure for me to take this opportunity to express my personal thanks to him for the many years of happy and productive cooperation that has marked the period of our Joint Editorship. Professor West is to maintain his association with *Analytica Chimica Acta* as one of our Editorial Advisers, so that we shall continue to derive benefit from his great experience.

I am pleased to announce that Dr. D. M. W. Anderson, who has been an Associate Editor of the Journal since 1975, will join me as Editor from October 1977.

A. M. G. Macdonald

Analytica Chimica Acta, 92 (1977) 235—249

FLOW INJECTION ANALYSIS
Part IX. A New Approach to Continuous Flow Titrations

J. RŮŽIČKA, E. H. HANSEN and H. MOSBÆK

Chemistry Department A, The Technical University of Denmark, Building 207, DK-2800 Lyngby (Denmark)

(Received 22nd April 1977)

SUMMARY

Studies of dispersion patterns in nonsegmented streams, flowing through narrow open tubes, show that it is possible to obtain highly reproducible concentration gradients within a sample zone injected into the moving stream. By varying the geometry of the flow path, low, medium and high dispersion patterns can be achieved; the high dispersion pattern forms the basis for a new approach to continuous flow titrimetry. In this type of titration, discrete samples are passed through a gradient device and are then mixed with a continuously flowing stream of titrant of fixed concentration. The new technique has been tested for potentiometric as well as spectrophotometric end-point indication. A simple one-channel system allows titrations to be performed automatically in less than 1 min.

In chemical analysis the choice between a direct measurement and a titrimetric determination depends on a number of criteria, such as the required precision, speed, availability of instrumentation and personal taste. Generally, titrations are regarded as slower and less sensitive yet more precise than direct methods, as the measurement of a volume of reagent, or its rate of delivery, can often be done more reproducibly than, e.g., measurement of the intensity of a colour, of an electric current, or of the magnitude of an electrode potential. Unless automated, titration equipment is usually also less expensive, because the indication of the equivalence point does not require a very refined detector, as it is the point of maximum change in colour intensity, potential etc. which is being sought.

The troublesome processes of collecting and plotting the data required for the titration curve, and the time-consuming operations stemming from the batchwise mode of performing titrations, are the main drawbacks of titrimetric procedures. This is perhaps the reason why in analytical practice titrations are now generally used only when the direct measurement does not yield acceptable results, as in the determination of all strong and weak acids and bases, of water by the Karl Fischer method, of dissolved oxygen by the Winkler procedure, etc.

The automation of titrimetry has made enormous progress within the last two decades and a number of automated titrators, based on the original

ideas of Robinson [1] and Lingane [2], are now commercially available. The extensive use of the classical Gran plot approach and derivative methods in potentiometric titrations have reduced the amount of data which must be collected and have also improved the precision of locating the equivalence points. Within the last few years, microprocessors have been incorporated into automated titrators as they allow the equivalence point to be predicted before it is actually reached [3], or the rate of titrant delivery to be varied in such a way that mixtures of several species with similar dissociation or stability constants can be titrated with good resolution [4]. Research within the field of automated titrations is very active; recently, a technique based on stepwise addition of equal volumes of titrant has been developed [5], which allows automated titrations with potentiometric as well as colorimetric indication to be done with a very high degree of precision.

However, nearly all automated titrimetric procedures are based on batch operation, which requires relatively complicated ancillary units to facilitate sample introduction, draining and washing of the titration vessel, and usually replenishing the titrant in the delivery unit. A discontinuous cycle reagent delivery is normally employed for titration of discrete samples. An exception, where a continuous flow operation has been used, is the work of Fleet and Ho [6] in which a gradient titration principle was ingeniously suggested. In their method the flow rates of the sample and of the titrant streams were maintained constant, the concentration of the titrant being increased in the form of a linear gradient. The resulting mixture of titrant and sample, forming a continuous stream, was monitored by an ion-selective electrode which thus indicated the end-point of the titration. This approach allowed discrete samples to be titrated with a minimum of manual handling, but the drawback of the technique was that each individual sample had to be assigned a separate cup of reagent solution, from which the concentration gradient of the titrant was created. Furthermore, periodic washout of the titrant gradient circuit required a certain time, which affected unfavourably the sampling frequency. This drawback, however, could in principle be avoided, by generating the reagent coulometrically in the sample stream, in the manner suggested by Pungor, Toth and Nagy [7] for continuous industrial monitoring.

Flow injection titrations

One of the important features of the flow injection method is the possibility of adapting the flow pattern to the requirements of a particular determination. Unlike the air-segmented continuous flow of the AutoAnalyzer type, where the air bubbles inselectively limit the dispersion of the sample zone, the unsegmented flow is capable of higher flexibility. By varying the diameter and length of the tube which accommodates the carrier stream and serves as the chemical reactor for the injected samples, and by appropriate selection of the linear velocity of the reagent stream(s), and also determining the length of the sample zone (sample volume), a wide range of concentration

gradients of the sample plug within the carrier solution can be obtained. In the absence of air segmentation, these profiles created by the forward motion of the stream, are highly reproducible and can be readily employed for analytical purposes.

Thus, if the original composition of the sample solution is to be measured, e.g. pH, pCa, conductivity, etc., a *small dispersion* of the sample zone is required to ensure that the readout, as obtained in the middle of the sample zone, is not affected by mixing with the surrounding carrier stream [8].

If, however, one or several chemical reactions, such as buffering or colour formation have to be effected, the centre of the sample zone must be mixed efficiently with the carrier stream and often with several other reagents in sequence. Such mixing must be done in a strictly controlled manner, while the sample moves towards the detector. This calls for an appropriate degree of *medium dispersion* of the sample zone, a suitable compromise being achieved between the requirement of mixing and reaction time on one hand, and maximum acceptable broadening of the sample zone on the other hand, as the latter factor affects the carryover and thus the sampling rate.

It is important to realize that the above cases utilize a direct measurement of the electrode potential or the colour intensity, which are recorded as a peak height. Therefore, flow conditions for medium and/or low dispersion of the sample zone must be selected. It will be shown below, however, that for the purpose of titrations a *large dispersion* has to be created as it is the width of the sample zone measured as it passes through a detector, which is proportional to the titrant consumption.

THEORY

The equivalence between a substance A and reagent B, which react according to the chemical reaction

$$A + nB \rightleftarrows AB_n \tag{1}$$

is reached when

$$C_A v_A = C_B v_B n, \tag{2}$$

where C_i denotes the concentration of component i and v_i the volume. If these two solutions are continuously mixed, then the volumes can be replaced by the flow rates f_A, f_B where $f = v/t$ (ml min^{-1}), provided that the mixing and the chemical reaction are instantaneous, or that the flow conditions are so arranged that any delay in reaction speed is accommodated by the chemical reactor preceding the readout device.

If substance A is to be determined by measuring the equivalent amount of B corresponding to the original concentration of A in the sample, C_A^s, it is most practical to keep C_B and f_A constant and to create a concentration gradient dC_A/dt of the injected sample solution as in this case the time t_{eq} between the start of the titration and the equivalence point will then be

directly proportional to v_B. The titration can thus be performed in an experimental arrangement such as that depicted in the flow diagram shown in Fig. 1, where G is the gradient device and R the chemical reactor in which the chemical reaction takes place. The circuit is operated by injecting a certain volume v_s of the sample solution through the injection port S into the carrier stream of a diluent, pumped at a rate f_A by a peristaltic pump (P) through the gradient device (G), having the volume V. Further downstream, titrant B of concentration C_B is continuously added at a rate f_B, and after passing through the reactor R, the resulting mixture is monitored by a flow-through detector D, before passing to waste, W. For each sample zone, two abrupt changes of the monitored signal will be observed as the two carrier stream-sample zone boundaries pass through the detector. The point of maximum change is located in that elementary section of the flowing stream where the equivalence condition is fulfilled, and therefore the time spans between these outer boundaries, t_{eq}, is proportional to $C_B v_B$ because f_B is constant. The creation of the concentration gradient from the injected sample zone is the key to performing the titration. If there is no dispersion of the sample zone (Fig. 2 left), the difference in concentration of two different samples C_A^1 and C_A^2 will not be measurable as the time span between the outer sample boundaries, as marked by the □—□ points, would be identical, merely reflecting the length of the sample plug. Dispersion of the sample zone (Fig. 2, right-hand side) gives rise to two concentration gradients on the sample zone boundaries which are, for various C_A^1 and C_A^2 concentrations, well reflected in the respective differences of the t_{eq} values for any constant C_B level.

The relationship between t_{eq} and C_A depends primarily on the form of the mathematical function which describes the concentration gradient created in the gradient device used. Depending on its geometry (i.e. length, L, and internal radius, a), the intensity of mixing, the flow rate (f), and the sample volume (v_s), various dispersion patterns and degrees might be achieved [10]. Thus for tubes of large L and small a, and for low f, symmetrical gradient profiles are obtained (Fig. 3) which can be described by a Gaussian curve [10, 11]:

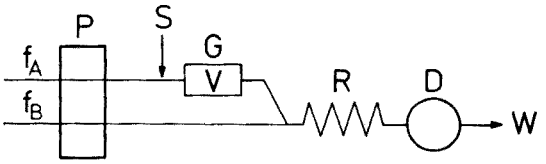

Fig. 1. Diagram depicting Flow Injection Titration. The sample (S) is injected into a carrier stream of diluent, pumped at rate f_A by means of a pump (P), then proceeds through a gradient chamber (G) of volume V and is titrated in coil R by the reagent pumped at rate f_B. The stream is continuously monitored by a flow-through detector (D) and then wasted (W).

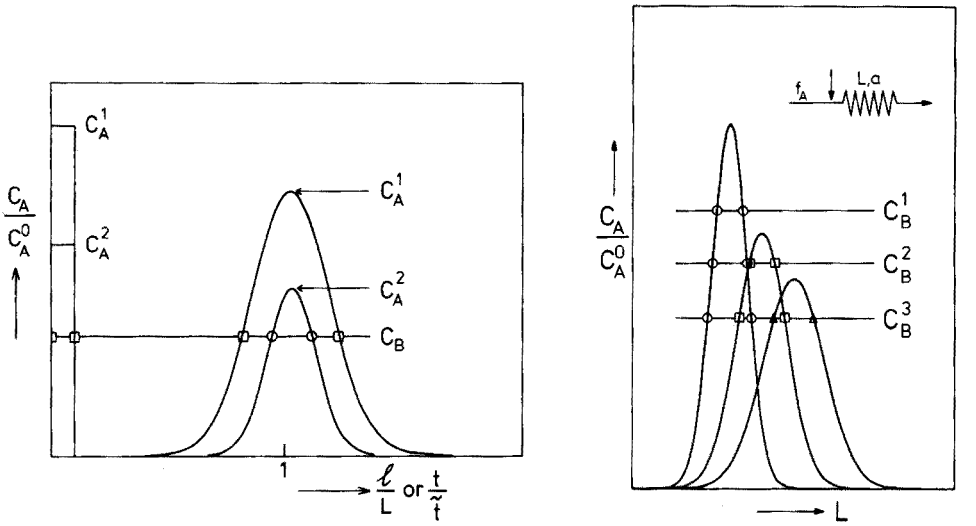

Fig. 2. Dispersion patterns in narrow open tubes. In the absence of dispersion, the injected sample (C_A^1, C_A^2) proceeds through the tube as a plug with a rectangular profile, as shown on the left. If the dispersion pattern can be described by eqn. (3), symmetrical profiles for these two sample concentrations, C_A^1, C_A^2, will be formed. Use of a fixed titrant level C_B then results in different t_{eq} values as shown by the difference in the time span between the two sets of points (○—○) and (□—□).

Fig. 3. The dispersion pattern of a sample zone in a long thin gradient tube as described by a Gaussian curve (eqn. 3). Note the increasing dispersion with increasing length of the tube (L).

$$\frac{C_A}{C_A^0} = \frac{v_s}{\pi a^2 L} \cdot \frac{1}{2(t/\bar{t})\delta)^{-1/2}} \, e^{-\frac{(1-(t/\bar{t}))}{4(t/\bar{t})\delta}} \qquad (3)$$

where $C_A^0 = C_A^s$ is the original concentration of the injected sample solution, $\bar{t} = (\pi a^2 L)/f$, and δ is the dispersion number characteristic of the flow employed [10]. Typically, f is in the vicinity of 1.5 ml min^{-1}, a is ca. 0.5 mm and L is 2—4 m. As shown in Fig. 3 the dispersion of the sample zone increases with L, the dispersion number δ being proportional to the variance of the curve (σ) in the well known manner. Thus, by choosing various C_B levels, different $t_{eq} = \Phi(C_A)$ are obtained, all being derived from the normal distribution curve for this type of dispersion pattern. Therefore, at least some of them will have a fair chance to be linearized either in a semilog plot for low C_B values or in a probability plot for a high C_B. The drawbacks of this type of gradient are the obvious difficulty in obtaining a wider linear range and the fact that a fairly long time (of the order of minutes) is needed for this type of flow pattern to develop, which adversely affects the sampling rate.

A better approach is therefore to use a gradient device with a shorter holding time, having low L (up to 25 cm) and larger a (up to 1.5 mm i.d.). Here, assymmetrical gradients will be produced (Fig. 4) with an increasing

degree of dispersion and decreasing skewness as L (and time t for the same linear velocity, $u = L/t$) increases. This system can be described by a tank-in-series model which fits to a G- or Pearson III-type statistical function [10]:

$$\frac{C_A}{C_A^0} = \left(\frac{t}{\bar{t}_i}\right)^{N-1} \frac{1}{(N-1)!} e^{-t/\bar{t}_i} \quad (4)$$

where $\bar{t}_i$ is the mean residence time in one hypothetical tank, while N is the number of these tanks containing the sample zone. Thus N affects the degree of skewness and $\bar{t}$, as well as the degree of dispersion. Again, by choosing the level of C_B various t_{eq} functions can be obtained. It is worth noting that the curve for $N = 2$ leading to a simplified eqn. (4):

$$C_A/C_A^0 = (t/\bar{t}_i)\, e^{-t/\bar{t}_i} \quad (5)$$

is assymmetrical to such a degree that, if a lower titrant concentration is being chosen (say C_B^2 in Fig. 4), the rising part of the curve will contribute negligibly to t_{eq}. In contrast, the falling part is nearly exponential at the lower end, and corresponds to a large dispersion of the rear sample zone boundary. Thus, a suitable choice of the titrant concentration C_B, makes it possible to select that section of the curve for titration which conforms with the simplest mathematical treatment, i.e., that of a well-mixed gradient chamber.

The well-mixed gradient chamber (Fig. 5, a) yields a pure exponential concentration gradient, corresponding to one stirred tank ($N = 1$, eqn. 4):

$$C_A/C_A^0 = e^{-t/\bar{t}} \quad (6)$$

where $\bar{t}$ is the mean residence time, related to the half-wash time by $t_{1/2} = \bar{t} \ln 2$, and $C_A^0 = C_A^s/V$. Rewriting eqn. (6) gives

$$\log C_A = \log C_A^0 - (t/2.3\,\bar{t}) \quad (7)$$

and inserting the equivalence condition (eqn. 2) as well as expressing the gradient chamber holding time t as V/f_A gives

$$t_{eq} = \frac{V}{f_A} 2.3 \log C_A^0 - \frac{V}{f_A} 2.3 \log C_B \frac{f_B}{f_A} n \quad (8)$$

This expression shows t_{eq} as a function of C_A^0 in semilogarithmic coordinates to be a straight line with a slope of $2.3\ V/f_A$. By extrapolation to $t_{eq} = 0$ the corresponding value of C_A^0 will, after volume correction (i.e., $C_A^0 = C_A^s\, v_s/V$), yield the sensitivity limit of the titration. To increase the sensitivity, the sample volume—chamber volume ratio should be increased and/or C_B, f_A decreased. The slope of the calibration curve depends, however, on the V/f_A ratio, hence a suitable compromise must be found experimentally, as a mere increase in the chart paper speed may lead simply to a loss of reproducibility. Usually a straight line can be obtained over more than one decade of sample concentration, if v_s is small compared to V and if the additional dispersion in the reactor coil R is negligible compared to the

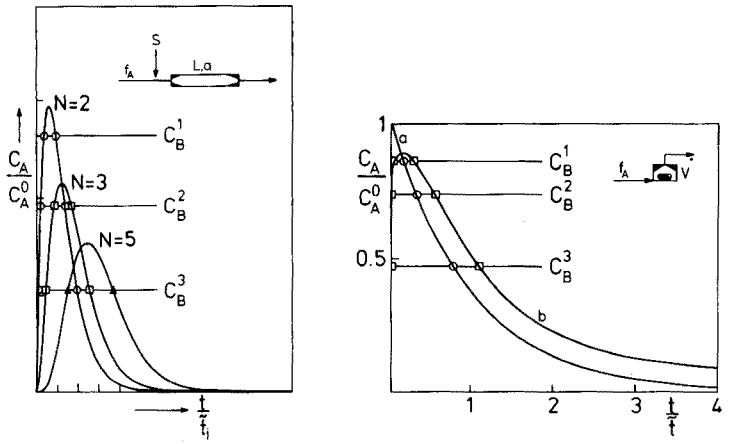

Fig. 4. The dispersion pattern of a sample zone in a short tube of a larger diameter (d), resulting in the formation of assymmetrical concentration gradients, described by eqn. (4). The shorter and wider the tube, the more pronounced will be the skewness; by adjusting this as well as the level of titrant (C_B^1 to C_B^3), various calibration curves of increasing linear range can be obtained (for details see text).

Fig. 5. The dispersion of a sample zone with a mixing chamber. This results in the formation of a pure exponential concentration gradient (curve a), the pattern of which corresponds to $N = 1$ in eqn. (4). In practice, a gradient of slight curvature, corresponding to $1 \leqslant N \leqslant 2$, is often obtained (curve b), but this can be rectified by a suitable choice of the level of C_B^1 to C_B^3.

dispersion produced by the gradient chamber. Even if a slight deviation of the actual dispersion curve occurs (Fig. 5, curve b) this can be rectified by choosing a slightly lower level of titrant, say C_B^2 instead of C_B^1, as the rounded part of the concentration gradient curve b will remain untitrated. For the same reason, when the gradient tube is used rather than the mixing chamber (Fig. 4), deviations from linearity are observed at very low and very high sample concentrations, as these fall outside a purely exponential concentration gradient, in analogy with Fig. 2.

The short gradient tube (Fig. 4) can therefore be treated by the same model as the mixing chamber, except that its physical volume $V(\pi a^2 L)$ has to be corrected by a factor which takes into account the incompleteness of the mixing. The presence of different flow regions (dead water combined with dispersed plug) in an incompletely stirred gradient chamber can be described by various multiparametric models and linearized by choosing suitable coordinates [10]. It is therefore a question of taste whether one would prefer to linearize the curve experimentally or by calculus.

Finally, a special case where $f_A = f_B$ should be briefly mentioned. Here, eqn. (8) simplifies to:

$$t_{eq} = (V/f)\ 2.3 \log (C_A^0/C_B)n \qquad (9)$$

This approach can be used experimentally either in a two-channel instrument

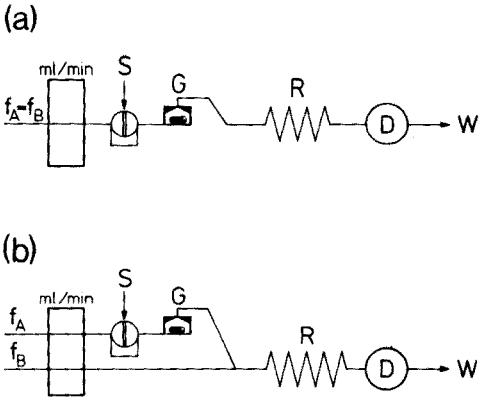

Fig. 6. One-channel (a) and two-channel (b) manifold for Flow Injection Titration. For symbols, see Fig. 1; the used flow rates, f_A and f_B, are stated in the text.

(Fig. 6, b) where the flow rates f_A and f_B are identical, or in a simple one-channel instrument (Fig. 6, a) where the stream of titrant serves simultaneously as the diluent. The experimental verification of these two systems with both spectrophotometric and potentiometric detection is described below. Experiments with the mixing chamber and gradient tube are also discussed.

EXPERIMENTAL

Apparatus

Peristaltic pump. An Ismatec model MP 13 GJ-4 (Ismatec S/A, Switzerland) was operated at speed 10 with suitable pump tube diameters to obtain the desired flow rates.

Spectrophotometer. A Corning model 254, equipped with a Hellma flow-through cuvette, type OS 178.12 (volume 18 μl, light path 10 mm) was connected to a Servograph REC 61 recorder, furnished with a REA 112 high-sensitivity unit (Radiometer A/S, Denmark).

Potentiometer. A PHM 64 digital pH meter (Radiometer) was connected to a Servograph REC 61 recorder, furnished with a REA 110 500-mV interface (Radiometer).

Potentiometric flow cell. This was identical with that described in detail previously [8, 12, 13] housing a calcium ion-selective electrode [14] and a reference electrode (saturated calomel — K 401, Radiometer); the dead volume of the flow cell was less than 10 μl.

Injection port. This was a precisely made rotary valve [9, 13] with a bore volume of 30 μl (exchangeable cores allowed injection of volumes between 100 and 5 μl), and furnished with a bypass of a higher flow resistance. Thus, while the sample is being injected by a syringe into the volumetric bore, the carrier solution is continuously bypassing the injection port. Only when the valve has been turned, the stream in the bypass comes

to a standstill and the precise amount of the sample solution is injected by the carrier stream from the volumetric bore into the reaction line. Larger sample volumes (200 μl) can equally well be injected manually through a flap-type valve [8, 15]. To avoid the effect of manual injection on the mixing pattern in the gradient chamber, a short (50 cm, 0.75 mm i.d.) delay coil was placed between the chamber and the injection port.

Gradient chamber. This was machined from Perspex, consisting of two parts, a lower circular unit of 13-mm inner diameter housing a Teflon-covered magnetic stirring bar 7-mm long, and an upper part with a dome-shaped inner cavity (see Fig. 6) to avoid entrapment of air. When assembled, a rubber gasket was placed between the two parts to ensure complete tightness. The total volume of the chamber was 0.98 ml, the hole for the incoming solution being drilled at the base of the lower part and the outlet being drilled in the center of the upper part. The chamber was placed on a magnetic stirrer; in practice it was found that mixing was equally effective if the stirrer was operated anywhere in the range 60—240 r.p.m.

Gradient tube. This was simply a piece of PVC tubing (1.74 mm i.d.). For student exercises, a much simplified one-channel system can be employed; this comprises the flap valve injection port, the gradient chamber, a Beckman B spectrophotometer with a Servogor recorder attached, and a single-channel pump.

Reagents

Potassium hydroxide, carbonate-free, was prepared from a 0.1 M Titrisol standard solution (Merck, West Germany) by further dilution with double-distilled water, to which bromthymol blue was added in $8 \cdot 10^{-4}$% concentration. Hydrochloric acid solutions, of required molarities, were also prepared from Titrisol standards. The $5 \cdot 10^{-4}$ M EDTA-containing borate buffer used in the calcium titrations was made by dissolving the appropriate amount of $Na_2EDTA \cdot 2H_2O$ in the buffer, prepared by mixing 500 ml of 0.2 M H_3BO_3 with 100 ml of 0.5 M NaOH (pH 9.2).

Manifolds and measurement technique

Manifolds (Figs. 1 and 6) were made from polyethylene tubing (0.75 mm i.d.) and Lego building blocks as described earlier [8, 15]. In the one-channel system (Figs. 1 and 6, b) the sample S was injected directly into the titrant pumped at a rate of $f_A = f_B$; the mixture then entered the gradient chamber G (or gradient tube) from where it was led through coil R to the detector D and finally to waste (W).

In the two-channel system, the sample was injected into a flow of water (f_A), and only after the gradient had been created in the chamber (G) was the solution mixed in coil R with the titrant added at flow rate f_B.

Whether a spectrophotometric or potentiometric flow-through cell was used, the signal from the detector was continuously monitored on a recorder operated at high paper speed (e.g. 5 s cm^{-1}). In both cases, the

peak shape consisted of a rising curve and a falling part, the peak width being equal to t_{eq}. As soon as the signal reached the base line, indicating that the gradient chamber had been thoroughly washed, the next sample could be injected.

RESULTS AND DISCUSSION

Potentiometric titration of calcium

The potentiometric titration of calcium with EDTA was done in a single-channel manifold (Fig. 6a) with a gradient chamber (V = 0.98 ml) and a short coil (R = 25 cm, i.d. 0.75 mm), by pumping the carrier solution at a rate of 0.84 ml min^{-1}. By injecting 200 μl of a sample solution, containing calcium in the range $5 \cdot 10^{-3}$—$5 \cdot 10^{-2}$ M, into the carrier stream containing $5 \cdot 10^{-4}$ M EDTA, a series of titration curves was obtained (Fig. 7). Each titration is initiated by an abrupt increase of the potential, corresponding to the ascending part of curve b, Fig. 5, followed by a typical S-shaped descending part, in which the inflexion point marks the end of the titration. By choosing a fixed potential, t_{eq} was read off and plotted versus the concentration of the injected sample (Fig. 8, line c). In agreement with eqn. (9), a straight line was obtained over the whole concentration range, its position in semilogarithmic coordinates depending: (a) on the volume of the injected sample (compare curves a—d), because the v_s/V ratio changes; and (b) on the concentration of EDTA. The slope of the calibration curve,

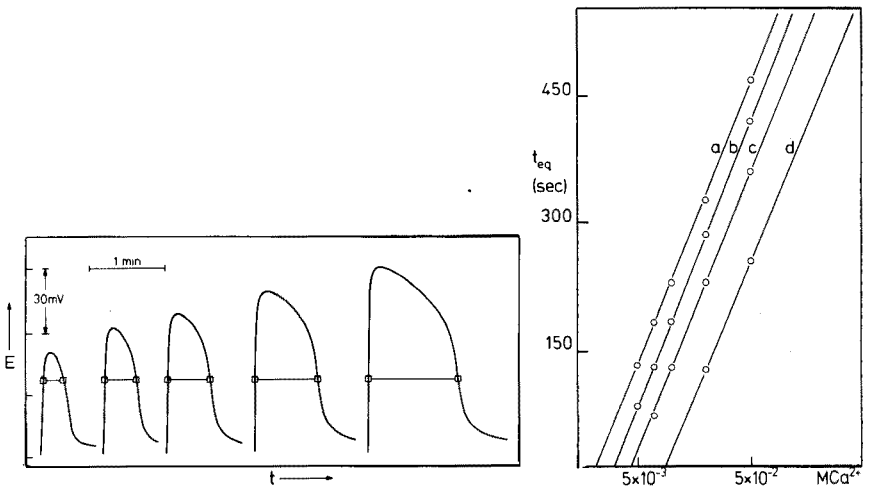

Fig. 7. Potentiometric titration of calcium with EDTA. From left to right $5 \cdot 10^{-3}$ M, $7 \cdot 10^{-3}$ M, $1 \cdot 10^{-2}$ M, $2 \cdot 10^{-2}$ M, and $5 \cdot 10^{-2}$ M $CaCl_2$. The t_{eq} values read off between points □—□ are plotted in Fig. 8 as line c. Sample volume, 200 μl; EDTA, $5 \cdot 10^{-4}$ M; one-channel manifold with f = 0.84 ml min^{-1} (Fig. 6, a).

Fig. 8. The equivalence time t_{eq} (s) as a function of the calcium concentration in the sample solution (log C_A^0) in titrations of different sample volumes (a = 400 μl; b = 300 μl; c = 200 μl; and d = 100 μl). Titrant, $5 \cdot 10^{-4}$ M EDTA; f = 0.84 ml min^{-1}.

as predicted by eqn. (8), depends on the pumping rate f (where $f_A = f_B$ in this case), but for different pumping rates (0.46 ml min^{-1} to 1.6 ml min^{-1}, curves a—c, Fig. 9) all the lines intersect at approximately the same $t_{eq} = 0$, corresponding to the detection limit of the titration, which is given by v_s/V and the concentration of titrant C_B. The chamber volume V, as calculated from the slope, was 0.98 ml corresponding to that determined by the weight of water necessary to fill the chamber. It is worth noting that the shape of the titration curve is assymmetrical (as best seen on the last curve to the right of Fig. 7), which is due to a certain degree of sensitivity of the calcium electrode towards sodium ions (the selectivity constant being $pK_{Ca/Na} = 5.2$ [14]). Therefore, in the presence of approximately 0.1 M Na^+, stemming from the borate buffer constituting the carrier stream, the maximum attainable sensitivity corresponded to pCa = 7.2, as the sodium ions simulate this calcium level, although the "true calcium activity" at the end of the titration, i.e. 100% overtitrated sample, would be as low as pCa = 9.3 ($\log K_{CaEDTA} = 10.7$) at pH 9. However, the overall changes of potentials during the titration agree very well with those expected theoretically. Thus, if a sample/chamber ratio of 1:5 is considered and instantaneous reaction is assumed for that fraction of the total amount of sample calcium which is equivalent to the EDTA present in the chamber at the moment of introduction, the actual pCa values at the very beginning of the titration cycle (top of the curve), as recorded in Fig. 7 from left to right, should theoretically be: $6 \cdot 10^{-4}$ M; $1 \cdot 10^{-3}$ M; $1.6 \cdot 10^{-3}$ M; $3.6 \cdot 10^{-3}$ M; and $9.6 \cdot 10^{-3}$ M, respectively, leading to the following potential jumps: 58 mV; 64 mV; 70 mV; 81 mV; and 93 mV (as computed from the calibration curve [14]). The actual values found from the graph were: 52 mV; 61 mV; 67 mV; 77 mV; and 89 mV, respectively. It can thus be concluded that the Ca—EDTA titration as performed by the Flow Injection system has exactly the same course as if carried out in the conventional batch mode.

Spectrophotometric titrations

The spectrophotometric titrations differ from the potentiometric ones mainly because the change of the indicator at the equivalence point does not encompass such a wide range of ionic activities as does the electrode measurement. For example, in titrations of strong acid by strong base, with bromothymol blue (3,3′-dibromothymolsulphonephthalein) as indicator [16], which has $pK = 7.1$ and a yellow acidic form ($\lambda_{max} = 435$ nm) and a blue basic form ($\lambda_{max} = 620$ nm), only the pH range from 6.1 to 8.1 can be followed, and therefore the resulting titration curves will be more abrupt, having a plateau on the top as well as at the base line. Model titrations of hydrochloric acid with sodium hydroxide were tested in the one-channel (Fig. 6a) and two-channel (Fig. 6b) systems, with the 0.98-ml gradient chamber or a gradient tube.

When the one-channel system was used, 200-μl sample volumes were injected and $1 \cdot 10^{-3}$ M sodium hydroxide containing $8 \cdot 10^{-4}$% of bromothymol

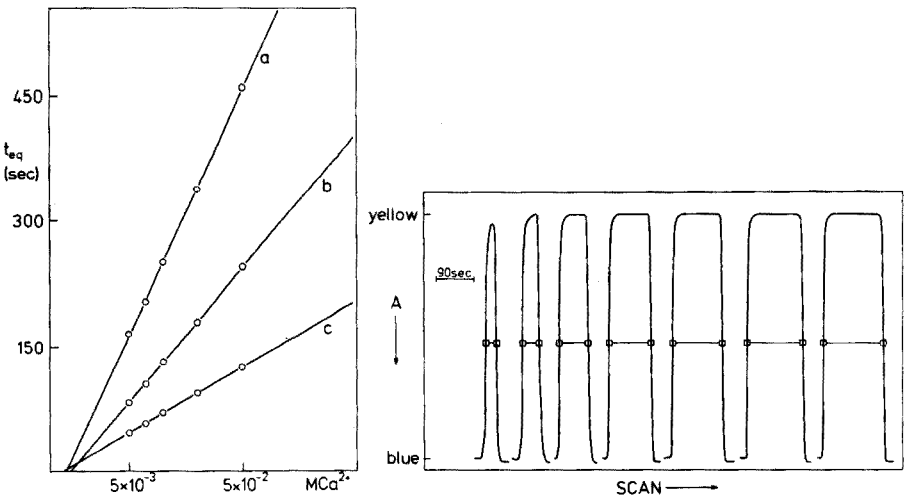

Fig. 9. The influence of the flow rate f on the slope of the calibration curve as obtained by titration of 300 μl Ca-sample volumes by $5 \cdot 10^{-3}$ M EDTA in a one-channel manifold with the potentiometric flow through cell. The flow rates are: a = 0.46 ml min^{-1}; b = 0.84 ml min^{-1}; and c = 1.60 ml min^{-1}; t_{eq} in sec. plotted versus log C_A^0 (M Ca^{2+}).

Fig. 10. The colorimetric titration of a strong acid by a strong base in the one-channel manifold of Fig. 6a, with bromothymol blue as indicator. Conditions are given in the text. Sample concentration, from left to right: $7 \cdot 10^{-3}$ M; $1 \cdot 10^{-2}$ M; $2 \cdot 10^{-2}$ M; $4 \cdot 10^{-2}$ M; $6 \cdot 10^{-2}$ M; $8 \cdot 10^{-2}$ M; and $1 \cdot 10^{-1}$ M HCl. The equivalence time, t_{eq}, plotted vs. log C_A^0 (M HCl) yields a straight line over the entire concentration range.

blue was pumped at a rate (f) of 1.35 ml min^{-1}. After thorough mixing in the gradient chamber, the solution was passed to the detector via a 0.5-m (0.75 mm i.d.) reaction coil and monitored at 620 nm. The shapes of the resulting titration curves (Fig. 10) were identical, consisting of an abruptly rising part, a plateau and an abruptly falling part, the peak width (t_{eq}) being proportional to the logarithm of the concentration of the injected acid (eqn. 9). Thus, t_{eq} as a function of C_A^0 gave a straight line, the intercept for $t_{eq} = 0$ indicating the limit of detection. By varying the concentration of the base C_B, the range of titration can be adjusted to suit best, in terms of reproducibility and sampling rate, the concentration of acid present in the samples.

The two-channel system, however, offers greater versatility. In this system (Fig. 6b), with the gradient chamber, 200-μl samples were injected into the carrier stream of water pumped at a rate of 1.35 ml min^{-1} (f_A). After the gradient profile had been created, the solution was mixed with the indicator-containing base solution in the 0.5-m long (0.75 mm i.d.) reaction coil and then passed through the flow-through detector while the absorbance was measured at 620 nm. Again, titration curves, identical in shape to those in Fig. 10, were obtained; and t_{eq} plotted vs. log C_{HCl}^0 yielded a straight line over more than one decade of sample concentrations. At a fixed flow rate of

f_A, the limit of sensitivity may be changed by changing f_B and/or changing the concentration of the base C_B. In this way, by changing the flow rate f_B at a fixed concentration of base, the calibration curve is parallely shifted (Fig. 11, line a), while the change in f_A results in a change of slope (Fig. 11, line b).

The use of a gradient tube has the advantage of simplifying the experimental setup, as the stirring table is not needed, but the price paid is a shorter linear measuring range (see eqns. 5 and 6). This way of creating a concentration profile from an injected sample was tested in both the one- and two-channel systems for the acid—base titration with spectrophotometric indication described above. It was found that in the manifold of Fig. 6b, where the sample volume was 30 μl, $f_A = f_B = 1.66$ ml min^{-1} and $R = 1.0$ m (0.75 mm i.d.), a 25-cm long PVC gradient tube of 1.74-mm i.d. yielded the most satisfactory dispersion pattern. Titration curves obtained with this manifold were identical in shape to those shown in Fig. 7, and when the resulting t_{eq} values were plotted vs. the logarithm of C^0_{HCl}, calibration curves such as those shown in Fig. 12 (a and b) were obtained; the linear portion comprised ca. 0.7 decade of concentration, and the deviations from linearity at high and low concentrations were due to departure from a purely exponential concentration gradient in these regions. The methods for adjusting the linear range to suit the sample concentrations are the same as those described in connection with the two-channel titration with the mixing chamber (Fig. 11). Thus, when the concentration of the titrant was changed from $1 \cdot 10^{-3}$ M NaOH (Fig. 12, curve a) to $5 \cdot 10^{-3}$ M NaOH (curve b), the linear range was shifted from $5 \cdot 10^{-3}$—$2 \cdot 10^{-2}$ M to $3 \cdot 10^{-2}$—$1 \cdot 10^{-1}$ M (C^0_{HCl}), while the slope of the calibration curve with all other parameters fixed remained constant. By extrapolation to $t_{eq} = 0$, C^0_{HCl} of curve a was

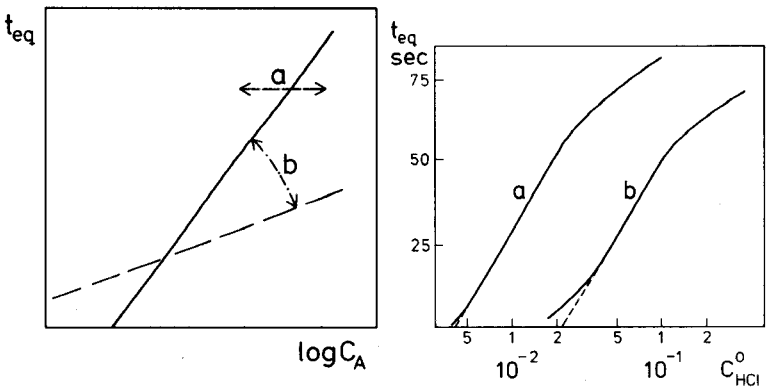

Fig. 11. The influence of pumping rates (f), sample volume (v), gradient chamber volume (V), and titrant concentration (C_B) on the relative position (a) and the slope (b) of the calibration curve (for details see text, and eqns. 7 and 8).

Fig. 12. The equivalence time, t_{eq}, as a function of the HCl concentration in the sample (C^0_{HCl}) in the spectrophotometric titration of 30-μl sample volumes in the two-channel system with a gradient tube (25-cm long, 1.74-mm i.d.).

found to be $4.1 \cdot 10^{-3}$ M while that of curve b was $2.1 \cdot 10^{-2}$ M, i.e., the ratio between them agrees well with the theoretical value of 5. From the slope of the two curves (32.32 s/decade; eqn. 9) and the physical volume of the gradient tube, the correction factor accounting for the effectiveness of mixing was calculated to be 0.65. Thus, even in such a short gradient tube, a relatively efficient mixing is obtained.

Sampling frequency and repeatability

The sampling frequency of the Flow Injection titrations can be estimated roughly from Figs. 7, 10 and 12; within 1.5 t_{eq}, one titration cycle is possible, as a time span in excess of one t_{eq} is needed for the sample to reach the detector and to re-establish the "pure gradient chamber" situation. Obviously, about 60 titrations per hour can be performed. In all cases within the linear range the repeatability of titration was within about 1%, depending on the duration of t_{eq}. A more detailed study of the relation of flow rates, sample volumes, chamber and/or gradient tube volumes and reproducibility of titrations is in progress.

To summarize, the one-channel system with a mixing chamber, is fully described by eqn. (9) and is very easy to construct and operate. It is very well suited for screening purposes and gives well reproducible results, provided that the flow rate is constant and does not pulsate much, and that the samples are injected with a good reproducibility. The two-channel system requires a virtually pulse-free pump (as otherwise the f_A/f_B ratio changes with pulsation), but it is more versatile and sensitive. Systems with gradient tubes are most difficult to design, but also most interesting to study.

CONCLUSIONS

The preliminary results obtained with this new titration technique confirm its feasibility and also illustrate how flexibly the dispersion of the sample zone can be controlled in unsegmented continuous flow systems. While limited dispersion has been found useful in direct measurements with, e.g. ion-selective electrodes, and medium dispersion mainly valuable in spectrophotometric analyses, large dispersion of the sample zone is now proved to be a useful tool for titrimetric analyses. Further exploitation of the large dispersion effect offers, however, other intriguing possibilities. Thus, kinetic measurements might well be based on formation of a well defined sample concentration gradient, created in a mixing chamber, which would be led to react with a reagent continuously added in a confluence arrangement. With only one flow-through cell to monitor the stream continuously, the rising and falling edge of the resulting peak could be recorded and subsequently analysed. The controlled concentration gradient could also be used to create a variable profile of pH or complexing reagent within the sample zone. This approach, combined with precipitation and adsorption–desorption techniques, might become a basis for simple and rapid separations.

As to titrations in general, the Flow Injection system has to be optimized, and the reproducibility of titrations critically evaluated at different sampling rates and sample dilutions. Currently, sampling rates of 20—60 titrations per hour are feasible, depending on the required repeatability. From a practical viewpoint, the simplicity of the non-batch mode of operation is an obvious advantage, as the replenishing of the titrant is continuous and also because the injection of the sample itself automatically initiates the next titration cycle.

The two methods described in the present paper, i.e. titration of a strong acid by a strong base and Ca—EDTA titrations, served as reasonably good models. Whether or not several components in a mixture can be determined, or a stepwise titration is possible, remains to be seen. The reversibility of the chemical equilibria employed will undoubtedly play a role, and different indicating techniques will provide further versatility. Use of small sample volumes, e.g. 30 μl, could be advantageous if sample material is scarce, but would be a drawback in titrations of very dilute sample material, as the Flow Injection system is less sensitive than a batch technique, where a small volume of concentrated titrant can be added from a microburette to a large volume of a sample.

The authors express their appreciation to The Danish International Development Agency (DANIDA) for financial support (Project No. 104. Dan. 8/241). Thanks are also due to E. A. Zagatto CENA, Piracicaba, Brazil, for participating in the initial stages of this study.

REFERENCES

1 H. A. Robinson, Trans. Electrochem. Soc., 92 (1947) 445.
2 J. J. Lingane, Anal. Chem., 20 (1948) 797.
3 D. Betteridge, E. L. Dagless, P. David, D. R. Deans, G. E. Penketh and P. Shawcross, Analyst, 101 (1976) 409.
4 T. F. Christiansen, J. E. Busch and S. C. Krogh, Anal. Chem., 48 (1976) 1051.
5 L. Pehrsson and F. Ingman, Talanta, 24 (1977) 87.
6 B. Fleet and A. Y. W. Ho, Anal. Chem., 46 (1974) 9.
7 E. Pungor, K. Toth and E. Nagy, Hung. Sci. Instrum., 35 (1975) 1.
8 J. Růžička, E. H. Hansen and E. A. Zagatto, Anal. Chim. Acta, 88 (1977) 1.
9 J. Růžička, E. H. Hansen, H. Mosbæk and F. J. Krug, Anal. Chem., in press.
10 O. Levenspiel, Chemical Reaction Engineering, Chapter 9, 2nd edn., J. Wiley, New York, 1972.
11 O. Levenspiel and W. K. Smith, Chem. Eng. Sci., 6 (1957) 227.
12 E. H. Hansen, A. K. Ghose and J. Růžička, Analyst, in press.
13 E. H. Hansen, F. J. Krug, A. K. Ghose and J. Růžička, Analyst, in press.
14 J. Růžička, E. H. Hansen and J. Chr. Tjell, Anal. Chim. Acta, 67 (1973) 155.
15 J. Růžička, J. W. B. Stewart and E. A. Zagatto, Anal. Chim. Acta, 81 (1976) 387.
16 E. Bishop, Indicators, Pergamon Press, London, 1972.

Analytica Chimica Acta, 92 (1977) 251—260

POTENTIOMETRIC DETERMINATIONS WITH THE SILVER SULFIDE MEMBRANE ELECTRODE
Part II. Determination of Sulfur Compounds

H. CLYSTERS and F. ADAMS*

Department of Chemistry, University of Antwerp (U.I.A.), Universiteitsplein 1, B-2610 Wilrijk, Belgium)

(Received 15th February 1977)

SUMMARY

A simple, sensitive and fast titrimetric method for sulfur determinations with the silver sulfide membrane electrode is described. Sulfide and sulfate can be determined in one sample. A sensitive sulfate determination is possible after reduction with hydrogen iodide—sodium hypophosphite—acetic acid. Other inorganic sulfur compounds can also be determined. Sparingly soluble metal sulfides can be determined after treatment with strong acid. A reduction with Raney nickel is suitable for the estimation of elementary sulfur and organic sulfur compounds; combustion of the samples in an oxygen flask may be necessary. The methods outlined are applied to the determination of sulfur in steel, some petroleum products and aerosols. When different methods are used, different kinds of sulfur compounds present in an unknown sample can be distinguished.

As has been shown [1] the silver sulfide membrane electrode can be successfully applied to the determination of cyanide. Sulfur compounds can be determined with the sulfide electrode either directly as sulfide, or in conjunction with a titration with silver(I) as sulfite, thiosulfate, thiourea, etc. Several sulfur compounds can be reduced to sulfide before the determination. Finally, sulfate can be titrated with lead(II) using the lead-selective electrode, which consists of a silver sulfide—lead sulfide membrane, for end-point indication. The principles and theory of the ion-selective sulfide electrodes used have already been discussed [1].

Here special attention is focused on the selective determination of different types of sulfur compounds. In addition to sulfide in solution, sparingly soluble metal sulfides can be determined after treatment with strong acid; the hydrogen sulfide evolved is absorbed in alkaline solution. Sulfate and other inorganic sulfur compounds are reduced to sulfide with a strong reductant [2]. For the reduction of sulfate with hydriodic acid—sodium hypophosphite—acetic acid, Vandael [3] has shown that the overall reaction is $H_2SO_4 + 4PO_2^{3-} \rightarrow H_2S + 4PO_3^{3-}$. This reaction may be separated into the following steps: $H_2SO_4 + 2HI \rightarrow H_2SO_3 + H_2O + I_2$; $H_2SO_3 + 3PO_2^{3-} \rightarrow H_2S + 3PO_3^{3-}$; $I_2 + H_2O + PO_2^{3-} \rightarrow PO_3^{3-} + 2HI$. Hydriodic acid and sodium

hypophosphite are both necessary for quantitative reduction; the first step in the successive reactions is rate-determining The hydrogen sulfide is evolved and measured. Sulfate determined in this way can be compared with the method relying on a determination with the lead-selective electrode [4].

Elementary sulfur and some organic sulfur compounds can be reduced with Raney nickel [5], which acts as a surface catalyst. The sulfur is directly bound to the nickel surface, and on acidification hydrogen sulfide is released and determined as described for the metal sulfides. For other samples, decomposition of the matrix is necessary. One of the simplest methods of decomposition is the oxygen flask combustion method [6], which is suitable not only for determinations of sulfur, but also for chloride, bromide, mercury, etc. Combination of the flask method with reduction to sulfide provides a very sensitive method for trace organic sulfur determinations.

By using these selective methods, a single sample can be analyzed for different chemical states of sulfur.

EXPERIMENTAL

Apparatus

A Radiometer PHM 64 millivoltmeter was used with an Orion model 94-06A sulfide or a 94-82A lead electrode and a Tacussel double-junction $Hg/HgO/OH^-$ reference electrode with 1 M sodium hydroxide in the outer compartment. For titrations a Radiometer ABU 11 automatic burette was used. The oxygen flask combustions were done with the Heraeus Mikro K Schöniger apparatus. A Siemens SRS-1 sequential x-ray spectrometer with a Kristalloflex 4 generator was employed for the x-ray fluorescence measurements.

Reagents

All chemicals were of analytical-reagent grade.

Sulfate reductant. Place 100 ml of hydriodic acid (57%; $d = 1.7$), 25 ml of acetic acid (98%) and 2.5 g of sodium hypophosphite in a flask fitted with a condenser, and boil for 1 h with nitrogen bubbling through the solution. Continue to bubble nitrogen until the solution has cooled to room temperature. Store the solution in the dark. The solution can be used for several weeks.

Raney nickel. Place 0.5 g of a 50% nickel—50% aluminium alloy, in a 25-ml flask and add 5 ml of 2.5 M sodium hydroxide: a vigorous reaction starts and the aluminum dissolves. After 10 min decant the supernatant liquid. Wash the activated nickel three times with 10 ml of distilled water, avoiding contact of the catalyst with air. Finally, wash with 10 ml of isopropanol, and store the catalyst under another 10 ml of isopropanol.

Determination of sulfide

Sulfide is preferably determined with the silver sulfide membrane electrode by a titrimetric method. Add the titrant (lead(II) nitrate), quickly until about

90% of the sulfide has precipitated. Then add the titrant in small equal portions (one hundredth of the volume used at the end-point), noting the potential after each addition. After the end-point, add a few more portions. Establish the end-point using the second derivative of the titration curve. A complete determination requires only 5 min.

Determination of sulfide and sulfate

Sulfide and sulfate can be titrated successively with lead(II) solution using the lead-selective electrode [4]. Measure 10 ml of the sample containing sulfide and sulfate into the titrating vessel. Adjust the pH to 12 with 1 M sodium hydroxide and titrate the sulfide. Acidify to pH 4 with perchloric acid, add 20 ml of methanol and titrate the sulfate.

Determination of sparingly soluble metal sulfides

Place the sample containing the metal sulfide into the distillation flask of the evolution apparatus described earlier (see Fig. 1 of ref. 1). Add 8 M hydrochloric acid slowly from the dropping funnel and heat the solution. Pass nitrogen to sweep the hydrogen sulfide to the absorber, which contains 50 ml of 1 M sodium hydroxide. Dip the sulfide and reference electrodes into this solution and record the potential. When the potential reading has stabilized, which indicates that no more hydrogen sulfide is evolved, start the titration.

Determination of sulfur compounds

Two reducing agents have been evaluated for the reduction of sulfur compounds to sulfide prior to the determination.

Reduction with hydriodic acid—hypophosphite—acetic acid. Place the sample in a 25-ml distillation flask, and evaporate to dryness. Assemble the evolution apparatus, add 3 ml of reducing agent through the dropping funnel, and heat the flask quickly with a small bunsen flame. In this manner some sulfur compounds can be reduced quickly; within 5 min the hydrogen sulfide is absorbed in the sodium hydroxide solution. After stabilization of the potential titrate the sulfide. Then change the absorbing solution and the flask for the next determination. Four to five determinations per hour are possible.

Reduction with Raney nickel. Measure the sample into the flask containing the activated nickel in isopropanol. Assemble the evolution apparatus and heat gently until gas evolves from the nickel surface. Then shake the mixture. After 15 min, add 0.1 ml of 2.5 M sodium hydroxide, and heat to boiling. After another 15 min, add 10 ml of 8 M hydrochloric acid slowly while boiling the solution. Collect the hydrogen sulfide and titrate as before. The time necessary for a complete analysis is 1 h.

Determination of sulfide after combustion of the sample

Place the sample on a 4-cm^2 ash-free filter paper and burn it in the usual manner in a 750-ml oxygen flask containing 5 ml of distilled water and 5 drops of 30% hydrogen peroxide. After the combustion, shake the flask for several minutes, to ensure complete absorption and oxidation of sulfur dioxide [7]. For the reduction add 1 ml of 1 M sodium hydroxide and an aliquot of the sample, evaporated to dryness and analyzed as described above.

X-ray fluorescence analysis

The results of the sulfur determinations after oxygen flask combustion were compared with those obtained by x-ray fluorescence. In the latter method the sulfate was precipitated as barium sulfate by an excess of barium chromate. The precipitate was filtered off, and the K_α line of sulfur was measured [8, 9] with a wavelength-dispersive sequential spectrometer.

RESULTS AND DISCUSSION

Determination of sulfide

The following methods of using the sulfide electrode have been compared: calibration curve, standard addition, standard subtraction and titration. Titration with lead(II)-nitrate gives the most precise results [10]. The end-point of the titration may be evaluated from the second derivative, graphically or by linearization [11]. All these methods give similar results, but the first is most convenient. The precision of sulfide titrations with lead nitrate based on the second derivative is listed in Table 1. Either a sulfide electrode or a lead electrode can be used.

Determination of sulfide and sulfate

Because of the relatively high solubility product of lead(II) sulfate, sulfate is usually titrated in mixed solutions, e.g. 1:1 water—dioxane or 1:2 water—methanol. The former gives a more pronounced potential jump, and a better precision. For example in, the titration of $2.55 \cdot 10^{-3}$ M sulfate, the standard

TABLE 1

The precision of titrations of sulfide with lead(II) nitrate for different concentrations

Sulfide (M)	Standard deviation for triplicate determination (%)	Titrant strength (M)
$9.16 \cdot 10^{-2}$	0.1	10^{-1}
$8.78 \cdot 10^{-3}$	0.3	10^{-2}
$8.54 \cdot 10^{-4}$	0.8	10^{-3}
$6.65 \cdot 10^{-5}$	3.9	10^{-3}
$6.43 \cdot 10^{-6}$	5.4	10^{-3}

deviations were 0.39% and 7.0%, respectively. However, for the titration of sulfide and sulfate in one sample, the addition of dioxane gives low results for the sulfate determination. This negative error can be suppressed by filtering off the precipitated lead sulfide (Table 2).

In the water—methanol medium, sulfide and sulfate can be titrated with a lower limit for sulfate of 10^{-3}M. Sulfide interferes with the sulfate determination when a four-fold excess is present. The sulfide determination is not affected by the sulfate present (Table 2).

Determination of sulfur compounds

The hydriodic acid—sodium hypophosphite reagent reduces most common inorganic sulfur compounds, whereas Raney nickel is suitable for the reduction of organically bound and elemental sulfur.

Reduction of inorganic sulfur compounds. Sulfate is determined as sulfide after reduction with hydriodic acid—sodium hypophosphite—acetic acid. The accuracy and precision for different quantities of sulfate are summarized in Table 3. The precision is optimal for 10μg of sulfur, but only 96% of the sulfate is recovered; for lower quantities the efficiency of the reduction is higher, but the standard deviation increases. After standardization of the method with known amounts of sulfate, the best results are obtained in the range 1—10 μg of sulfur. If a 5-ml absorption vessel with reduced diameter is used, as little as 0.1 μg of sulfur can be determined. The sulfates of calcium, barium and lead can also be determined accurately. Some other inorganic

TABLE 2

Titration of sulfate and sulfide in one sample in water—dioxane (1:1 v/v) and water—methanol (1:2 v/v) solutions

Sample	Sulfate concentration ($\cdot 10^{-3}$ M)		Sulfide concentration ($\cdot 10^{-3}$ M)	
	Present	Found	Present	Found
Water—dioxane				
1	2.55	2.55	—	—
2	2.55	1.77	0.50	0.51
3	2.55[a]	2.50	1.00	0.98
4	2.55	0.79	1.90	1.83
Water—methanol				
5	2.55	2.55	—	—
6	2.55	2.56	2.00	2.04
7	2.55	2.51	4.50	4.32
8	1.02	0.96	—	—
9	1.02	0.92	4.00	4.11
10	1.02	0.77	9.80	9.71

[a]With filtration of PbS.

TABLE 3

Accuracy and relative standard deviation (s_r) for the determination of sulfate after reduction

Sulfate (μg S)		Recovery (%)	s_r	No. of detns.
Present	Found			
160.3	139.2	86.8	—	—
100.0	90.2	90.2	1.3	4
80.2	73.9	92.3	—	—
32.1	30.7	95.6	—	—
16.03	15.40	96.2	0.6	7
1.603	1.600	99.8	4.6	5
0.160	0.154	96.3	16.0	7

TABLE 4

Reduction of inorganic sulfur compounds with hydriodic acid—sodium hypophosphite—acetic acid

Ion	SO_3^{2-}	$S_2O_3^{2-}$	$S_2O_7^{2-}$	$S_2O_8^{2-}$
Present (μg S)	15.40	15.40	15.40	15.40
Found (μg S)	15.18	14.97[a]	15.28	15.60

[a] After reduction for 40 min. The results after 12 and 20 min were 11.67 and 13.03 μg S, respectively.

sulfur compounds can also be determined in this way (Table 4). The reductions proceed in the same manner as for sulfate and are fast, except for the reduction of thiosulfate.

All samples must be evaporated to dryness because water lowers the yield of the reduction. Another possible interferent is nitrate [12]. When 15.4 μg S (as sulfate) was determined, 1.5 mg of nitrate did not interfere, but results became increasingly low with 5 and 10 mg of nitrate, and no sulfur was recovered when 40 mg of nitrate were present. The presence of an interfering substance is indicated by the red color of the reducing agent; when the circumstances for the reduction of sulfate are not favorable, there is no decolorization of the reagent, because of the presence of iodine. Addition of zinc acetate and heating for 1 h at 320°C removes the nitrate [13].

Raney nickel is not suitable for the reduction of inorganic sulfur compounds Values not significantly different from blanks were obtained even when high concentrations of sulfate and the ions listed in Table 4 were present.

Reduction of elemental sulfur and organic sulfur compounds. The reduction of elemental sulfur with the hydriodic acid—hypophosphite reagent is not quantitative; carbon tetrachloride and benzene as solvents for sulfur give different yields for the reduction (84% and 75%, respectively). Raney

nickel provides very precise and accurate results in the 100-μg range (Table 5); the precision becomes worse for lower concentrations. Because of the relatively high blank value of the nickel used, the limit of determination is about 2 μg.

The reduction of organic sulfur compounds with hydriodic acid—hypophosphite reagent is unsatisfactory. Thiourea yields about 5% of its sulfur as hydrogen sulfide; thiocyanate yields about 30%. Various organic sulfur compounds are reduced to sulfide [5, 14]. Here the method was only checked by analyzing a light petroleum fuel (see below).

Combustion of organic samples

The above methods are satisfactory for several kinds of sulfur compound, but some samples, e.g. coals, give very low results. Complete decomposition of the sample is essential, and the oxygen flask combustion method was chosen for convenience. Table 6 shows the sulfur contents of different coal-containing samples. The results obtained by the reductive method of analysis after the flask combustion and by the x-ray fluorescence method for sulfate agree closely.

Applications to other samples

A National Bureau of Standards sample of Bessemer steel (NBS-10g) was analyzed by the evolution method with the hydriodic acid—hypophosphite reagent with satisfactory results (Table 7).

TABLE 5

Reduction of sulfur with Raney nickel

Sulfur (μg)		s_r	No. of detns.
Present	Found		
97.3	96.9	1.6	4
22.6	22.2	4.3	4
4.4	4.1	12.2	9

TABLE 6

Comparison between the sulfide electrode and x.r.f. determination for coal-containing samples; filter paper (1 cm^3) containing 300—600 μg of particulate matter was used for all samples

Sample	Reduction/electrode		x.r.f.	
	S (μg)	s_r	S (μg)	s_r
1	27.0	2.7	28.1	1.9
2	26.6	2.1	25.7	1.8
3	29.5	2.8	30.4	2.3

TABLE 7

Determination of sulfur in N.B.S. samples

N.B.S. sample	Method	Sulfur (%)		s_r	No. of detns.
		Present	Found		
Bessemer steel (SRM—10g)[a]	HI—NaH_2PO_2—HAc	0.109	0.104	0.8	5
Light distillate fuel (SRM-1624)[b]	Raney nickel	0.211	0.209	2.3	4
Crude oil (SRM-1623)[b]	Raney nickel	0.268	0.233	3.9	3

[a] A 100-mg steel sample was finely divided and added to the reducing medium.
[b] 100-μl samples were used.

Because of the importance of sulfur determinations in petroleum products, special attention was devoted to this problem. In a light distillate fuel (N.B.S. SRM 1624) sulfur was determined by reduction with Raney nickel with good results. This contrasts with the case of crude oil (SRM 1623), where the sulfur was not completely recovered (Table 7), probably because some is present in inorganic or inaccessible forms.

If larger samples are taken for the Raney nickel reduction, sulfur concentrations down to 0.4 p.p.m. can be determined, as was shown by the analysis of industrial ethylbenzene samples. Two separate samples (200 μl) gave results of 0.42 p.p.m. and 0.8 p.p.m. with standard deviations of about 8% (5 determinations). Recoveries of 98% and 104% were obtained when 4 μg of sulfur in benzene was added to these samples and the analyses repeated.

Considerable attention has been devoted recently to the determination of sulfur in aerosols [15—18]. Particulate sulfur compounds formed in the atmosphere from sulfur dioxide emission are a suspected long-term health hazard. Most studies of suspended sulfur compounds in pollution aerosols rely on conventional wet-chemical techniques. Instrumental methods such as x-ray fluorescence or neutron activation are not suitable for accurate determinations. With the methods outlined above, not only are more accurate sulfur determinations possible, but different chemical forms of sulfur, especially sulfate and non-sulfate, can be distinguished.

A standard reference dust sample from the European Economic Community was analyzed, and the results were compared with those obtained in other laboratories. Two aerosol samples collected from the atmosphere by filtration through Whatman-41 filters with a high-volume sampler were also examined. The results are given in Table 8. Direct evolution from 8 M hydrochloric acid provides results on the sulfide present, which appeared to be below the detection limit. Reduction treatment with Raney nickel should determine organic sulfur compounds; again, there were no detectable amounts. The reduction with hydriodic acid—hypophosphite reagent should provide a

TABLE 8

Determination of sulfur in aerosols by different methods

Method	S found (%)		
	Standard sample	Filter sample 1	Filter sample 2
Evolution HCl 8 M	< 0.001	< 0.001	< 0.001
Reduction:			
Raney nickel	< 0.01	< 0.01	< 0.01
Reduction:			
HI—NaH_2PO_2—HAc	2.83 ± 0.19(5)[a]	2.95 ± 0.29(3)	3.12 ± 0.18(3)
Flask combustion	5.32 ± 0.23(3)	4.62 ± 0.44(3)	3.28 ± 0.13(3)
S(%)[b]	4.0 ± 1.5	—	—
% S as sulfate[c]	2.73 ± 0.10	—	—

[a]Number of determinations in parentheses.
[b]Mean result from other laboratories.
[c]By the turbidimetric $BaSO_4$ method [19].

result on the sulfur present as sulfate; the result obtained (Table 8) correspond to the sulfate concentration obtained by turbidimetry [19]. Oxygen flask combustion, however, provides a much higher result.

The difference in the sulfur contents obtained by the two methods indicates that some of the element is present in a form which is accessible by the combustion method but not by the reduction. At least part of the missing sulfur is probably present either bound organically or as pyrite in the carbon particles which result from incomplete combustion processes. The EEC aerosol sample contains 40% carbon, filter sample 1 up to 50%. Filter sample 2 was sampled near an iron smelter and contained a much smaller quantity of combustion products. A sulfur content of 3—4% in the carbon fraction would explain the discrepancy; further work is in progress to check this. Roberts and Friedlander [20] have compared the results obtained for sulfur by vaporization at 1200°C with flame photometric detection and by an unspecified wet chemical procedure. They obtained good agreement for samples taken downwind from a sulfuric acid plant, but in other samples they obtaine results lower by a factor of two for the vaporization method, probably because part of the sulfur was not volatile.

REFERENCES

1 H. Clysters, F. Adams and F. Verbeek, Anal. Chim. Acta, 83 (1976) 27.
2 L. Gustaffson, Talanta, 4 (1960) 227.
3 C. Vandael, Chim. Anal., 44 (1962) 295.
4 R. N. Heistand and C. T. Blake, Mikrochim. Acta, (1972) 212.
5 L. Granatelli, Anal. Chem., 31 (1959) 343.
6 W. Schöniger, Mikrochim. Acta, (1955) 123.
7 L. Gildenberg, Microchem. J., 3 (1959) 167.
8 P. Tschoepel, A. Disam, V. Krivan and G. Tölg, Z. Anal. Chem., 271 (1974) 106.

9 B. Magyar and G. Kaufmann, Talanta, 22 (1975) 267.
10 H. Clysters, Analytical Determinations with the Silver Sulfide Membrane Electrode, doctorate thesis, University of Antwerp, Belgium, 1976.
11 G. Gran, Analyst, 77 (1962) 662.
12 C. M. Johnson and H. Nishata, Anal. Chem., 24 (1952) 736.
13 A. Sinclair, R. D. Hall, D. Burns and W. P. Hayes, Talanta, 18 (1971) 194.
14 A. Fensom, K. Dimnoch and G. Duff, Analyst, 96 (1971) 194.
15 P. T. Roberts and S. L. Friedlander, Atmos. Environ., 10 (1976) 403.
16 J. D. Husar, R. Husar and P. Stubits, Anal. Chem., 47 (1975) 2062.
17 K. Potzl, Staub. Reinhalt. Luft, 34 (1974), 55.
18. J. L. Johnson, Mikrochim. Acta, (1974) 145.
19. R. Dams, J. Billiet, C. Block, M. Demuynck and M. Janssens, Atmos. Environ., 9 (1975) 1099.
20 P. T. Roberts and S. K. Friedlander, Atmos. Environ., 10 (1976) 403.

Analytica Chimica Acta, 92 (1977) 261—265

POTENTIOMETRIC STUDIES OF DITHIOOXAMIDE WITH A SULPHIDE-SELECTIVE MEMBRANE ELECTRODE

N. M. SHEINA§, V. P. IZVEKOV, M. K. PÁPAY, K. TÓTH and E. PUNGOR*

Institute for General and Analytical Chemistry, Technical University, 1502 Budapest (Hungary)

(Received 7th March 1977)

SUMMARY

The sulphide-selective electrode is applicable to the determination of dithiooxamide by titration with silver nitrate. The effect of the alkali content of the solutions on the reaction has been studied. The reaction products are silver sulphide, oxalic acid, and nitric acid. If the alkali concentration of the solution is lower than that equivalent to the acid formed during the titration, the amount of sulphide produced by hydrolysis decreases and the equilibrium potential is established more slowly. The determination is rapid and accurate in the presence of 1 M sodium hydroxide.

Some earlier potentiometric studies of organic sulphur compounds have already been reported [1—3]. Dithiooxamide is a well known analytical reagent for the determination of copper, cobalt, nickel and other metals [4—6]. In the present paper, a rapid and accurate potentiometric method is described for the determination of dithiooxamide with a sulphide-selective membrane electrode. The products of the reaction with silver nitrate titrant have been identified.

EXPERIMENTAL

E.m.f. values were measured with a Radelkis Precision pH meter Type OP-205 (Radelkis, Budapest, Hungary). A Radelkis sulphide-selective membrane electrode (Type OP-S-711) and a Metrohm pH glass electrode were used as indicator electrodes and a saturated calomel electrode as reference electrode. The calomel electrode was connected with the sample solution by a 0.1 M potassium nitrate agar salt bridge.

I.r. spectra were recorded with a Perkin-Elmer 421 instrument.

All reagents used were of analytical grade.

A dithiooxamide stock solution ($5 \cdot 10^{-2}$ M) was prepared in ethanol. Silver nitrate standard solutions of the same concentration as the sample solution were used as titrant in every case.

---

§Present address: Chemical Faculty, Institute of Analytical Chemistry, Moscow University, U.S.S.R.

RESULTS AND DISCUSSION

Dithiooxamide can be titrated in the presence of 1 M, 10^{-1} M and 10^{-2} M sodium hydroxide, or in aqueous 2% and 5% ammonia solution with standard silver nitrate solution (Figs. 1—3). The changes which occur during titration are followed sensitively by the sulphide-selective electrode. There is only one potential jump on the titration curves. The ratio of the titrand and titrant at the point of equivalence is constant over wide concentration limits, corresponding to a ratio of 1:4. The equilibrium potential is established quickly in the presence of 1 M NaOH. The potential change at the equivalence point is very large, 800—850 mV.

However, the titration of 10^{-4} M dithiooxamide takes a long time, as establishment of the equilibrium potential at the electrode is slow at this low concentration; in this case $5 \cdot 10^{-3}$ M silver nitrate was used as titrant. The lower limit of determination of dithiooxamide is affected by the reduced rate of the establishment of the equilibrium potential, although the potential jump still occurs at a ratio of 1:4.

The equilibration of the potential is also slower when the titration is carried out in distilled water or if the concentration of NaOH is less than 10^{-1} M. If

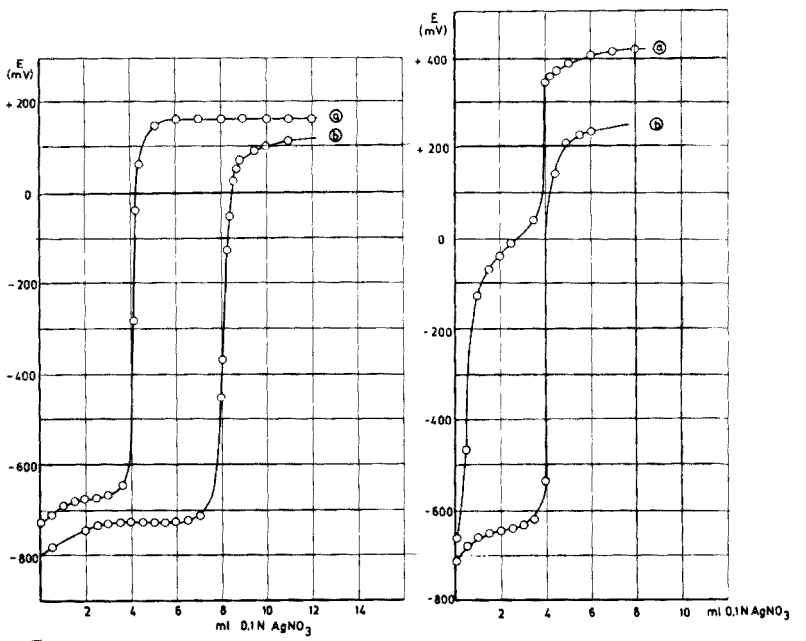

Fig. 1. Potentiometric titration curves of $5 \cdot 10^{-2}$ M dithiooxamide in 1 M NaOH solution. (a) 2.00 ml dithiooxamide. (b) 4.00 ml dithiooxamide.

Fig. 2. Potentiometric titration curves of $5 \cdot 10^{-2}$ M dithiooxamide in, (a) 10^{-2} M NaOH, (b) 10^{-1} M NaOH.

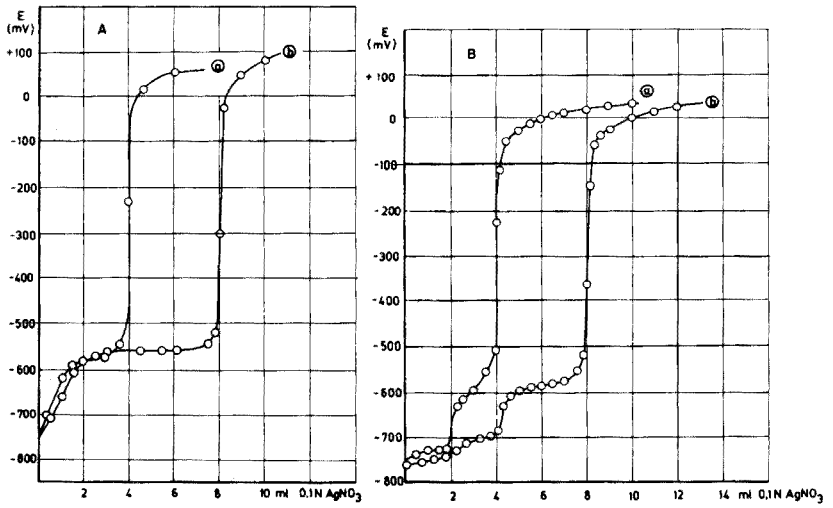

Fig. 3. Potentiometric titration curves of $5 \cdot 10^{-2}$ M dithiooxamide, (A) In 2% ammonia solution. (B) In 5% ammonia solution. (a) 2.00 ml of dithiooxamide, (b) 4.00 ml of dithiooxamide.

the titration is carried out in the presence of 5% ammonia, the titration curve is different from those mentioned above. There are two potential jumps, the molar ratio being 1:2 at the first, and 1:4 at the second.

Identification of the products of titration

The titration of dithiooxamide with silver nitrate solution in the presence of 1 M sodium hydroxide involves only one potential jump. Up to this jump, one molecule of dithiooxamide reacts with four molecules of silver nitrate to form a black precipitate. The precipitate was filtered, washed, and found to be silver sulphide. The i.r. spectrum of the solid residue obtained from the filtrate after extraction with ether and evaporation to dryness is recorded in Fig. 4, Curve (b); the spectrum of pure dithiooxamide is also given (Fig. 4, Curve a).

From the general concepts of chemical bonding, it is reasonable to expect that the structural formula of dithiooxamide is $H_2N—CS—CS—NH_2$. This formula could lead to two heavy-atom arrangements, i.e. the planar *cis* and *trans* forms, but dithiooxamide exists in the *trans* form [7, 8]. In the spectrum of pure dithiooxamide (Fig. 4) the strong band at 830 cm^{-1} can be assigned to the stretching vibration of the C=S group. The bands at 3110, 3190 and 3280 cm^{-1} are assigned to the stretching vibrations of hydrogen-bonded NH_2 groups [8, 9]. In the i.r. spectrum of the solid residue obtained after the titration, the ν_{CS} and ν_{NH_2} vibrations are absent. This means that the reaction product does not contain C=S and NH_2 groups; a new band at 1720 cm^{-1} can be interpreted [10] as the carbonyl stretching vibration of sodium hydrogen-

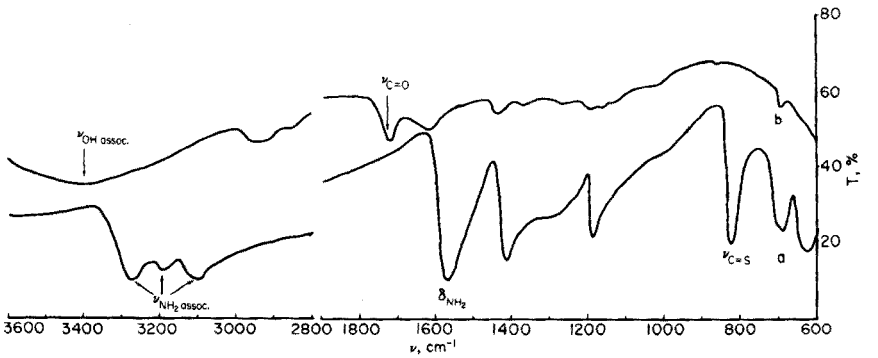

Fig. 4. Infrared spectra of (a) pure dithiooxamide, (b) the solid residue obtained from the filtrate after titration in 1 M NaOH solution.

oxalate. The broad band with the maximum at 3420 cm^{-1} is the stretching vibration of a hydrogen-bonded OH group. The results of the potentiometric titrations and the i.r. investigation indicate the following reaction mechanism between dithiooxamide and silver nitrate in 1 M sodium hydroxide

$$\begin{matrix} S=C-NH_2 \\ | \\ NH_2-C=S \end{matrix} + 4AgNO_3 \xrightarrow{NaOH} 2Ag_2S + \begin{matrix} C\equiv N \\ | \\ C\equiv N \end{matrix} + 4NaNO_3$$

(*trans*-form)

$$\begin{matrix} C\equiv N \\ | \\ C\equiv N \end{matrix} \rightarrow \begin{matrix} COONa \\ | \\ COOH \end{matrix}$$

As mentioned above, two potential jumps occur when dithiooxamide is titrated in 5% ammonia solution. Up to the first potential jump, one molecule of the dithiooxamide reacts with two molecules of silver nitrate to form a black precipitate. Again, the reaction product is also silver sulphide, but the by-product, the i.r. spectrum of which is presented in Fig. 5, is different. This spectrum is more complicated than the spectrum of pure dithiooxamide or sodium hydrogenoxalate. The band at 830 cm^{-1} remains in the spectrum of the solid residue (cf. Fig. 4a) but it is less intense. The band at 1580 cm^{-1}, which is the deformation vibration of the NH_2 group [11] is also present; the reaction product therefore contains NH_2 and C=S groups. A new band at 1680 cm^{-1} characteristic of a hydrogen-bonded carbonyl group [12] is also present. The stretching vibrations of the NH_2 group usually observed at 3100—3200 cm^{-1} are masked by the very broad absorption band of the OH group. Thus, the results indicate that the first potential jump corresponds to the following reaction

$$\begin{matrix} S=C-NH_2 \\ | \\ NH_2-C=S \end{matrix} + 2AgNO_3 \xrightarrow{NH_3} \begin{matrix} COOH \\ | \\ S=C-NH_2 \end{matrix} + Ag_2S + 2NH_4NO_3$$

The filtrate obtained in a parallel experiment, after removal of silver sulphide was titrated further with silver nitrate; silver sulphide was formed during

the titration. The product obtained in this titration, as shown by its i.r. spectrum, was ammonium hydrogen oxalate.

$$S=C(COOH)(NH_2) + 2AgNO_3 \xrightarrow{NH_3} Ag_2S + C(COONH_4)(COOH) + 2NH_4NO_3$$

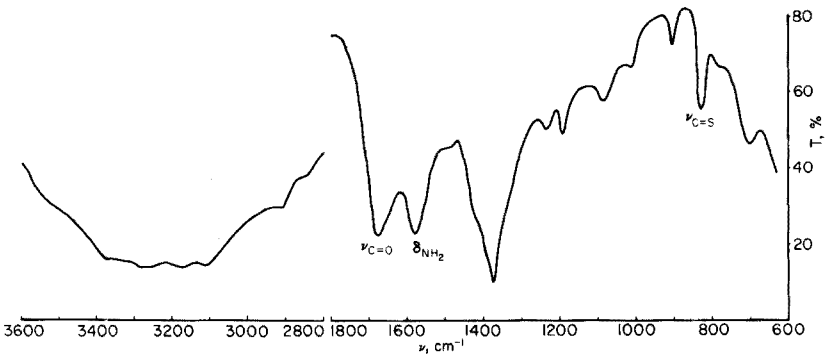

Fig. 5. Infrared spectrum of the by-product after the first potential jump in 5% ammonia solution.

REFERENCES

1 M. K. Pápay, K. Tóth and E. Pungor, Anal. Chim. Acta, 56 (1971) 291.
2 M. K. Pápay, K. Tóth, V. P. Izvekov and E. Pungor, Anal. Chim. Acta, 64 (1973) 409.
3 M. K. Pápay, V. P. Izvekov, K. Tóth and E. Pungor, Anal. Chim. Acta, 69 (1974) 173.
4 S. A. Voznesenskii, I. Pazelskii and I. M. Tsinn, Trans. Inst. Pure Chem. Reagents (U.S.S.R.) 16 (1939) 98.
5 G. E. Kalbus, R. D. Wesley and L. H. Kalbus, Analyst, 96 (1971) 488.
6 D. A. Williams, I. J. Holcomb and D. F. Boltz, Anal. Chem., 47 (1975) 2025.
7 P. J. Wheatley, J. Chem. Soc., (1965) 396.
8 T. A. Scott and E. L. Wagner, J. Chem. Phys., 30 (1959) 465.
9 A. Ray and D. N. Sathyanarayana, Indian J. Chem., 12 (1974) 1092.
10 J. Flett, Spectrochim. Acta, 18 (1962) 1537.
11 D. Hadzi, J. Chem. Soc., (1957) 847.
12 L. J. Bellamy, Advances in Infrared Group Frequencies, Methuen, London, 1969, p. 172.

Analytica Chimica Acta, 92 (1977) 267—275

MICROCOULOMETRIC DETERMINATION OF TOTAL INORGANIC SULPHUR IN WATER BY A HYDROIODIC ACID REDUCTION METHOD

M. C. van GRONDELLE, F. van de CRAATS and J. D. van der LAARSE
Koninklijke/Shell-Laboratorium (Shell Research B.V.), Amsterdam (The Netherlands)
(Received 22nd March 1977)

SUMMARY

A method has been developed for the determination of trace amounts of total inorganic sulphur in aqueous solutions. It is based on rapid reduction of the sulphur compounds by a mixture of hydroiodic acid and hypophosphite to hydrogen sulphide, followed by oxidation to sulphur dioxide and instantaneous microcoulometric titration. The high sensitivity of the titration technique allows the detection of sulphur in concentrations as low as 0.01 mg l^{-1}; each analysis requires only 3—4 min. Metals, phosphorus and halogens do not interfere. The method is usable for aqueous samples such as boiler water, plant effluents and solutions obtained after appropriate destruction of organic and inorganic materials.

The determination of traces of sulphate in aqueous solutions is frequently needed, either as such or as a finish after combustion or destruction of organic and inorganic samples in analyses for total sulphur.

A widely used method is the titration with a barium salt solution (e.g. ASTM 516) with either a thorin indicator or a turbidimetric end-point. The detection limit is a few micrograms of sulphur in both cases. When special apparatus is used, such small amounts can be measured even in small samples, as indicated by Coleman et al. [1]. The interference from many metals, phosphate and high concentrations of halogens restricts the applicability of methods based on precipitation with barium(II). Procedures for eliminating such interferences have been reviewed by Griepink et al. [2]. All of them, even the best (ion exchangers), have an adverse effect on the limit of detection.

An alternative approach based on a different principle is reduction of sulphur compounds to hydrogen sulphide, followed by titrimetric or colorimetric detection. This procedure is attractive, because the sulphur is separated as a gas from other compounds which could interfere with the detection. Furthermore, there are several sensitive and selective methods for measuring sulphide. The two main methods of reducing sulphate to hydrogen sulphide are those using tin(II) solutions and hydroiodic acid—hypophosphoric acid mixtures. The various reduction mixtures described in the literature are listed in Table 1.

TABLE 1

Survey of reduction mixtures for inorganic sulphur compounds

Composition of reaction mixture	Ref.
$SnCl_2$ in H_3PO_4	Kiba and Kishi [3], Nagashima et al. [4]
Sn dissolved in H_3PO_4	Griepink et al. [2]
HI + red P + HCOOH	St. Lorant [5], Johnson and Nishita [6]
HI + H_3PO_2 + HCl	Luke [7], Tölg [8], Millet [9]
HI + NaH_2PO_2 + CH_3COOH	Gustafson [10]
HI + NaH_2PO_2 + $(CH_3CO)_2O$	Davis and Lindstrom [11]
HI + H_3PO_2 + HCOOH	Keay et al. [12]

The reduction with tin in concentrated phosphoric acid has been applied mainly to non-aqueous samples, e.g. minerals. A temperature of 280—300°C is needed for fast reaction. In our experience this type of reduction mixture is not suitable for aqueous samples. More practicable for aqueous solutions is the reduction with hydroiodic acid at 100—125°C, which is also easier to handle. Combining all the information from the literature leads to the following conclusions: (a) high concentrations of hydroiodic acid (maximum 57%, constant boiling mixture) are favourable for more complete conversion to H_2S; (b) the actual form of the phosphorus is not essential, so that red phosphorus or hypophosphorous acid or its sodium salt may be used; and (c) the addition of other acids to the reaction mixture seems to be of secondary importance.

Microcoulometry has become recognized as a fast and accurate means of determining traces of reactive gases. A few nanograms can easily be determined. The suitability of this technique for detecting the gaseous sulphur compounds formed on the reduction of sulphate and other sulphur compounds was therefore investigated. The speed of the existing reduction procedures had to be increased correspondingly to derive full benefit from the fast automatic titration. The present paper describes how this problem has been solved.

The basic principles of the procedure are as follows. The aqueous sample, maximum 1 ml, is injected into a reaction vessel containing a mixture of hydroiodic acid and sodium hypophosphite at 124°C. The gaseous sulphur compounds formed (H_2S and some SO_2) are stripped from the reagent in a fractionating column. Water originating from the sample is collected in a reflux trap and can be drained off. The gas stream passes through an absorption vessel for removal of hydrogen iodide vapour before the hydrogen sulphide is converted to sulphur dioxide in a small combustion tube. The gas stream is finally dried in a scrubber containing sulphuric acid. The sulphur dioxide is titrated microcoulometrically in an iodimetric titration cell.

EXPERIMENTAL

A line diagram of the apparatus is shown in Fig. 1.

Reduction

The sulphur compounds are reduced in the reaction flask (A) (Fig. 2). The round-bottom flask has a gas inlet tube, a thermocouple well and a silicone rubber septum for sample injection. The flask is provided with a Vigreux column, a reflux trap and a small spiral-type reflux condenser about 20 cm long. The flask contains a mixture comprising 50 ml of hydroiodic acid (57% azeotrope with water) and 10 ml of a saturated solution of sodium hypophosphite. The system is heated by an 80 W mantle, and kept under a nitrogen stream (125 ml min^{-1}). The temperature of the reagent is critical for good performance and can be controlled by means of the water content. The optimum temperature range is 122—124°C. At lower temperatures the reaction becomes too slow; at higher temperatures excessive amounts of interfering phosphine are formed.

The addition to the reaction mixture of other organic or inorganic acids (see Table 1) was found to have no important effect. However, chromium(II) improved the reducing power considerably. Therefore approximately 0.1 g of chromium(II) chloride was added to the reaction mixture.

Water trap and hydroiodic acid absorber

The reflux trap allows a large number of samples to be analyzed without renewal of the reaction mixture (see Fig. 2A). The refluxing liquid is collected

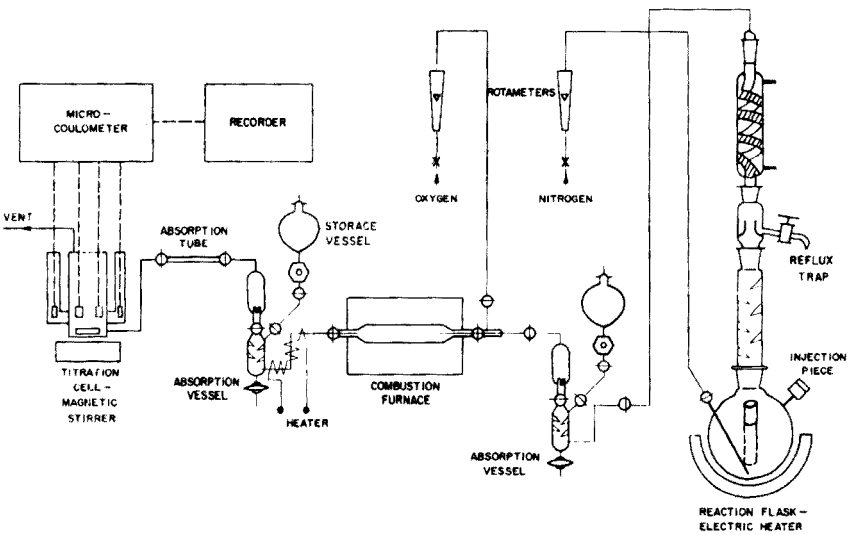

Fig. 1. Diagram of apparatus.

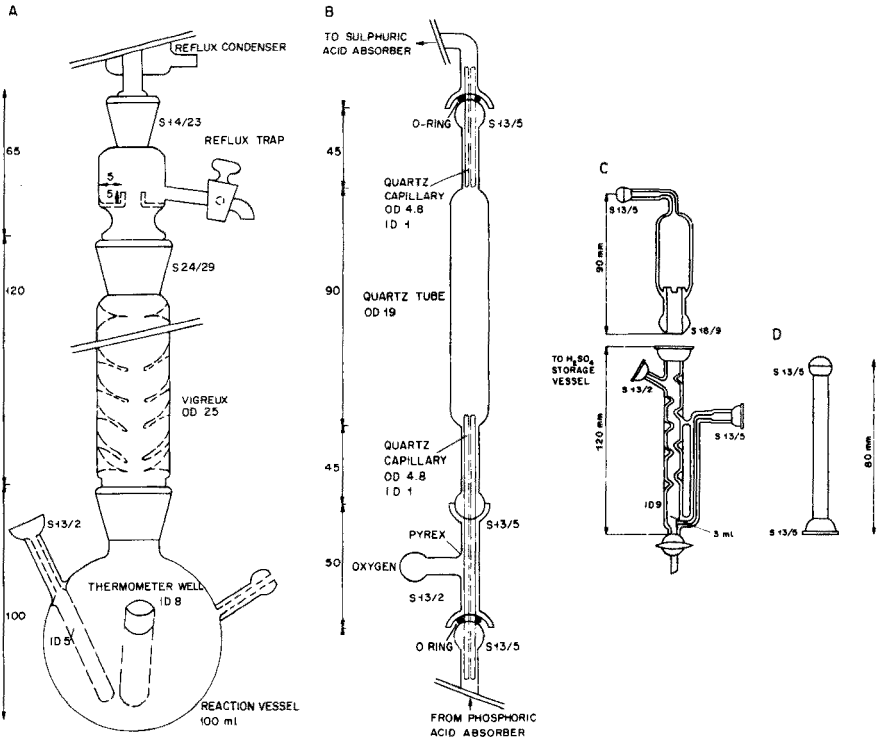

Fig. 2. Details of reaction vessel (A), combustion section (B), absorption vessel with foam destroyer (C), and silver wool tube (D).

in a ring-shaped tray which can be drained when the temperature of the reaction mixture becomes too low. The Vigreux column serves to diminish losses of hydroiodic acid; the drained water usually contains less than 1%.

To prevent undesirable reactions between iodine and sulphur dioxide formed during combustion, hydroiodic acid must be removed before it can enter the combustion tube. A small absorber containing a solution of 10%(w/w) orthophosphoric acid and 5%(w/w) sodium hypophosphite proved to be suitable (see Figs. 1 and 2C). The phosphite prevents oxidation of HI to I_2.

Combustion

Because only traces of H_2S and some PH_3 have to oxidized, the combustion can be carried out in a small quartz tube heated at 725°C, through which oxygen (25 ml min^{-1}) is passed (see Fig. 2B). Under these mild oxidizing conditions, complete conversion of H_2S to SO_2 was observed. Sulphur trioxide is not formed and need not be co-determined. Phosphine which interferes with the titration is converted to phosphoric acid and phosphorus pentoxide, giving a harmless deposit in the capillary on the outlet side of the quartz tube. The capillary must be cleaned daily with water.

Titration

For the titration, the Dohrman microcoulometric titration system (Dohrman Instruments Company, Mountain View, Calif.) was used. The electrolyte prescribed for the titration cell was replaced by an aqueous solution containing 2%(w/w) KBr, 0.001%(w/w) KI and 0.05%(w/w) acetic acid. The lowering of the iodide content by a factor of 50 was found to make this electrolyte much more stable. Uncontrolled oxidation of iodide caused by oxygen, light or nitrogen oxides has much less influence. The choice of "bias", which may vary from cell to cell, is also important. This was determined by measuring the baseline shift caused by iodine evaporation at a nitrogen flow of 200 ml min^{-1}, and adjusting the bias until a shift of 2 μA was obtained.

Before entering the cell, the gases are dried by means of an absorber containing 75%(w/w) sulphuric acid (see Figs. 1 and 2C) the inlet capillary of which is heated to 100°C. Finally the last traces of iodine are removed in an absorption tube containing silver wool (see Fig. 2D).

The procedure for the day-to-day maintenance of the scrubbers is as follows: refill with the respective absorption liquids; rinse the entrance capillary of the sulphuric acid-containing scrubber with water; regenerate the silver wool by heating the tube to about 600°C while passing a stream of nitrogen through it.

RESULTS AND DISCUSSION

Aqueous solutions

The procedure has been applied to various samples with different sulphur contents. In addition, test samples with different types of sulphur compound were analyzed. Table 2 shows that the sulphur is quantitatively determined not only in sulphate but also in ions such as sulphite, sulphide, thiocyanate, pyrosulphate as well as elemental sulphur. The time required for one analysis is 3—4 min.

The H_2S/SO_2 ratio in the reduction mixture is unknown, but it can be presumed that little SO_2 will leave the reduction unit, because further reduction takes place in the Vigreux column, where a large amount of HI refluxes. The formation of some SO_2 in the reaction mixture is not important in this method, as all H_2S is eventually converted to SO_2.

In general, the limit of detection is 0.01 mg l^{-1}. Although the sensitivity of the titration allows measurements below 0.01 mg l^{-1}, they are of little practical importance. Injection syringes must be made wholly of inert materials such as glass, Teflon and platinum. Syringes with steel plungers and needles give inconsistent results, because the needle is attacked by the hydrogen iodide vapours in the reaction vessel. To avoid overloading the titration system, the maximum amount of sulphur per injection is limited to 3 μg. The repeatability of the final method was found to be 5% (relative).

Besides relatively pure aqueous solutions, the method also gives good results for samples containing high concentrations of salt, mineral acid or

TABLE 2

Results obtained for various test samples and blanks

Sample	Sulphur content ($mg\ l^{-1}$)		Sample	Sulphur content found ($mg\ l^{-1}$)
	Added	Found		
Na_2SO_4 in water	37.5	36.8, 37.4	HCl, 37%, Merck, p.a.	0.13, 0.13
Na_2SO_3 in water	47.4	46.1, 47.4	Double-distilled water,	
S in water	12.5	12.5, 12.0	Sample A	0.010, 0.013
$(NH_4)_2S$ in water	22.8	23.8, 24.0	Double-distilled water,	
KSCN in water	40.5	40.0, 40.4	Sample B	0.005, 0.005
$K_2S_2O_7$ in water	30.0	30.3, 30.3	Demineralized water	0.015, 0.024
Na_2SO_4 in 20% HCl	12.6	13.0, 13.0	Tapwater, Amsterdam	26.9, 27.7

alkali. Metals like Ag, Hg, Fe, Ni, Cu, Cd, Co, Cr, Pb, Ca or Ba cause no interference. (Some metals, especially chromium, even had a positive effect on performance.) Manganese interferes with the reduction: injection of a 2% solution of $MnCl_2$ gave rise to white fumes containing PH_3, which resulted in incomplete combustion and deposits of red phosphorus in the outlet capillary.

High concentrations of oxidizing materials such as hydrogen peroxide and nitrates interfere with the reduction. Amounts up to 10 mg of hydrogen peroxide or 100 μg of nitrate per injected volume can be tolerated. Perchloric acid does not interfere. Apart from possible interferences, oxidizing materials consume hypophosphite. If no more hypophosphite is present (indicated by the appearance of a brownish colour (free I_2) in the reaction mixture), the values obtained will be too low. Injection of about 4 ml of a saturated solution of NaH_2PO_2 is then necessary to "reactivate" the reaction mixture.

The removal of water from the injected sample by means of the water trap makes it possible to analyze a large number of samples (up to one thousand) in succession. It is not necessary to replace the reaction mixture after just a few determinations, as is required with all other methods in the literature.

Water may also contain sulphur in organic form, e.g. sulphonates and sulphates originating from detergents. The extent to which the various types of such sulphur compounds are co-determined, has not been investigated in this study. Davis and Lindstrom [11] and Freney [13] state that only a few sulphur compounds are completely reduced, e.g. alkyl sulphates, whereas the conversion of sulphonates is low. The direct measurement of inorganic sulphur in the presence of organically bound sulphur is therefore not generally possible.

Inorganic solids and organic materials

The method has found extensive use in this laboratory as a finish for various destruction techniques. Insoluble inorganic materials such as silica- or alumina-based catalysts can be dissolved after a simple fusion technique. About 10 mg of sample is weighed in a platinum boat, covered with a flux (60—100 mg, unweighed, of a 4:1 mixture of sodium hydroxide and sodium

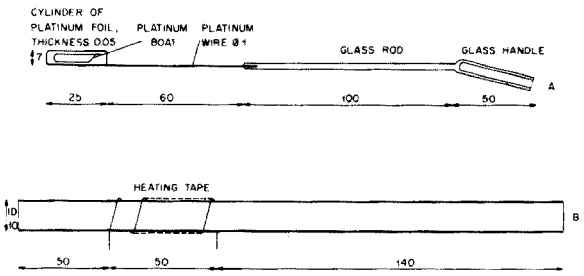

Fig. 3. Ladle (A) and quartz tube (B).

peroxide) and introduced with the aid of a ladle into a quartz tube as illustrated in Fig. 3. To prevent foaming, heating is done in two steps: 3 min at 400°C, followed by 4 min at 700°C. After cooling, the ladle is placed in a calibrated test tube, the melt dissolved in about 5 ml of water and the volume made up to 10 ml with hydrochloric acid (1 + 1). The solution obtained can be injected into the reduction flask.

Results obtained for various pure inorganic compounds by the fusion method (Table 3) show complete recovery, even for elemental sulphur. Table 4 gives some results for practical samples in comparison with more traditional methods. It can be concluded that the method fails for the coal samples containing both organic and inorganic sulphur compounds. Only the Eschka sintering procedure gives correct results for coal. An improved destruction technique for sulphur in coal has been developed [14].

Organic materials are usually burned in an oxygen flask or a Wickbold oxyhydrogen flame before titration, e.g. with barium(II) solution and thorin as the indicator. As the barium titration is subject to interference by metals, phosphorus or halogens, these elements have to be removed beforehand, usually by ion exchange. In the new method, they do not interfere. Even in cases where the ion-exchange treatment yields inaccurate data, the new method gives good results (Table 5).

TABLE 3

Results obtained on pure inorganic compounds after fusion

Compound	Sulphur (%)		Compound	Sulphur (%)	
	Theory	Found		Theory	Found
Cd S	22.4	22.1, 21.7	KSCN	33.0	33.7, 33.5
$NaHSO_3$	30.8	30.2, 31.4	$(NH_4)_2 S_2O_8$	28.1	26.5, 26.5[a]
$Na_2S_2O_3 \cdot 5H_2O$	25.8	25.3, 26.4	S	100	100, 105
$Na_2S_2O_5$	33.7	33.9, 32.4			

[a]Purity unknown.

TABLE 4

Results obtained with different analytical techniques on several materials

Sample type	% Sulphur			
	Microcoulometric finish preceded by			Leco procedure ASTM 354-73
	Fusion	Schöniger[a]	Eschka	
Fly ash	0.47	0.45		
	0.49	0.43		
Platforming catalyst, Al_2O_3 + Pt	0.87	0.70		
	0.86	0.41		
Deposit ex platformer furnace	10.0	8.1		
	10.0	8.9		
Hydrodesulphurization catalyst (0.3% C)	0.03			0.03
	0.04			0.03
Hydrodesulphurization catalyst (8% C)	13.1	14.3	13.2	13.7
	13.8	14.2	13.4	13.6
Hydrodesulphurization catalyst (17% C)	6.45[b]	7.1	6.9	6.3
		7.0	6.5	6.5
Hydrodesulphurization catalyst (24% C)	19.3		19.0	17.2
	18.8		18.0	17.2
Hydrocracking catalyst (0.2% C)	4.7		5.0	5.2
	4.8		5.4	5.2
Coal, lignite, 9% ash	0.42	0.55	0.62	
	0.46	0.56	0.60	
Coal, Welsh anthracite, 5% ash	0.74	0.91	0.96	
	0.51	0.93	0.98	

[a] 20 μl of decalin added before combustion.
[b] Average of 4 results (range 6.3—6.6).

TABLE 5

Comparison of the Schöniger combustion—coulometric procedure with other techniques (Results are given as %S.)

Method	Castrol dope A (5.8% P + 9.7% Zn)	Castrol dope B (9.2% Ba + 0.4% Sn + 1.0% P)	Castrol dope C (1.4% Pb)	Dialkylsulphonic acid, Ca salt (6.5% Ca)
X-ray fluorescence	16.6	2.91	1.43	—
Thorin titration after ion exchange	19.1	1.86	1.22	4.27
Coulometric titration	16.6	2.98	1.40	4.47

REFERENCES

1 R. L. Coleman, W. O. Shults, M. T. Kelley and A. J. Dean, Anal. Chem., 44 (1972) 1031.
2 B. Griepink, J. Slanina and J. Schoonman, Mikrochim. Acta, 5 (1967) 984.
3 T. Kiba and I. Kishi, Bull. Chem. Soc. Jpn., 30 (1957) 44.
4 S. Nagashima, M. Yoshida and T. Ozawa, Bull. Chem. Soc. Jpn., 45 (1972) 3446.
5 I. St. Lorant, Z. Physiol. Chem., 185 (1929) 245.
6 C. M. Johnson and H. Nishita, Anal. Chem., 24 (1952) 736.
7 C. L. Luke, Anal. Chem., 21 (1949) 1369.
8 G. Tölg, Z. Anal. Chem., 194 (1963) 20.
9 R. Millet, Chim. Anal., 45 (1963) 174.
10 L. Gustafson, Talanta, 4 (1960) 236.
11 J. B. Davis and F. Lindstrom, Anal. Chem., 44 (1972) 524.
12 J. Keay, P. H. Menagé and G. A. Dean, Analyst, 97 (1972) 897.
13 I. R. Freney, Soil Science, 86 (1958) 241.
14 W. Lädrach and J. D. van der Laarse, Anal. Chim. Acta, in press.

Analytica Chimica Acta, 92 (1977) 277—283

A NEW pH ELECTRODE FOR GAS-SENSING PROBES

MARCO MASCINI* and CARLO CREMISINI

Istituto di Chimica Analitica, Università di Roma, 00185 Roma (Italy)

(Received 15th February 1977)

SUMMARY

A pH-dependent electrode obtained by thermomoulding a mixture of powdered antimony and a thermoplastic polymer is shown to be highly reproducible and reliable. The electrodes are useful in gas-sensing probes for NH_3, CO_2 and SO_2. Calibration curves, selectivity and response times are evaluated.

Gas-sensing membrane probes have recently enjoyed much attention and their practical applications in chemical analysis have increased greatly [1, 2, 3]. Their high selectivity makes these electrodes very attractive for determinations of some inorganic species, and when the electrodes are coupled with enzymes, some organic species can also be determined [4].

The most popular gas-sensing probes are based on the use of a glass electrode with a flat surface and a reference electrode, both of which are separated from the sample solution by a plastic membrane. The electrodes are immersed in an electrolyte solution, the composition of which depends on the gas to be measured. The gas from the sample diffuses through the plastic membrane, varying the pH of the electrolyte solution and causing a variation in the potential of the glass electrode. Most gas-sensing probes depend on the dimensions and characteristics of the glass electrode. Such dimensions are generally standard and large (6—10 mm diameter), so that the fabrication of microelectrodes is not practicable.

This paper reports the use in a gas-sensing probe of a new pH-dependent electrode obtained by thermomoulding a mixture of antimony metal powder and a thermoplastic polymer powder. The electrodes prepared in this way are highly reproducible, for the moulding procedure ensures reliability. They provide excellent stability of the potential values, and high mechanical strength; the dimensions are easily controlled and can be varied from 1 mm to 10 mm, which is suitable for the development of micro or mini gas-sensing probes for new applications. The resistance of the electrodes is very low compared to that of the glass electrode, because of the metal content. The new electrodes have advantages over simple antimony electrodes with respect to reproducibility and to the passivity phenomena which occur after prolonged use with the classical antimony billet electrode.

The new pH-dependent electrodes have been tested in sensors for NH_3, CO_2 and SO_2.

EXPERIMENTAL

Preparation of antimony powder electrode

Antimony powder (analytical grade; Carlo Erba) was thoroughly mixed with a thermoplastic polymer and the mixture was moulded to obtain a compact pellet. This was heat-moulded in a suitable plastic tube of the same polymer composition. Polyethylene was mainly used because of its thermoplastic properties (Montedison Italy); its low softening point allows moulding at temperatures below 120°C and pressures around 100 kg cm^{-2}.

The pellets usually contained 10—20% (by weight) of polyethylene; pellets containing 30% polyethylene had high resistances and so were unsuitable. The weight ratio of polyethylene to antimony mainly used was 10:90, which allows a compact pellet of low electrical resistance to be prepared. The powders were mixed thoroughly in a mortar and set in a suitable stainless steel mould with polished rams. The thickness of the pellets was about 3—5 mm The diameter of the pellets was variable depending on the mould dimensions. Pellets with diameters of 1—8 mm were found to give identical results.

The pellet was placed in a polyethylene tube and heat-welded in a suitable mould. The electrode shown in Fig. 1 (A) was obtained. The Ag/AgCl wire was the reference electrode and the stainless steel cylinder provided the electrical contact. The dimensions shown in Fig. 1 were those used through this work but are obviously not critical. Figure 1 (B) shows how the probe was arranged conventionally as in most commercial gas-sensing probes.

Reagents and Standards

All chemicals used were of analytical-reagent grade. Ammonia standards were prepared from ammonium chloride, sulphur dioxide standards from potassium metabisulphite, and carbon dioxide standards from potassium hydrocarbonate. The solutions added to samples in a 1:10 volume ratio for pH adjustment were 1 M sodium hydroxide solution for ammonia and 1 M sulphuric acid for sulphur dioxide and carbon dioxide.

The gas-permeable membrane of the gas-sensing probes was Teflon FHLP (Millipore; pore size, 0.5 μm).

RESULTS AND DISCUSSION

Evaluation of the antimony powder electrode

Figure 2 shows the calibration curve obtained for the antimony powder electrode with a saturated calomel reference electrode and standard buffer solutions (0.05 M potassium hydrogenphthalate, 0.025 M sodium monohydrogenphosphate and 0.025 M potassium dihydrogenphosphate, 0.1 M borax, and calcium hydroxide solution saturated at 25°C) [5]. Solutions checked with

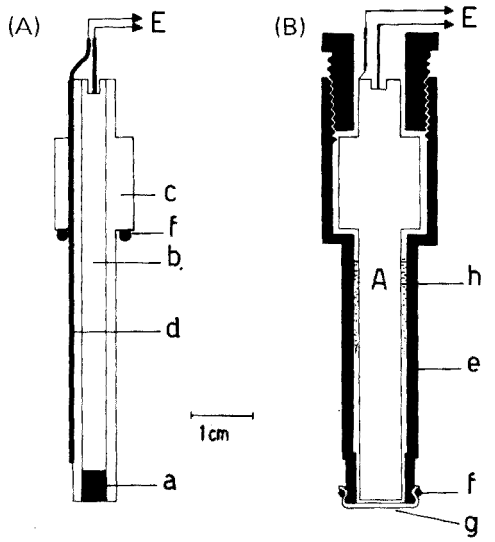

Fig. 1. (A) Construction of pH-sensing electrode. (a) Antimony–polyethylene pellet. (b) Stainless steel or brass for contact. (c) Polyethylene tube. (d) Silver–silver chloride reference electrode. (f) Rubber O-ring. (E) Contacts to potentiometer, (B) Assembly of the gas sensing probe. (e) PVC external tube. (f) Rubber O-ring. (g) Teflon membrane. (h) Internal solution. (A) The entire body described in Fig. 1A.

a conventional glass electrode were also used; the chemical systems were hydrochloric acid, acetate buffer, ammonia buffer and sodium hydroxide. Attempts to use buffers containing compounds such as citric and tartaric acids were unsuccessful because of their well-known complexing effect on antimony ions. Deviations up to 1 pH unit toward alkaline values were observed.

The maximum difference obtained in such calibration curves with a dozen different antimony powder electrodes was about 2 mV, which proves the high reproducibility of the pH-responsive probe and the reliability of the calibration curves. The same curve was found useful after 6 months of operation. Antimony billet electrodes became passive and needed polishing for restoration after about a month. Cleaning treatments were not found necessary during such a period with the antimony powder electrodes. No simple immediate explanation of the difference in behaviour between the antimony billet and powder electrodes is apparent.

The calibration curves show that the antimony powder electrode is suitable in the pH range 2—11. The slope is constant at 55 mV/pH at room temperature. Table 1 reports the millivolt values obtained for solutions of different pH with five antimony powder electrodes of different sizes and ages. The reproducibility of these values is very satisfactory.

TABLE 1

Reproducibility of different antimony electrodes made at different times and of different sizes (Solutions 1—4 were: (1) 0.01 M HCl; (2) 0.05 M potassium hydrogenphthalate; (3) 0.025 M phosphate buffer; (4) 0.01 M borax. The electrodes were: A, B, C, 4-mm diam., five and two months old and just prepared, respectively; D, E, 8-mm diam., five and two months old, respectively.)

Electrode	Potential (mV vs. SCE)			
	1	2	3	4
A	−130	−228	−382	−509
B	−127	−224	−379	−506
C	−126	−224	−377	−505
D	−126	−223	−380	−508
E	−128	−225	−381	−509

Calibration of the gas-sensing probes

The pH range 2—11 permits the antimony powder electrodes to be used as pH sensors in gas-sensing probes. The only disadvantage of the antimony electrode compared to the glass electrode, i.e. its sensitivity to strong oxidants and hydroxyl-containing compounds in solution, is eliminated when the electrodes are used as pH sensors in the gas-sensing probes. The advantages are

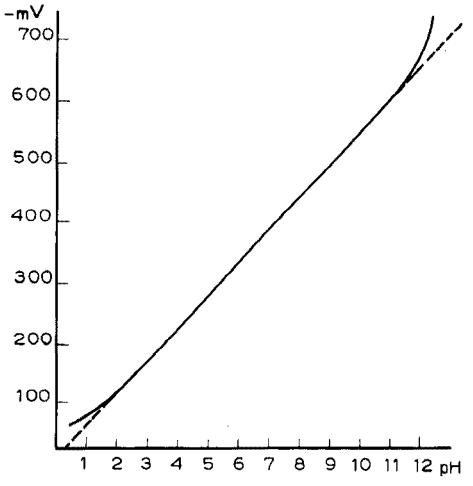

Fig. 2. Calibration curve of antimony powder electrode. The solutions were the standard buffers and solutions of HCl, NaOH, acetate, phosphate and ammonia buffers.

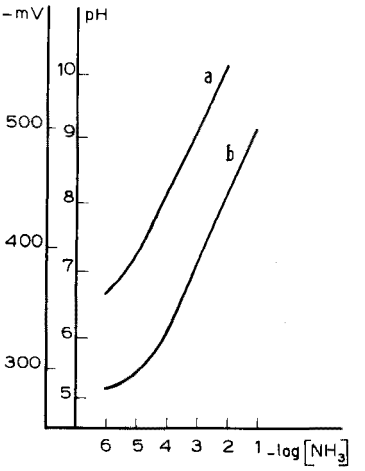

Fig. 3. Calibration curves for the NH_3-sensing probe. Internal solutions (a) 10^{-3} M NH_4Cl; (b) 10^{-1} M NH_4Cl.

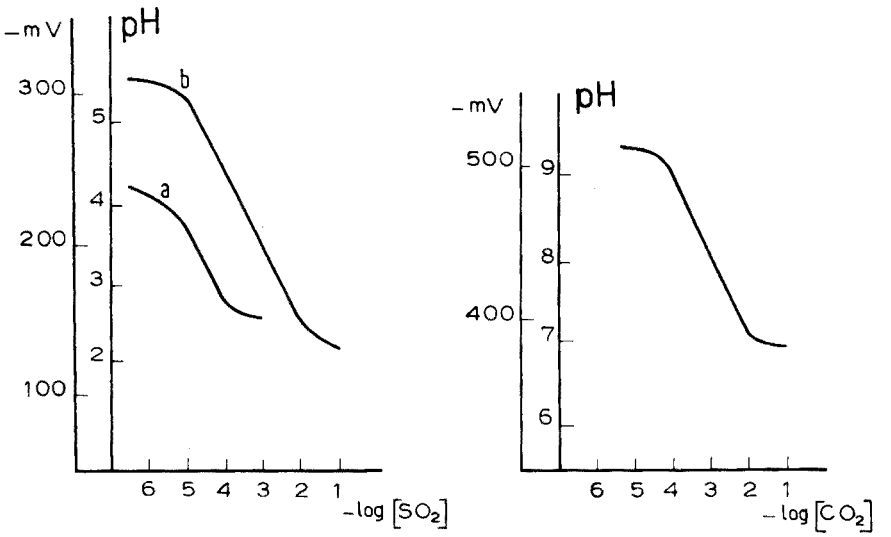

Fig. 4. Calibration curves for the SO_2-sensing probe. Internal solutions: (a) 10^{-3} M $Na_2S_2O_5$; (b) 10^{-1} M $Na_2S_2O_5$.

Fig. 5. Calibration curve for the CO_2-sensing probe. The internal solution was 10^{-1} M $NaHCO_3$.

many. The perfect geometrical shape of the sensor allows a well defined contact with the layer of electrolyte in the internal solution; a perfectly flat surface in a glass electrode is difficult to obtain practically because of the soldering joint, so that the contact between the flat surface and the electrolytic layer is generally ill defined. The superior mechanical strength of the antimony powder electrode is obvious. The low electrical resistance obviates the electronic noise of glass electrodes, which often poses difficult problems despite shielded cables and high-impedance amplifiers.

Figures 3—5 show the experimental responses of the NH_3, SO_2 and CO_2 probes, respectively. The internal solutions were ammonium chloride, potassium metabisulphite and sodium hydrogen carbonate, respectively, for the NH_3, SO_2 and CO_2 probes. The responses were obtained with internal electrolyte concentrations of 10^{-1} and 10^{-3} M, and were reproducible to ± 2 mV. The responses are reported in mV, and these potentials were converted to the pH values shown, by means of the calibration graph in Fig. 2. The agreement with commercial glass sensing probes is fairly good. The response of the CO_2 probe is reported only for an internal electrolyte concentration of 10^{-1} M; with a 10^{-3} M internal electrolyte the measuring range is so limited that the probe is analytically useless.

The response speeds for the ammonia and sulphur dioxide sensors are reported in Fig. 6. As has been carefully described [1, 2] the speed of response depends on several parameters, two of the most important being the geometry of the film of internal electrolyte, and the response time of

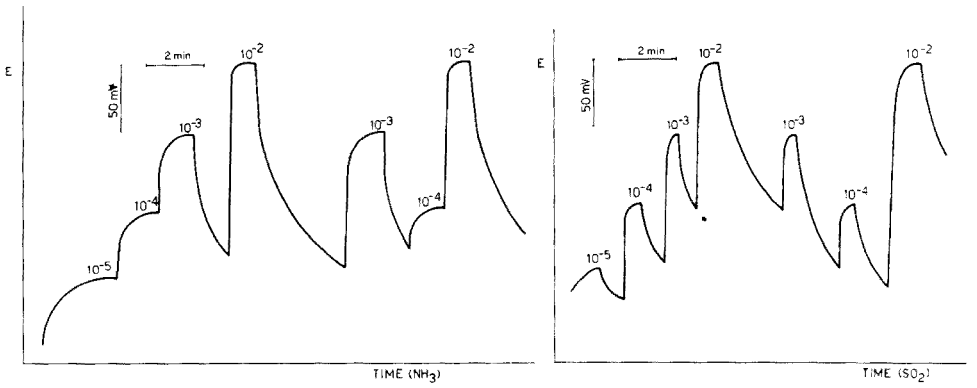

Fig. 6. Response times for increasing and decreasing concentrations. (a) NH_3 (b) SO_2.

the electrode. Obviously, the shape of the pH electrode must determine the response speed of the probe through the geometry of the contact. The speed of the response to both increasing and decreasing concentrations can be appreciated from Fig. 6. Actually, these speeds are similar to those reported with glass electrodes, but the problems associated with electrode shape have not been considered in such studies. In our experience with glass electrode probes, the response speed is not a simple reproducible characteristic of the gas sensor, but can vary considerably, depending on the method of assembly. This does not happen with the proposed sensors.

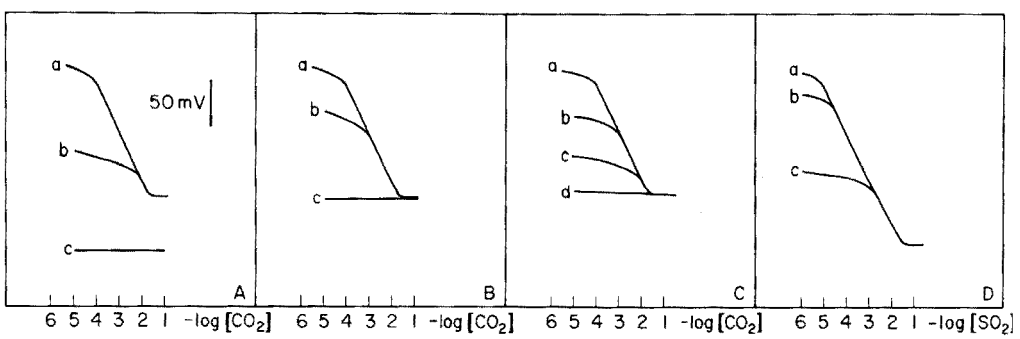

Fig. 7. Selectivity of the gas sensors. (A) SO_2 interference on CO_2 sensors with samples at pH 1: (a) without interference; (b) with 10^{-4} M H_2SO_3: (c) with 10^{-3} M H_2SO_3. (B) SO_2 interference on CO_2 sensor with samples at pH 4: (a—c) as in part A. (C) HF interference on CO_2 sensor with samples at pH 3; (a) without interference; (b) with 10^{-4} M HF; (c) with 10^{-3} M HF; (d) with 10^{-2} M HF. (D) Interference effects on SO_2 sensor with samples at pH 3: (a) without interference; (b) with 10^{-1} M HCO_3^-; (c) with 10^{-1} M HF.

Selectivity

Any gas-sensing membrane probe suffers direct interference from dissolved gaseous species that can produce pH variations in the thin layer of electrolyte in contact with the pH electrode. As a general rule, a volatile strong acid will interfere with a sensor for a weak acid, and analogously for bases. Accordingly, sulfur dioxide, hydrogen fluoride and acetic acid interfere with carbon dioxide probes. This interference can be calculated from the pK values of the acids and bases [6]; some experimental curves are shown in Fig. 7.

Conclusion

Replacement of the glass electrode in gas sensors by the proposed pH-sensitive antimony powder electrode is obviously useful. The advantages are more practical than theoretical, and may be appreciated most by those with experience of conventional gas-sensing probes. Probably the most interesting facet of the new system is the possibility of making microelectrode probes; work in this direction is in progress.

REFERENCES

1 J. W. Ross, J. H. Riseman and J. A. Krueger, Pure Appl. Chem., 35 (1973) 473.
2 P. L. Bailey and M. Riley, Analyst, 100 (1975) 145.
3 J. Růžička and E. H. Hansen, Anal. Chim. Acta, 69 (1974) 129.
4 L. D. Bowers and P. W. Cair, Anal. Chem., 48 (1976) 544A.
5 R. G. Bates, Concepts and Determination of pH, Treatise on Analytical Chemistry Vol. I, Part I, I. M. Kolthoff and P. J. Elving (Eds.), Interscience, New York, 1959, p. 374
6 M. Mascini and C. Cremisini, to be published.

Analytica Chimica Acta, 92 (1977) 285—291

TITRIMETRIC APPLICATIONS OF MULTIPARAMETRIC CURVE-FITTING

Part VI. Determination of Strong Acids in the Presence of Weak Acids by Potentiometric Titration

DALE MURTLOW[§] and LOUIS MEITES*

Department of Chemistry, Clarkson College of Technology, Potsdam, New York 13676 (U.S.A.)

(Received 2nd March 1977)

SUMMARY

By non-linear regression onto appropriate titration-curve equations it is possible to determine hydrochloric acid in very dilute solutions containing substantially larger concentrations of acetic acid by potentiometric titration with a strong base. The results are much superior to those obtained by techniques that involve end-point location, and the use of non-linear regression further makes it possible to detect and determine very small concentrations of basic impurities.

The determination of a strong acid in the presence of a larger concentration of a weak acid is a difficult problem in potentiometric titrimetry, and one to which several different kinds of approaches have been suggested [1—6]. Earlier papers in this series showed that the use of non-linear regression makes it possible to locate the equivalence point of a potentiometric acid—base titration even if the titration curve has no point of maximum slope [7] or if the reagent has not been previously standardized [8]. Briggs and Stuehr [9] independently employed non-linear regression analysis to detect traces of strong acid in solutions of nicotinamide adenine dinucleotide; the standard error in such a procedure was discussed by Meites et al. [10]. The evaluation of these results was complicated by the fact that the strong acid was an unexpected impurity in the materials used by Briggs and Stuehr [9], so that there was no independent or reliable information about its concentrations in the solutions analyzed.

This paper describes the results of an investigation of the utility of non-linear regression analysis in determinations, by potentiometric titration with

---

[§]This paper is based on a report submitted by Dale Murtlow to the Faculty of Clarkson College of Technology in partial fulfilment of the requirements for the degree of M.S. in Chemistry, December, 1976.

standard base, of hydrochloric acid in the presence of acetic acid under such conditions that there is no useful point of maximum slope near the hydrochloric acid equivalence point.

EXPERIMENTAL

Stock solutions of sodium hydroxide and of hydrochloric and acetic acids were prepared by mixing the reagent-grade materials with boiled distilled water and with enough potassium chloride (J.T. Baker Chemical Co., Analyzed Reagent, Lot 409484) to yield a 3.00 M solution. More dilute solutions were prepared by volumetric dilution of the stock solutions with a 3.00 M solution of potassium chloride prepared in the same way. All solutions were stored in such a way as to guard them against contamination by carbon dioxide. Calibrated glassware was used throughout.

Titrations were performed under nitrogen by the procedure described by Barry and Meites [7]. In this work, however, a water-jacketed 300-cm^3 glass vessel was used to facilitate maintenance of the temperature of a titration mixture at 25.0°C throughout each titration. Measurements of pH were made with a Sargent-Welch Model NX pH meter (reading to 0.01 pH unit) equipped with Corning glass and calomel electrodes. The meter was standardized against a solution of potassium hydrogentartrate saturated at 25°C and 0.01 M borax [11]; the standardization was checked against three other solutions having defined pH-values on the NBS scale. Measurements having the desired precision and accuracy could not be made with electrodes that had been allowed to stand at room temperature, because unconscionably long times were required for these to reach equilibrium with solutions at 25°C; consequently, the electrodes (and all the solutions) were continuously kept at 25.0°C. The thermal hysteresis of calomel electrodes is well known, and Mattock [12] long ago recommended storing glass electrodes at the temperature at which they are to be used.

Approximately 35—40 points were secured in each titration. In titrations of mixtures these were spaced in a way that emphasized the portion of the titration during which hydrochloric acid was being neutralized. For example, when 100 cm^3 of a mixture containing $5 \cdot 10^{-4}$ M hydrochloric acid and $3 \cdot 10^{-3}$ M acetic acid was titrated with 0.04 M sodium hydroxide, the titrant was added in increments of 0.06 cm^3 until a total of 1.6 cm^3 had been added, then in increments of 0.4 cm^3 until the acetic acid equivalence point had been passed. The resulting data were fitted to appropriate equations by means of a general computer program for effecting least-squares fits [13]. Most of the fits were made on either an IBM 360/44 or an IBM 360/65 computer operated in FORTRAN IV.

RESULTS AND DISCUSSION

Data were obtained for four different sets of titrations. In the first, weighed portions of potassium hydrogenphthalate were titrated with the stock solution of sodium hydroxide, which was approximately 0.25 M. In the second and third, the solution of sodium hydroxide thus standardized was used to titrate aliquots of the stock solutions of hydrochloric and acetic acids, which were approximately 0.05 and 0.1 M, respectively. In the fourth, mixtures of the two acids, prepared by diluting their stock solutions, were titrated with dilute sodium hydroxide. By comparing the results secured from these four sets of titrations, it was possible to form accurate estimates of the reliabilities of the values obtained.

It was first assumed, as was done by Barry and Meites [7], that the solutions were free from acidic or basic impurities. Regression onto standard titration-curve equations yielded the values listed in the first column of Table 1. Barry and Meites [7] had obtained $K_a = 1.313 \cdot 10^{-5}$ M and $y_{H^+} = 1.746$ at 23.5°C; the values given here for 25.0°C are in reasonable agreement with these. However, these results were deemed to be unacceptable because the calculated concentrations of the acids in mixtures are systematically low, and the errors become worse as the concentrations become smaller. In solutions containing about $1.5 \cdot 10^{-3}$ M hydrochloric acid and $9 \cdot 10^{-3}$ M acetic acid, the calculated concentration of hydrochloric acid is about 3% too low while that of acetic acid is about 0.4% too low. In solutions containing $4 \cdot 10^{-4}$ M hydrochloric acid and $3 \cdot 10^{-3}$ M acetic acid, each error is about three times as large. A similar increase of the relative error with decreasing concentration was observed by Barry and Meites, but in their titrations of acetate ion with hydrochloric acid the relative errors were positive with dilute solutions.

These facts showed clearly that the potassium chloride contained a basic impurity, and an investigation of the nature and concentration of this impurity was consequently undertaken. Assuming it to be a strong base also yielded unacceptable results, but assuming it to be weak and monofunctional within the range of pH values covered by these fits yielded the values shown in the last column of Table 1. The values of K_w (for the titrations that were continued beyond their equivalence points), y_{H^+}, and K_a are somewhat more closely concordant, and both the concentrations of hydrochloric acid and the sums of the concentrations of the two acids in the mixtures agree much more closely with the expected values. The weighted average concentration C_i of the basic impurity is $6.1_4 \cdot 10^{-5}$ M according to the values, given in part D of Table 1, from titrations of mixtures in which the total concentration of acid was between $3.4 \cdot 10^{-3}$ and $1.2 \cdot 10^{-3}$ M. In the titrations employed for standardization the concentration of acid was much larger: in the standardizations of hydrochloric acid, for example, the initial concentration of the acid was about 0.02 M, while in those of acetic acid and sodium hydroxide it was about 0.03 M.

TABLE 1

Calculated values of the parameters
(Each section of this table lists the parameters that were evaluated in fitting the data obtained in 5—7 replicate titrations. It gives the mean values secured for these parameters by making the different assumptions described in the text. For each mean value it also gives (in parentheses), the standard deviation of the individual values corresponding to the separate titrations.)

	Assumption	
	No impurity	Weakly basic impurity
A. Standardization of NaOH		
1 Concentration of NaOH (C_b), M	0.25742 (±0.00049)	0.25727 (±0.00055
2, 3. Concentration dissociation constants of *o*-phthalic acid:		
K_1, M	$1.249\ (\pm 0.056)\cdot 10^{-3}$	$1.300\ (\pm 0.076)\cdot 10^{-3}$
K_2, M	$1.721\ (\pm 0.012)\cdot 10^{-5}$	$1.786\ (\pm 0.044)\cdot 10^{-5}$
4. Ion-concentration product of water (K_w), M^2	$5.92\ (\pm 0.23)\cdot 10^{-15}$	$6.06\ (\pm 0.20)\cdot 10^{-15}$
5. Apparent single-ion molarity activity coefficient of hydrogen ion (y_{H^+})	1.873 (±0.008)	1.822 (±0.035)
6. Concentration of impurity (C_i), M	—	$4.3\ (\pm 1.5)\cdot 10^{-5}$
7. pK_a for conjugate acid of impurity (pK_i)	—	8.6 (±1.8)
B. Standardization of HCl		
1. Concentration of HCl (C_{HCl}), M	$5.2753\ (\pm 0.0005)\cdot 10^{-2}$	$5.281\ (\pm 0.009)\cdot 10^{-2}$
2. K_w, M^2	$6.69\ (\pm 0.21)\cdot 10^{-15}$	$6.55\ (\pm 0.20)\cdot 10^{-15}$
3. y_{H^+}	1.695 (±0.017)	1.700 (±0.016)
4. C_i, M	—	$9.1\ (\pm 1.8)\cdot 10^{-5}$
5. pK_i	—	6.99 (±0.03)
C. Standardization of HOAc		
1. Concentration of HOAc (C_{HOAc}), M	$9.983\ (\pm 0.018)\cdot 10^{-2}$	$9.962\ (\pm 0.017)\cdot 10^{-2}$
2. Concentration dissociation constant of HOAc (K_a), M	$1.361\ (\pm 0.030)\cdot 10^{-5}$	$1.307\ (\pm 0.041)\cdot 10^{-5}$
3. K_w, M^2	$6.38\ (\pm 0.14)\cdot 10^{-15}$	$6.01\ (\pm 0.12)\cdot 10^{-15}$
4. y_{H^+}	1.662 (±0.031)	1.747 (±0.062)
5. C_i, M	—	$7.1\ (\pm 2.7)\cdot 10^{-5}$
6. pK_i	—	8.1 (±1.1)
D. Titrations of mixtures		
(i) Mixture I		
1. C_{HCl}, M	$1.3422\ (\pm 0.0085)\cdot 10^{-3}$	$1.3987\ (\pm 0.0075)\cdot$
Expected C_{HCl}	$1.3988\cdot 10^{-3}$	$1.4004\cdot 10^{-3}$
Mean error, %	−4.0	−0.10
2. C_{HOAc}, M	$8.840\ (\pm 0.037)\cdot 10^{-3}$	$8.819\ (\pm 0.036)\cdot 10^{-3}$
Expected C_{HOAc}	$8.850\cdot 10^{-3}$	$8.831\cdot 10^{-3}$
Mean error, %	−0.11	−0.13
3. K_a, M	$1.342\ (\pm 0.033)\cdot 10^{-5}$	$1.338\ (\pm 0.031)\cdot 10^{-5}$
4. y_{H^+}	1.673 (±0.032)	1.677 (±0.030)
5. C_i, M	—	$5.93\ (\pm 0.29)\cdot 10^{-5}$
6. pK_i	—	7.9 (±1.2)

TABLE 1 (continued)

	Assumption	
	No impurity	Weakly basic impurity
(ii) Mixture II		
1. C_{HCl}, M	$1.558\ (\pm 0.011)\cdot 10^{-3}$	$1.615\ (\pm 0.013)\cdot 10^{-3}$
Expected C_{HCl}	$1.580\cdot 10^{-3}$	$1.582\cdot 10^{-3}$
Mean error, %	−1.4	+2.0
2. C_{HOAc}, M	$9.903\ (\pm 0.032)\cdot 10^{-3}$	$9.861\ (\pm 0.042)\cdot 10^{-3}$
Expected C_{HOAc}	$9.983\cdot 10^{-3}$	$9.963\cdot 10^{-3}$
Mean error, %	−0.81	−1.0
3. K_a, M	$1.321\ (\pm 0.006)\cdot 10^{-5}$	$1.323\ (\pm 0.017)\cdot 10^{-5}$
4. y_{H^+}	1.697 (±0.008)	1.702 (±0.025)
5. C_i, M	—	$6.22\ (\pm 0.37)\cdot 10^{-5}$
6. pK_i	—	6.40 (±0.46)
(iii) Mixture III		
1. C_{HCl}, M	$4.301\ (\pm 0.015)\cdot 10^{-4}$	$4.904\ (\pm 0.0023)\cdot 10^{-4}$
Expected C_{HCl}	$4.741\cdot 10^{-4}$	$4.746\cdot 10^{-4}$
Mean error, %	−9.3	+3.3
2. C_{HOAc}, M	$2.964\ (\pm 0.012)\cdot 10^{-3}$	$2.949\ (\pm 0.016)\cdot 10^{-3}$
Expected C_{HOAc}	$2.995\cdot 10^{-3}$	$2.989\cdot 10^{-3}$
Mean error, %	−1.0	−1.3
3. K_a, M	$1.338\ (\pm 0.020)\cdot 10^{-5}$	$1.345\ (\pm 0.019)\cdot 10^{-5}$
4. y_{H^+}	1.659 (±0.030)	1.679 (±0.034)
5. C_i, M	—	$6.6\ (\pm 0.5)\cdot 10^{-5}$
6. pK_i	—	6.70 (±0.25)

Because there was much less of the impurity in proportion to the amount of acid being titrated in these standardizations, the individual values of C_i are much less certain than those for the dilute mixtures. Nevertheless, the weighted average value of C_i from all of the standardization titrations, $6.4_0\cdot 10^{-5}$ M, does not differ significantly from the more reliable value cited above.

Definite proof of the identity of this impurity could not be obtained, although its presence and weakly basic nature were confirmed in other ways, but it is believed to have been hydrogencarbonate ion. If it was, the assumption that it was monofunctional was an oversimplification, and the value obtained for pK_i would depend on the way in which the data points were distributed. The standardization titrations were continued until pH-values near 12 had been reached, and the data obtained in these titrations included a number of points at which appreciable concentrations of carbonate ion would have been present. In these titrations the value of pK_a obtained for a presumably monofunctional impurity should therefore have been somewhere between the values of pK_1 and pK_2 for carbon dioxide, or approximately 8.3. However, the titrations of mixtures were stopped before the pH-values had increased above about 9. The resulting data included many points that were affected by the carbon dioxide—hydrogencarbonate equilibrium, but

very few that were affected by the hydrogencarbonate—carbonate equilibrium, and therefore they should have given a value of pK_a that was not far from that of pK_1. It may be seen from Table 1 that the titrations of mixtures gave values of pK_a well below those obtained from the standardization titrations, and the comparison would be even clearer if it were not partially obscured by citations of average values in Table 1. For example, the eight titrations of potassium hydrogenphthalate summarized in part A gave the following values of pK_a: 6.998, 6.999, 6.996, 6.999, 7.002, 10.65, 9.91 and 10.33. The first five of these correspond reasonably well to pK_1, as do the last three to pK_2. The difference arises from the fact that the data points were distributed differently in different titrations.

The average standard deviation from regression onto the equations that took the weakly basic impurity into account was $3.6 \cdot 10^{-3}$ pH unit in the standardizations of sodium hydroxide, $3.1 \cdot 10^{-3}$ pH unit in the standardizations of hydrochloric acid, $4.8 \cdot 10^{-3}$ pH unit in the standardizations of acetic acid, and $2.5 \cdot 10^{-3}$ pH unit in the titrations of mixtures. These figures were surprising because the pH meter could be read to 0.005 unit only with some difficulty.

CONCLUSIONS

Figure 1 is a plot of the data obtained in one of the titrations of Mixture III. Only the region around the hydrochloric acid equivalence point is shown here. In this very dilute solution, and in the presence of a substantial excess of acetic acid, some suggestion of an inflection point can be detected on very close inspection, but no technique of end-point location (including a Gran plot) yields a result within even 10% of the truth. Non-linear regression gives the concentration of hydrochloric acid with a mean error of only 3% and a standard deviation of only 0.5%. This is further evidence that this technique is superior to any other for the analysis of titration curves.

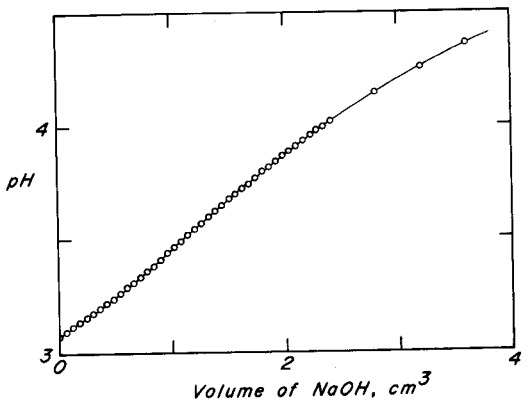

Fig. 1. The first portion of the titration curve obtained during the titration, with 0.0386 M sodium hydroxide, of 100.005 cm^3 of a solution containing $4.75 \cdot 10^{-4}$ M hydrochloric acid and $2.99 \cdot 10^{-3}$ M acetic acid.

On the basis of the errors they incurred in similar analyses of data obtained in titrating extremely dilute solutions of acetate with hydrochloric acid, Barry and Meites [7] concluded that it is advantageous to decrease the number of adjustable parameters in unfavorable cases by fixing the values of those, such as K_a and y_{H^+}, that can be evaluated in separate titrations. In titrations of $1.6 \cdot 10^{-4}$ M acetate ion with $1.7 \cdot 10^{-3}$ M hydrochloric acid, for example, they obtained an average relative error of +11% when the concentration of acetate, K_a (the concentration dissociation constant of acetic acid), and y_{H^+} were all taken as adjustable parameters. Using values of K_a and y_{H^+} obtained from other titrations decreased the relative error to only −1.4%.

For the present titrations we were unable to obtain substantial confirmation of this conclusion. The values given in the last column of Table 1 for Mixture II were obtained from fits involving six adjustable parameters. Decreasing this number to four by taking $K_a = 1.313 \cdot 10^{-5}$ and $y_{H^+} = 1.746$, which are the values obtained by Barry and Meites, led to the average values $C_{HCl} = 1.662\ (\pm 0.078) \cdot 10^{-3}$ M and $C_{HOAc} = 9.808\ (\pm 0.071) \cdot 10^{-3}$ M. Both are less precise and less accurate than the results of the six-parameter fits. The errors observed by Barry and Meites at the lowest concentrations of acetate were therefore due to the presence of a trace of weakly basic impurity.

Perhaps the most unexpected result of this work is the consistency of the values of C_i. It is not surprising that something like $6 \cdot 10^{-5}$ M basic impurity can be detected, and determined with reasonable precision, by titrating a solution containing a total of only $3.5 \cdot 10^{-3}$ M acid, for at this ratio the impurity consumes an appreciable fraction of the amount of acid that is present. It is much more surprising that this is possible even if the total concentration of acid is 0.1 M, as it was in the standardizations of acetic acid.

This work was supported by the National Science Foundation under grants CHE76-17247 and MPS74-17519.

REFERENCES

1 H. T. S. Britton and A. E. Young, J. Chem. Soc., (1932) 2467.
2 K. J. Jensen and R. J. Mundy, in C. J. Rodden et al. (Eds.), Analytical Chemistry of the Manhattan Project, McGraw-Hill, New York, 1950, p. 214.
3 N. H. Furman and J. I. Watters, in C. J. Rodden et al. (Eds.), Analytical Chemistry of the Manhattan Project, McGraw-Hill, New York, 1950, p. 584.
4 H. A. Pagel and F. W. McLafferty, Anal. Chem., 20 (1948) 272.
5 H. A. Pagel, P. E. Toren, and F. W. McLafferty, Anal. Chem., 21 (1949) 1150.
6 D. B. Bruss and G. E. A. Wyld, Anal. Chem., 29 (1957) 232.
7 D. M. Barry and L. Meites, Anal. Chim. Acta, 68 (1974) 435.
8 D. M. Barry, L. Meites, and B. H. Campbell, Anal. Chim. Acta, 69 (1974) 143.
9 T. N. Briggs and J. E. Stuehr, Anal. Chem., 46 (1974) 1517.
10 L. Meites, J. E. Stuehr, and T. N. Briggs, Anal. Chem., 47 (1975) 1485.
11 V. E. Bower and R. G. Bates, J. Res. Nat. Bur. Stand., 59 (1957) 261.
12 G. Mattock, pH Measurement and Titration, Heywood, London, 1961, p. 102.
13 L. Meites, The General Multiparametric Curve-Fitting Program CFT4, Computing Laboratory of the Department of Chemistry, Clarkson College of Technology, Potsdam, N. Y., 1976.

Analytica Chimica Acta, 92 (1977) 293—300

MOLECULAR EMISSION CAVITY ANALYSIS
Part XI. The Determination of Carbonyl Compounds

MOUAYED Q. AL-ABACHI, R. BELCHER, S. L. BOGDANSKI and ALAN TOWNSHEND*

Chemistry Department, Birmingham University, P.O. Box 363, Birmingham B15 2TT, (England)

(Received 14th March 1977)

SUMMARY

Formaldehyde (2—750 μg), acetaldehyde (0.05—1.0 mg) and acetone (0.4—3.5 mg) can be determined in aqueous solution (≤ 17.5 ml) by MECA. Sodium sulphite solution (5 ml, 500 p.p.m. S) and 1.5 ml of 1 M phosphoric acid are added and the delayed S_2 emission from the sulphite addition compound in 5 μl of the solution is measured in a MECA cavity; a hydrogen—nitrogen flame is used. Mixtures of formaldehyde and acetone can be determined simultaneously on the basis of the resolved MECA peaks of their sulphite addition compounds, after evaporation of the excess of sulphite from the cavity.

It is well documented that many aldehydes and ketones form hydrogen-sulphite addition compounds in the presence of excess sodium sulphite [1].

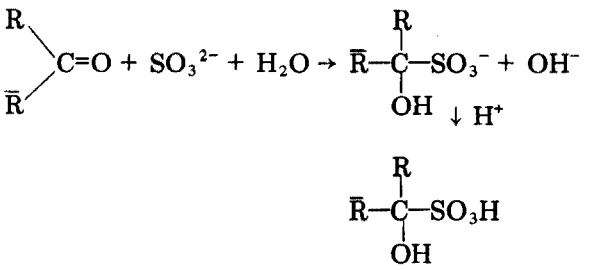

Schwartz and Weihrauch [2], for example, used the reaction for the isolation and characterization of constituents of natural products by passing micro-molar amounts of carbonyl compounds in hexane or carbon tetrachloride through a column packed with celite impregnated with sodium hydrogen-sulphite. Aliphatic and aromatic aldehydes were rapidly and quantitatively extracted.

Recently, it has been shown that trace amounts of inorganic and organic sulphur compounds can be determined via their S_2 emission at 384 nm by molecular emission cavity analysis (MECA) [3, 4]. Formaldehyde, acetaldehyde and acetone have been found to delay the S_2 emission from hydrogen-sulphite in the presence of phosphoric acid. When excess of sodium sulphite

is present, the peak from the unreacted sulphite appears first, followed by that of the bound hydrogensulphite. By measuring the peak height of the S_2 emission from the latter, it should be possible to determine nanogram amounts of these carbonyl compounds. This paper describes an investigation of this possibility and the development of MECA methods for the determination of individual carbonyl compounds and for the simultaneous determination of formaldehyde and acetone.

EXPERIMENTAL

Apparatus

A modified Unicam SP 900 flame emission spectrophotometer and Servoscribe 1S recorder were used, as described previously [5]. A 0.3-mm slit (spectral bandpass = 8 nm at 384 nm) and a stainless steel cavity with silica liner [4] were used. The cavity was pitched at 7° below the horizontal, 9 mm into the flame, with the centre of the cavity 22 mm above the top of the burner. The cavity had a volume of 40 μl.

Reagents

Analytical reagent-grade chemicals were used. Sodium sulphite solutions (500 p.p.m. S, 250 ml) were stabilized by 2 ml of 0.1 M disodium EDTA solution. All the solutions were freshly prepared daily except for the 1 M phosphoric acid.

The sulphite and formaldehyde solutions were standardized iodimetrically [6] by addition of an excess of iodine, and back-titration with thiosulphate.

Determination of formaldehyde (2—750 μg), acetaldehyde (50—1000 μg) and acetone (0.4—3.5 mg)

For calibration purposes, add to each of a series of 25-ml volumetric flasks, 5 ml of sodium sulphite solution (500 p.p.m. S) followed by aliquots of 0.2—12.5 ml of 50-p.p.m. formaldehyde solution, 0.5—10 ml of 100-p.p.m. acetaldehyde solution or 1—17.5 ml of 200-p.p.m. acetone solution. Leave the solution for 15 min (formaldehyde and acetaldehyde) or 2 h (acetone). Add to each flask 1.5 ml of 1 M phosphoric acid and dilute to volume with distilled water. Inject 5 μl of each solution into the cavity which is fixed in position above the burner. Immediately ignite the flame (H_2, 1.70 l min^{-1}; N_2, 4.0 l min^{-1}) and measure the emission intensity at 384 nm against time until emission has ceased. Extinguish the flame and cool the cavity to room temperature with a cold air blower. Measure the height of the complexed sulphite peak. Plot a graph of the amount of carbonyl compound against peak height. For unknown samples, take $\leqslant$ 17.5 ml of aqueous sample through the above procedure.

Determination of formaldehyde and acetone in admixture

Use the procedure described above for acetone except that after injection of 5 μl of the aqueous solution inside the cavity, wait for 25 s before igniting the flame. Measure the peak height for sulphite—formaldehyde and the peak

area for sulphite—acetone. For unknown samples, the aqueous sample solution should contain $\leqslant$ 500 μg of formaldehyde and $\leqslant$ 4 mg of acetone. Obtain the respective concentrations from calibration plots obtained from measurements made on individual standards under the same conditions.

RESULTS AND DISCUSSION

Formaldehyde, acetaldehyde and acetone form sulphite addition compounds when mixed with an excess of aqueous sodium sulphite solution in the presence of 0.06 M phosphoric acid. The delayed MECA peaks are shown in Fig. 1. The S_2 emission resulting from each addition compound has a characteristic t_m value (time from igniting the flame to maximum intensity). The values for formaldehyde, acetaldehyde and acetone are 18, 18 and 8 s, respectively (Fig. 1). These compare with a t_m value for sulphite itself under the same conditions of 2 s. Therefore, resolution of the unreacted sulphite peak from that of the sulphite addition compound peak can easily be achieved under the recommended conditions.

Effect of gas flows

Variation in the flame gas flows affects emission intensity and t_m values (Table 1). An increasing nitrogen flow cools the flame, so that the emission intensity (as measured by peak height) is reduced, whereas the t_m value is increased. Increasing hydrogen flows generally decrease intensity and t_m value. The optimal conditions for achieving reasonable sensitivity and a good separation of the addition compound peak from that of the unreacted sulphite are considered to be 1.7 and 4.0 l min^{-1} for hydrogen and nitrogen, respectively. Less than 4.0 l min^{-1} of nitrogen is not recommended because the flame becomes unstable and difficult to ignite.

Effect of reaction conditions

Order of addition of reagents. Figure 2 shows that addition of phosphoric acid to the sulphite solution before addition of formaldehyde results in slow formation of the addition compound, as evidenced by the slow growth of the MECA peak, whereas the peak forms immediately and thereafter remains constant if the phosphoric acid is added last.

Reaction time. Aldehydes generally undergo nucleophilic addition with sulphite more readily than ketones. This difference in reactivity seems to be due to a combination of electronic and steric factors [7]. Results obtained by MECA show that formaldehyde and acetaldehyde react faster than acetone with hydrogensulphite (Table 2). The reaction with acetaldhyde is complete almost instantaneously, that with formaldehyde in 5 min, but acetone requires 2 h if phosphoric acid is added last. This is due to the steric hindrance of the second methyl group in acetone. The methyl group in acetaldehyde makes the carbonyl carbon more positively charged than that in formaldehyde, thus enabling acetaldehyde to react more quickly than formaldehyde.

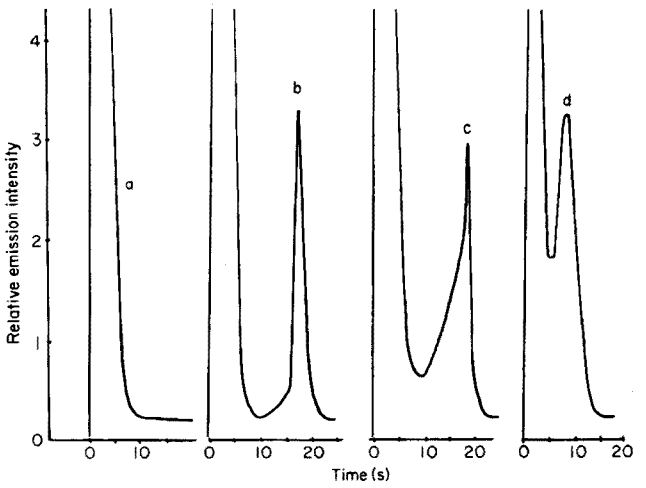

Fig. 1. MECA response from 500 ng of sulphur as Na_2SO_3 (a) alone; (b) with 25 ng of formaldehyde; (c) with 80 ng of acetaldehyde; (d) with 400 ng of acetone.

Phosphoric acid concentration. The effect of phosphoric acid concentration (added after 15 min) on the height of the sulphite addition compound peak measured after 15 min of mixing aldehyde and sulphite is shown in Fig. 3. Addition of a moderate amount of phosphoric acid enhances S_2 emission from the addition compound but the emission is depressed by a large amount of acid. This enhancing effect can be explained by the elimination of cationic depression from sodium ions. Addition of phosphoric acid converts the addition compound to its acid form. Similar effects have been observed on addition of phosphoric acid or phosphate buffer to inorganic sulphur anions [4, 5]. Depressive effects by larger amounts of phosphoric acid have also been observed for inorganic sulphur ions.

TABLE 1

Effect of gas flow rates on the formaldehyde—sulphite S_2 emission peak[a]

H_2 flow rate (l min^{-1})[b]	1.15	1.70	2.30	2.90	3.40
Emission intensity (mV)	8.4	8.5	7.2	7.2	6.8
t_m (s)	19.0	18.5	14.0	13.5	13.5
N_2 flow rate (l min^{-1})[c]	1.50	3.0	4.0	5.5	7.0
Emission intensity (mV)	9.2	9.8	8.5	5.8	2.2
t_m (s)	14	16.5	18.5	20	18

[a] From a solution containing Na_2SO_3 (5 ml of 100 p.p.m. S), 5 ml of 0.002 M formaldehyde and 2.5 ml of 1 M H_3PO_4, diluted to 25 ml.
[b] With a N_2 flow rate of 4.0 l min^{-1}.
[c] With a H_2 flow rate of 1.70 l min^{-1}.

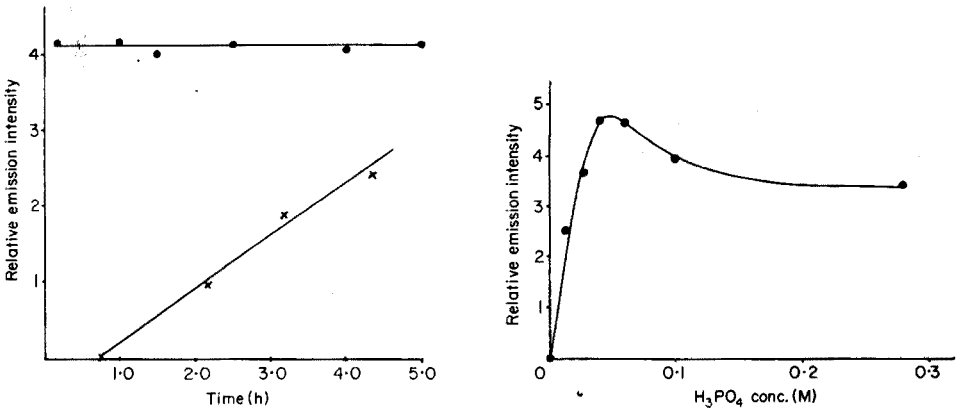

Fig. 2. Effect of order of reagent addition (final solution $6.3 \cdot 10^{-4}$ M Na_2SO_3 and 0.1 M H_3PO_4); phosphoric acid added to sulphite solution (×) before and (•) after adding formaldehyde ($4 \cdot 10^{-4}$ and $2.8 \cdot 10^{-4}$ M, respectively).

Fig. 3. Effect of phosphoric acid concentration on emission (peak height) from the sulphite—formaldehyde compound ($6.3 \cdot 10^{-4}$ M Na_2SO_3, $2.8 \cdot 10^{-4}$ M formaldehyde).

TABLE 2

Effect of time on the emission intensity from various addition compounds

Time (min)	Relative emission intensity (peak height, mV)		
	Formaldehyde[a]	Acetaldehyde[b]	Acetone[c]
0	4.6	16.0	0.9
5	15.7	16.0	
10	15.7	15.8	2.7
30	16.1	15.0	3.3
60	15.9	16.0	4.3
90			5.0
105			6.0
120	15.5	15.8	6.6
240			6.6

[a] = Na_2SO_3 (5 ml of 500 p.p.m. S), 1.5 ml of 125 p.p.m. formaldehyde and 1.5 ml of 1 M H_3PO_4 in 25 ml.
[b] = Na_2SO_3 (5 ml of 500 p.p.m. S), 5 ml of 100 p.p.m. acetaldehyde and 1.5 ml of 1 M H_3PO_4 in 25 ml.
[c] = Na_2SO_3 (5 ml of 500 p.p.m. S), 7.5 ml of 200 p.p.m. acetone and 1.5 ml of 1 M H_3PO_4 in 25 ml.

Analytical applications

By measuring the peak height of the sulphite addition compound, 0.4—150 ng of formaldehyde, 10—200 ng of acetaldehyde or 80—700 ng of acetone can be determined in a 5-μl aliquot. The calibration graphs are shown in Fig. 4. Sensitivity, precision and detection limits are given in Table 3.

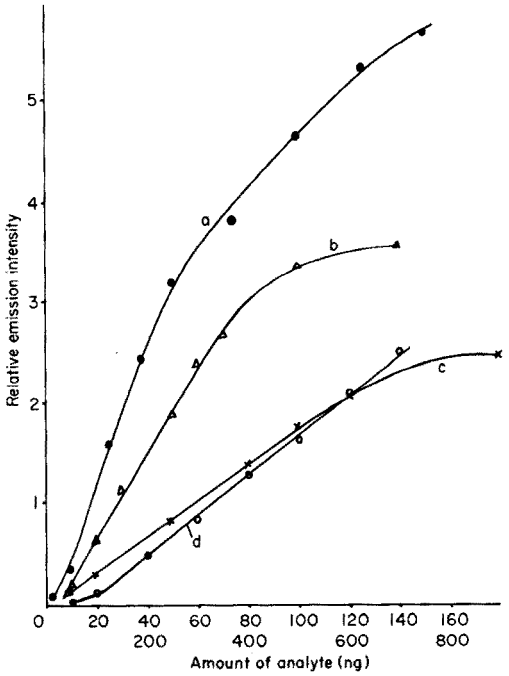

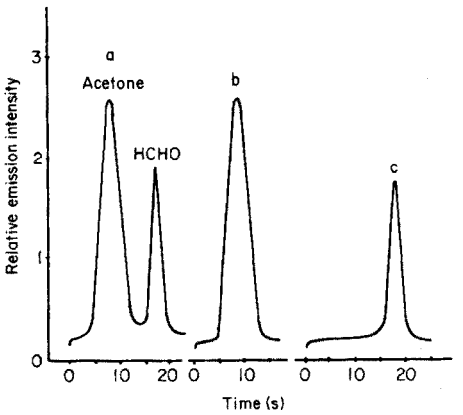

Fig. 4. Calibration graphs for (a) formaldehyde; (b) sulphite (as ng of sulphur); (c) acetaldehyde; (d) acetone (50—700 ng). The upper scale relates to (a), (b) and (c), and the lower scale to (d).

Fig. 5. MECA response from (a) a mixture of formaldehyde (40 ng) and acetone (400 ng); (b) acetone (400 ng); (c) formaldehyde (40 ng), after evaporation of excess sulphur dioxide.

TABLE 3

Sensitivity, detection limits and precision for some carbonyl addition compounds

Compound	B.p. (°C)	t_m(s)	Detection limit (2σ) (ng/5 μl)	Sensitivity (mV ng^{-1})	Precision
Formaldehyde	−21	18	2	0.5	50 ± 2 ng[a]
Acetaldehyde	20	18	10	0.15	80 ± 2 ng[a]
Acetone	56	8	40	0.031	400 ± 5 ng[a]

[a]Standard deviation for seven measurements.

It is interesting to note that the t_m value of the addition compounds increases with increasing stability of the addition compound. Thus, mixtures of formaldehyde (10—100 ng, t_m = 18 s) and acetone (80—800 ng, t_m = 8 s) in 5-μl samples gave two completely resolved peaks in addition to the uncomplexed sulphite peak. Similar resolutions have been achieved for inorganic sulphur compounds [5], organophosphorus [8] and organotin [9] compounds. A typical response from a mixture of formaldehyde— and acetone—sulphite complexes is shown in Fig. 5. A slight overlap of the sulphite peak with the sulphite—acetone peak was eliminated by igniting the flame 25 s after injecting the solution into the cavity, thus giving time for much of the unbound sulphite to volatilize. This effect is illustrated in Fig. 6. The unreacted sulphite peak disappears after 20 s. The height or area of each peak was independent of the concentration of the other component of the mixture in all instances. The relative standard deviation for determining formaldehyde in the presence of acetone and vice versa was 5% (seven measurements by peak height).

Mixtures of acetaldehyde and acetone gave only partly resolved peaks. This resolution might be improved by using a water-cooled cavity.

Preliminary experiments have shown that this procedure can be applied to the determination of formaldehyde produced by the Malaprade reaction of *vic*-diols. After oxidation, excess of sulphite is added; periodate and iodate oxidize some of the sulphite to sulphate, so that three MECA peaks are

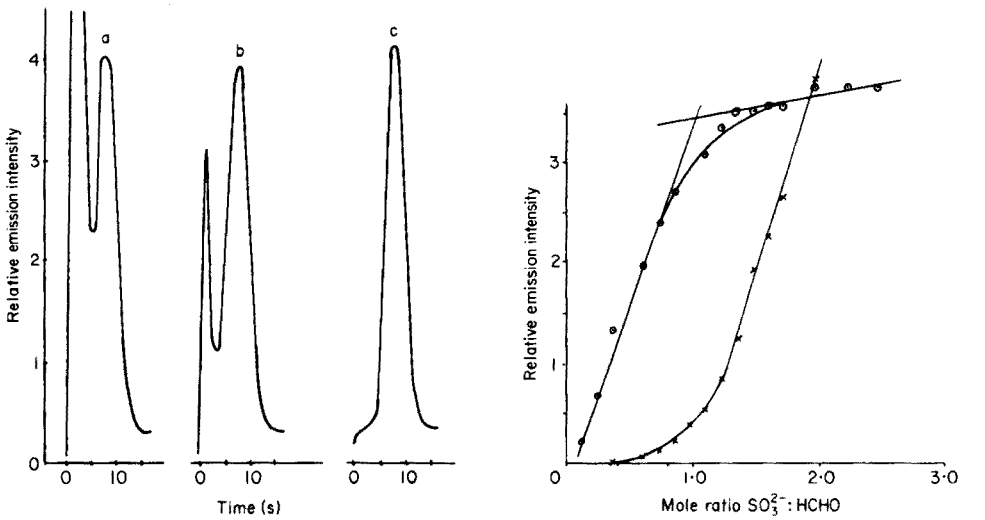

Fig. 6. Effect of time of evaporation of excess of sulphur dioxide on the acetone peak (Na_2SO_3 (500 ng of sulphur) and acetone (480 ng)). (a) 0 s; (b) 10 s; (c) 20 s.

Fig. 7. Mole ratio plot for the formaldehyde—sulphite compound (total formaldehyde concentration = $4.96 \cdot 10^{-4}$ M).

finally obtained — from free sulphite, the addition compound and sulphate. Detailed results will be published later.

The procedure can also be utilized for the determination of sulphite (10—140 ng of sulphur) by measuring the response from the sulphite—formaldehyde compound in the presence of a constant amount of formaldehyde, with a relative standard deviation of 3.6% (seven measurements by peak height). This could be useful if the sulphite peak needs to be shifted to present overlap with peaks from other sulphur anions.

Nature of the complex

The mole ratio [10] method was used to establish the composition and stability constant of the addition compound. A plot is shown in Fig. 7. It shows that the compound is a 1:1 species, in agreement with previous workers [11]. The stability constant, calculated as the mean from two such experiments, was $1 \cdot 10^4$ l mol^{-1}.

M. Q. Al-Abachi thanks the Ministry of Higher Education and Scientific Research, Republic of Iraq, for a scholarship.

REFERENCES

1 J. von Redtenbacker, Ann., 65 (1848) 37.
2 D. P. Schwartz and J. L. Weihrauch, Microchem. J., (1973) 249.
3 R. Belcher, S. L. Bogdanski and A. Townshend, Anal. Chim. Acta, 67 (1973) 1.
4 R. Belcher, S. L. Bogdanski, D. J. Knowles and A. Townshend, Anal. Chim. Acta, 77 (1975) 53.
5 M. Q. Al-Abachi, R. Belcher, S. L. Bogdanski and A. Townshend, Anal. Chim. Acta, 86 (1976) 139.
6 R. Belcher and A. J. Nutten, Quantitative Inorganic Analysis, 3rd edn., Butterworths, London, 1970.
7 R. T. Morrison and R. N. Boyd, Organic Chemistry, 2nd edn., Allyn and Bacon, Boston, 1966, p. 639.
8 R. Belcher, S. L. Bogdanski, O. Osibanjo and A. Townshend, Anal. Chim. Acta, 84 (1976) 1.
9 C. O. Akpofure, R. Belcher, S. L. Bogdanski and A. Townshend, Anal. Lett., 8 (1975) 921.
10 J. H. Yoe and A. L. Jones, Ind. Eng. Chem., Anal. Ed., 16 (1944) 11.
11 W. M. Lauer and C. M. Langkammerer, J. Am. Chem. Soc., 57 (1935) 2360.

Analytica Chimica Acta, 92 (1977) 301—305

DETERMINATION OF SMALL AMOUNTS OF TUNGSTEN BY ATOMIC ABSORPTION SPECTROMETRY AFTER EXTRACTION SEPARATION

J. MUSIL

The Metal Works, Mníšek pod Brdy (Czechoslovakia)

J. DOLEŽAL*

Department of Analytical Chemistry, Charles University, Albertov 2030, 128 40 Prague 2 (Czechoslovakia)

(Received 3rd March 1977)

SUMMARY

Small amounts of tungsten can be determined by atomic absorption spectrometry, after reduction with tin(II) and separation of the thiocyanate complex into methyl isobutyl ketone. The organic phase is aspirated into an acetylene—nitrous oxide flame. There are no interferences from 1000-fold amounts of Zr or Cr(III), 200-fold amounts of U or Ti, 100-fold V or 10-fold Mo. Interference from large amounts of iron(III) is avoided by prior reduction. The method was successfully applied to the determination of tungsten in steels and zirconium alloys.

Tungsten can readily be determined by a.a.s. with high-temperature flames, but the sensitivity of the determination is rather poor [1]. The direct determination is usually limited to concentrations above 1% [2—4]. In addition to the low sensitivity, serious interferences are encountered in analyses of many samples [3, 5]. To remove these drawbacks, tungsten has been separated by extraction with methyltricaprylammonium chloride [6], toluene-3,4-dithiol [7], α-benzoinoxime [8] and tri-n-octylamine oxide [9], when concentrations below 1% are determined. Sometimes solvents unsuitable for aspiration into flames have been used [7, 9]. The present paper deals with the extraction of the thiocyanate complexes of tungsten and the subsequent a.a.s. determination.

EXPERIMENTAL

Reagents and instrumentation

A stock solution of tungsten (1 mg ml^{-1}) was prepared by dissolving 1.261 g of pure tungsten trioxide, previously ignited at 750°C, in 25 ml of 2 M sodium hydroxide and diluting with water to 1 l. Solutions of other metals were prepared by dissolving the pure metals in hydrochloric acid. A fresh 5% $SnCl_2$ solution in 6 M HCl was prepared.

A Perkin-Elmer model 303 instrument with a C_2H_2—N_2O flame was used; the fuel and N_2O flow rates were 6.1 l min^{-1} and 11.8 l min^{-1}, respectively. A 0.48 × 50 mm slit burner was used. The height of the red zone of the flame was about 60 mm during nebulization of methyl isobutyl ketone (MIBK). The height of the beam axis above the burner orifice was 10 mm. A Perkin-Elmer tungsten hollow-cathode lamp, powered at 40 mA, was used; wavelengths of 255.1 nm (spectral slit width, 0.24 nm) and 400.9 nm (slit width, 0.68 nm) were followed. Scale expansion (3—5 ×) was used as required. Measurements at 255.1 nm were recorded with a recorder in a common circuit.

Procedure

To a solution of 0.1—1 mg W in ca. 11 M HCl, add 5 ml of 5% $SnCl_2$ solution. Adjust the volume to about 50 ml after 10 min, add 5 ml of a 20% NH_4SCN solution, and extract for 2 min with 10 ml of MIBK in a separatory funnel. Then separate the aqueous phase, wash with 10 ml of MIBK for 1 min, combine the organic phases, and dilute with MIBK to 25 ml in a volumetric flask. Leave the organic solution for 2 h (to collect the dispersed water at the bottom of the flask) and then aspirate into the flame. Adjust the zero position by using a corresponding blank solution.

RESULTS AND DISCUSSION

The effect of acid concentration

The reduction of tungsten(VI) with tin(II) chloride requires a medium at least 10 M in HCl. The dependence of the signal on the HCl concentration of the solution to be extracted was studied (Fig. 1) by measuring the combined extracts as described above, and by measuring the two extracts independently, after dilution to 25 ml. The dependence involves the effect of the HCl concentration on the percentage extraction and the possible effect of co-extracted HCl on the absorption measurement. The sum of the absorbances of the independent extracts always equalled the absorbance of the combined extracts; of course, the concentration of the co-extracted HCl in the solution aspirated was higher in the latter case. It can be concluded that the effect of co-extracted HCl on the signal is a minor factor and that the dependence found represents primarily the effect on the extraction.

Measuring conditions and sensitivity

The efficiency of atomization increases with increasing reducing properties of the flame, but an increase in the fuel flow-rate above the specified value leads to excessive deposition of carbon at the edges of the slit. The maximum of the signal dependence on the beam height is rather sharp (Fig. 2) and its position changes little on variation of the fuel-to-oxidant ratio; consequently, adjustment of the optimum flame is easy.

Under the optimum experimental conditions, a signal of $A = 0.0044$ (on

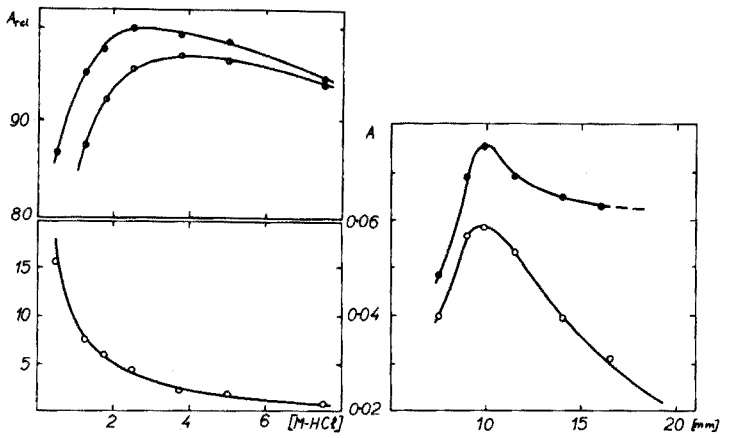

Fig. 1. The signal dependence on the HCl concentration in the aqueous phase (the relative signal value with respect to the maximum value attained in the combined extracts). ◦ 1st extract, ○ 2nd extract, • combined extracts.

Fig. 2. Flame profile. •, 6.1 l C_2H_2 min^{-1}, ○ 4.9 l C_2H_2 min^{-1}. The N_2O flow rate was always 11.8 l min^{-1}.

the basic scale) was attained for a concentration of 5.5 μg W ml^{-1} MIBK, at 400.9 nm. The sensitivity found is about four times that commonly attained in aqueous solutions. Use of the line at 255.1 nm almost doubles the sensitivity, but the signal-to-noise ratio is substantially less favourable, so that the detection limit is not sufficiently low; this line is, therefore, less suitable for the determination of low tungsten concentrations.

The calibration curve constructed for pure tungsten solutions by the recommended procedure is linear up to 1 mg W, i.e. up to a concentration of 40 p.p.m. W in the organic phase, and passes through the origin. The results can be evaluated either by using the calibration curve or by the standard addition method. Standard addition plots are parallel to the calibration plot, which verifies the absence of interferences.

Interferences

Iron(III) consumes an equivalent amount of the reductant, which may lead to a decrease in the tungsten extraction. With high iron contents, prior reduction with tin(II) chloride is essential. Other reductants (SO_2 and $NH_2OH \cdot HCl$) were also tested, but the most suitable procedure is that described below for the analysis of steel. Small amounts of iron, manifested by a reddish colour of the extract, do not interfere in the determination (Table 1).

The effect of the other elements studied is evident from Table 1. It was

TABLE 1

The effect of various elements on the signal for tungsten (0.5 mg W)

Element	Amount added (mg)	Absorption (%)	Element	Amount added (mg)	Absorption (%)
(W alone)		2.68	U	100	2.61
Mn[a]	500	2.70	Cr(III)	500	2.65
Zr	500	2.68	Ti	100	2.65
V ($VOCl_2$)	50	2.60	Mo	5	2.60
Fe	5	2.68		10	2.40
	500	1.17	Nb	50	0.63
	500[b]	2.68			

[a]Plus 500 mg Ca + 1000 mg Na.
[b]Reduced with $SnCl_2$.

found in the practical application of the method that common components of medium-alloy steels do not interfere.

Interferences may occur by two different mechanisms. Some interferents affect the reduction of tungsten by consuming the reductant (e.g. iron) or by shifting the redox potential in the solution; others form competing complexes with thiocyanate (Ti, Mo, Nb). Excessive amounts of Mo, Ti, Cu and some others also prevent rapid phase separation.

Non-selective absorption during the measurement itself is negligibly small and thus the deuterium corrector need not be used.

Practical applications

Determination of tungsten in steel. A 0.2-g steel sample is dissolved in 10 ml of warm 11 M HCl and 15 M HNO_3 is added dropwise until the residue dissolves (about 0.5 ml of HNO_3). The solution is evaporated to 2—3 ml, 15 ml of 11 M HCl is added, the solution is heated to boiling, heating is stopped, and the $SnCl_2$ solution is immediately added dropwise, until the solution turns colourless (about 10 ml), followed by 5 ml in excess. After 10 min, 5 ml of the thiocyanate solution are added and the recommended procedure in Experimental is followed.

Determination of tungsten in zirconium and its alloys (10% Cu, V, Fe, Mo). A 0.2-g sample is dissolved in 5 ml of HF (1+7) in a Teflon beaker, about 0.2 ml of HNO_3 (1 + 1) is added, and the decomposition is completed by heating. The solution is allowed to cool, and 5 ml of a 5% solution of boric acid, 15 ml of 11 M HCl and 5 ml of the $SnCl_2$ solution are added. The recommended procedure is then followed.

Typical results are given in Table 2, where the accuracy is also verified. The standard relative deviation is about 4% in the analysis of steel and about 15% in the analysis of the zirconium alloy.

TABLE 2

Typical results of the determination of tungsten

Sample	W present (%)	W found (%)
Steel standard sample ČKD 165	0.02[a]	0.034; 0.038
Steel standard sample ČKD 166	0.06[a]	0.056; 0.058
Steel standard sample ČKD 167	0.14[a]	0.13; 0.13
Zr alloy	0.002[b]	0.0018; 0.0018

[a]Certified value. [b]Photometric determination with dithiol.

REFERENCES

1 M. D. Amos and J. B. Willis, Spectrochim. Acta, 22 (1966) 1325.
2 B. F. Quin and R. R. Brooks, Anal. Chim. Acta, 65 (1973) 206.
3 A. M. Saltykova, N. K. Davidovich and S. H. G. Melamed, Zh. Anal. Khim., 27 (1973) 1216.
4 J. Husler, At. Absorpt. Newsl., 10 (1971) 60.
5 R. C. Rooney and C. G. Pratt, Analyst, 97 (1972) 400.
6 P. Dharma Rao, At. Absorpt. Newsl., 9 (1970) 131.
7 R. W. Morrow, Rep. At. Energy Comm. U.S. Y-1812 (1972).
8 J. S. Korrey and P. D. Goulden, At. Absorpt. Newsl., 14 (1975) 33.
9 I. G. Yudelevich and N. P. Shaburova, Chem. Anal., 19 (1974) 941.

Analytica Chimica Acta, 92 (1977) 307—320

AN IMPROVED GENERAL METHOD FOR THE REDUCTION OF ANALYTICAL ERRORS IN FLAME EMISSION AND ATOMIC ABSORPTION SPECTROMETRY†

R. K. HANSEN* and R. H. HALL

Owens-Illinois, Inc., P.O. Box 1035, Toledo, Ohio 43666 (U.S.A.)

(Received 4th January 1977)

SUMMARY

A general method of analysis by flame emission and atomic absorption spectrometry is described. The method, broadly applicable to a variety of samples, including glasses, minerals and metals, consists of preparing standards and samples in a common matrix of 0.4% (w/v) CsCl and 2% (v/v) HCl. Analytical errors caused by "matrix effects" are reduced, and laboratory efficiency is improved by reducing the need for special sample treatment and dilutions as well as error-compensating techniques such as standard additions or matrix-matching. The analytes studied include Li, Na, K, Ca, Mg, Sr, Ba, Al, Cr, Mn, Fe, Co, Cu and Zn. The potential interferences tested include all of the above analytes plus lead, usually at interferent-to-analyte ratios of 33:1. Modification of the basic CsCl—HCl method is necessary only for the determination of chromium. Results are given for the analysis of several NBS reference materials, including glass, steel, aluminum alloy, feldspar and limestone.

EVALUATION OF PREVIOUS ROUTINE METHODS (MATRIX INTERFERENCE STUDY)

The development of the proposed analytical method is a result of a systematic evaluation of former routine methods with regard to accuracy, precision and efficiency. The study included Li, Na, K, Ca, Mg, Sr, Ba, Al, Cr, Mn, Fe, Co, Cu and Zn.

Preparation of samples for analysis by flame techniques can vary depending on the type of sample. Major levels of silicon are usually determined by classical wet-chemical methods for high accuracy. Therefore, the general method of preparation of samples containing silicon for flame spectrometry involves acid attack by HF and $HClO_4$, i.e. volatilization of SiF_4. The excess of HF is removed by evaporating to dryness with $HClO_4$. Teflon or platinum dishes are required. Most sample residues dissolve readily in dilute HCl. Depending on the sample, an ionization suppressor or a releasing agent,

---

†Presented at the 27th Pittsburgh Conference on Analytical Chemistry and Applied Spectroscopy, March, 1976, Cleveland, Ohio, U.S.A.

e.g. La_2O_3, may be needed; and the mode of analysis, e.g. flame emission or atomic absorption, type of flame and instrumental parameters, must be chosen, together with the selection of appropriate standards. These decisions may require considerable experience on the part of the analyst. The situation can be difficult if the sample history and composition is not known; the probability of analytical errors then increases. Even if these errors are subsequently discovered, time is lost in a repeat analysis.

Because of the wide variety of samples analyzed here, several methods have been used to deal with analyses requiring different approaches after the dissolution stage (see Table 1). The alkali metals were usually determined by flame emission spectrometry (f.e.s.; Method A). Ionization suppressors were not normally used since all the common ones were frequently present as analytes in the same sample. Matrix matching was used when deemed necessary, but this required a preliminary analysis to establish the relative concentration levels of the alkali metals; moreover, if KCl was added as an ionization suppressor, then only Li and Na could be determined.

The determination of Al, Ca, Mg, Ba, and Sr was done by atomic absorption spectrometry (a.a.s.; method B). KCl was added as an ionization suppressor because the high flame temperature virtually guaranteed severe ionization effects, especially for Ba, Ca, and Sr. The La_2O_3 was added as a releasing agent for potential interferences [1—6]; its usefulness had been established prior to the widespread use of the nitrous oxide—acetylene flame and improved burner—nebulizer systems.

The analytes Mn, Fe, Ca, Cu and Zn were determined by a.a.s. (Method C). La_2O_3 was added, but KCl was omitted because ionization suppression was unnecessary, and attempts were made to keep the total solids as low as possible. Finally, chromium was determined by a.a.s. (Method D); again ionization suppression was considered unnecessary. Sulfuric acid was present because of a different sample preparation procedure. Samples containing chromium were treated with HF, H_2SO_4 and H_2SO_3 rather than with HF and $HClO_4$, to ensure formation of Cr(III) and prevent losses of Cr(VI) by volatilization as CrO_2Cl_2 [7, 8]. Samples to be analyzed for

TABLE 1

Previous routine methods

	Method A	Method B	Method C	Method D
Analyte	Li, Na, K	Ca, Mg, Ba, Sr, Al	Mn, Fe, Co, Cu, Zn	Cr
Flame	Air—C_2H_2	N_2O—C_2H_2	Air—C_2H_2	N_2O—C_2H_2
Mode	F.e.s.	A.a.s.	A.a.s.	A.a.s.
Solution type[a]	2% HCl	2% HCl, 1% KCl, 0.5% La_2O_3	2% HCl, 0.5% La_2O_3	2% HCl, 0.5% La_2(2% H_2SO_4

[a] % = v/v (liquids) or w/v (solids).

chromium were not fumed to dryness to remove excess acid as in the usual procedure when $HClO_4$ was used.

Four separate methods were therefore used to analyze samples by flame spectrometry. Standard solutions containing the required acids and buffers for Methods A—D were maintained for each individual analyte. If an unknown piece of soda-lime glass were to be analyzed for Na_2O, K_2O, CaO, MgO, Al_2O_3, and Fe_2O_3 (e.g. NBS 620), duplicate samples, dissolved by the $HF—HClO_4—HCl$ treatment, were diluted appropriately and contained 2% HCl. The K_2O could be determined readily by Method A (provided that the sodium level did not cause a significant error from ionization suppression). The Na_2O could also be determined by Method A after appropriate dilution. The CaO and MgO could be determined by Method B on a dilution from the original. Two other aliquots from each original were needed for the determination of Al_2O_3 (Method B) and Fe_2O_3 (Method C), because of the different additives required. Thus with the previous methods, four separate aliquots of each original sample solution were required to complete the analysis of even a common sample (only one aliquot is necessary with the new method). This caused considerable inefficiency in laboratory operations. Errors sometimes occurred because ionization suppressors were not used when they should have been, and trace impurities (Ca, Al, and Mg) in La_2O_3 added uncertainty to the determination of low levels of these analytes.

To simplify these analytical methods, the determination of 14 analytes was investigated to identify serious errors from matrix effects or lack of precision. The research was conducted by omitting techniques of questionable usefulness (e.g. the use of La_2O_3 as a releasing agent) and retaining others thought to be necessary (e.g. the use of KCl as an ionization suppressor for Al, Ca, Mg, Ba, Sr). Thus, if matrix errors affected the determination of a particular element under these test conditions, the reason for the error or its elimination could be investigated more fully.

Procedure for observing matrix interference effects

The analytical signal from a solution containing the analyte alone was compared with that from a solution containing the analyte plus a matrix element. In each case a blank solution containing only the matrix was prepared to check for background or trace analyte impurity. The data were taken in the order: deionized water, matrix blank, analyte, and analyte-plus-matrix. This sequence was repeated four times for most of the analytes tested. Matrix elements tested included all 14 analytes listed previously, plus lead.

The ratio of matrix-to-analyte chosen was 33:1, except for Al_2O_3 for which a level of 10:1 was necessary to obtain an adequate signal. The ratio of 33:1 represents the case of determining 0.3% of analyte (as oxide) in the presence of 10% of matrix i.e. 3μg ml^{-1} and 100 μg ml^{-1}, respectively (for alumina, 10 μg ml^{-1} and 100 μg ml^{-1}, respectively).

TABLE 2

Optimal instrumental conditions for routine analyses

Analyte	F.e.s.			A.a.s.		
	Li_2O	Na_2O	K_2O	CaO	MgO	BaO
99% Confidence criterion	0.8	0.8	0.5	4.2	2.3	5.8
Flame[a]	AA	AA	AA	NA	NA	NA
Stoich.[b]				Rich	Rich	Rich
Burner[c]	1	1	1	AB-50	AB-50	AB-50
Slit (μm)	100	100	300	50	100	50
Band pass (nm)	0.33	0.33	0.99	0.165	0.33	0.165
Lamp current (mA)	—	—	—	7	3	10
Red filter	Yes	No	Yes	No	No	No
Wavelength (nm)	670.8	589.0	766.5	422.7	285.2	553.6

[a] AA, Air—acetylene, NA, Nitrous oxide—acetylene.
[b] Rich, 1/2 in. red zone. Lean, 1/8 in. red zone. (Interconal zone of N_2O—C_2H_2 flame.)
[c] 1 in., Custom-made slot burner or AB-50. AB-50, Varian-Techtron burner for nitrous oxide—acetylene. AB-51, Varian-Techtron burner for air—acetylene.

It was assumed that combinations of matrices do not act differently from the same single matrices. Also, it was assumed that if interference was not observed for a matrix-to-analyte ratio of 33:1, then smaller ratios would not cause interference.

Standard materials and apparatus

The test solutions were prepared by dilution from individual stock solutions, containing 1000 μg ml^{-1} of the desired analyte or matrix, prepared from Ultrex or reagent grade chemicals (J. T. Baker) or Johnson Matthey Specpure metals. All acids used were analytical-reagent grade. The atomic absorption and flame emission measurements were done on a Varian-Techtron AA-5 equipped with digital readout. The instrumental conditions are listed in Table 2.

Statistical procedures

Accepted statistical procedures were used to calculate the precision or relative standard deviation and also to describe a suitable criterion for determining whether an observed matrix effect could be termed significant.

The precision for a given analyte was calculated from the standard deviation obtained for a series of 10 readings of the analyte signal. The coefficient of variation at the 95% confidence level was calculated by multiplying the r.s.d. by two.

The significance criterion [9, 10] was developed statistically from a formula for calculating confidence intervals. The 99% confidence level was

A.a.s.							
SrO	Al_2O_3	Cr_2O_3	MnO	Fe_2O_3	CoO	CuO	ZnO
6.7	5.4	2.8	4.1	5.2	5.8	2.1	3.0
NA	NA	NA	AA	AA	AA	AA	AA
Rich	Rich	Lean					
AB-50	AB-50	AB-50	AB-51	AB-51	AB-51	AB-51	AB-51
50	50	100	50	50	50	50	200
0.165	0.165	0.33	0.165	0.165	0.165	0.165	0.66
10	10	10	5	10	10	3	5
No	No	No	No	No	No	No	No
460.7	309.3	357.9	279.5	248.3	240.7	324.7	213.9

chosen to strengthen the certainty of an observed matrix interference being described as valid. The formula for the criterion was

$$\text{Criterion} = \pm [t_{0.995,\ n-1}\, s(2/m)^{\frac{1}{2}}] 100/\bar{x}$$

where $t_{0.995}$ is the statistical t-distribution; s = standard deviation; n = number of readings to obtain s; m = number of comparisons of solution of analyte versus analyte + matrix; $\bar{x}$ = average value of analyte alone.

Any observed matrix interference effect was transformed to a % relative error and its magnitude compared with the significance criterion for that analyte. If its absolute value was larger than that of the criterion, then the matrix effect was regarded as a valid observation.

Results of the evaluation of earlier routine methods

The tests for observing matrix interferences were done as previously described. The results are shown in Table 3. As an aid in visualizing trends, the data can be reduced to those shown in Table 4. The results showed the following to be significant: (a) Li_2O, Na_2O and K_2O suffered numerous matrix errors, which confirms the extensive ionization interferences known to occur under those conditions; (b) relatively few interferences were observed for the alkaline earths and Al, which were determined by the N_2O—C_2H_2 flame with KCl as ionization suppressor; (c) Cr_2O_3 suffered severe interferences, many of which seemed to suggest ionization suppression; (d) all the remaining analytes seemed to suffer considerable interferences in the air—C_2H_2 flame.

TABLE 3

Results of evaluation of previous routine methods (matrix interference study)
(Instrumental conditions as in Table 2 unless specified otherwise.)

Analyte	2σ C.v.	99% Criterion	% Relative error from matrix effects														
			Matrix														
			Li_2O[a]	Na_2O[a]	K_2O[a]	CaO[b]	MgO[b]	BaO[b]	SrO[b]	Al_2O_3[b]	Cr_2O_3[a]	MnO[a]	Fe_2O_3[a]	CoO[a]	CuO[a]	ZnO[a]	PbO[a]
Li_2O	0.7	1.1	—	+4.8	+5.6	+1.6	−0.6	+3.0	+3.0[c]	+0.6	+0.6	+0.5	+0.2	+0.6	+0.4	+0.6	+1.7
Na_2O	0.6	1.0	+2.8	—	+7.2	−0.2	+1.5	+1.4	−0.8	−0.8	+1.7	+0.4	−2.0	−0.5	−0.3	−1.1	+0.9
K_2O	0.6	1.0	+7.4	+9.4	—	+3.4	+5.5	+1.0[c]	+4.6	+2.4	+2.2	+2.3	+1.1	+1.0	+1.2	+0.4	−0.3
CaO	2.0	3.2	+0.2	−0.3	—	—	−0.2	−0.1	−0.3	−2.3	−0.8	−0.3	−0.8	−0.4	−3.3	−5.3	−0.8
MgO	1.3	1.5	−0.3	−1.3	—	−2.1	—	−0.8	−0.6	−0.6	−1.0	0	−1.1	−1.5	+0.2	−1.2	+0.1
BaO	5.7	6.5	+2.5	−0.2	—	+0.5	−0.2	—	+0.2	−2.8	+2.1	−0.4	+0.8	0	−3.3	−1.0	−1.3
SrO	3.2	3.3	−1.7	−0.6	—	−0.3	+0.7	+1.8	—	−3.1	+0.2	−1.4	−1.3	−0.3	−4.1	−2.2	−0.6
Al_2O_3	2.4	2.7	+3.0	+1.5	—	−0.5	+1.5	+0.5	+0.5	—	0	+1.0	−1.0	−1.6	+2.1	+2.3	+2.3
Cr_2O_3[d]	3.4	3.9	+23	+19	+17	+19	+15	+5.2	+16	+11	—	+11	−14	−11	−3.0	+10	+1.5
Cr_2O_3[e]	1.4	1.6	+10	+9.6	+7.7	+5.5	+2.4	+1.2	+2.4	+1.2	—	+1.8	−0.6	+0.6	−1.8	+1.8	−3.0
MnO	0.8	0.9	+5.9	+6.3	+5.9	+5.4	+2.8	+4.1	+4.4	+1.6	+3.1	—	+2.8	+2.2	+1.9	+1.9	+3.1
Fe_2O_3	3.2	3.6	+3.8	+3.6	+3.7	+1.6	+1.2	+2.4	+3.6	+2.0	+2.9	+1.6	—	+0.8	+1.6	+2.9	+0.8
CoO	1.2	1.4	+4.0	+4.0	+4.0	+2.2	+2.2	+2.2	+2.7	+0.4	+0.9	+3.7	+1.3	—	+1.4	−0.4	+2.7
CuO	0.9	1.1	+3.0	+3.6	+3.7	+2.7	+1.8	+2.7	+2.1	+2.1	+3.1	+4.0	+2.2	+3.1	—	+1.9	+3.4
ZnO	0.8	1.0	+1.0	+1.3	+2.4	+1.1	+1.7	+1.3	+1.9	+1.8	+2.0	+0.9	+2.2	+1.7	+2.2	—	+1.4

[a] 2% (v/v) HCl solution. [b] 2% (v/v) HCl—0.5% (w/v) KCl solution. [c] Corrected for background. [d] In fuel-rich N_2O—C_2H_2 flame. [e] In fuel-lean N_2O—C_2H_2 flame.

TABLE 4

Summary of data in Table 3

Analyte	Li_2O	Na_2O	K_2O	CaO	MgO	BaO	SrO
99% Criterion	0.6	1.2	1.6	3.2	1.5	6.5	3.3
No. of matrix errors	13	4	6	2	2	0	1
Analyte	Al_2O_3	Cr_2O_3	MnO	Fe_2O	CoO	CuO	ZnO
99% Criterion	2.7	3.9	0.9	3.6	1.4	1.1	1.0
No. of matrix errors	1	12	14	4	10	14	12

Of the data for the analytes done in the absence of KCl (Li_2O, Na_2O, K_2O, Cr_2O_3, MnO, Fe_2O_3, CoO, CuO, ZnO) 90% showed a small positive bias caused by the 100 μg ml^{-1} matrices. This contrasted sharply with the 32% of the data showing this trend for CaO, MgO, BaO, SrO and Al_2O_3, all of which contained 0.5% of KCl in addition to the matrix elements. This positive bias for the other analytes in the absence of 0.5% KCl may indicate the presence of subtle lateral diffusion effects [11] or some other undetermined cause. Possibly, the high KCl concentration masked these effects for the analytes for which the positive bias was not observed.

The tests for matrix interferences were conducted with the flame conditions and instrumental parameters that had been routinely employed. With the N_2O—C_2H_2 flame, the flame stoichiometry or fuel-to-oxidant ratio was an important variable. A fuel-lean flame caused serious negative errors in the determination of Ca, Ba and Sr in the presence of Al; a fuel-rich flame reduced those errors significantly. Another well-known important variable is the height of observation in the flame. For example, in the classical case of Al interference on Ca, the relative error for calcium varies greatly with the height of observation. Fortunately, in a fuel-rich flame there is a range of observation heights at which the interference is essentially eliminated for the Al_2O_3 to CaO ratio of 33:1.

These evaluations of former routine methods showed that the most serious matrix interferences encountered resulted from ionization suppression, an improper choice of flame conditions and/or height of observation, and possible lateral diffusion effects. There was little support for the continued use of La_2O_3 as a releasing agent under the conditions used. Therefore, it seemed possible to develop a general routine flame spectrometric method based on the universal use of an ionization suppressor coupled with optimization of flame stoichiometry and height of observation.

DEVELOPMENT OF CsCl—HCl METHOD

Ionization suppressors

The main goal was to find an ionization suppressor having the best characteristics for routine analyses. The compounds tested included LiCl, KCl, NaCl, and CsCl. Cesium chloride was as good as, or better than, the

other compounds tested for ionization suppression. Cesium chloride was a logical choice for further investigation; in addition to having a low ionization potential, it is available in high purity, is not normally present in samples, and has a relatively simple spectral background. Subsequent testing and evaluation were designed to show whether or not CsCl satisfied all the requirements.

Of several brands of CsCl analyzed for impurities by emission spectroscopy with both flame and d.c. arc excitation, that from E. Merck (Darmstadt) was chosen on the basis of purity and cost; the impurity levels were at or below those stated by the supplier.

The optimum CsCl concentration was determined by measuring its ability to suppress the ionization of barium in the N_2O—C_2H_2 flame. Under the conditions employed for routine analysis, barium is the most easily ionized of all the analytes tested. The emission from solutions containing BaO (10 μg ml^{-1}), plus varying CsCl concentrations, was measured. The results are shown in Fig. 1; 0.4% CsCl (4000 μg ml^{-1}) was chosen as an acceptable level to evaluate for routine use. This provided a compromise between the ability to suppress ionization and a relatively low level of total solids in solution. As Fig. 1 shows, the plot of barium intensity vs. CsCl concentration has not completely leveled off at 0.4% CsCl. However, the slope of the curve at that point suggests that the formation of barium atoms is relatively insensitive to further large changes in CsCl concentration. The KCl level of 0.5% used in the earlier matrix interference study was selected by a similar experiment with barium.

Additional tests verified that large changes in other alkali metal concentrations would not affect the determination of BaO significantly in the presence of 0.4% CsCl and 2% HCl. The BaO was determined in several solutions which contained varying amounts of LiCl and KCl in addition to the matrix of 0.4% CsCl and 2% HCl (Table 5). The largest error observed was +6.4% occurring from the effect of KCl (10,000 μg ml^{-1}) on BaO

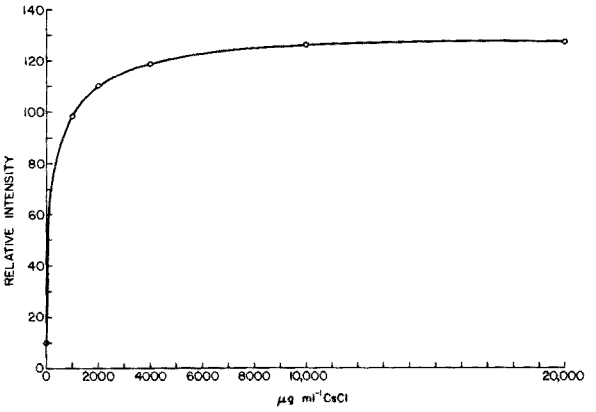

Fig. 1. Effect of CsCl on intensity of the Ba 553.5-nm line in the fuel-rich N_2O—C_2H_2 flame (10 μg ml^{-1} BaO).

TABLE 5

Effectiveness of CsCl in preventing ionization errors in solutions containing BaO (10 μg ml^{-1}), CsCl (4000 μg ml^{-1}) and varying LiCl and KCl (tested by f.e.s. at 553.5 nm)

LiCl added (μg ml^{-1})	% Rel. error in BaO[a]	KCl added (μg ml^{-1})	% Rel. error in BaO[a]
57	−0.2	10	+0.04
568	+0.7	100	−0.04
2,840	+1.5	1,000	+2.2
5,681	+1.4	5,000	+5.0
11,362	+0.3	10,000	+6.4

[a]C.v. (95%) for 10 μg ml^{-1} BaO plus 4000 μg ml^{-1} CsCl = 0.93% for this test.

(10 μg ml^{-1}). In practice, this effect would be negligible because it would represent a +6.4% error in determining 0.1% BaO in a sample of essentially 100% KCl.

Description of the CsCl—HCl method

The method consists of preparing samples and standards alike in a common aqueous matrix of 0.4% CsCl and 2% HCl. Sets of working standards in CsCl and HCl are maintained for routine use. If subsequent dilutions of the samples are necessary, additional CsCl and HCl can be added to the diluted samples to maintain the proper concentrations. Convenience in adding these reagents is necessary both for accuracy and efficiency. Cesium chloride can be stored as an 8% (w/v) solution in a borosilicate bottle equipped with a suitably accurate 0—10 ml variable dispenser; 5 ml of this stock solution per 100-ml final volume gives the required 0.4% CsCl. The concentrated HCl is stored in a similar container and dispensed from a 25-ml self-filling buret. Previous work showed that close control of acid concentration is important.

To ensure the proper flame stoichiometry and burner height settings for CaO, MgO, BaO, and SrO, it is desirable to maintain two test solutions. One test solution contains 3 μg ml^{-1} of CaO, MgO, SrO and BaO. The other contains the same plus 100 μg ml^{-1} Al_2O_3. Both solutions contain 2% HCl and 0.4% CsCl. When CaO, MgO, BaO and SrO are determined, it is necessary to adjust the operating parameters until essentially the same reading is obtained from each test solution. This eliminates or minimizes any interference effect from Al_2O_3.

Procedure for testing the CsCl—HCl method

The performance of the CsCl—HCl method was compared with the results obtained without CsCl in the earlier matrix interference study. Compared with the original matrix interference study, some changes in procedure were made to simplify the work. Rather than test each analyte

with each individual matrix as before, the 14 analytes were combined and tested with one matrix at a time. In all these tests, the levels of matrices (100 μg ml^{-1}) and analyte (3 μg ml^{-1}, except for Al_2O_3 at 10 μg ml^{-1}) were kept the same as in the earlier matrix interference study. Also, several "synthetic sample" solutions which contained several analytes together with several matrices were prepared to see if there were any combined interference effects; these solutions were selected to represent worst-case situations based on interferences observed in the original matrix interference study. It was assumed that there would be no interference between analytes at the low concentration levels tested and that variations in solids content up to 12% relative would not affect the results. Both of these conditions are frequently encountered in routine analyses.

The outline of the testing of the new method is shown in Tables 6 and 7. For example, in Table 6, solution number 2 containing the analytes Na_2O through ZnO in a Li_2O matrix was compared with control solution number 1 containing just analytes, etc. In Table 7, solution number 17 containing the analytes ZnO, MgO, SrO, CaO and BaO and matrices Li_2O, Na_2O, K_2O, Al_2O_3 and CuO was compared with control solution number 1. Precision data were again collected by making 10 measurements of each analyte on control solution number 1. Duplicate readings were taken for each comparison between the various solutions and solution number 1. Errors were again judged for significance by the 99% confidence criteria.

Results of the testing of the CsCl—HCl method

The complete results of these tests, shown in Tables 6 and 7, are summarized in Table 8; only four "significant errors" were found in testing the new method. These errors, which occurred for the determination of CaO in solution 14, Cr_2O_3 in solutions 5 and 6, and MgO in solution 17, were considered to be statistically marginal. The number of errors found in the original matrix study was 95.

In addition to testing for matrix effects caused by cations, a limited check was made for matrix effects arising from sulfate and perchlorate, which could be present in a sample or be added during the dissolution or pre-treatment steps. Solutions containing all the analytes (3 μg ml^{-1} except Al_2O_3 = 10 μg ml^{-1}) were checked for interference compared with similar solutions containing 1% H_2SO_4 and 1% $HClO_4$. All solutions also contained 0.4% CsCl and 2% HCl. The results are shown in Table 9.

Precipitation of $BaSO_4$ and $SrSO_4$ caused low results for BaO and SrO, but this cannot be considered to be a spectroscopic interference. Enhancements occurred for Cr_2O_3 (+11.0%) and Na_2O (+2.7%) in the presence of H_2SO_4. Sulfate also caused a serious depression for Fe_2O_3 (—27.0%), but this interference was removed by using the N_2O—C_2H_2 flame instead of the air—C_2H_2 flame. The presence of perchlorate resulted in a large enhancement for Cr_2O_3 (+9.5%), a small enhancement for K_2O (+1.8%), and a medium depression for ZnO (—4.4%). Thus, the results indicate that the CsCl—HCl

TABLE 6

Results of testing CsCl—HCl method: effect of a single element matrix on combined analytes (Matrix added, 100 $\mu g\ ml^{-1}$; analyte added, 3 $\mu g\ ml^{-1}$, except for Al_2O_3, 10 $\mu g\ ml^{-1}$.)

Analyte	Solution no.	% Relative error Control 1	2	3	4	5	6	7	8	9	10	11	12	13	14	15	16
	Matrix	None	Li_2O	Na_2O	K_2O	CaO	MgO	BaO	SrO	Al_2O_3	Cr_2O_3	MnO	Fe_2O_3	CoO	CuO	ZnO	PbO
	2 σ C.V.	99% Criterion															
Li_2O	0.5	0.8	—	−0.2	0.0	+0.4	+0.5	+0.2	+0.7	+0.6	−0.1	+0.2	+0.2	+0.1	−0.1	−0.5	+0.2
Na_2O	0.5	0.8	+0.3	—	0.0	−0.6	−0.3	+0.3	+0.5	0.0	+0.3	+0.1	−0.1	−0.3	−0.1	−0.2	−0.4
K_2O	0.3	0.5	−0.2	0.0	—	−0.1	+0.2	+0.2	−0.2	+0.1	−0.1	−0.1	+0.1	0.0	+0.2	+0.1	+0.1
CaO	2.7	4.2	+0.7	−0.7	+1.3	—	−1.5	−1.1	+0.9	−2.8	−2.1	+0.4	−1.2	+0.8	+4.6	−0.2	+2.8
MgO	1.5	2.3	0.0	0.0	−1.4	−1.3	—	−0.2	+0.2	−0.1	−0.7	0.0	−0.7	−0.6	+0.8	−0.2	+0.2
BaO	3.6	5.8	+2.5	−0.3	−2.7	+1.6	−0.9	—	−0.3	+1.0	−2.8	+0.7	−4.1	+0.3	−0.4	−1.2	−1.5
SrO	4.2	6.7	+0.6	−1.4	+1.3	0.0	−1.9	+2.4	—	+0.4	0.0	−2.1	−1.1	−1.5	−1.4	−1.5	−0.4
Al_2O_3	3.4	5.4	−2.6	0.0	−1.7	−1.4	−0.8	−0.1	−0.9	—	−2.6	−0.4	−1.6	−1.8	−1.2	−2.2	+1.9
Cr_2O_3	1.8	2.8	+2.3	−1.1	−0.4	−2.9	−3.1	+0.7	−0.1	−1.9	—	+0.3	−1.0	−1.6	−0.1	+1.6	+0.8
MnO	2.6	4.1	−0.3	−0.8	−0.1	−0.6	−0.4	−0.4	−0.8	−0.8	−0.2	—	+0.5	−0.5	+0.6	−0.3	+0.4
Fe_2O_3	2.8	5.2	−3.5	+2.9	−1.4	+0.1	+0.2	0.0	+0.7	+0.3	−0.7	+0.1	—	+1.0	−0.9	−3.5	+0.3
CoO	3.6	5.8	+1.0	+1.5	−0.7	−1.8	−0.1	−1.1	+0.1	+1.5	+0.2	+0.1	−0.2	—	+0.2	−0.6	−0.9
CuO	1.3	2.1	−0.1	−1.5	+0.7	−1.0	−0.1	+0.2	0.0	−2.0	0.0	−0.5	−0.4	−0.8	—	−1.2	−0.3
ZnO	1.9	3.0	−0.8	−0.9	−0.6	−0.5	−0.6	−0.7	+0.1	−0.4	−1.4	−0.7	+0.2	−0.3	0.0	—	−1.0

TABLE 7

Results of testing CsCl—HCl method: effect of mixed matrices on mixed analytes (Analytes, 3 $\mu g\ ml^{-1}$ each, except for Al_2O_3, 10 $\mu g\ ml^{-1}$. Matrices, 100 $\mu g\ ml^{-1}$ each.)

Solution 17			Solution 18			Solution 19		
Matrix Li_2O, K_2O, Na_2O, Al_2O_3, CuO			Matrix Fe_2O_3, Cr_2O_3, MgO, CaO, SrO, BaO			Matrix CaO, MgO, SrO, BaO, Fe_2O_3, CoO		
Analyte	99%	Rel. error (%)	Analyte	99%	Rel. error (%)	Analyte	99%	Rel. error
ZnO	3.0	+1.8	Li_2O	0.8	−0.1	Cr_2O_3	2.8	+1.5
MgO	2.3	+0.5	Na_2O	0.8	−0.6	MnO	4.1	+0.3
CaO	4.2	+4.5	K_2O	0.5	−0.3	Al_2O_3	5.4	+0.2
SrO	6.7	−1.0	CuO	2.1	+1.5			
BaO	5.8	+2.8						

Solution 20			Solution 21		
Matrix Li_2O, Na_2O, ZnO, MnO, PbO			Matrix Li_2O, Na_2O, K_2O, Cr_2O_3, CuO, PbO		
Analyte	99%	Rel. error (%)	Analyte	99%	Rel. error (%)
Fe_2O_3	5.2	+0.5	MnO	4.1	+0.1
CoO	5.8	+1.7	Fe_2O_3	5.2	+1.6
CaO	4.2	0.0	BaO	5.8	−3.4
Cr_2O_3	2.8	+1.4	Al_2O_3	5.4	+0.2
CuO	2.1	−0.2			
K_2O	0.5	+0.4			

TABLE 8

Results of matrix interference study for the new CsCl—HCl method (Li_2O, Na_2O and K_2O were determined by f.e.s. All others were determined by a.a.s.)

Analyte	99% Criteria	Matrix errors found	Analyte	99% Criteria	Matrix errors found
Li_2O	0.8	0	Al_2O_3	5.4	0
Na_2O	0.8	0	Cr_2O_3	2.8	2
K_2O	0.5	0	MnO	4.1	0
CaO	4.2	1	Fe_2O_3	5.2	0
MgO	2.3	1	CoO	5.8	0
BaO	5.8	0	CuO	2.1	0
SrO	6.7	0	ZnO	3.0	0

method was not severely affected by sulfate or perchlorate except for the case of Cr_2O_3 and possibly ZnO. It is therefore recommended that Cr_2O_3 be determined with the fuel-lean N_2O—C_2H_2 flame, but with standards and samples which contain 2% H_2SO_4, 2% HCl and 0.4% CsCl. Sample preparation must be done carefully to prevent loss of chromium(VI) by volatilization as CrO_2Cl_2.

TABLE 9

Effect of anions on mixed analytes in 0.4% CsCl—2% HCl. Statistically significant errors are asterisked.

Analyte	% Relative error		Analyte	% Relative error	
	1% H_2SO_4	1% $HClO_4$		1% H_2SO_4	1% $HClO_4$
Li_2O	+0.3	+1.0	Al_2O_3	+7.4	+3.7
Na_2O	+2.7*	+0.9	Cr_2O_3	+11.0*	+9.5*
K_2O	+0.6	+1.8*	MnO	−1.6	+0.6
CaO	−0.7	−0.3	Fe_2O_3	−27.0*	+2.8
MgO	+1.2	−0.3	CoO	+1.5	+1.5
BaO	−92.0*	0	CuO	+0.3	+1.3
SrO	−24.0*	+0.7	ZnO	−2.3	−4.4*

Applications of the CsCl—HCl method — Analysis of NBS reference materials

The CsCl—HCl method was applied to the analysis of several NBS reference materials. The initial sample treatment depended on the material, but in general the samples were dissolved in Pt or Teflon dishes with HF—$HClO_4$, accompanied by volatilization of the SiF_4. A second treatment with $HClO_4$ aided in removal of traces of fluoride. The samples were dissolved in dilute HCl, transferred to volumetric flasks and made to contain 2% (v/v) HCl and 0.4% (w/v) CsCl prior to analysis. The results of these analyses (Table 10) show that the CsCl—HCl method gave good accuracy. Where variations from certified values occurred, the magnitude was within normal instrumental error for flame spectrometric analyses. The principal benefit of the new method, i.e. successful application to a wide variety of sample types, with a reduction of analytical errors, is accomplished with a significant gain in laboratory efficiency through standardization of procedures without sacrifice in precision.

TABLE 10

Applications of the CsCl—HCl method

Analyte	Cert (%)	Found (%)	Cert (%)	Found (%)
	NBS 1B Limestone 1970		*NBS 99a Feldspar 1965 (Prov.)*	
Na_2O	0.04	0.05, 0.06	6.2	6.34, 6.32
K_2O	0.25	0.25, 0.26	5.2	5.32, 5.33
CaO	50.9	50.6	2.14	2.16, 2.17
MgO	0.36	0.33, 0.32	0.02	0.01, 0.01
BaO			0.26	0.25, 0.26
SrO	0.14	0.15, 0.15		
Al_2O_3	1.12	1.15, 1.16	20.5	20.7, 20.8
MnO	0.20	0.20, 0.20		
Fe_2O_3	0.75	0.77, 0.76	0.065	0.065, 0.066

TABLE 10 (continued)

Analyte	Cert. (%)	Found (%)	Cert. (%)	Found (%)	Cert. (%)	Found (%
	NBS 89 Pb—Ba Glass 1932		*NBS 91 Opal Glass 1931*		*NBS 93 Borosilicate 1*	
Na_2O	5.70	5.69, 5.64	8.48	8.53, 8.65	4.16	4.36, 4.3
K_2O	8.40	8.34, 8.32	3.25	3.34, 3.29	0.16	0.14, 0.1
CaO	0.21	0.23, 0.23	10.48	10.51, 10.36		
BaO	1.40	1.40, 1.33				
Al_2O_3	0.18	0.20, 0.19	6.01	5.86, 5.96	1.94	1.94, 1.9
MnO	0.088	0.092, 0.092				
Fe_2O_3	0.049	0.051, 0.049	0.081	0.067, 0.067[a]	0.076	0.067, 0.(
ZnO			0.08	0.089, 0.088		
	NBS 620 Soda-Lime Glass 1972 (Prov.)		*SS-181 NBS 55181 Spodumene 1958 (Prov.)*			
Li_2O			6.4	6.41, 6.36		
Na_2O	14.40	14.51	0.8	0.88, 0.89		
K_2O	0.41	0.39, 0.39	0.3	0.31, 0.31		
CaO	7.12	7.08, 7.10				
MgO	3.69	3.65, 3.69				
Al_2O_3	1.81	1.81, 1.78				
Fe_2O_3	0.042	0.050, 0.046				
	NBS 85B Al Alloy 1957		*NBS 106B Steel 1961*			
Mg	1.49	1.46, 1.48				
Al	—	— —	1.07	1.03, 1.05		
Mn	0.61	0.60, 0.58	0.506	0.50, 0.50		
Fe	0.24	0.25, 0.23				
Cu	3.99	3.95, 4.00	0.117	0.11, 0.11		
Zn	0.030	0.033, 0.033				

[a] Analyzed spectrophotometrically and found to contain 0.068% Fe_2O_3.

REFERENCES

1 J. Yoffe and R. Finklestein, Anal. Chim. Acta, 19 (1958) 166.
2 C. H. Williams, Anal. Chim. Acta, 22 (1960) 163.
3 J. I. Dinnin, Anal. Chem., 32 (1960) 1475.
4 D. J. David, Analyst, 85 (1960) 495.
5 C. B. Belcher and K. A. Brooks, Anal. Chim. Acta, 29 (1963) 202.
6 R. E. Dickson and C. M. Johnson, Appl. Spectrosc., 20 (1966) 212.
7 F. W. Smith, Ind. Eng. Chem., Anal. Ed., 10 (1938) 360.
8 J. I. Hoffman and G. E. F. Lundell, J. Res. Nat. Bur. Stand., 22 (1939) 465.
9 G. N. Lauer, Owens-Illinois, Inc., Computer Technology Dept., personal communication, 1975.
10 B. Ostle, Statistics in Research, Iowa State University Press, Ames, Iowa, 2nd edn., 1963, p. 119.
11 A. C. West, V. A. Fassel and R. N. Kniseley, Anal. Chem., 45 (1973) 1586, 2420.

Analytica Chimica Acta, 92 (1977) 321—328

THE DEVELOPMENT OF A GAS CHROMATOGRAPHY—FURNACE ATOMIC ABSORPTION COMBINATION FOR THE DETERMINATION OF ORGANIC LEAD COMPOUNDS. ATOMIZATION PROCESSES IN FURNACE ATOMIZERS

J. W. ROBINSON, E. L. KIESEL, J. P. GOODBREAD, R. BLISS and R. MARSHALL

Department of Chemistry, Louisiana State University, Baton Rouge, Louisiana 70803 (U.S.A.)

(Received 12th January 1977)

SUMMARY

A carbon furnace atomizer has been developed which can be directly attached to a gas chromatography column. The atomizer exhibits high sensitivity and eliminates many of the problems involved with interferences encountered with furnace atomization. The functioning of the instrument is demonstrated for tetraalkyllead in various brands of gasoline, and for organic lead compounds in air. The process of atomization in furnace atomizers, and the numerous problems which lead to sensitive but unreliable data when normal commercial furnace atomizers are used, are discussed. The atomizer described overcomes most of the problems discussed.

The determination of the total amount of a given metal in a sample gives limited information about the chemical effects of the trace metal. This is particularly true in studies of toxicity, pollution, and biological effects, where the chemical form affects the reactivity of the element. Gas chromatography (g.c.) has found widespread application for the separation of various samples into their components. When specific detectors are used, information on the chemical composition of these components can be obtained by utilizing retention times for identification. Further positive identification may be used if necessary.

Recently, combinations of g.c. and various forms of atomic absorption spectrometers have been used; these have usually involved coupling a commercial g.c. with a commercial atomic absorption instrument [1—8]. Although these techniques illustrate the feasibility of the process and can be very convenient, particularly when flame atomizers are used, they are nevertheless not readily streamlined for routine use. Numerous applications have already been demonstrated, but particularly in the case of carbon atomizers, the combinations are unwieldy in many respects. In addition, many of the problems involved with commercial carbon atomizers persist when they are used in g.c.—a.a.s. combination systems.

It has been our experience and the experience of many routine analysts that commercial carbon furnace atomizers are unreliable. The commercial

systems are certainly capable of performing analyses at very high levels of analytical sensitivity and precision, but the development of reliable quantitative analytical procedures is much more difficult.

An examination of the furnace atomization step reveals the problems involved in obtaining accurate quantitative data.

ATOMIZATION IN CARBON ATOMIZERS

The atomization step with a furnace or rod atomizer is very difficult to examine; the formation of atoms is a very fast process. The number of atoms formed depends on many variables and the population never reaches a steady state. Consequently, to control the percentage of atoms formed (atomization efficiency) and the total number of free atoms entering the light path during optical measurement, it is vital to control all the variables which affect the rate and the degree of atomization. The difficulty involved in effective control can be more readily understood when the entire atomization process is considered. Many sample atomizers involve three steps: (1) evaporation of the solvent at a relatively low temperature; (2) ashing of the sample at an increased temperature; and (3) atomization at a relatively high temperature.

When a carbon rod or a tube is used, the liquid sample diffuses into the carbon to a lesser or greater extent depending on the physical form of the carbon. If the carbon is impervious and the surface is shiny, as is the case when pyrolytic carbon is deposited on the surface the liquid sample will not penetrate the carbon; atomization will then be relatively rapid. However, if the carbon is not impervious, then the liquid sample soaks into the carbon and the subsequent evaporation, ashing and atomization steps are slowed down because the components of the solution must first re-emerge from the carbon.

The atomization and ashing steps both depend on the chemical form of the sample. Extensive studies by West et al. [9] indicate that the chemical interferences with carbon atomizers can lead to serious errors. With commercial atomizers, the chemical interferences can be overcome to some extent by rigidly controlling the complete atomization step, with regard to timing, rate of heating, and temperatures. However, it is quite impossible to control these steps completely since the normal sample is often not completely characterized. It is much easier to obtain accurate and reproducible results from 'pure' solutions, than from real samples, such as river water, plant streams, etc.

A further problem relates to the variation of the electrical resistance of the carbon rod or tube with use. Thus, with a standardized atomization program, the temperatures achieved will differ somewhat as the carbon ages, although the time and voltage remain the same, and this will affect the atomization rate.

With these atomizers, the free atoms are swept through the light path in a very brief period of time. Short, sharp peaks are frequently recorded and the

peak heights are usually measured. Recent commercial equipment in which the peak area is integrated is more accurate because peak areas correspond more to the total number of atoms than to the maximum number of atoms produced. A problem frequently arises with coupling a furnace atomizer to equipment purchased for flame atomizers. The latter equipment usually utilizes amplifiers and read-out systems with slow response times which are totally unsuitable for use with furnace atomizers. Such equipment can give answers which are more a measure of response time than of metal concentration.

Despite the above variables, it is possible to obtain precise measurements. The reproducibility may be very good for a given instrument under strictly controlled conditions. However, when actual samples are run, the rates at which the samples diffuse into and out of the carbon rod change, the rates of decomposition vary because of chemical interferences, and quite erroneous answers may be obtained even though every precaution has been taken to match the samples and the standards used. The processes never reach equilibrium. Under these non-ideal conditions, which might be compared with the conditions encountered in gravimetric analysis before the days of thermogravimetric analysis, highly reproducible data are possible, but the production of accurate, reliable results is a very different matter. These considerations have led to the development of the atomizer with different processes described below.

CARBON ATOMIZER

A schematic diagram of the atomizer is shown in Fig. 1. The atomizer is left hot at all times when in use. The effluent from the gas chromatograph enters

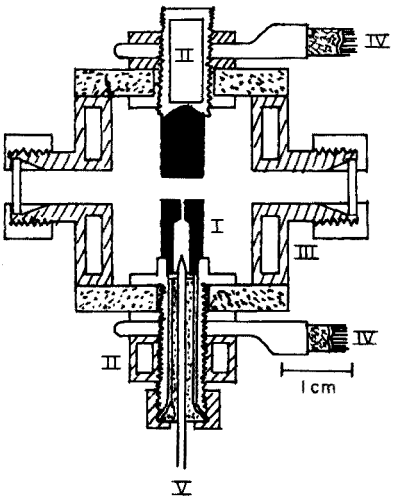

Fig. 1. Schematic diagram of atomizer. I, Carbon resistance atomization chamber. II, Water-cooled electrodes. III, Water-cooled housing. IV, Power Supply (welding cables). V, Pyrex capillary transfer line from g.c. to atomizer.

the base of the atomizer where the gaseous sample is decomposed and atomization takes place. The atoms flow into the cross-piece, which is in the optical light path. The advantage of the process is that the peak of the solvent used is quite separate from the peak of the metal-bearing component on the gas chromatogram. The gas chromatograph separates the metal-bearing components from the rest of the material, which eliminates much of the problems encountered in the solvent evaporation step and other matrix effects. Decomposition is fairly rapid, although several seconds elapse from the time that the sample enters the carbon atomizer before the atoms reach the optical light path. This permits chemical decomposition to take place and virtually eliminates chemical interference, which is usually caused by varying rates of atomization from different compounds rather than by prevention of decomposition. Even if the rate varies, decomposition is virtually complete before the free atoms enter the light path.

The peak height is a product of the metal concentration and the resolution of the g.c. column. The definition of sensitivity as that concentration which results in 1% absorption is therefore unrealistic. Sensitivity measurements were based on peak area data.

The atomizer is just a few cm long (Fig. 1) and can be fitted into almost any commercial a.a.s. unit. Fast electronics are not necessary because the metal concentration is measured as a gas chromatographic peak which takes several seconds to evolve.

The atomizer overcomes many of the difficulties involved in commercial furnace carbon atomizers. As a demonstration process, gasoline samples were analyzed to indicate how metal-bearing components can be distinguished from a multitude of organic compounds.

EXPERIMENTAL

Equipment

The following standard components were used: Sargent Model XK recorder with variable range attachment; Microtek GC-2000-R gas chromatograph; Varian-Techtron Type M1 (SI-RO-SPEC) grating monochromator; Heathkit Photometric readout amplifier Model EU-703-31; Hewlett-Packard Model 6515A high voltage power supply; Hammatsu Model R-106 photomultiplier; stepdown transformer (Signal Transformer Co., Model 6-260, 6 V, 250 A maximum); variable autotransformer (Superior Electric Co., Powerstat 2KVA); Hamilton 0—1 μl microliter syringe.

The atomizer is shown if Fig. 1.

The parameters for the gas chromatograph were: Teflon column, $\frac{1}{8}$ in. diameter, 8 ft. long, packed with 20% TCP on Chromosorb W; argon carrier gas at 30 cm^3 min^{-1}; column temperature, 100°C; injection port temperature, 125°C; transfer line temperature, 100°C.

The atomic absorption parameters were: lamp current, 8 mA; high voltage 350 d.c.; slit width, 50 μm; absorption wavelength, 283.3 nm. The atomizer temperature was roughly estimated as 2000°C.

Procedure

A 1-μl quantity of a mixed alkyl lead solution containing five alkyl lead compounds known to be present in leaded gasolines in n-heptane was injected into the system to measure the relative retention times of the alkyl lead compounds on the g.c. column. The compounds were tetramethyllead (TML), trimethylethyllead (TMEL), dimethyldiethyllead (DMDEL), methyltriethyllead (MTEL) and tetraethyllead (TEL).

After determination of the relative retention times, samples of different gasolines were injected into the system and analyzed for alkyllead content. The system was calibrated with dilutions of tetraethyllead in heptane.

After calibration, the lead hollow-cathode lamp was replaced by a deuterium lamp, and the entire group of samples was re-run to determine molecular background.

Dilutions of 1-chloro-2-methylpropane, chlorobenzene, n-butanethiol, and tripropylamine in hexane were made. These samples were run with the lead hollow-cathode lamp.

RESULTS AND DISCUSSION

Some typical chromatograms of commercially available gasolines are shown in Fig. 2. In all cases, molecular background absorption measurements were taken to eliminate error from incomplete combustion of organic compounds [1]. It was discovered that except for the solvent peaks which flooded the atomizer, the organic compounds were broken down. Absorption was detected from large concentrations of chlorine, nitrogen and sulfur compounds, and the atomizer could probably be used for the determination of such compounds in organic mixtures. Typical chromatograms are shown in Fig. 3.

The studies on the gasolines showed clearly that the different brands contained different mixtures, which is of course well known. The unleaded gasolines showed significant absorption of the lead lines but this proved to be organic in nature since it occurred also with the background correction. When the temperature of the atomizer was increased, the absorption by the non-lead materials increased, indicating that the absorption was due to a combustion product rather than to incomplete combustion of the solvent molecules. This phenomenon will be studied further.

Evaporation of gasoline

Some studies were undertaken on the effect of evaporation on the concentrations of lead components in the anti-knock materials. These results are shown in Fig. 4. Under some circumstances, tetramethyllead tended to evaporate more rapidly than the other forms of lead; this is not surprising since it is the most volatile of the lead components. However, it should be stressed that under the conditions of these studies, large quantities of gasoline were evaporated. It is very unlikely that this kind of evaporation would take place in practice.

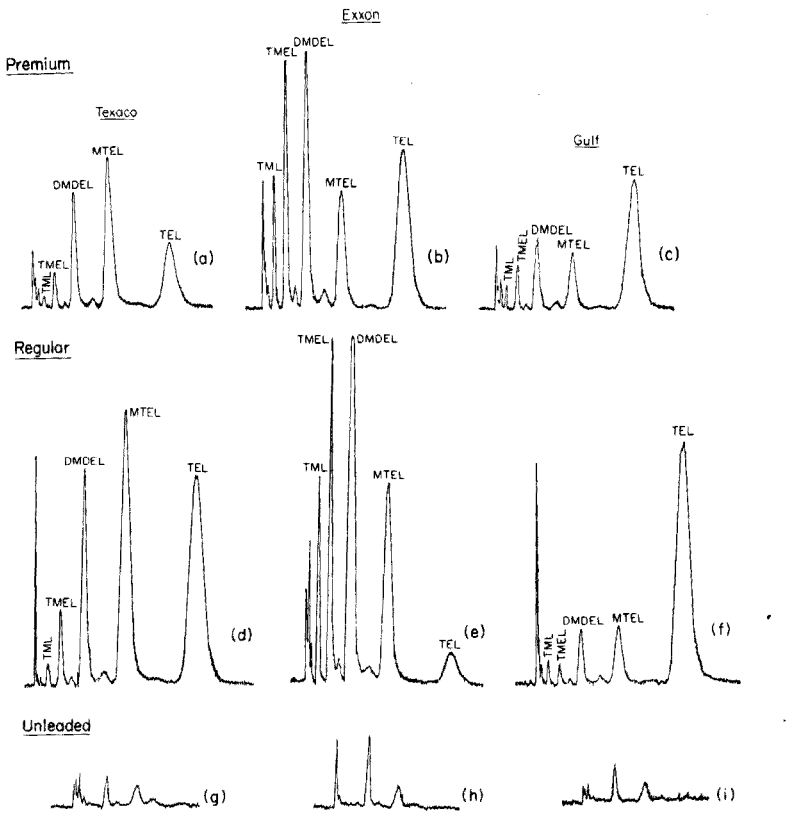

Fig. 2. G.c. traces for different gasolines. See text for abbreviations. (a) Texaco Premium, 0.5-μl sample. (b) Exxon Premium, 1-μl sample. (c) Gulf Premium, 0.5-μl sample. (d) Texacc Regular, 1-μl sample. (e) Exxon Regular, 1-μl sample. (f) Gulf Regular, 1-μl sample. (g) Texaco Unleaded, 2-μl sample. (h) Exxon Unleaded, 2-μl sample. (i) Gulf Unleaded, 2-μl sample.

One interesting application of this technique was the determination of the source of gasoline which had leaked from some gasoline stations. Inasmuch as these stations were different brands, the lead alkyl composition was different, so that it was easy to identify from which station the gasoline had leaked. Other studies with this instrument have shown that the sensitivity is of the order of 10^{-10} g.

Lead compounds in the atmosphere

In previous work [10] relatively high concentrations of "molecular lead" were found in the atmosphere. However, the concentrations of TEL in the atmosphere are known to be very low. In an attempt to discover the chemical identity of the "molecular lead" observed earlier, relatively large volumes of air ($\geqslant 1$ m^3) were pulled through a cryogenic trap. The trapped material

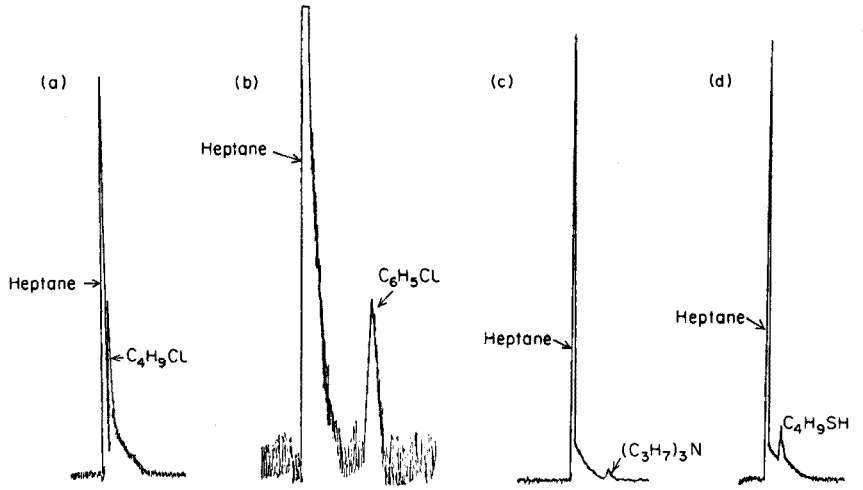

Fig. 3. G.c. traces for pure organic compounds in heptane solution measured at the Pb 283.3-nm line. (a) 1-Chloro-2-methylpropane as a 0.2% solution. (b) Chlorobenzene as a $2.2 \cdot 10^{-7}$ g ml^{-1} solution. (c) Tripropylamine as a 1% solution. (d) n-Butanethiol as a 0.4% solution.

was then put into the gas chromatograph under conditions suitable for tetraethyllead or other organic lead compounds. The concentrations of TEL were so small that in 9 cases out of 10 none was detected; in the 10th case some lead was detected but the compound could not be identified. These results confirm that the TEL concentrations in the atmosphere are very low. Thus the "molecular lead" [10] cannot be tetraethyllead and did not originate from evaporation of TEL from gasoline. The chemical form of the lead previously detected is being studied.

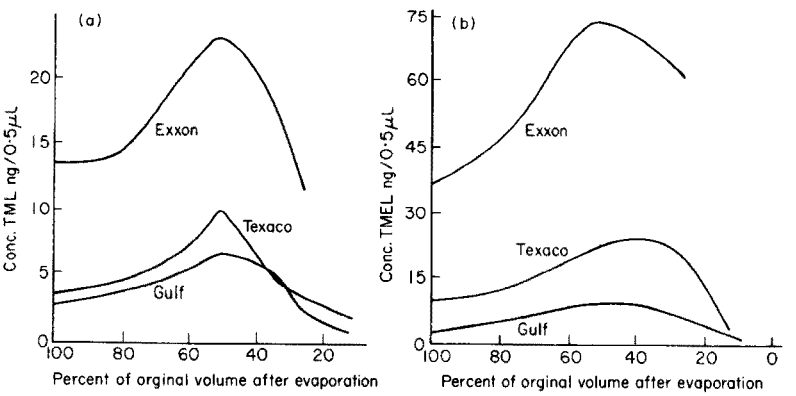

Fig. 4. Loss of anti-knock agents during evaporation of gasoline. (a) Tetramethyllead. (b) Trimethylethyllead. Loss of other agents was less severe during the evaporation.

REFERENCES

1 J. W. Robinson, L. E. Vidaurreta, D. K. Wolcott, J. P. Goodbread, and E. Kiesel, Spectrosc. Lett., 8 (1975) 491.
2 D. A. Segar, Anal. Lett., 7 (1974) 89.
3 J. G. Gonzalez and R. T. Ross, Anal. Lett., 5 (1972) 683.
4 Y. K. Chau, P. T. S. Wong and P. D. Goulden, Anal. Chem., 47 (1975) 2279.
5 N. K. Rudnevesicii, D. A. Vyakhirev, V. T. Demarin, M. V. Zueva, and A. I. Lukyanova, Dokl. Akad. Nauk. SSSR, 223 (1975) 887.
6 D. T. Coker, Anal. Chem., 47 (1975) 386.
7 H. Hey, Z. Anal. Chem., 256 (1971) 361.
8 B. Kolb, G. Kemmner, F. H. Schleser, and E. Wiedeking, Z. Anal. Chem., 221 (1966) 166.
9 L. Ebdon, G. F. Kirkbright, and T. S. West, Anal. Chim. Acta, 58 (1972) 39.
10 J. W. Robinson, L. Rhodes, and D. K. Wolcott, Anal. Chim. Acta, 78 (1975) 474.

Analytica Chimica Acta, 92 (1977) 329—335

CHROMATOGRAPHY OF PHENOLS AND AROMATIC CARBOXYLIC ACIDS ON ANION-EXCHANGE RESINS IN AQUEOUS ETHANOL

LUTFUL MAJID JAHANGIR and OLOF SAMUELSON*

Department of Engineering Chemistry, Chalmers University of Technology, Fack, S-402 20 Göteborg (Sweden)

(Received 29th March 1977)

SUMMARY

An efficient group separation of various phenolic compounds from aromatic carboxylic acids can be achieved on the acetate form of an anion-exchange resin in aqueous ethanol (e.g. 80% w/w) acidified with acetic acid (0.01—0.1 M). The carboxylic acids are then eluted at high concentration of acetic acid. The method permits separation of individual compounds in the same run.

Both phenolic compounds and benzoic acids are retained strongly by anion-exchange resins in the acetate form [1—4]. Acetic acid in aqueous solution is a suitable eluent for chromatographic separations [3, 4], but in analyses of complex mixtures containing both types of compounds, it has the disadvantage that phenolic compounds held very strongly by the resin are eluted among the carboxylic acids. This is a serious handicap in analyses of complex mixtures of unknown compounds such as industrial effluents.

The main purpose of the present work was to devise a method for a group separation of phenolic compounds from benzoic acids. The method is based on the observation that the distribution coefficients of many phenolic compounds can be depressed by the addition of organic solvents. In contrast, experiments with anion-exchange resins in the sulphate form have shown that strongly polar phenolic compounds are held very strongly in aqueous ethanol [5]. To establish appropriate conditions it was therefore necessary to determine the distribution coefficients of different types of solutes at different compositions of the eluent. The results are also of interest when it is desired to combine the group separation with a chromatographic separation of individual compounds.

EXPERIMENTAL

The volume distribution coefficients (D_v) were determined and the chromatographic separations were made by the methods described previously [3]

($D_v = \bar{V}/(X - \epsilon)$, where $\bar{V}$ is the peak elution volume, X the bed volume and ϵ the interstitial fraction). The bed volume was determined at 30°C with 0.1 M acetic acid in 80% ethanol; no correction was applied for swelling changes. In this medium, D_v of the phenolic compounds was reproducible within ±1% for at least one month and unaffected when the applied amounts varied between 0.5 and 5 μg. Variations in the nominal linear (empty tube) flow from 1.8 cm min^{-1} to 3.7 cm min^{-1} had no effect. In 0.01 M acetic acid the strongly acidic phenols gave fronting peaks, indicating a nonlinear sorption isotherm.

In preparing the eluents a weighed amount of glacial acetic acid was introduced into a volumetric flask which was then filled to the mark with aqueous ethanol of the composition (% w/w) reported below.

RESULTS AND DISCUSSION

Table 1 shows the distribution coefficients of some phenolic compounds on the acetate form of an anion-exchange resin at different ethanol concentrations. For all compounds the addition of ethanol resulted in a marked decrease in D_v. This can, at least in part, be ascribed to decreased hydrophobic interactions. With increasing concentration of ethanol D_v passed through a minimum. The ethanol concentration which gave the lowest D_v was much lower for strongly polar compounds (about 40% for guaiacylglycerol) than for the more hydrophobic phenols (about 80% for the chlorinated phenols). Moreover, the compounds with a hydrophilic side

TABLE 1

Volume distribution coefficients (D_v) in 0.1 M acetic acid in water and aqueous ethanol at 30°C on Dowex 1-X10 (7—10 μm)

Compound	Water	Aqueous ethanol, % by weight					
		20%	40%	60%	80%	90%	98%
Phenol	26	13.0	3.34	1.35	1.09	1.62	2.70
1,3-Dihydroxybenzene	88	34	10.2	5.66	7.01	13.9	33
1,2-Dihydroxybenzene	46	22	8.20	4.44	5.32	10.3	24.7
1,4-Dihydroxybenzene	38	17	5.70	3.42	4.37	8.50	19.9
2-Chlorophenol	19	46	7.78	2.47	1.85	2.61	5.27
2,5-Dichlorophenol	>300	200	18.5	4.18	2.61	3.60	8.30
2,6-Dichlorophenol	>300	71	8.90	2.55	1.73	2.30	3.60
R'CH(OH)CH(OH)CH_2OH[a]	1.58	0.80	0.59	0.70	1.79	4.70	14
R'CH(OH)CH(OH)R'[a]	14.5	3.58	1.27	0.90	2.02	6.42	27

a R' = 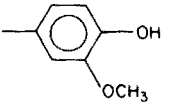

chain were held more strongly at the highest ethanol concentration than in aqueous medium. For the chlorinated compounds this change in ethanol concentration led to a drastic decrease in D_v. Analogously, the decrease observed for phenol was much greater than that observed for the more hydrophilic dihydroxybenzenes.

In aqueous ethanol, strongly polar solutes such as sugars and alditols are retained effectively by ion-exchange resins, because the ethanol concentration in the resin phase is lower than that in the external solution [6]. As predicted from solubility measurements, D_v increases drastically with an increased ethanol concentration in the eluent [7]. Solute—resin interactions can, however, not be disregarded. Partition chromatography in aqueous ethanol has not been reported for the acetate form of anion exchangers and for this reason experiments were made in 0.1 M acetic acid with glycerol, erythritol and glucitol. In agreement with results obtained for ion exchangers with other counter ions, the D_v values (1.1, 1.7 and 3.5 in 80% ethanol) increased with increasing number of hydroxyl groups in the polyol and with increasing ethanol concentration (2.1, 5.2 and 15 in 90% ethanol). Hence, the same mechanism applies for the acetate form. It was therefore concluded that the mechanism also applies for the phenolic compounds with a hydrophilic side chain, dihydroxybenzenes and for trihydroxybenzenes (Table 2).

Conversely, the higher ethanol concentration in the external solution than in the resin phase must tend to push the chlorinated phenols and other hydrophobic compounds into the external solution. The observation that their D_v values increased markedly when the ethanol concentration was increased from 80% to 98% indicates that increased contributions from hydrogen bonding of the phenolic proton to proton-accepting groups in the resin and possibly additional interactions are more important within this concentration range. These factors must also contribute to the increase in D_v observed for the other phenols.

Table 1 refers to the elution of phenolic compounds with eluents which were 0.1 M with respect to acetic acid. A higher acid concentration leads to low distribution coefficients for the benzoic acids while a lower concentration might facilitate the group separation. Experiments were therefore also made in 0.01 M acetic acid. For weakly acidic phenolic compounds (Table 2) including monochlorophenols and dihydroxybenzenes (Table 3) the D_v values were slightly higher than in 0.1 M acetic acid. When no acetic acid was present, these compounds were held more strongly than in 0.01 M acid. In this case the elution curves were fronting and the peak positions less reproducible. These values are not included in the tables.

The D_v values of the most strongly acidic phenols, e.g. those containing two and more chloro substituents or a carbonyl group linked to an aromatic ring (vanillin, pK = 7.40 and the last compound in Table 2), increased markedly when the eluent concentration was changed from 0.1 M to 0.01 M. The results suggest that these solutes are ionized to an appreciable extent at the lower eluent concentration and that ion exchange contributes significantly

TABLE 2

Volume distribution coefficients (D_v) for Dowex 1-X10 (7—10 μm) in 0.01 M and 0.1 M acetic acid in aqueous ethanol at 30°C

Compound[a]	80% ethanol		40% ethanol
	0.01 M	0.1 M	0.1 M
1 Phenol	1.1	1.09	3.50
2 1,3,5-Trihydroxybenzene	54	47	33
3 R'CH_2OH	0.92	0.86	1.14
4 R'$CH_2CH_2CH_2OH$	0.48	0.46	1.02
5 R'CH(OH)CH(OH)CH_2OH	1.97	1.79	0.59
6 R'CHO	2.05	1.02	2.45
7 R'CH(OH)CH(OH)R'	2.13	2.02	1.27
8 R'CH(OH)CHOR''	0.48	0.41	0.75
9 R'CH(OH)CH_2OR''	0.58	0.50	2.18
10 R'''CH(OH)CHOR''	0.10	0.08	0.27
11 R'CH(OH)CHR'	1.60	1.46	1.08
12 R'$COCH_2$R'	3.46	2.55	8.54

a 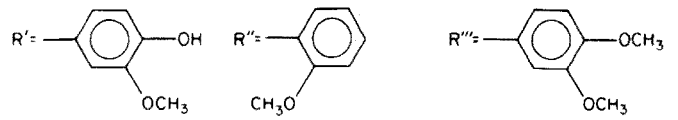

to their retention. A comparison between the observed difference in D_v and published dissociation constants supports this conclusion. In addition, the D_v value of 3-nitrophenol (pK = 8.38 in water) increased by less than 10% while those of 2-nitrophenol (pK = 7.21) and 4-nitrophenol (pK = 7.16) increased by more than 300%.

In 0.01 M acetic acid, those dichlorophenols and trichlorophenols for which data are available [1, 2] appeared in the order of increasing acid strength, while the elution order in 0.1 M acetic acid was reversed for some species. Among the dichlorophenols investigated, 2,6-dichlorophenol is by far the most acidic compound. Large contributions of ion exchange to its D_v explains why it was held much more strongly than its isomers in 0.01 M acetic acid. The observation that it was held less strongly than its isomers in 0.1 M acetic acid is explained by intramolecular hydrogen bonding and steric hindrance for hydrogen bonding with the resin (cf. ref. 4). Similarly the low D_v value of 2-nitrophenol in 0.1 M acetic acid can be ascribed to internal hydrogen bonding.

TABLE 3

Volume distribution coefficients (D_v) in 0.01 M and 0.1 M acetic acid in aqueous ethanol at 30°C on Dowex 1-X10 (7—10 μm)

	80% (w/w) ethanol		73% ethanol
	0.01 M HAc	0.1 M HAc	0.01 M HAc
Phenol	1.1	1.09	1.2
1,2-Dihydroxybenzene	5.5	5.32	4.8
1,3-Dihydroxybenzene	7.3	7.01	6.1
1,4-Dihydroxybenzene	4.4	4.37	3.7
2-Chlorophenol	2.1	1.85	2.2
3-Chlorophenol	1.8	1.60	1.9
4-Chlorophenol	1.6	1.50	1.7
2,3-Dichlorophenol	4.2	3.15	
2,4-Dichlorophenol	3.8	2.75	
2,5-Dichlorophenol	4.3	2.61	
2,6-Dichlorophenol	9.0	1.73	
2,4,6-Trichlorophenol	110	11.5	
2,4,5-Trichlorophenol	16.4	5.04	
3,4,5-Trichlorophenol	5.6	3.35	
2,3,4,5-Tetrachlorophenol	110	15.5	
2-Nitrophenol	8.7	2.25	9.7
3-Nitrophenol	3.0	2.75	3.3
4-Nitrophenol	17.3	5.55	19.8

Table 4 shows that all the benzoic acids investigated were held very strongly in 0.1 M acetic acid in 80% ethanol. Benzoic acid was eluted before the derivatives, and as expected 2-hydroxybenzoic and 2-chlorobenzoic acids, which are the strongest acids, exhibited the highest D_v values. Except for 1,3,5-trihydroxybenzene, all the phenolic compounds studied were eluted ahead of the benzoic acids. This means that this eluent is suitable for a group separation of the benzoic acids from most phenolic compounds. The latter can be obtained as a group or, when desired, separated chromatographically from each other. It is impractical to use this eluent for the elution of the carboxylic acids. Their elution is favoured by an increased acetic acid concentration. Hence an efficient elution of all the species investigated was obtained with 5 M acetic acid in 93% ethanol. To speed up the group separation when 2-hydroxybenzoic acid was present, a higher acetic acid concentration was used, e.g. 7 M.

In 5 M acetic acid in aqueous ethanol the separation factors are favourable for a separation of the individual carboxylic acids (Table 4). The optimum

TABLE 4

Volume distribution coefficients (D_v) of benzoic acids in 0.1 M and 5 M acetic acid in aqueous ethanol at 30°C on Dowex 1-X10 (7—10 μm)

Acid	0.1 M acetic acid	5 M acetic acid	
	80% ethanol	40% ethanol	93% ethanol
Benzoic	33	1.9	1.2
2-Hydroxybenzoic	>200	83	37
3-Hydroxybenzoic	170	7.0	5.9
4-Hydroxybenzoic	58	5.0	4.3
4-Hydroxy-3-methoxybenzoic	41	2.4	2.3
2-Chlorobenzoic	>200	10.8	6.5
3-Chlorobenzoic	145	5.9	2.4
4-Chlorobenzoic	97	4.0	1.6

ethanol concentration depends on the acids present. Hence, benzoic and 4-hydroxy-3-methoxybenzoic acids exhibit a more favourable separation factor at 93% than at 40% ethanol while the reverse holds true for most of the other acids. It should be emphasized that acetic acid in aqueous ethanol is by no means the ideal method for separation of individual aromatic carboxylic acids. The reproducibility is impaired by ester formation which makes it impossible to employ a high elution temperature.

As already mentioned, the group separation can be combined with a separation of individual phenolic compounds. A practical separation at 30°C of six phenols on Dowex 1-X10 is illustrated in Fig. 1A. Under the applied conditions the total retention time for the last compound was 85 min. An identical chromatogram was recorded in a parallel run in which the sample solution in addition to the phenolic compounds contained benzoic, 4-hydroxybenzoic and 4-hydroxy-3-methoxybenzoic acids (5 μg of each).

Variations in the structure of the resin have an influence on the separations. Figure 1B shows that the elution order of the phenolic compounds was the same on Aminex A-28 as on Dowex 1-X10. For some compounds the separation factors were more favourable on the former resin while for others the latter resin was more effective. The effect of the resin on the separation factors was larger than observed during anion-exchange chromatography of strongly polar acids and during partition chromatography of strongly polar nonelectrolytes in aqueous ethanol. The results support the conclusion that several types of sorption mechanisms are involved and that their relative importance depends on the structure of the solutes.

Experiments with Dowex 1-X10 at 70°C showed that, as expected, the peaks were much sharper and that the flow rate could be increased without excessive peak broadening and increase in pressure. The D_v values of phenol and 2,6-dichlorophenol were virtually unaffected, while the D_v values of the other compounds decreased by 25—30%. This means that 2,6-dichlorophenol

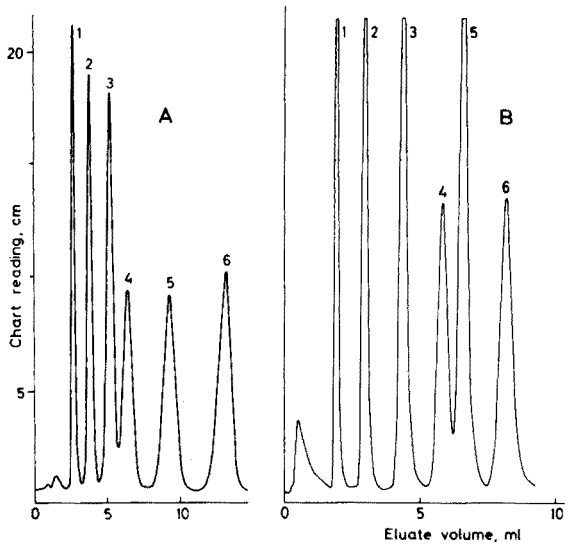

Fig. 1. Separation of: (1) phenol, (2) 2,6-dichlorophenol, (3) 2,5-dichlorophenol, (4) 3,4,5-trichlorophenol, (5) 2,4,5-trichlorophenol, (6) 1,3-dihydroxybenzene at 30°C. Eluent: 0.1 M acetic acid in 80% ethanol. Nominal linear (empty tube) flow: 3.2 cm min^{-1} A. Dowex 1-X10, 7-10 μm (347 × 2.5 mm). Added amounts, 2.0—3.5 μg. B. Aminex A-28, 8—12 μm (346 × 1.9 mm). Added amounts, 0.5—0.8 μg.

and 2,5-dichlorophenol were not separated while a sample from which one of these compounds was excluded was well separated within 50 min at 70°C. In routine analyses of mixtures containing known compounds, it is often possible to take advantage of the improved column efficiency at high temperature. Since our work was directed towards methods for separations of complex mixtures of unknown compounds including those unstable at high temperature, the influence of the temperature was not explored further.

In applications for the analysis of very complex mixtures of aromatic compounds such as those present in spent liquors from pulp mills, it is advantageous to elute the phenolic compounds by stepwise elution with acidified (0.02 M acetic acid) aqueous ethanol of increasing ethanol concentration before the elution of the carboxylic acids.

The financial support of the Swedish Board for Technical Development is gratefully acknowledged.

REFERENCES

1 D. Logie, Analyst, 82 (1957) 563.
2 J. Drahoňovský and Z. Vacek, Collect. Czech. Chem. Commun., 36 (1971) 3431.
3 L. M. Jahangir, L. Olsson and O. Samuelson, Talanta, 22 (1975) 973.
4 L. Olsson, N. Renne and O. Samuelson, J. Chromatogr., 123 (1976) 355.
5 M. Palu and O. Samuelson, Talanta, in press.
6 H. Rückert and O. Samuelson, Acta Chem. Scand., 11 (1957) 303, 315.
7 E. Päärt and O. Samuelson, J. Chromatogr., 85 (1973) 93.

Analytica Chimica Acta, 92 (1977) 337—344

PHTHALDIALDEHYD-REAKTIONSDETEKTOR FÜR DIE HOCHDRUCK-FLÜSSIGKEITS-CHROMATOGRAPHISCHE ANALYSE BIOGENER AMINE

G. SCHWEDT*

Institut für Arbeitsphysiologie an der Universität Dortmund Ardeystrasse 67, D-46 Dortmund (B.R.D.)

(Eingegangen den 1. Februar 1977)

ZUSAMMENFASSUNG

Für die Gruppe der Katecholamine (Adrenalin, Noradrenalin, Dopamin und 3,4-Dihydroxyphenylalanin (Dopa) als Vorstufe der Amine) sowie für Histamin, Serotonin, Tyramin und Tryptamin ergeben sich mit der Hochdruck-Flüssigkeits-Chromatographie (HPLC) sowohl durch Ionenaustausch als auch "reversed-phase"-Chromatographie günstige Möglichkeiten für eine vollständige und schnelle Trennung. Zur empfindlichen fluorimetrischen Bestimmung können die primären Amine mit *o*-Phthaldialdehyd im Anschluß an die HPLC-Säule mit einem Reaktionsdetektor bestehend aus einer Reaktionseinheit mit Flüssigkeits-Dosierpumpe und Fluorimeter umgesetzt werden. Bei möglichst hohen linearen Durchflußgeschwindigkeiten des Reaktionsgemisches aus mobiler Phase und Reagenz im Reaktionssytem kann die Verringerung der HPLC-Auflösung gering gehalten werden.

SUMMARY

A phthalaldehyde reaction detector for the high-pressure liquid chromatography of amines of pharmacological importance

Both ion-exchange and reversed-phase high-pressure liquid chromatography can be used for complete rapid separations of the catecholamine group (adrenaline, noradrenaline, dopamine and 3,4-dihydroxyphenylalanine (Dopa) and of histamine, serotonine, tyramine and tryptamine. For a sensitive fluorimetric determination, the primary amines are treated with *o*-phthalaldehyde in a reaction chamber connected to the h.p.l.c. column and consisting of a Gilson pump, a mixing spiral and a fluorimeter. With the highest possible linear flow velocity of the reaction mixture from the mobile phase and of the reagent in the reaction system, the decrease in the h.p.l.c. resolution can be kept at a low level.

Als "biogen" werden im allgemeinen solche Amine bezeichnet, die in Organismen infolge physiologischer Reaktionen gebildet werden. Seiler et al. [1] rechnen zu dieser Gruppe im engeren Sinn nur die Katecholamine Dopamin, Noradrenalin und Adrenalin sowie Serotonin und Histamin. In die

*Neue Anschrift: Gesamthochschule Siegen, Fachbereich 8, Adolf-Reichwein-Str. 2, D-59 Siegen 21, B.R.D.

vorliegenden Untersuchungen wurden außerdem Tryptamin (als dem Serotonin chemisch verwandte Verbindung), Tyramin (chemisch verwandt mit Dopamin) und das 3,4-Dihydroxyphenylalanin (Dopa) aus dem Katecholamin-Stoffwechsel einbezogen. Für die Bestimmung von Serotonin und Histamin findet vor allem die Umsetzung mit *o*-Phthaldialdehyd zu fluoreszierenden Derivaten Verwendung [2, 3].

Dieses Reagenz setzt sich im Alkalischen in wenigen Minuten mit Verbindungen um, die über primäre Aminogruppen verfügen; es wird in erster Linie zur fluorimetrischen Analyse von Aminosäuren eingesetzt [4, 5]. Am Beispiel dieser Reaktion sollten die Möglichkeiten und Grenzen einer fluorimetrischen Analyse mit einem Reaktionsdetektor [6] nach der hochdruckflüssigkeits-chromatographischen (HPLC-)Trennung verschiedener Substanzen untersucht werden. Ein weiteres Ziel dieser Arbeit war es, die genannten Amine mit Hilfe der HPLC sowohl durch Ionenaustausch als auch "reversed-phase"-Chromatographie zu trennen und mit dem optimierten Reaktionsdetektor auf der Basis der *o*-Phthaldialdehyd-Reaktion empfindlich zu bestimmen.

EXPERIMENTELLER TEIL

Geräte

HPLC. Hochdruckpumpe Modell 6000 A (Waters, Königstein); Probeninjektionssystem Modell U 6 K (Waters); Zweistrahl-Mehrwellenlängen-UV/VIS-Photometer Modell 440 (Waters); 6-Wege-Ventil als Probenaufgabeventil mit 100-μl Schleife ("Valco"-Prinzip; Dupont, Bad Nauheim) für die HPLC mit Reaktionsdetektor.

Reaktionsdetektor, bestehend aus: Gilson Spectro/Glo Filtor Fluorimeter mit "Fluorescamin"-Filtern (Anregung: durchlässig von etwa 350—400 nm, Emission: durchlässig von etwa 440—550 nm, Maximum 500 nm) und Durchflußküvette (Pyrex-Glasrohr, OD 6 mm, ID ca. 4 mm); Gilson Minipuls II Pumpe (Abimed, Düsseldorf) als Flüssigkeits-Dosierpumpe.

Reaktionseinheit. (Fließschema siehe Abb. 1) (aus Hajoka-Ersatzteilen der Fa. Kleinfeld, Hannover); Phasenschlange (Mischspirale) 1,2 ml, 2,4 mm ID (Katalog-Nr. K-157-0202-07); Verbindungsstück HO; Entlüfter C 5; Pumpenschläuche aus Polyäthylen (ID in inch, siehe Abb. 1); Verbindungsschlauch (1/16-in. ID). Die Glasteile sind untereinander bzw. mit den Schläuchen durch Schlauchstücke und "Nipples" (N 5 und N 6) verbunden.

Chemikalien und Lösungen

Adrenalin (L-Adrenalin bitartrat), Noradrenalin (L-Noradrenalin bitartrat) und Isopropylnoradrenalin (DL-Isopropylarterenol hydrochlorid): pharm Serva. Dopamin (3-Hydroxytyramin hydrochlorid) und Dopa (DL-3,4-Dihydroxyphenylalanin): puriss Fluka. Tyramin (Tyramine hydrochloride) Tryptamin (Tryptamine hydrochloride) und Histamin (Histamine dihydrochloride): Regis. Serotonin (5-Hydroxytryptamine oxalate): Sigma.

Alle übrigen Chemikalien mit dem Reinheitsgrad "zur Analyse" (Merck).

Amine und Dopa: in 0,1 N Salzsäure, Stammlösung je 1 mg freien Amins je ml.

Reagenz A (für Katecholamine): 0,05 Vol. % Mercaptoäthanol (reinst; Serva) — 0,04 Gew. % *o*-Phthalaldehyd (z.A.; Serva) in 0,2 M Boratpuffer pH 10.

Reagenz B (für die übrigen Amine): 0,05 Vol. % Mercaptoäthanol — 0,02 Gew. % *o*-Phthalaldehyd in 0,2 M Boratpuffer pH 9.

ERGEBNISSE UND DISKUSSION

Umsetzung mit o-Phthaldialdehyd (OPT)

Die Umsetzung der Amine und der Aminosäure Dopa wurde in Abhängigkeit vom pH-Wert (pH 7—10), von der Konzentration an *o*-Phthaldialdehyd und Mercaptoäthanol in der Reagenzlösung [5] sowie der Pumpengeschwindigkeit im automatischen Analysensystem (Fließschema Abb. 1) ohne Hochdruck-Flüssigkeits-Chromatographen untersucht und optimiert (siehe Tabelle 1).

Für eine Analyse der Substanzen ist im Hinblick auf die Abtrennungsmethoden aus biologischem Material eine Aufteilung in zwei Gruppen sinnvoll. Die Katecholamine und Dopa werden selektiv bei pH 8,4 an Aluminiumoxid adsorbiert (siehe z.B. 7), die übrigen Amine lassen sich durch Flüssig-flüssig-Verteilung abtrennen und anreichern [7].

Für eine gemeinsame Bestimmung in diesen Gruppen ergeben Umsetzungen bei pH 9,5—10 für die Katecholamine und pH 9 für die übrigen Amine mit Reagenzlösungen, die 0,05 % Mercaptoäthanol und 0,04 bzw. 0,02 % *o*-Phthaldialdehyd enthalten, bei einer Pumpengeschwindigkeit von speed

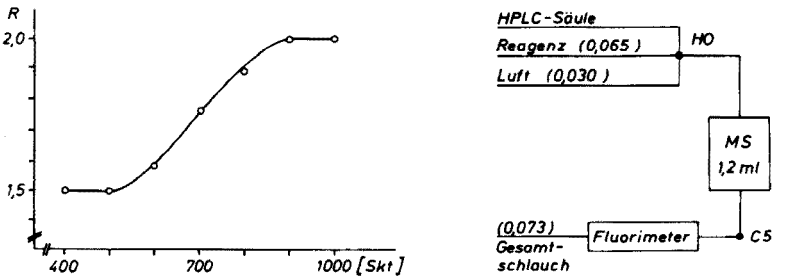

Abb. 1. Fließschema für das automatische Analysensystem (Reaktionssystem) des Reaktionsdetektors. MS = Mischspirale (zur Optimierung der Umsetzungen: statt HPLC-Säule Probenschlauch 0,60-in. ID.).

Abb. 2. Abhängigkeit der Auflösung R im automatischen Analysensystem von der Pumpengeschwindigkeit (Speed-Zahl in [skt]). Probenschlauch 0,60 in. ID, 15-s Saugzeit, 15-s Spülzeit. [Skt der Speed-Zahl] x 0,0043 = [ml min^{-1}] Durchflußrate.

TABELLE 1

Optimale Reaktionsbedingungen für die Umsetzung mit *o*-Phthaldialdehyd im automatischen Analysensystem (siehe Abb. 1)

Verbindung	pH-Wert	*o*-Phthalaldehyd (%)	Mercaptoäthanol (%)	Speed Zahl
Dopa	9,5—10	0,04—0,08	0,05	700
Dopamin	8,5—10	0,01—0,04	0,05—0,2	800
Noradrenalin	9 —10	0,01—0,04	0,05—0,1	800
Histamin	7,5—10	0,01—0,04	0,05—0,2	800—900
Serotonin	7,5—9,5	0,004—0,02	0,05—0,2	800
Tyramin	7,5—9	0,01—0,04	0,05—0,2	700
Tryptamin	7,5—10	0,004—0,01	0,05—0,1	800

700 die höchsten Fluoreszenzausbeuten im beschriebenen Reaktionssystem (Abb. 1). Automatisch-fluorimetrische Systeme auf der Grundlage der Phthaldialdehyd-Reaktion sind z.B. bereits für Serotonin beschrieben worden [8, 9], jedoch unter anderen Reaktionsbedingungen und mit weitaus komplizierteren Reaktionseinheiten, da keine Trennung von anderen Aminen, wie in der vorliegenden Arbeit, durchgeführt wurde.

Einflüsse aus den physikalischen Parametern des automatischen Analysensystems auf die Auflösung getrennter Substanzen

Die Signal-Verbreiterung σ in einem Reaktionssystem kann durch die Segmentierung des Flüssigkeitsstromes mit Luftblasen verringert werden [10]. Infolge der Segmentierung nach dem AutoAnalyzer-Prinzip werden übermäßige Diffusionen verhindert. Nach Deelder und Hendricks [10] haben auf σ die mittlere Stärke des Flüssigkeitsfilms an den Wänden (d), die Länge (L) und der Durchmesser ($2r$) des Reaktionssystems (bzw. der Mischspiralen), die Länge eines Flüssigkeits-Segmentes (l) und die lineare Strömungsgeschwindigkeit im System (Q) einen Einfluß: $\Delta\sigma^2 = 2\pi^2 d\, L\, l\, r^3/Q$.

Bei vorgegebenen geometrischen Abmessungen des Reaktionssystems (Abb. 1) wurde der Einfluß der beiden zuletzt genannten Größen auf die Auflösung geprüft. Die Länge des Flüssigkeits-Segmentes kann durch die Frequenz der Luftblasen, d.h. durch Veränderung des inneren Durchmessers des Luftschlauches, die lineare Strömungsgeschwindigkeit durch die Pumpengeschwindigkeit im Analysensystem beeinflußt werden. Eine Verringerung der Länge der einzelnen Flüssigkeits-Segmente durch die Erhöhung der Luftblasen-Frequenz um den Faktor 3 (Durchmesser des Luftschlauches: 0,03—0,065 in.) ergab keine Verbesserung in der Auflösung zweier Signale. Jedoch konnte zwischen der linearen Strömungsgeschwindigkeit im Analysensystem (dargestellt durch die Pumpengeschwindigkeit = Speed-Zahl) und der Auflösung R eine ausgeprägte Abhängigkeit festgestellt werden (Abb. 2). Die günstigste Auflösung im automatischen Analysensystem wird bei hohen Speed-Zahlen erreicht.

Daraus ergibt sich für die Verbindung einer hochdruck-flüssigkeits-chromatographischen Trennung mit einem automatischen Analysensystem als Reaktionsdetektor die Folgerung, daß die geringsten Verluste an chromatographischer Auflösung durch eine hohe lineare Strömungsgeschwindigkeit im Reaktionsdetektor zu erzielen sind.

Hochdruck-Flüssigkeits-Chromatographie

Die HPLC-Trennung der Katecholamine mit Ionenaustauschern ist bereits häufig beschrieben worden (siehe [11]). Für die einzelnen Untersuchungen wurden verschiedene Puffer mit dem pH 4 als mobile Phasen für die Trennung an Nucleosil 10-SA eingesetzt: Formiat, Acetat, Citrat und Phosphat (0,5 M). Die günstigste Trennung (vollständige Trennung bei kürzester Trennzeit) wurde mit einem 0,5 M Citratpuffer pH 4 erreicht (Abb. 3a).

Die übrigen Amine haben an 10-μm Materialien sehr lange Retentionszeiten [12]. An sauren Ionenaustauschern mit größerem Teilchendurchmesser und geringeren Bödenzahlen wie z.B. Vydac 401-SA gelingt eine Trennung der Amine Tyramin, Tryptamin und Serotonin (Histamin wird vom UV-Detektor bei 280 nm nicht angezeigt) mit Acetat- oder Citratpuffern in wenigen Minuten (Abb. 4a).

Die "reversed-phase"-chromatographische Trennung der Katecholamine an speziell vorbehandeltem ODS/TMS-Kieselgel (6 μm) mit einer mobilen

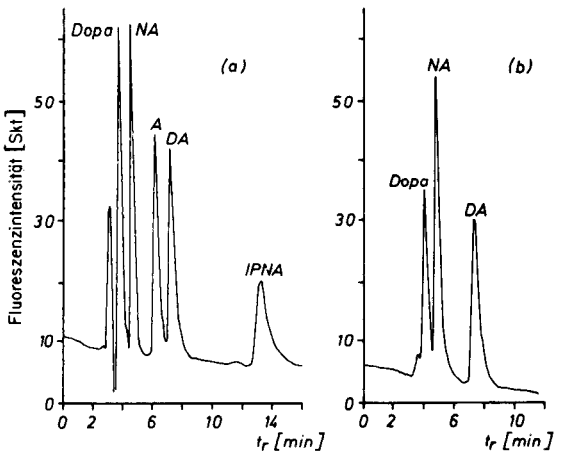

Abb. 3. HPLC-Trennung (Ionenaustausch) der Katecholamine (Dopa = 3,4-Dihydroxyalanin, NA = Noradrenalin, A = Adrenalin, IPNA = Isopropylnoradenalin). Säule, 300 mm × 4 mm ID. Packungsmaterial, Nucleosil 10-SA. Mobile Phase, 0,5 M Na-Citrat-Puffer pH 4. Durchfluß, 1 ml min^{-1}. Druck, 105 bar. Temperatur, 20°C. Dosiervolumen, (a) 25 μl (je 500 ng der Amine), (b) 100 μl (je 500 ng der Amine).

(a) UV-Detektor, 280 nm, 0,05 AUFS. (b) Reaktionsdetektor, Reagenz A, speed 900, Fluorimeter 1/100 der maximalen Empfindlichkeit.

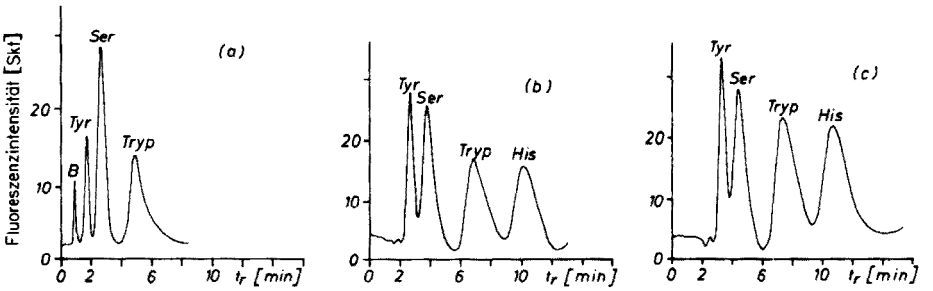

Abb. 4. HPLC-Trennung (Ionenaustausch) von Tyramin (Tyr), Tryptamin (Tryp), Serotonin (Ser) und Histamin (His) (B = Blindwert) Säule, 500 mm × 2,1 mm ID. Packungsmaterial, Vydac 401-SA trocken gepackt. Mobile Phase, 0,2 M Na-Acetat-Puffer pH 6. Durchfluß, 2 ml min^{-1}. Druck, 112 bar. Temperatur, 19°C. Dosiervolumen, wie Abb. 3.

(a) UV-Detektor, 280 nm. (b) Reaktionsdetektor, Reagenz B, speed 900. (c) Reaktionsdetektor, Reagenz B, speed 400. Empfindlichkeiten der Detektoren wie Abb. 3.

Phase aus Acetonitril—Wasser—konz. Schwefelsäure (10:90:0,3 v/v) wurde von Knox und Pryde [13] bzw. Knox und Jurand [14] mitgeteilt. An Nucleosil 10-C_{18} sind Trennungen der Katecholamine mit rein wäßrigen Formiat puffern [11] möglich. Die k'-Werte für Noradrenalin, Dopamin und Dopa sind pH-abhängig (Abb. 5), bei etwa pH 3,2 ist die Trennung am günstigsten (Abb. 6a). Für die zweite Gruppe der Amine kann der mobilen Phase Methanol zugesetzt werden, um kurze Trennzeiten bei vollständiger Trennung zu erreichen (Abb. 7a).

Die Ergebnisse aus der Verbindung der HPLC-Trennung mit dem Reaktionsdetektor zeigen die Abbildungen 3b, 4b, 6b. Erst unter diesen Bedingungen gelingt es, Histamin im Chromatogramm durch die fluorimetrische

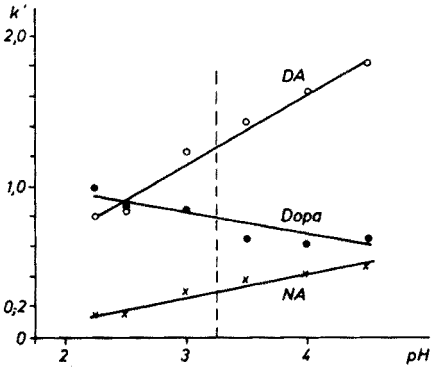

Abb. 5. pH-Abhängigkeit der k'-Werte für Noradrenalin (NA), Dopamin (DA) und Dopa bei der "reversed-phase"-Chromatographie (0,2 M Formiatpuffer) Säule und sonstige Bedingungen wie Abb. 6.

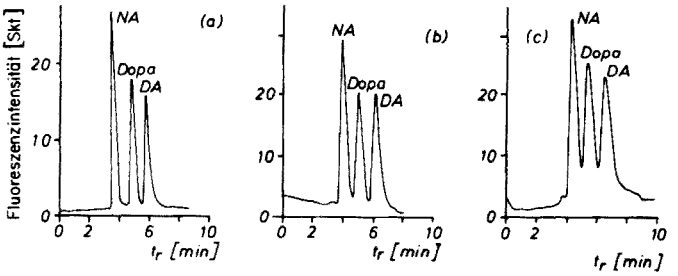

Abb. 6. HPLC-Trennung ("reversed-phase") der Katecholamine. Säule, Fertigsäule (Macherey—Nagel) 200 mm × 4 mm ID. Packungsmaterial, Nucleosil 10—C_{18}. Mobile Phase, 0,2 M Na-Formiatpuffer pH 3,2. Durchfluß, 1 ml min^{-1}. Druck, 91 bar. Temperatur, 20°C. Dosiervolumen, siehe Abb. 3.

(a) UV-Detektor. (b) Reaktionsdetektor, speed 900. (c) Reaktionsdetektor, speed 400. Übrige Angaben siehe Abb. 3.

Anzeige zu erkennen (Abb. 4b u. 7b). Den Einfluß der Pumpengeschwindigkeit (Speed-Zahl) auf die Trennung zeigt der Vergleich der Chromatogramme 4b and 4c sowie 6b and 6c.

Die Verbindung der HPLC-Trennung mit der anschließenden Umsetzung mit *o*-Phthaldialdehyd in dem beschriebenen Reaktionsdetektor eröffnet somit Möglichkeiten zur schnellen und empfindlichen fluorimetrischen Analyse biogener Amine in biologischem Material. Adrenalin als sekundäres Amin kann jedoch durch diese Reaktion nicht erfaßt werden.

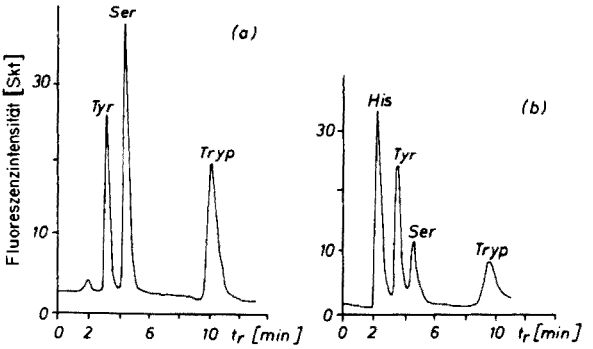

Abb. 7. HPLC-Trennung ("reversed-phase") von Tyramin, Tryptamin, Serotonin und Histamin. Säule, wie Abb. 6. Mobile Phase, 10% Methanol—90% 0.2 M Ameisensäure. Durchfluß, 1 ml min^{-1}. Druck, 91 bar. Dosiervolumen, wie Abb. 3.

(a) UV-Detektor. (b) Reaktionsdetektor (Reagenz B). Übrige Angaben, siehe Abb. 3.

LITERATUR

1 N. Seiler, L. Demisch und H. Schneider, Angew. Chem., 83 (1971) 53.
2 M. Yusem et al., Anal. Chim. Acta, 44 (1969) 403.
3 R. P. Maichel und F. D. Miller, Anal. Chem., 38 (1966) 1937.
4 M. Roth, Anal. Chem., 43 (1971) 880.
5 J. R. Benson und P. E. Hare, Proc. Nat. Acad. Sci. U.S.A., 72 (1975) 619.
6 G. Schwedt, Chromatographia, 10 (1977) 92.
7 S. Udenfriend, Fluorescence Assay in Biology and Medicine, Academic Press, New York, 1964 and 1969.
8 J. Korf, H. H. Schutte und K. Venema, Anal. Biochem., 53 (1973) 146.
9 J. D. Peuler und P. G. Passon, Anal. Biochem., 52 (1973) 574.
10 R. S. Deelder und P. J. H. Hendricks, J. Chromatogr., 83 (1973) 343.
11 G. Schwedt, J. Chromatogr., Biomed. Applic., (1977) im Druck.
12 L. J. Riceberg, R. H. Abiles und H. Van Vunakis, in Application AH343 Catecholamines, Waters, U.S.A., 1974.
13 J. H. Knox und A. Pryde, Advan. Chromatogr., Proc. X, Int. Symp., 3—6 Nov. 1975, München (1975) 171.
14 J. H. Knox und J. Jurand, J. Chromatogr., 125 (1976) 89.

Analytica Chimica Acta, 92 (1977) 345—352

SOME APPLICATIONS OF BONDED-PHASE HIGH-PERFORMANCE LIQUID CHROMATOGRAPHY TO THE ANALYSIS OF PHARMACEUTICAL FORMULATIONS

G. B. COX, C. R. LOSCOMBE and K. SUGDEN

Laboratory of the Government Chemist, Cornwall House, Stamford Street, London SE1 9NQ (Great Britain)

(Received 15th April 1977)

SUMMARY

Chromatographic procedures are presented for the determination of guaiphenesin, phenylephrine hydrochloride, phenylpropanolamine hydrochloride, pholcodine, methyl and propyl 4-hydroxybenzoates, and tyrothricin in some pharmaceutical products. An investigation of the contamination of lozenges with aspirin, paracetamol, phenacetin, prednisone and prednisolone is reported, together with the preparation of a novel bonded weak cation-exchange packing used.

Analytical investigation of pharmaceutical products encompasses the determination of a vast and ever-increasing range of compounds. The analysis of complex mixtures and the detection of traces of contaminants are problems for which conventional methods can be both tedious and difficult. Many obstacles may be overcome by the use of methods based on high-pressure liquid chromatography (h.p.l.c.): approximately one-third of the papers published in this field are devoted to pharmaceutical or closely related problems [1]. Unfortunately, many of the published chromatographic systems are designed for the analysis of pure materials rather than of formulated products which, by their nature, can limit the usefulness of a particular procedure. This paper reports the application of h.p.l.c. to the analysis of some formulated pharmaceutical products; bonded-phase microparticulate column packing materials are particularly useful in such analyses.

EXPERIMENTAL

Chromatographic apparatus

The work was performed with instruments previously assembled within this Laboratory from a variety of commercially available equipment [2—4]. Columns, made from stainless steel tubing (15 cm × 4.6 mm i.d.), were packed by the procedure previously reported [2].

TABLE 1

Methods of sample preparation and chromatographic conditions of analysis

Compound	Type of sample	Preparation of sample	Column	Mobile phase	Flow rate (ml min^{-1})	λ (nm)
1 Tyrothricin	Lozenges	2.5 g continuously extracted for 1 h in ethanol, made up to 10 ml	ODS	80% methanol 20% water	1	220
2 Methyl and propyl 4-hydroxybenzoates	Ointment	0.5 g dissolved in 5 ml chloroform, made to 10 ml with methanol	ODS	60% methanol 40% water	1	257
3 Pholcodine	Linctus	25 ml linctus diluted to 50 ml with methanol	ODS	methanol with pH adjusted to 8.9 with 5 M aqueous NH_3	1	220
4 Guaiphenesin, phenylephrine hydrochloride and phenylpropanolamine hydrochloride	Cough mixture	10 ml diluted to 100 ml with water	SCX	0.1 M KH_2PO_4 in 10% aqueous ethanol at pH 4.4	0.5	198
5 Contamination study	Lozenges	0.5 g ground lozenge dissolved in 10 ml ethanol	WCX	0.005 M ammonium formate in 2.5% aqueous ethanol	0.5	240
Phenacetin, Prednisolone, Prednisone						
Paracetamol, Aspirin			ODS	70% methanol 30% water	0.5	240

chromatography for the analysis of complex mixtures such as pharmaceutical formulations is that the equilibration processes are rapid [6]. Compounds not eluted under the conditions necessary for analysis may be removed periodically by a change in mobile phase composition without incurring the penalty of lengthy re-equilibration processes. Hence clean-up of the samples may be reduced to a minimum; this, in turn, leads to a faster and more accurate analysis.

Determination of tyrothricin

Tyrothricin is a peptide mixture obtained as an alcohol-soluble fraction from *Bacillus brevis* fermentation, and is used for treatment of infections of the mouth and throat and of wounds and burns. Among antibiotics it is notable for its relatively high toxicity. It is of current interest as it will be controlled under a proposed EEC cosmetics directive. The major constituents of tyrothricin are the decapeptides (60—80%); the remainder consists of gramicidins [7]. Currently the commonest analytical method for tyrothricin is based on a microbiological examination although, under favourable circumstances, a spectro photometric method may be employed. Chromatography of tyrothricin USP on a microparticulate reversed-phase column with aqueous methanol as mobile

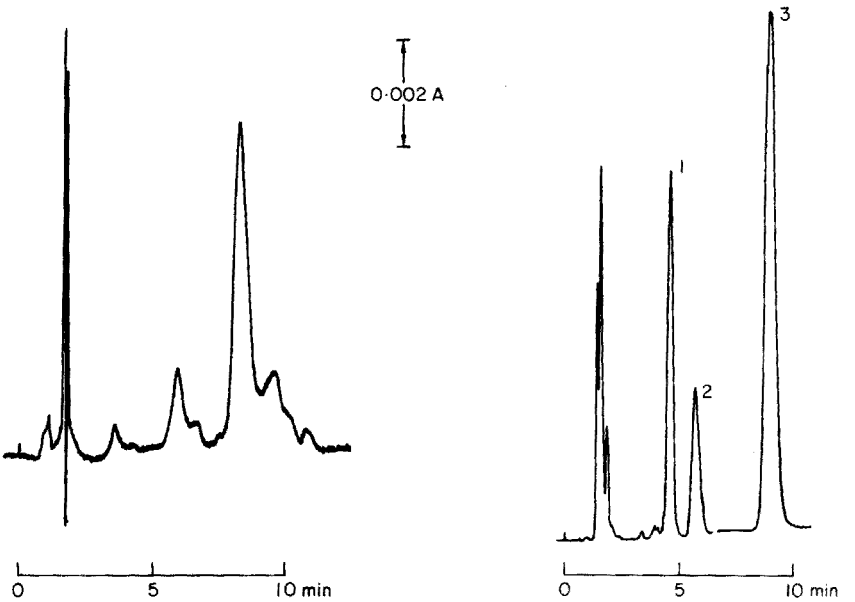

Fig. 1. Chromatogram of tyrothricin USP standard. Sample size, 600 ng. Column, Spherisorb S5.ODS, 15 cm × 4.6 mm. Eluent, 80% methanol—water at a flow rate of 1 ml min^{-1}. Detector wavelength, 220 nm.

Fig. 2. Analysis of an elixir. 1, Phenylephrine hydrochloride (88 ng); 2, Phenylpropanolamine hydrochloride (101 ng); 3, Guaiphenesin (1.6 μg); Column, Spherisorb S5W—strong cation exchanger, 15 cm × 4.6 mm. Eluent, 0.1 M potassium dihydrogenphosphate in 10% aqueous ethanol, pH 4.6, at a flow rate of 1 ml min^{-1}. Detector wavelength, 198 nm.

phase gave rise to five distinct peaks (see Fig. 1) when a detector wavelength of 220 mm was used. Under the conditions of analysis, neither benzocaine nor cetylpyridinium chloride, which are often present in tyrothricin formulations, were retained by the column. Since tyrothricin is soluble in ethanol and is stable at 100°C for at least 1 h [7], a procedure involving Soxhlet extraction of ground tablets with ethanol for 1 h was employed; extraction for longer periods did not increase the recovery of tyrothricin. The extracts gave chromatograms sufficiently similar to standard tyrothricin for the determination to be carried out by comparison of the heights of the major peaks. The limit of detection (defined as thrice the baseline noise level) corresponded to 60 ng of tyrothricin as injected.

Determination of methyl and propyl 4-hydroxybenzoates

Methyl and propyl 4-hydroxybenzoates are used as preservatives for foods, cosmetics, and pharmaceuticals. They are active against moulds, fungi, and yeasts. Reports of their determination in foodstuffs and pharmaceuticals by h.p.l.c. with silica [5], anion-exchange [8], polysiloxane Permaphase ETH [9] and ODS [10] packings have been published. Consideration of the problem of the determination of the esters in an ointment suggested the use of a microparticulate octadecyl reversed-phase column packing. It was intended that the ointment should be dissolved and analysed without further treatment; since it contained appreciable quantities of water, the use of adsorption chromatography was ruled out. Ion-exchange or reversed-phase columns requiring a predominantly aqueous mobile phase were not used because of the likelihood of precipitation of water-insoluble excipients. The microparticulate column packing required a relatively high methanol concentration in the mobile phase and dilution of the dissolved sample in the latter produced no visible precipitation. In addition, the microparticulate column packing can cope with small quantities of precipitated material more efficiently than the pellicular packings by virtue of its higher surface area. The ointment, a formulation containing 2% antazoline hydrochloride, 0.2% methyl 4-hydroxybenzoate and 0.1% propyl 4-hydroxybenzoate, was dissolved in 50% chloroform—ethanol (v/v); extraction with ether or ethanol alone gave erroneous results. Analysis of the solution resulted in separation of the two esters within 8 min with no interference from the other components.

Determination of pholcodine

Pholcodine, the 3-(2-morpholinoethyl) ether of morphine, has cough suppressant and mild sedative action. It is frequently used in association with ephedrine, menthol, eucalyptol, guaiphenesin, and many other materials. In common with many basic materials, pholcodine is not eluted from microparticulate reversed-phase columns at neutral pH, nor, presumably because of the strongly basic morpholino group, even with pure methanol as mobile phase. Adjustment of the eluent to an apparent pH of 8.9 with 5 M aqueous ammonia, however, resulted in the elution of pholcodine with a retention

time of 10.8 min. Analysis of the sample was achieved simply by dilution and injection. The advantage of the chromatographic system employed is that only very strongly basic materials were retained; neutral components in the formulation were rapidly eluted and did not interfere with the analysis.

Determination of guaiphenesin, phenylephrine hydrochloride, and phenylpropanolamine hydrochloride

Phenylephrine and phenylpropanolamine hydrochlorides are sympathomimetic agents used in the treatment of hypertensive states and as nasal decongestants. Guaiphenesin (3-(*o*-methoxyphenoxy)propane-1,2-diol) is an expectorant; in large quantities it functions as a skeletal muscle relaxant. All three compounds are used in formulations for the treatment of colds. No single liquid chromatographic system for their analysis has been published. Liquid chromatographic analyses of phenylephrine [11] and phenylpropanolamine [12] have been carried out individually on strong cation-exchange columns, but under vastly different mobile phase conditions; guaiphenesin has been separated from paracetamol, biclotymol, and neosynephrine on silica gel [5]. A microparticulate bonded-phase strong cation exchange packing material prepared in this laboratory [2] was used for the separation of phenylephrine and phenylpropanolamine hydrochlorides with 0.1 M potassium dihydrogenphosphate in 10% aqueous ethanol as mobile phase. Fortuitously, the neutral guaiphenesin was also eluted under these conditions. The separation of neutral molecules on resin-based ion-exchangers is well documented, and simple experiments were carried out to determine if this somewhat unexpected result fell into such a category. On reduction of the ionic strength of the mobile phase by 50%, the peaks given by phenylephrine and phenylpropanolamine were observed at longer retention times whilst that of guaiphenesin maintained its original value. Further evidence for a partition mechanism for guaiphenesin was obtained from measurement of its capacity factor k' at three different solvent compositions; k' had values of 24, 14, and 12 for water, water—ethanol (19:1) and water—ethanol (9:1), respectively. The extinction coefficients for u.v. absorption of both phenylephrine and phenylpropanolamine hydrochlorides at wavelengths above 210 nm are too low for the reliable analysis of formulations containing ca. 0.1% of either compound. Studies with various substances have shown that the use of end absorption for chromatographic detection has a similar precision to the more conventional employment of absorption maxima in other regions of the u.v. spectrum. Thus at 198 nm, the lowest wavelength attainable with the detector (CE 212 variable wavelength u.v. monitor), as little as 1 ng of each of the components injected could be detected. A chromatogram for an elixir containing all three components is shown in Fig. 2. Brompheniramine maleate, which was also present, was not eluted under the chromatographic conditions employe

Contamination studies

A difficult problem in the area of pharmaceutical analysis is that of products cross-contaminated by other drug substances. This occurs with drugs such as

steroidal hormones which can have a marked physiological effect when administered in microgram quantities. A review of methods for the detection of cross-contamination has recently been published [13].

Lozenges containing the bacteriostatic agent ambazone have been investigated. Contamination with a wide range of drugs, e.g. aspirin, paracetamol, phenacetin, prednisolone and prednisone, was suspected. The separation of aspirin, paracetamol, and phenacetin on strong cation-exchange columns is well known [14] but attempts to employ a microparticulate cation exchanger were foiled by co-elution of components from the lozenges with the compounds of interest. A new weak cation-exchange column gave a separation of all five possible contaminants (see Fig. 3) although aspirin and paracetamol were eluted very close to the solvent and were obscured by components from the lozenges. Such conditions, nevertheless, could be used for the analysis of formulations containing some or all five compounds as major components. The use of phenacetin in medicines is now actively discouraged; the system described represents a convenient, rapid screening of formulations which may contain it. No single system enabled all five compounds to be separated from each other as well as from those in the lozenges. Two systems, the weak

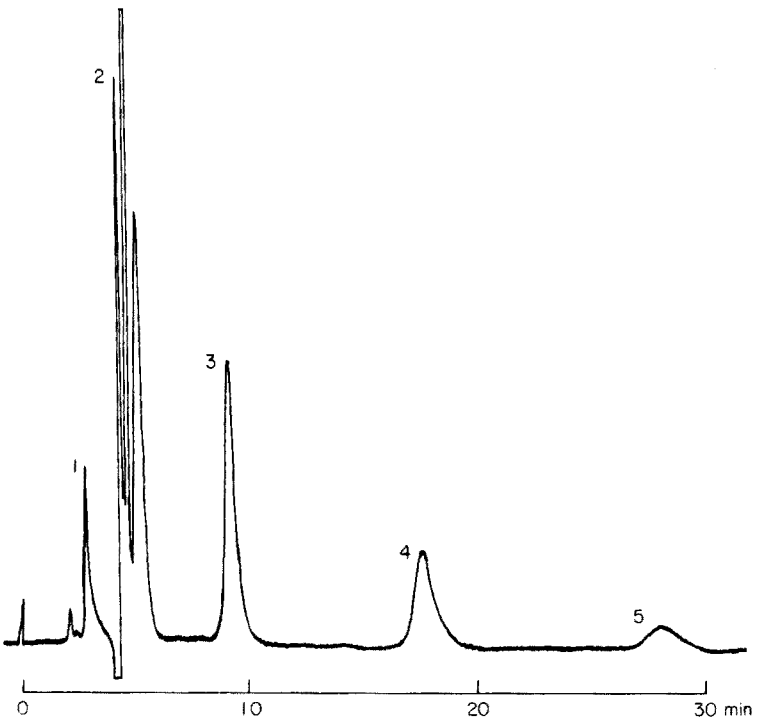

Fig. 3. Chromatogram of aspirin (24 ng)(1), paracetamol (29 ng) (2), phenacetin (27 ng) (3), prednisone (11.8 ng) (4) and prednisolone (36 ng) (5). Column, weak cation-exchange packing prepared from bis(3-chloropropyl)silyl-substituted LiChrosorb SI60, 15 cm × 4.6 mm. Eluent, 0.005 M ammonium formate in 2.5% aqueous ethanol at 0.5 ml min^{-1}. Detector wavelength, 240 nm.

cation-exchanger for phenacetin, prednisolone and prednisone and an octadecyl reversed-phase packing for aspirin and paracetamol were therefore employed. For a 5% solution of the ground lozenge, the detection limits for aspirin, paracetamol, phenacetin, prednisone and prednisolone were 0.016, 0.001, 0.002, 0.006 and 0.008%, respectively. The levels quoted for the two steroids are much higher than those which are potentially harmful, thus for such compounds the present method is limited to gross contamination studies. The same weak cation-exchanger column was also used to check for phenacetin contamination of tablets containing aspirin, chloroquine and prednisolone; the weak cation exchanger was prepared via a route similar to that reported previously [2] except that a dichlorosilane with two chloropropyl groups was used in place of monochloropropyltrichlorosilane. Although it was hoped that this would give a final product with a capacity higher than the previous material, the two phases were similar in this respect; the new material gave 0.24 meq g^{-1} compared with 0.17 meq g^{-1} for the earlier ion-exchanger. It is probable that the differences between the two weak ion-exchangers result from non-ionic groups on the surface of the silica which arise from hydrolysis of the 3-chloropropyl function. The reasons for the reaction of a lower proportion of chloropropyl groups with β-alanine in the bis-substituted phase than in the other are not clear: presumably, either the rate of hydrolysis in the phase is greater because of synergic effects of the second chloropropyl group, or the acid group, once bonded, sterically hinders further substitution.

We thank colleagues in the Health Services Division of this Laboratory for the supply of some challenging samples and standard materials, and for constructive comment on this paper.

REFERENCES

1 J. H. Knox, J. Jurand and A. Pryde, Proc. Anal. Div. Chem. Soc., 13 (1976) 14.
2 G. B. Cox, C. R. Loscombe, M. J. Slucutt, K. Sugden and J. A. Upfield, J. Chromatogr., 117 (1976) 269.
3 G. B. Cox, J. Chromatogr., 83 (1973) 471.
4 G. B. Cox, J. Chromatogr., 116 (1976) 244.
5 M. Caude and Le Xuan Phan, Chromatographia, 9 (1976) 20.
6 R. E. Majors, Bonded Stationary Phases in Chromatography, Ann Arbor, 1974, 139.
7 Martindale, The Extra Pharmacopoeia, Pharmaceutical Press, 26th edn, 1974.
8 J. J. Nelson, J. Chrom. Sci., 11 (1973) 28.
9 M. J. Saxby, BFMIRA Tech. Circular, 557 (1974).
10 R. H. King, L. T. Grady and J. T. Reamer, J. Pharm. Sci., 63 (1974) 1591.
11 T. C. Kram, FDA By-lines, 1 (1974) 290.
12 T. L. Spriek, J. Pharm. Sci., 63 (1974) 591.
13 G. F. Phillips, Process Biochem., 11 (1976) 3.
14 J. H. Knox and J. Jurand, J. Chromatogr., 82 (1973) 398.

Analytica Chimica Acta, 92 (1977) 353—360

A POLAROGRAPHIC STUDY OF SOME *N*-OXYGENATED PRODUCTS OF *N*-ETHYL-β-METHOXY-β-(3′-TRIFLUOROMETHYLPHENYL)-ETHYLAMINE (SK AND F 40652A)

A. H. BECKETT, N. N. RAHMAN and W. FRANKLIN SMYTH*†

Pharmacy Department and †Chemistry Department, Chelsea College, University of London, Manresa Road, London SW3 6LX (England)

(Received 22nd March 1977)

SUMMARY

The polarographic behaviour of *N*-hydroxy-β-methoxy-β-(3′-trifluoromethylphenyl)-ethylamine, *N*-ethyl-*N*-hydroxy-β-methoxy-β-(3′-trifluoromethylphenyl)ethylamine and β-methoxy-β-(3′-trifluoromethylphenyl)acetaldoxime has been studied over the pH range 0—14. The hydroxylamines gave rise to anodic and cathodic behaviour whereas the oxime gave only a cathodic wave. The mechanism of the oxidation and reduction processes was investigated by d.c. polarography and preparative micro-coulometry. The optimum pH values for analytical purposes were 7, 8 and 4 for the two hydroxylamines and the oxime, respectively. The polarographic behaviour of a mixture of the three compounds was studied and the determination of traces of such compounds by differential pulse polarography is discussed.

N-Hydroxy-β-methoxy-β-(3′-trifluoromethylphenyl)ethylamine (II), *N*-ethyl-*N*-hydroxy-β-methoxy-β-(3′-trifluoromethylphenyl)ethylamine (III) and β-methoxy-β-(3′-trifluoromethylphenyl)acetaldoxime (IV) are the three important in vitro metabolic products of *N*-ethyl-β-methoxy-β-(3′-trifluoromethylphenyl)ethylamine (I) [1] which is being investigated clinically as an anorectic agent and is structurally similar to the non-stimulant anorectic drug fenfluramine. Since the hydroxylamines (II, III) are not amenable to gas—liquid chromatography and are difficult to separate from the oxime (IV)

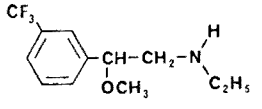

I

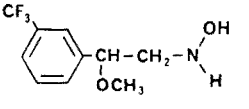

II

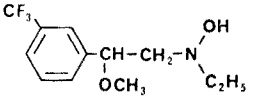

III

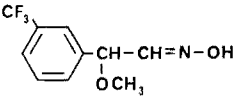

IV

by t.l.c., a direct sensitive polarographic method of analysis of these compounds was investigated. Unlike the parent amine (I) and the oxime (IV), the corresponding hydroxylamine may be oxidized at the dropping mercury electrode as has been demonstrated for some aliphatic hydroxylamines in alkaline media [2—4]. The mechanism was thought to involve formation of the nitroso derivative involving a 2e step [3] but the value of n was less than 2, probably because of competing side-reactions.

The electrochemical reduction of a number of oximes has been investigated [5]. In acidic solution, these oximes exhibited a single pH-dependent wave which disappeared on increasing the pH. The mechanism of reduction involved four electrons resulting in the formation of the parent amine. The waves obtained for many oximes are, however, affected by the concentration and nature of the supporting electrolyte and competing hydrolytic reactions (as demonstrated in the determination of cyclohexanoxime [6]); care must be taken to find the optimum conditions for analysis.

EXPERIMENTAL

Apparatus

A polarographic analyser (PAR Model 174) connected with a recorder (Bryan XY-26000 A4) operated in the sampled-d.c. and differential pulse modes, was used in conjunction with a 3-electrode cell with a platinum counter electrode and a saturated calomel reference electrode [7]. The scan speed was 2 mVs^{-1} and the dropping mercury electrode had the following characteristics: outflow velocity $m = 1.73 \cdot 10^{-6}$ kgs^{-1}; drop time, $t = 2.03$ s at the potential of the saturated calomel electrode and at a mercury height of 0.5 m. Preparative constant-potential microcoulometry was carried out in a cell with a mercury pool electrode, connected to the polarograph [7].

Preparative thin layer chromatography was performed on glass plates (20 × 20 cm) coated with Silica Gel GF254 (0.5 mm thickness) in the solvent systems chloroform—methanol (4:1) and benzene—ethyl acetate (3:1). Spots were detected under u.v. with reference to known compounds.

Gas—liquid chromatography was conducted with a Perkin-Elmer F11 gas chromatograph with a flame ionization detector and a Hitachi Perkin-Elmer Model 56 1-mV recorder. The column used was 1 m long, with o.d. 6.25 mm, i.d. 3 mm. The glass column contained A/W DMCS-treated GasChrom W.HP(80-100 mesh) coated with 7.5% carbowax 20 M and conditioned at 190°C for 24 h before use. Operating conditions were 109 ml N_2 min^{-1}; H_2 pressure, 1.4 kg cm^{-2}; air pressure, 1.05 kg cm^{-2}; oven temperature, 140°C.

Mass spectra (solid inlet) of the electrolysis products from preparative experiments were recorded on a VG micromass 12F at an ionization potential of 70 eV.

E.s.r. experiments were carried out with a Varian E-4 EPR spectrometer.

Reagents and compounds

Samples of the *N*-hydroxy compounds (II, III) and the oxime (IV) were synthesized from the corresponding amines [1]. Stock solutions of each compound (10^{-3} M) were prepared in AnalaR methanol and kept under refrigeration. A stock Britton—Robinson BR buffer solution (pH 2.0), 0.04 M in boric acid, phosphoric acid and acetic acid, was prepared from AnalaR reagents. From this stock solution, buffer solutions of varying pH were prepared by suitable addition of 0.2 M sodium hydroxide. Sulphuric acid (0.1 M) and 1 M hydrochloric acid were prepared from the AnalaR materials. Other compounds were of analytical grade and organic solvents were redistilled before use.

Procedures

For the mechanistic studies, d.c. (or sampled-d.c.) polarography was used. The buffer (4.5 ml) of appropriate pH was deaerated with nitrogen for 3 min; 0.5 ml of the 10^{-3} M stock solution of the electroactive species was added. After deaeration for a further 30 s the *i*—*E* curves were recorded at scan rate 2 mVs^{-1}, modulation amplitude 100 mV and time constant 0.3 s.

For the microcoulometric experiments, 10 ml of a 10^{-3} M solution of the hydroxylamine (II) in buffer pH 7.0/10% MeOH was deaerated for 10 min before applying a potential (relating to the plateau of the wave, i.e. +0.05 V) across the cell for 30 min. A similar experiment was carried out at —1.35 V for the oxime (IV) in buffer pH 4.0/10% MeOH. In both cases, aliquots of the electrolysis mixture were taken after each 10 min; the products were extracted into chloroform and subjected to e.s.r. in an attempt to identify any long-lived free radical intermediates. At the end of the electrolysis, the products of the hydroxylamine (II) oxidation were extracted with diethyl ether at neutral pH, whereas for the oxime the pH was adjusted with 5 M NaOH to pH 8 before extraction with ether. The electro-oxidation and reduction products were identified by g.l.c. and mass spectrometry in relation to appropriate reference samples.

Calibration curves were recorded in the differential-pulse mode for both the anodic and cathodic waves of the primary hydroxylamine (buffer pH 7.0/10% MeOH), the anodic wave of the secondary hydroxylamine (buffer pH 8.0/10% MeOH) and the cathodic wave of the oxime (buffer pH 4.0/10% MeOH).

RESULTS AND DISCUSSION

Variation of $E_{1/2}$ and i_{lim} with pH

Cathodic and anodic behaviour of N-*hydroxy-β-methoxy-β-(3'-trifluoromethylphenyl)ethylamine (II).* The d.c. polarographic investigation of the primary hydroxylamine (II) yielded a reduction wave in the pH range 3—8 ($i_{c'}$) corresponding to the reduction of the protonated form. Above pH 8 a further ill-defined cathodic wave appeared ($i_{c''}$) which might be due to

reduction of the CF_3 group, since unprotonated aliphatic hydroxylamines are not reducible.

The variation of $E_{1/2}$ with pH for $i_{c'}$ showed two linear portions giving an inflexion at pH 6 which can be associated with the polarographic pK_a value of the primary hydroxylamine (II). This is in agreement with the value of 4.01 obtained by potentiometric titration since polarographic pK_a values are generally several units higher than the corresponding pK_a values.

The primary hydroxylamine gave a well-defined anodic wave in the pH range 6—8, corresponding to oxidation of the unprotonated form. Above pH 8 the main wave began to disappear with the appearance of several small waves, presumably because of adsorption processes. The total wave height corresponding to these anodic processes remained constant in this pH region. The $E_{1/2}$ for the main anodic wave varied linearly with pH, i.e. 90 mV per pH unit. The main wave was diffusion-controlled at pH 7 since i_{lim} varied linearly with $h^{1/2}$.

Anodic and cathodic behaviour of N-*ethyl*-N-*hydroxy*-β-*methoxy*-β-(3′-*trifluoromethylphenyl)ethylamine (III).* The variation of $E_{1/2}$ with pH for the anodic oxidation of the secondary hydroxylamine (III) was performed in the pH range 6—9. At pH 7 an ill-defined anodic wave was close to the decay curve of the supporting electrolyte but below pH 7 no anodic wave was observed. The best anodic wave was at pH 8 ($E_{1/2}$ = —0.03 V) where the process was diffusion-controlled. The cathodic behaviour of this compound was also similar to that of the primary hydroxylamine (II).

Cathodic behaviour of β-*methoxy*-β-(3′-*trifluoromethylphenyl)-acetaldoxime (IV).* This compound (IV) showed no anodic behaviour but gave rise to a well-defined cathodic wave in the range pH 2—5. At higher pH values, the oxime yielded an ill-defined wave. Plots of i_{lim} vs. h and i_{lim} vs. $h^{1/2}$ showed the wave at pH 4 to be diffusion-controlled.

Determination of αn_α and p values

For the anodic wave of the primary hydroxylamine (II) in buffer pH 7/10% MeOH, a plot of $E_{d.e.}$ vs. log $(i_d - i)/i$ gave a slope of 0.045 V and an intercept on the E axis of —0.071 V which corresponded to the $E_{1/2}$ value. The value of αn_α calculated from the slope was 1.3. The plot of $E_{d.e.}$ vs. log $(i_d - i)/i$ for the anodic wave of secondary hydroxylamine (III) in buffer pH 8.0/10% MeOH, however, gave 2 linear portions with αn_α values of 0.92 and 0.62. A plot of $E_{d.e.}$ vs. log $i/(i_d - i)$ for the cathodic wave of the oxime (IV) (buffer pH 4/10% MeOH) yielded a value of αn_α of 0.375.

The number of protons p involved in the rate-determining steps of the electrochemical oxidations and reduction was calculated from the equation $dE_{1/2}/d\,pH = -0.059\, p/\alpha n_\alpha$. Values of 2.2, 0.864 and 1 were obtained for the primary and secondary hydroxylamines (II, III) and the oxime (IV) respectively.

Controlled-potential microcoulometry

When controlled-potential microcoulometry experiments were carried out on 10^{-3} M solutions of the hydroxylamine (II) and the oxime (IV), the

oxidation and reduction waves of the parent compounds dropped to 10—20% of their original heights, and the polarographic scan showed no oxidation or reduction waves other than those of the remaining hydroxylamine (II) and the oxime (IV). Aliquots (2 ml) taken after electrolysis for 10 and 20 min were extracted into chloroform and examined by e.s.r.; traces of free radicals were not detected.

T.l.c. and g.l.c. of the electrolysis products of the electrooxidation of the hydroxylamine (II) showed three products apart from the hydroxylamine (II). The mass spectral analysis of the extracts of the spots obtained from the t.l.c. plates showed that the main oxidation product was the oxime (IV). The other two products were the hydrolytic products, i.e. α-hydroxy-α-(3′-trifluoromethylphenyl)acetaldehyde (V) and 3′-trifluoromethylphenylglyoxal (VI), [1]. T.l.c. and g.l.c. of the extract of the electrolysis products corresponding to the reduction of the oxime (IV) gave the corresponding amine (VII, SK and F 39993A), a small amount of the hydroxylamine (II), unreduced oxime (IV), and α-hydroxy-α-(3′-trifluoromethylphenyl)acetaldehyde (V); the latter may be a result of hydrolysis of the oxime in acidic media.

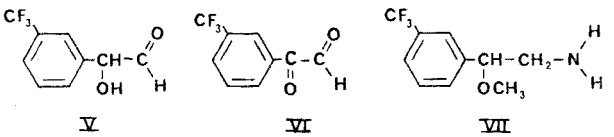

V VI VII

Proposed polarographic mechanism

The possible reaction schemes for anodic oxidation and cathodic reduction of the primary hydroxylamine (II), the secondary hydroxylamine (III), and the cathodic reduction of the oxime (IV) are shown in Figs. 1 and 2.

For the secondary hydroxylamine (III) one electron is involved in the rate-determining step, forming an intermediate nitroxide. The intermediate nitroxide either undergoes disproportionation (Path A, [8], [9]), or forms hydroperoxide (Path B, [10]) to give a nitrone which further oxidizes to give

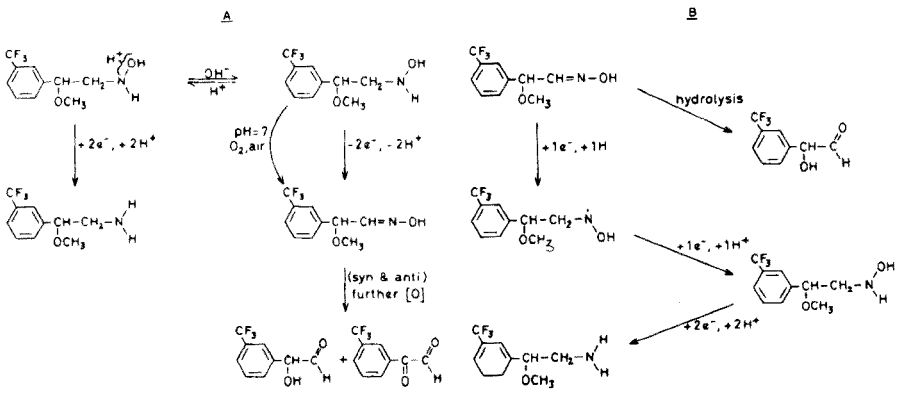

Fig. 1. Mechanism (A) for the anodic and cathodic behaviour of the primary hydroxylamine (II) at pH 7 and (B) for the cathodic behaviour of the oxime (IV) at pH 4.

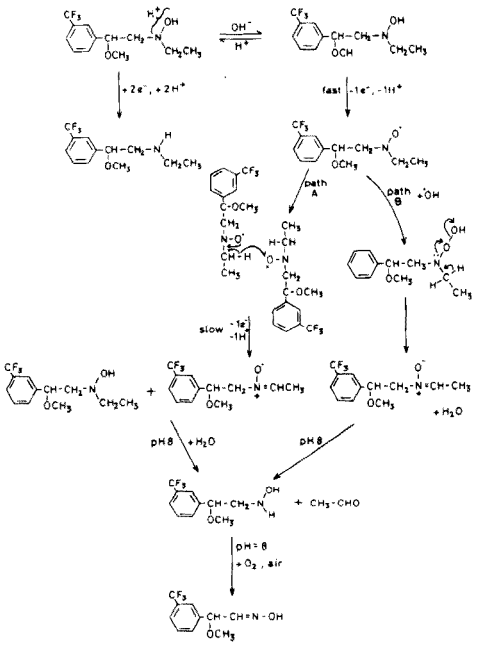

Fig. 2. Mechanism of the anodic and cathodic behaviour of *N*-ethyl-*N*-hydroxy-β-methoxy-β-(3′-trifluoromethylphenyl)ethylamine (III) at pH 8.

the oxime (IV). One electron was involved in the rate-determining step for the electro-reduction of the oxime (IV) and the reaction consumed 4 electrons per molecule.

Analytical application of polarography for the determination of hydroxylamines (II) and (III) and the oxime (IV)

Linear calibration plots of i_p vs. concentration were obtained for both the anodic (E_p = —0.07 V) and cathodic (E_p = —0.856 V) waves of the primary hydroxylamine (II) in the range 10^{-4}—10^{-6} M (buffer pH 7.0/10% MeOH). For the cathodic reduction, the line did not pass through the origin, presumably because of the effect of the large maximum, which could not be removed by the addition of Triton X-100. Below 10^{-6} M, both the anodic and cathodic waves were swamped by the decay of the supporting electrolyte; the anodic wave was best suited for analytical purposes. A linear calibration plot of i_p vs. concentration was also obtained for the anodic wave of the secondary hydroxylamine (III) in buffer pH 8.0 (E_p = —0.03 V) in the range 10^{-4}—10^{-5} M, below which the peak disappeared into the supporting electrolyte decay. The differential pulse polarogram of the cathodic wave was broad and gave two peaks of —0.80 and —0.85 V.

The differential pulse polarogram of the cathodic wave of the oxime (IV) showed two peaks at pH values above 7.0 (E_p = —1.30 V (*anti*); E_p = —1.45 V (*syn*)) which also corresponded to the breakdown products of the hydroxylamine

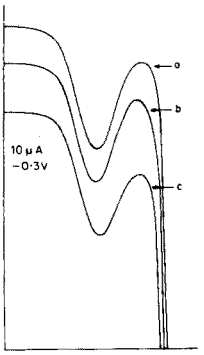

Fig. 3. The effect of secondary hydroxylamine (III) and oxime (IV) on the anodic wave of primary hydroxylamine (II), all at 10^{-5}M, by differential pulse polarography in buffer pH 7. (a) Compound II alone. (b) Compounds II and IV. (c) Compounds II, III and IV.

(II) at higher pH values. A calibration plot of i_p vs. concentration in the range 10^{-4}—10^{-6} M was obtained by recording the differential pulse polarogram at pH 4 (E_p = —1.16 V). This was linear in the range $5 \cdot 10^{-5}$—10^{-6} M, although the plot did not pass through the origin.

To establish an analytical method for the primary hydroxylamine (II) the differential pulse polarogram of the anodic wave at a concentration 10^{-5} M was run in buffer pH 7 and then the mixture of the two hydroxylamines (II, III; each 10^{-5} M) was run at the same pH. Secondly, the polarogram of a mixture of the hydroxylamines (II, III) and the oxime (IV), each at 10^{-5} M (pH 7), was recorded; equal concentrations of the oxime and the secondary hydroxylamine contributed only slightly to the wave obtained for the primary hydroxylamine (Fig. 3).

A similar experiment was also performed for the cathodic reduction of the oxime (IV) at pH 4; this showed that the oxime could be determined in a mixture of the three species.

Polarography, therefore, offers a specific method of analysis for the determination of the primary hydroxylamine (II), based on its anodic wave, down to a concentration of 10^{-6} M even when it is present in a mixture of the secondary hydroxylamine (III) and the oxime (IV). Reductive polarography can be used to determine the oxime (IV) in the presence of the two hydroxylamines (II, III).

One of us (Mrs. N. N. Rahman) thanks the Bangladesh Government and Dacca University for financial support. The authors also thank Dr. M. R. Smyth and Mr. J. Burmicz for technical advice.

REFERENCES

1 A. H. Beckett and N. N. Rahman, to be published.
2 P. E. Iversen and H. Lund, Acta Chem. Scand., 19 (1965) 2303.
3 P. E. Iversen and H. Lund, Anal. Chem., 41 (1969) 1322.

4 P. E. Iversen, Chem. Ber., 104 (1971) 2195.
5 H. Lund, Acta Chem. Scand., 13 (1959) 249.
6 Ya. I. Turyan and V. V. Smekalova, Zavod. Lab., 28 (1962) 923.
7 M. R. Smyth, Ph.D. Thesis, University of London, (1976).
8 H. Sayo, S. Ozaki and M. Masui, Part III, Chem. Pharm. Bull. (Tokyo), 21 (1973) 415.
9 H. Sayo, S. Ozaki and M. Masui, Chem. Pharm. Bull. (Tokyo), 21 (1973) 1988.
10 A. H. Beckett and P. M. Belanger, J. Pharm. Pharmacol., 27 (1975) 547.

Analytica Chimica Acta, 92 (1977) 361—368

CYCLIC VOLTAMMETRIC INVESTIGATION OF THE REDUCTION OF TIN(II) CHLORIDE IN ACETONITRILE

D. POOL[§], L. K. YOUNG[§], R. J. WILLIAMS and J. W. ROGERS*

Department of Chemistry, Midwestern State University, Wichita Falls, TX 76308 (U.S.A.)

(Received 4th February 1977)

SUMMARY

Cyclic voltammetric data collected at mercury and platinum electrodes are presented for the reduction of tin(II) chloride in acetonitrile and acetonitrile—tetramethylammonium chloride solutions. The data taken on mercury generally confirm the nature of the electrode processes postulated from polarographic and spectrophotometric data. Voltammetric data taken on platinum suggest the production of a soluble tin species via a 1e-reduction of the $SnCl_3^-$ ion.

Polarographic and spectrophotometric data presented previously show that tin(II) chloride is a weak electrolyte in dilute acetonitrile solutions [1]. The dominant tin(II) species, molecular $SnCl_2$, exists in a labile equilibrium with the ions $SnCl^+$ and $SnCl_3^-$. Free chloride is a strong ligand in acetonitrile toward the acceptor species $SnCl_2$ forming the ion $SnCl_3^-$. Two polarographic waves at negative potentials are consistent with the reduction of the species, $SnCl_2$ and $SnCl_3^-$. Evidence was presented that $SnCl_3^-$ is reduced at the higher potential wave in a 2e-step that is reversible only in the presence of excess of chloride. It was postulated that $SnCl_2$ is reduced at the lower potential wave, which exhibits a limiting current partially controlled by the formation of $SnCl_3^-$ at the electrode surface via the sequence: $SnCl_2 + 2e^- + Hg \rightarrow Sn(Hg) + 2Cl^-$; $SnCl_2 + Cl^- \rightarrow SnCl_3^-$.

Since several aspects of the complex reduction processes were not well understood, cyclic voltammetric data were collected for tin(II) chloride and tin(II) chloride—chloride solutions in acetonitrile at hanging mercury drop (h.m.d.e.) and planar platinum disc (p.p.d.e.) electrodes in an attempt to define each polarographic step further.

MERCURY ELECTRODE DATA

A typical cyclic voltammogram of tin(II) chloride, 1.0 mM in acetonitrile containing 1.0 M tetra-*N*-propylammonium perchlorate (TPAP) as supporting electrolyte and recorded at an h.m.d.e., is shown in Fig. 1(a). This wave,

---

[§] Robert A. Welch Foundation Undergraduate Scholars.

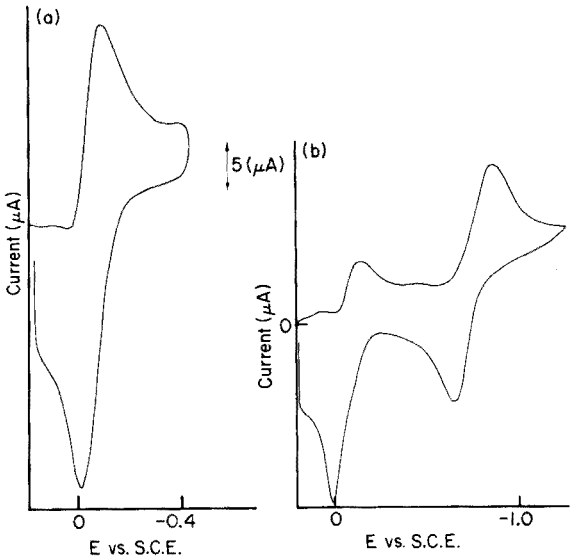

Fig. 1. Cyclic voltammograms of tin(II) chloride, 1.0 mM in acetonitrile containing 1.0 M TPAP and recorded at an h.m.d.e. (a) Switching potential 200 mV more negative than first polarographic $E_{\frac{1}{2}}$. (b) Switching potential 200 mV more negative than second polarographic $E_{\frac{1}{2}}$.

corresponding to the low potential cathodic polarographic wave, exhibits a notable anodic current component [1]. Complete cyclic voltammetric data are given as a function of potential sweep rate (v) in Table 1. The cathodic peak potential, $(E_p)_c$, and current function, $(i_p)_c v^{-\frac{1}{2}}$, are invariant to changes

TABLE 1

Cyclic voltammetric data for reduction of tin(II) chloride in acetonitrile at h.m.d.e.[a]

Sweep rate (v) (V min^{-1})	$-(E_p)_c$ (V)	$(i_p)_a/(i_p)_c$[b]	$(E_p)_c/(2-(E_p)_c)$ (mV)	$(i_p)_c v^{-\frac{1}{2}}$ ($\mu A V^{-\frac{1}{2}}$ min$^{\frac{1}{2}}$)
Cathodic wave 1				
9.14	0.08	—	61	6.55
7.32	0.08	—	65	6.25
5.49	0.08	—	67	5.98
3.66	0.08	—	67	6.09
1.83	0.08	—	69	5.98
0.95	0.08	—	71	6.32
Cathodic wave 2				
13.38	0.90	—	104	2.57
1.34	0.89	—	85	2.72

[a] A constant size h.m.d.e. was generated with a micropipet. Solution was 1 mM in tin(II) chloride in spectroquality acetonitrile containing 0.1 M TPAP. E_λ = 120 mV.
[b] Reliable baseline could not be established for measurement of $(i_p)_a$.

in v, while the half-peak height to full-peak separation, $(E_p)_c/2 - (E_p)_c$, is broadened slightly with increasing v. Difficulty in establishing an appropriate baseline prevented a precise measurement of the ratio of anodic current, $(i_p)_a$, to cathodic current, $(i_p)_c$. However, the peak anodic current is enhanced at all values of v, resulting in a $(i_p)_c/(i_p)_a$ ratio of less than 1.0. This behavior is typical of a process in which the product of the electrode reaction is weakly adsorbed [2]. The lack of variation of the current function with changes in v is typical of an electron-transfer process (reversible or irreversible) uncomplicated by a coupled chemical reaction [3]. The broadening of the wave with increasing v is consistent with some irreversibility [3]. Consequently, the invariance of $(E_p)_c$ with v is unusual but may be the result of the effects of adsorption and slow electron-transfer kinetics [2, 3]. The structure of the cyclic wave is in near agreement with that expected for a near reversible $1e^-$ transfer (with weak adsorption of product). However, it is not possible so to define the process since a cyclic voltammogram associated with an irreversible process with an n (apparent) value greater than one may also be consistent with these data [3].

Voltage excursion with reversal at potentials past the second polarographic plateau generates a current response which also exhibits a significant anodic current (Fig. 1b). The anodic current of the least negative wave is greatly enhanced in amplitude and symmetry in voltammograms recorded in this manner relative to those presented in Fig. 1(a).

Limited data for the higher potential cathodic wave are given in Table 1. Hanging drop stability, and drop size duplication were extremely difficult to control in experiments of this nature. However, the half-peak to full-peak separation, current function and cathodic peak potential variation with v are consistent with an irreversible electrochemical couple [3].

Voltammograms recorded at an h.m.d.e. of 1.0 mM tin(II) chloride in acetonitrile solutions containing 1.0 mM tetra-*N*-methylammonium chloride (TMAC) as a source of uncomplexed chloride exhibit only one current response corresponding to the second polarographic plateau. The cathodic current of this wave is increased only at the expense of the first wave. Multicycle voltammograms of this system with sweep reversal at potentials past the second wave regenerate the couple corresponding to the first wave present in tin(II) chloride solutions containing no excess of chloride (Fig. 2). The wave increases in intensity with each succeeding cycle, but does not exhibit the enhanced, symmetric anodic current noted in Fig. 1(b).

Addition of TMAC exceeding 5 mM sharpens the cathodic current response of the higher potential wave. However, no significant cyclic voltammetric study could be completed under these conditions owing to the instability of the h.m.d.e. at potentials only slightly more negative than the cathodic peak.

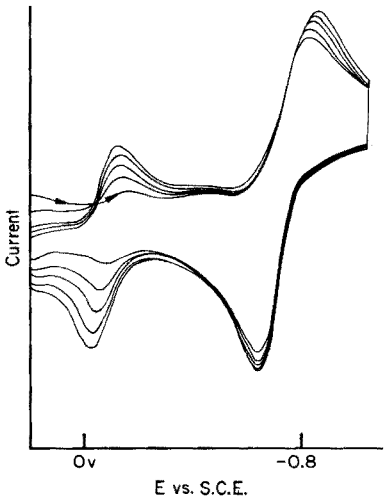

Fig. 2. Multi-cycle voltammogram of tin(II) chloride, 1.0 mM in acetonitrile containing 1.0 M TPAP and 1.0 mM TMAC and recorded at an h.m.d.e.

PLATINUM ELECTRODE DATA

A typical voltammogram recorded at a p.p.d.e. with voltage excursion and reversal at a potential past the most negative polarographic plateau is shown in Fig. 3(a). The voltammetric wave exhibits a significant anodic current response that appears to be uncomplicated by adsorption. The data given for this wave in Table 2 show behavior characteristic of a process in which an electroactive species is reversibly reduced to a soluble species which

TABLE 2

Cyclic voltammetric data for reduction of tin(II) chloride in acetonitrile at a p.p.d.e.[a]

Sweep rate (v) ($V\ min^{-1}$)	$-(E_p)_c$ (V)	$(i_p)_a/(i_p)_c$	$(E_p)_c/(2-(E_p)_c)$ (mV)	$(i_p)_c v^{-\frac{1}{2}}$ ($\mu A V^{-1/2}\ min^{1/2}$)
Cathodic wave 2 for 0.1 M TPAP—acetonitrile				
8.46	0.85	1.0	59	79.13
5.08	0.84	0.9	59	83.97
3.38	0.83	0.9	59	85.03
0.85	0.83	0.7	59	89.85
Cathodic wave 2 for 1.0 mM TMAC—0.1 M TPAP—acetonitrile				
8.46	0.86	0.8	62	107.87
5.08	0.85	0.7	59	117.64
3.38	0.85	0.7	59	119.79
0.85	0.83	0.6	59	121.93

[a]Platinum electrode was 0.78 cm^2 in area. Solution was 1 mM in tin(II) chloride in spectroquality acetonitrile containing 0.1 M TPAP. E_λ = 120 mV.

undergoes a relatively slow solution phase reaction [3]. It may be further noted that the $(E_p)_c/2 - (E_p)_c$ value of 59 mV and $(i_p)_a/(i_p)_c$ ratio near 1.0 at larger values of v are consistent with the values expected for a $1e^-$ process followed by a reaction that competes in rate with v.

No quantitative data are presented for the less negative wave on platinum. It is apparently complicated by adsorption of reactant and deposition of a metallic film (Fig. 3a). Voltage excursions with reversal at 120 mV past the first current peak on platinum also generate a series of curves showing a pronounced anodic buildup characteristic of the development of a metallic film (Fig. 4).

Addition of 1.0 mM TMAC to a 1.0 mM tin(II) chloride solution in acetonitrile also destroys the first voltammetric wave on platinum. The current of the second wave is enhanced, but the other current—voltage parameters remain largely unaltered (Table 2). The $(i_p)_a/(i_p)_c$ ratio is slightly diminished at all values of v, suggesting an increase in rate of chemical reactions following the heterogeneous electron transfer.

Addition of quantities of TMAC exceeding 5.0 mM significantly alters the character of the second wave. The wave narrows and grows in intensity with increasing amounts of chloride until limiting behavior is established at approximately 25 mM (Fig. 3b). The cathodic current at full peak height is

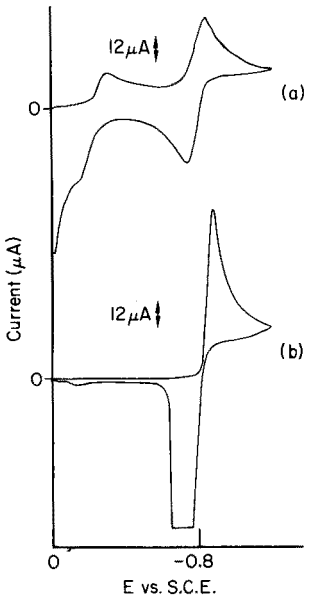

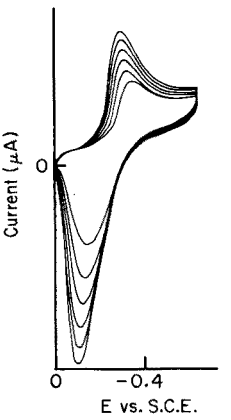

Fig. 3. (left) Cyclic voltammograms recorded at a p.p.d.e. of (a) tin(II) chloride 1.0 mM in acetonitrile containing 1.0 M TPAP, and (b) tin(II) chloride 1.0 mM in acetonitrile containing 1.0 M TPAP and 25 mM TMAC (complete anodic current not shown).

Fig. 4. (right) Multi-cycle voltammogram of tin(II) chloride, 1.0 mM in acetonitrile containing 1.0 M TPAP and recorded at a p.p.d.e. Switching potential 200 mV.

twice that of the corresponding peak observed for 1.0 mM tin(II) chloride—acetonitrile solutions containing no TMAC. The half-peak to full-peak separation of 29 mV is invariant to changes in v. These data, in addition to the enhanced and symmetric anodic current of the voltammetric wave, signify a rapid $2e^-$ reduction step resulting in the deposition of elemental tin.

DISCUSSION

Polarographic data presented previously suggest that the two cathodic current plateaux observed in the reduction of tin(II) chloride in acetonitrile may be attributed to the $2e^-$ reduction of molecular $SnCl_2$ at the lower potential wave and the trichlorostannate ion, $SnCl_3^-$, at the higher potential [1, 4]. It was postulated that the diffusion current behavior of the lowest potential wave is controlled by the production of $SnCl_3^-$ which is only reducible at the potentials of the second wave [1].

Cyclic voltammetric data taken at a mercury electrode are in general agreement with these conclusions. Voltammograms recorded with current reversal at potentials past the $E_{\frac{1}{2}}$ of the first polarographic wave but before advent of the second wave are not truly definitive of the electrode process. However, characteristics of the more negative voltammetric wave (Table 1), in addition to evidence that the n (apparent) value of the electrode process is 2.0 [1, 4], suggest that the wave is associated with an irreversible couple of the type: $SnCl_3^- + Hg + 2e^- \rightarrow Sn(Hg) + 3Cl^-$.

Regeneration of the low potential voltammetric wave by continuous voltage cycles, with reversal at a potential past the $(E_p)_c$ of the more negative wave (Fig. 2), in addition to the data presented in Table 1 for the low potential wave, suggest that it is also probably associated with an irreversible, two-electron couple, but involving $SnCl_2$: $SnCl_2 + Hg + 2e^- \rightarrow Sn(Hg) + 2Cl^-$.

All cyclic voltammograms of the lower potential process on platinum (Figs. 3 and 4) show significant anodic enhancement characteristic of the formation of a metallic film. It is therefore reasonable to conclude that this electrode process on platinum may be represented as: $SnCl_2 + 2e^- \rightarrow Sn^0 + 2Cl^-$.

Reduction of the $SnCl_3^-$ ion to elemental tin apparently only occurs in the presence of excess free chloride (Fig. 3). Voltammetric data associated with the reduction of this species from solutions containing only 1.0 mM tin(II) chloride and TPAP are consistent with the production of a relatively stable and soluble ionic species, (Fig. 3, Table 2). The approximate doubling of the cathodic peak current of this couple and apparent metallic film development on addition of excess of chloride suggest that the initial process is converted from an n (apparent) value of 1.0 to 2.0 or that the reversibility of an irreversible $2e^-$ process is altered by the presence of free chloride ion. The former suggestion is, however, more realistic in view of the data presented in Table 2.

EXPERIMENTAL

The instrumentation, cells, and electrodes were of conventional design and have been previously described [5, 6]. Spectroquality acetonitrile containing less than 0.03% water (Aldrich Chemical Company), polarographic-grade tetramethylammonium chloride (Southwestern Analytical Chemicals, Inc.), and anhydrous tin(II) chloride containing less than 1% Sn(IV) (Alpha Products Company) were used.

All polarographic and spectrophotometric solutions were prepared and transferred under a nitrogen atmosphere in a DRI-LAB glove box (Vacuum Atmospheres Corporation).

The authors gratefully acknowledge the financial support of the Robert A. Welch Foundation [R. J. Williams (AO-557), J. W. Rogers (AO-337)].

REFERENCES

1 A. R. Brajer, T. E. Farley, J. W. Kauffman, L. K. Young, R. J. Williams and J. W. Rogers, Anal. Chim. Acta, 91 (1977) 165
2 R. H. Wopschall and I. Shain, Anal. Chem., 39 (1967) 1515.
3 R. S. Nicholson and I. Shain, Anal. Chem., 36 (1964) 706.
4 F. G. Thomas and I. M. Kolthoff, J. Electroanal. Chem., 31 (1971) 423.
5 W. N. Greig and J. W. Rogers, J. Electrochem. Soc., 117 (1970) 1141.
6 R. L. Dickerson and J. W. Rogers, Anal. Chim. Acta, 71 (1974) 433.

Analytica Chimica Acta, 92 (1977) 369—378

QUANTITATIVE STUDIES OF THE SYNCHRONOUS EXCITATION METHOD IN SPECTROFLUORIMETRY: APPLICATION TO TRACER CONCENTRATION MEASUREMENTS IN HYDROLOGY

J. C. ANDRE*, M. BOUCHY, and M. NICLAUSE

I.N.P.L. Laboratoire de Chimie Générale, E.R.A. n° 136 du C.N.R.S., 1 rue Grandville, 54042 Nancy Cedex (France)

Ph. BAUDOT

Laboratoire de Chimie Minérale et de Toxicologie, Faculté des Sciences Pharmaceutiques et Biologiques, 5 rue Albert Lebrun, 54000 Nancy (France)

(Received 14th March 1977)

SUMMARY

The detection and measurement by spectrofluorimetry of trace quantities of fluorescent substance is often limited by interference from light at the excitation wavelength. This is the case for the classical tracers (fluorescein, eosin, sulforhodamine G, rhodamine B and WT) used for qualitative or quantitative purposes in hydrology. The need to measure ever decreasing concentrations of these tracers has led to the use of a special method of excitation, the synchronous excitation method, in which interference is avoided by scanning excitation and emission wavelengths simultaneously while maintaining a constant wavelength separation between the two. This technique gives a perceptible increase in sensitivity and reduces experimental errors. Spectrofluorimeters equipped with stepper-type motors can be modified cheaply and easily to record synchronous excitation spectra.

Mention of the use of tracers in hydrology conjures up the image of the speleologist using fluorescein qualitatively to detect the course of water underground. The rigour imposed by new methodologies (in hydrodynamics for example) has obliged hydrologists to measure the concentration of this fluorescent tracer with ever-increasing precision. Fluorescein, or, more exactly, its soluble form uranine, along with other xanthenic dyes, e.g. eosin, sulforhodamine G and rhodamine B and WT, display exceptional advantages such as low cost, high solubility, and the remarkable sensitivity of detection by fluorescence [1, 2]. However, dyes difficult to degrade are being used more and more frequently in field measurements and could in the long term be responsible for a form of pollution and for appreciable errors in measurement because of the presence in the water of extraneous tracer. These two considerations led to attempts to improve the method so that smaller quantities of tracer could be used.

The synchronous excitation spectrofluorimetry method, where excitation (λ_e) and emission or analysis (λ_a) wavelengths are varied simultaneously while maintaining a constant step c ($c = \lambda_e - \lambda_a$ = constant) between them, used by Lloyd [3, 4] and by John and Soutar [5] for qualitative purposes

only, can be applied to the problem of measuring low concentrations of fluorescent tracers, particularly when there is interference (Rayleigh diffusion and scattering light) at the excitation wavelength [6—8] (cf. Fig. 1).

The technique has been developed in the laboratories of the Centre d'Etudes Nucléaires de Grenoble (C.E.N.G.) and used in hydrological studies for several years (cf., for example, [9—11]).

The first part of this paper describes the synchronous excitation method [3, 4] in the absence of interference from light at the excitation wavelengths and discusses the potential interest of this method for the determination of trace quantities (about 10^{-2} p.p.b.) in the presence of such interference. In the second part, the technique is applied to the measurement of the concentration of fluorescent tracers and a lowering of the detection limit of the tracer is achieved.

THE SYNCHRONOUS EXCITATION METHOD

Some useful definitions are presented in Fig. 2. The spectral width l is the half-height width of the spectrum of light leaving a monochromator. Under

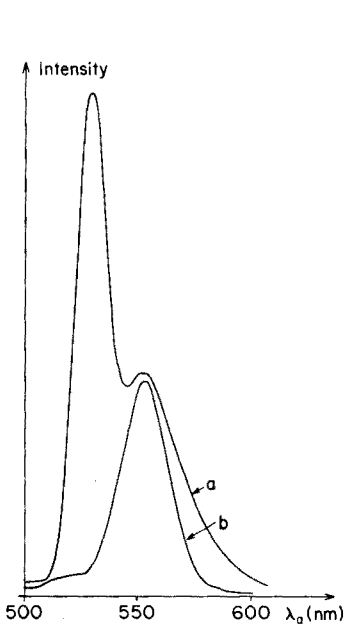

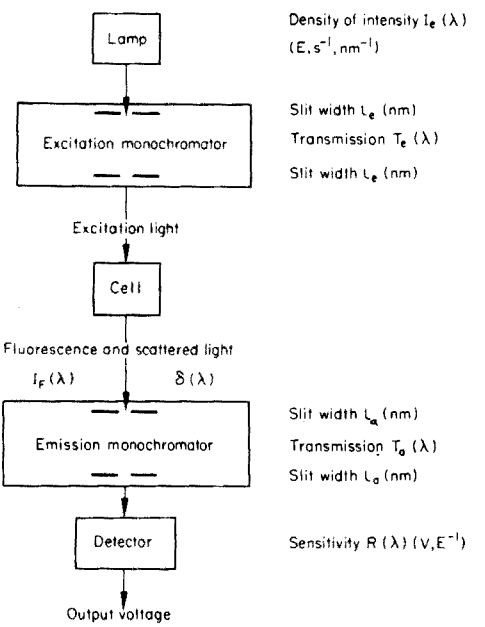

Fig. 1. Comparison between "constant step" spectrum and emission spectrum. Sample, sulforhodamine G (2 p.p.b.) in water. (a) Emission spectrum (excitation wavelength 530 nm). (b) "Constant step" spectrum ("constant step" of 25 nm). Excitation and emission slits, 10 nm. Temperature, 20°C.

Fig. 2. Schema of the apparatus and nomenclature.

normal conditions (slit widths of entrance and exit equal), the transmitted wavelengths are between $\lambda - l$ and $\lambda + l$, the largest intensity corresponding to the set wavelength λ.

The synchronous excitation method in the absence of interference from light at the excitation wavelength

For the visualization of this method a basic solution (pH 12) containing both fluorescein (excitation, 490 nm; emission, 516 nm) and acridine orange (excitation, 445 nm approximately; emission, 530 nm) was prepared. The concentration of each dye was chosen so that a maximum absorbance below 0.2 (no skin effect) and approximately equal fluorescence intensities at 516 and 530 nm were obtained. The wavelengths at which the fluorescence maxima of these two substances occur are very close; excitation of the mixture at wavelengths between 400 and 500 nm gives rise to a spectrum with a fluorescence maximum between 516 nm and 530 nm (cf. Fig. 3).

It is practically impossible to detect the presence of fluorescein and acridine orange by examining emission spectra alone. However, if a constant step c is maintained between excitation and emission wavelengths, it is possible (see Fig. 3) to obtain a spectrum (a) whose maximum corresponds

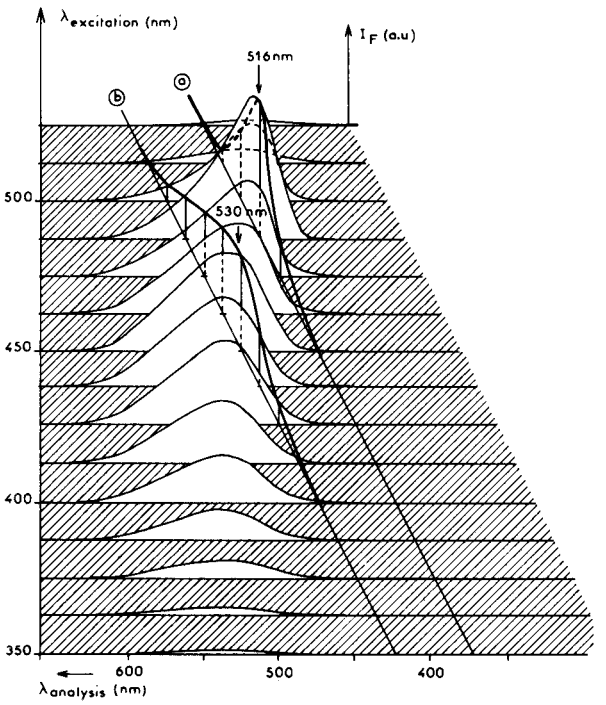

Fig. 3. Visualization of the synchronous excitation method. Application to the identification of fluorescein and acridine orange at pH 12. (a) c = 26 nm; (b) c = 75 nm.

to that of fluorescein (c = 26 nm) and a spectrum (b) whose maximum corresponds to that of acridine orange ($c \approx 75$ nm).

This is the method used [3—5] for the qualitative analysis of motor oils, fuels and soots.

The synchronous excitation method in the presence of interference from light at the excitation wavelength

If the spectral width of both excitation and emission monochromators is larger than, or of the order of, the difference between the excitation and emission wavelengths λ_e and λ_a for low concentrations of the fluorescent compound, the observed emission spectrum consists of a strong "scattering" band with the fluorescence band superimposed on it [cf. Fig. 1]. The intensity I recorded at the emission wavelength λ_a corresponds to both fluorescence and "scattering" intensities. In this case, it appears very difficult to estimate the nature and the concentration of the emitting compound. The problem is particularly acute for xanthenic dyes where emission is very close to absorption (cf. Table 1).

To visualize the method, several emission spectra have been obtained for sulforhodamine G in aqueous solution. The results are shown in Fig. 4. When the excitation range (depending on the slit width) does not overlap the absorption range, only scattered light is recorded; when the excitation wavelength is close to the maximum of absorption (λ_e^0), both scattering and fluorescence are recorded. Apparent elimination of scattered light can be obtained by the synchronous excitation technique (see Fig. 4).

TABLE 1

Spectrofluorimetric data

Compound	Fluorescein	Eosin	Sulforhodamine G	Rhodamine B	Rhodamine WT
Maximum excitation wavelength (nm)	490	515	557	555	555
Maximum fluorescence wavelength (nm)	516	539	534	581	582
c (nm)	26	24	23	26	27
$\Delta\lambda_e$ (nm)	39	51	48	45	37
$\Delta\lambda_a$ (nm)	33	32	32	31	32
Calculated $\Delta\lambda_c$ (nm)	21	23	22.5	21.5	20
Experimental $\Delta\lambda_c$ (nm)	21	24	23	23	23
Concentration at which $I_S \simeq I_F$ (p.p.b.)	$2 \cdot 10^{-2}$	$6 \cdot 10^{-2}$	$2 \cdot 10^{-2}$	$8 \cdot 10^{-2}$	$2.5 \cdot 10^{-1}$
Origin and form	Fluka solid	Fluka solid	Dupont de Nemours solid	Fluka solid	Dupont de Nemours solution

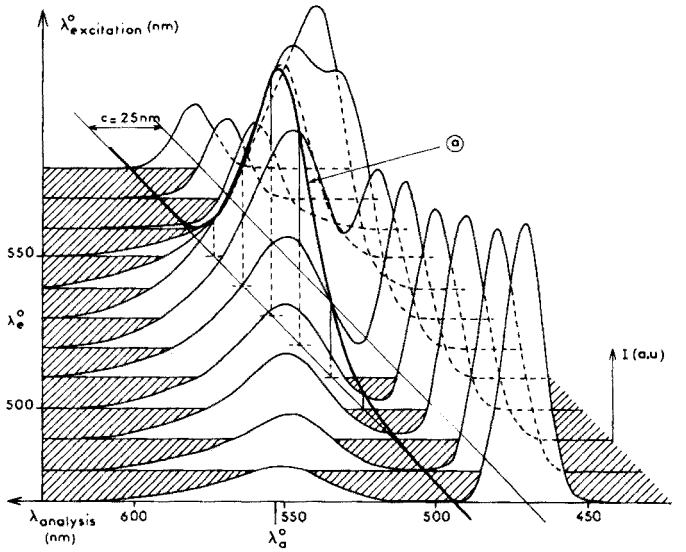

Fig. 4. Visualization of the synchronous excitation method. Application to the determination of a fluorescent tracer in the presence of interference from scattering light. Sulforhodamine G, 8 p.p.b. Temperature, 20°C. pH, 7. Emission and excitation slits 10 nm. (a) c, 25 nm.

Apparatus

Use of the "constant step" method necessitated providing the spectrofluorimeter (Farrand MKI) with a means of driving both monochromators simultaneously. Certain commercially available equipment is already fitted with this facility [7]. Stability and reproducibility of the wavelength difference is of the greatest importance. Mechanical coupling of the monochromators is not reliable enough, but if the latter are driven by stepper-type motors, perfectly satisfactory coupling may be obtained with a common pulse generator.

RESULTS AND DISCUSSION

Qualitative analysis

Detection of trace quantities in various media. Figure 1 shows the spectra obtained for sulforhodamine G by the "constant step" (curve b) and the usual (curve a) methods. Experimental conditions were the same in both cases.

An impressive demonstration of the effectiveness of the "constant step" method in dealing with highly scattering solutions was carried out as follows. A suspension of alumina was added to a fluorescent solution such that only 0.01% of the incident light was transmitted. Under these conditions, it is impossible to record the fluorescence spectrum with the usual method: the fluorescence spectrum is completely hidden by the scattering band (cf. Fig. 5,

curve a). With the "constant step" method, however, recording of the emission spectrum was perfectly feasible (cf. Fig. 5, curve b).

Shape of the "constant step" spectrum. Figure 6 shows fluorescence spectra for a number of common tracers. For each of these, two spectra were recorded as follows: (i) excitation at the maximum excitation wavelength, scanning the emission wavelength (usual method); (ii) scanning of both excitation and emission wavelength with average constant step of 25 nm (cf. Table 1). The "constant step" spectra have half-height widths less than those of the normal spectra: the half-height width of a "constant step" spectrum, $\Delta\lambda_c$ is given approximately by the following expression

$$\Delta\lambda_c \approx \Delta\lambda_e + \Delta\lambda_a - ((\Delta\lambda_a)^2 + (\Delta\lambda_e)^2)^{\frac{1}{2}} \quad (1)$$

where $\Delta\lambda_e$ and $\Delta\lambda_a$ are the half-height widths of the normal excitation and emission spectra, respectively. Values for $\Delta\lambda_c$ calculated by the above equation are in good agreement with those obtained experimentally (cf. Table 1). It should be noted that the half-height width $\Delta\lambda_c$ is always smaller

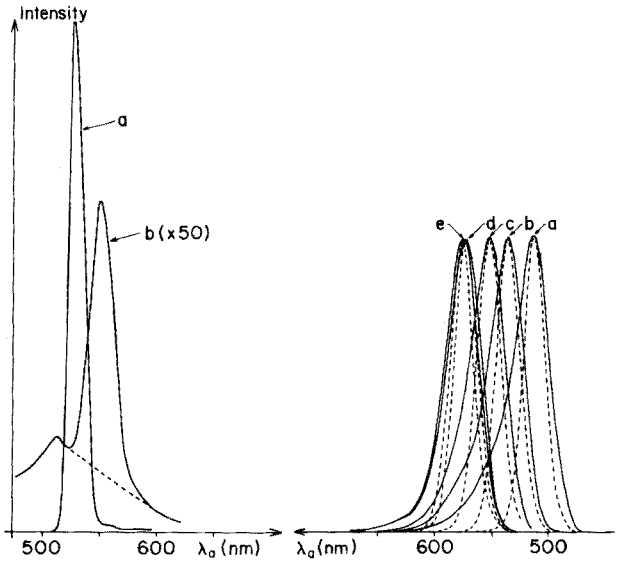

Fig. 5. Analysis of fluorescence in a highly scattering solution. Sample, solution of sulforhodamine G (20 p.p.b.) with alumina (see text). (a) Emission spectrum showing a strong "scattering" band (excitation wavelength 530 nm). (b) "Constant step" spectrum ("constant step" of 25 nm). Temperature, 20°C. Excitation and emission slits, 10 nm.

Fig. 6. Fluorescence (———) and synchronous excitation spectra (— — —) of fluorescent tracers. (a) Fluorescein (Fluka). (b) Eosin (Fluka). (c) Sulforhodamine G (Dupont de Nemours). (d) Rhodamine B (Fluka). (e) Rhodamine WT (Dupont de Nemours). Temperature, 20°C. pH, 7. Emission and excitation slits, 10 nm. *c*, 25 nm.

than the width $\Delta\lambda_a$ of the normal fluorescence spectrum; this can improve the selectivity of the technique when several fluorescent compounds are present simultaneously in the solution.

In the case of a normal fluorescence spectrum with structure, the modification of the shape of the spectrum can be considerable and depends on the value of c. When all the bands are still present, their relative amplitude is modified. In attempting to identify an unknown compound, it is necessary, therefore, to record reference spectra.

Raman emission can lead to interference when a fluorescence spectrum is recorded. The problem does not arise with xanthenic dyes, but the synchronous excitation method can partially eliminate this kind of interference [7].

Quantitative analysis: comparison with the usual method

Choice of optical variables. The fluorescence intensity is at a maximum when the excitation wavelength takes the value λ_e^0 corresponding to the maximum of the excitation spectrum and when the emission wavelength takes the value λ_a^0 corresponding to the maximum of emission spectrum.

In the "constant step" method ($c = \lambda_a^0 - \lambda_e^0$), excitation and emission wavelengths are scanned simultaneously. The intensity maximum is reached when $\lambda_e = \lambda_e^0$ and therefore $\lambda_a = \lambda_e^0 + c = \lambda_a^0$. For given values of λ_a and λ_e, the intensity of fluorescence I_F reaching the detector increases with the spectral widths of both monochromators; thus $I_F \propto (l_e \cdot l_a)^2$, where l_e and l_a are respectively the spectral widths of the excitation and the emission monochromators. However, the overlap of excitation and emission bands leads to a scattering intensity I_S whose value [see Appendix] is given by the expression: $I_S \alpha [l_e + l_a - (\lambda_a - \lambda_e)]^3$ when $l_e + l_a > (\lambda_a - \lambda_e)$, and it is necessary to limit the values of the spectral widths to reduce I_S.

It would seem sufficient to choose $l_e + l_a = \lambda_a^0 - \lambda_e^0 = c$, but this only holds for ideal optics (transmission bands triangular) and in practice one has to reduce by some nanometers the value of l_e and l_a: $l_e + l_a = 2l < (\lambda_a^0 - \lambda_e^0) = c$. Note that when the value $2l$ is chosen, I_F is at a maximum when $l_e = l_a = l$.

Comparison of the errors in the two methods. The intensity I of the light reaching the detector is given by $I = I_F + I_S$, where I_F is the fluorescence intensity and I_S the scattered light intensity. The measurement of I_F is made at the wavelengths $\lambda_e = \lambda_e^0$ and $\lambda_a = \lambda_a^0$, in both the usual and "constant step" methods. The values of these intensities are the same in both cases at these particular wavelengths (and only at these wavelengths).

For high concentrations of the fluorescent compound, $I_F \gg I_S$ and $I \approx I_F$, and the precision is equal in both methods. At low concentrations, it becomes necessary to subtract the value I_S from the experimental value I. I_S can be determined by interpolation or by recording a "blank" spectrum with a solution free of the fluorescent compound.

The curvature and the slope of the "scattering" band are very large and lead to appreciable error when the background is assessed by a simple inter-

polation procedure. However, with the "constant step" method, the scattered light is nearly constant in the fluorescence range and allows reliable interpolation (cf. Fig. 1).

In the "blank" spectrum, the values I and I_S have to be measured at the same wavelength $\lambda_a = \lambda_a^0$ in the recorded spectra. The error $d\lambda$ in the value of λ_a leads to the following errors

$$\Delta I_S = d\lambda \, (dI_S/d\lambda_a)_{\lambda_a^0} = \alpha_S \cdot d\lambda \tag{2}$$

$$\Delta I = d\lambda \, ((dI_F/d\lambda_a) + (dI_S/d\lambda_a))_{\lambda_a^0} \simeq \alpha_S \cdot d\lambda \tag{3}$$

$$I_F \simeq 2\alpha_S \cdot d\lambda \tag{4}$$

The maximum of the fluorescence spectrum is at the wavelength λ_a^0 and the slope of $I_F(\lambda_a)$ is nearly equal to zero.

When the "constant step" method is used, the slope α_S is very small, whereas with the usual method, the value of α_S is considerably higher and represents the major error in the value I_F. For example, in the case of sulforhodamine G, α_S is around 17 times smaller with the "constant step" method than with the usual method.

It appears that the intensity I_S [see Appendix] can be written

(i) for the "constant step" method

$$I_S \approx I_e(\lambda_e) \cdot T_e(\lambda_e) \cdot \delta(\lambda_e) \cdot T_a(\lambda_e + c) \cdot R(\lambda_e + c) \cdot (l_e + l_a - c)^3 \tag{5}$$

(ii) for the usual method

$$I_S \approx I_e(\lambda_e^0) \cdot T_e(\lambda_e^0) \cdot \delta(\lambda_e^0) \cdot T_a(\lambda_a) \cdot R(\lambda_a) \, [(l_e + l_a + \lambda_e^0) - \lambda_a]^3 \tag{6}$$

In the former case, the variations of I_S are related to the variations of the functions I_e, T_e, δ, T_a and R, which are small. But, in the latter case, the polynomial term λ_a^3 leads to an appreciable slope. One can obtain a smaller error, with the usual method, by reducing the spectral widths or by setting the wavelengths beyond the maxima. This method reduces the intensity I_F ($\propto l_e^2 \, l_a^2$) and leads to an increase in the error from electrical noise. With the "constant step" method, it is possible to set the wavelengths at the maxima, thus obtaining the highest value of I_F and hence only a small error from scattered light.

General conditions of use of the two methods

For highly fluorescent solutions ($I_S \ll I_F$), the interference arising from scattered light is negligible and the usual method is not improved by "constant step" scanning. With dilute solutions, ($I_S < I_F$), it is useful to subtract I_S from the experimental value I. With the "constant step" method, this correction can be made by a simple linear interpolation between the backgrounds on either side of the emission band. With the usual method, such an interpolation leads to considerable error.

For traces of fluorescent compound, ($I_S \approx I_F$), it is necessary to record a "blank" spectrum to obtain I_S [6, 8]. The error in the usual method is

markedly higher than that in the synchronous excitation technique. Indeed, where fluorescence intensity is low, the "constant step" method alone is capable of detecting the presence of the compound (cf. Fig. 7).

Advantages of the synchronous excitation technique in hydrological analysis

Before spectra are recorded, a "blank" must always be run (see Fig. 7) on the solvent (deionized water). A blank is necessary in the classical method to obtain by difference the fluorescence spectrum of the tracer. With the constant step method, however, when $I_S \approx I_F$, a blank determination is not necessary for qualitative analysis and is not indispensable for quantitative analysis since it may be obtained approximately by extrapolation. In addition the constant step method has the advantage of greater sensitivity.

Thus, this method is particularly suitable for detecting and measuring the concentration of fluorescent tracers used in hydrological studies (or in other fields) since it is very often impossible to carry out blank measurements in the field (the only background measurements possible would have to be carried out on samples taken before or long after injection of tracer into the phase to be marked). As sampling for tracer measurement may last several weeks, the concentration of interfering impurities has time to vary and since this variation is not predictable, results so obtained are suspect.

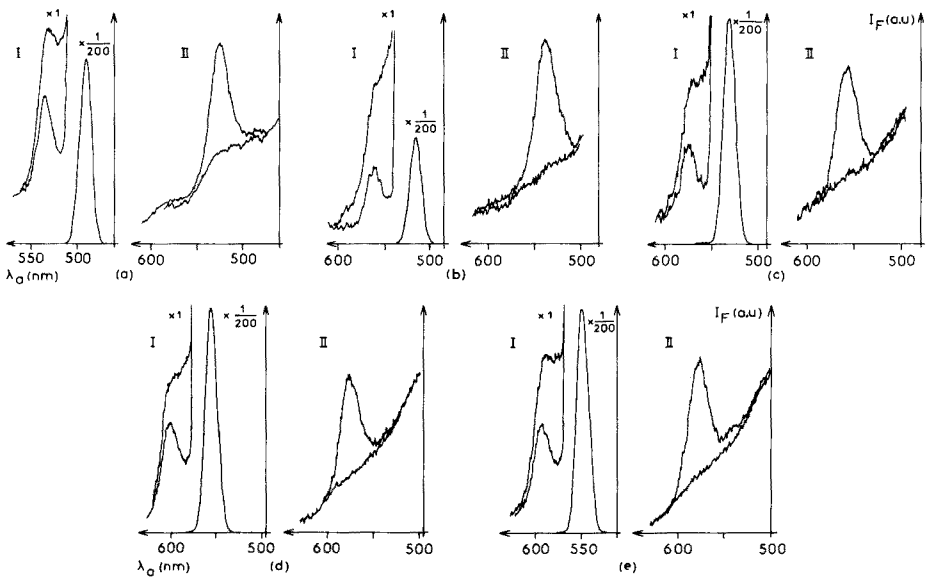

Fig. 7. Comparison between classical spectra (I) and synchronous excitation spectra (II) when $I_S \simeq I_F$. (a) Fluorescein, $2 \cdot 10^{-2}$ p.p.b. (b) Eosin, $6 \cdot 10^{-2}$ p.p.b. (c) Sulforhodamine G, $2 \cdot 10^{-2}$ p.p.b. (d) Rhodamine B, $8 \cdot 10^{-2}$ p.p.b. (e) Rhodamine WT, $2.5 \cdot 10^{-1}$ p.p.b. Temperature, 20°C. pH, 7. Emission and excitation slits, 10 nm. *c*, 25 nm. A "blank" was carried out in each case.

Simultaneous determination of several tracers

Since there is very little overlap between the synchronous excitation spectra of the tracers used, it should be possible to obtain, in a single experiment, the spectra of all the tracers present in a mixed-tracer sample by using a wavelength difference of the order of 25 nm (cf. Table 1). Caution, however, should be exercized, particularly when the concentrations of the tracers are not comparable.

We thank S. Joly for fabricating the electronics and J. Molinari (C.E.N.G.) for helpful discussions.

Appendix: Influence of spectral width on scattered light

Let λ_e and λ_a be the excitation and emission wavelengths respectively. Then

(i) $l_e + l_a \leqslant \lambda_a - \lambda_e$

The light which is scattered in the region of λ_e is not "seen" by the detector and the scattering intensity I_S is zero.

(ii) $l_e + l_a > \lambda_a - \lambda_e$ but with l_e and $l_a < \lambda_a - \lambda_e$.

Under these conditions, there is partial overlap between the "spectra" of the excitation light and the light transmitted by the emission monochromator.

The intensity of the scattered light can be expressed as

$$I_S(\lambda_e,\lambda_a) \propto \int_{\lambda_a - l_a}^{\lambda_e + l_e} I_e(\lambda)\, T_e(\lambda)\, [l_e - |\lambda - \lambda_e|] \cdot \delta(\lambda) \cdot T_a(\lambda) \cdot R(\lambda)$$
$$[l_a - |\lambda - \lambda_a|]\, d\lambda$$

where $\delta(\lambda)$ is the experimental "scattering" law ("scattering" is mainly reflexions at the faces of the cell). If the functions I_e, T_e, δ, T_a and R are almost constant in the integration range, then

$$I_S(\lambda_e,\lambda_a) \propto I_e(\lambda_e) \cdot T_e(\lambda_e) \cdot \delta(\lambda_e) \cdot T_a(\lambda_a) \cdot R(\lambda_a) \cdot [l_e + l_a - (\lambda_a - \lambda_e)]^3$$

REFERENCES

1 J. Molinari, Commissariat à l'Energie Atomique, Centre d'Etudes Nucléaires de Grenoble, Rapport DR/SAR-G/69, 1969, p. 36.
J. Molinari, Les techniques de traceurs dans l'étude des problèmes de pollution, in Nuisances et Environnement. Colloque des Techniques anti-pollution, Grenoble, 2—6 Oct. 1973.
2 J. C. Andre and J. Molinari, J. Hydrol., 28 (1976) 257.
3 J. B. F. Lloyd, Nature (Physical Science), 231 (1971) 64.
4 J. B. F. Lloyd, J. Forensic Sci. Soc., 11 (2) (1971) 83; 11 (3) (1971) 153; 11 (4) (1971) 135.
5 P. John and I. Soutar, Anal. Chem., 48 (1976) 520.
6 J. U. White, Anal. Chem., 48 (1976) 2089.
7 J. C. Andre, Ph. Baudot and M. Niclause, Clin. Chem. Acta, 76 (1977) 55.
8 J. C. Andre, M. Bouchy, Ph. Baudot and M. Niclause, C. R. Acad. Sci., in press.
9 D. Steinmetz, Commissariat à l'Energie Atomique, Centre d'Etudes Nucléaires de Grenoble, Rapport SARR/INT/74-289/DS, 1974, pp. 9.
10 J. Molinari and M. B. Florez, Commissariat à l'Energie Atomique, Centre d'Etudes Nucléaires de Grenoble, Rapport SARR/GARTHY/75-14/JM/MC, 1975, pp.12.
11 R. Charriere, thèse de 3ème Cycle, Grenoble (1974).

Analytica Chimica Acta, 92 (1977) 379—386

EXTRACTION—SPECTROPHOTOMETRIC DETERMINATION OF TRACES OF ANTIMONY IN COPPER AND LEAD METALS AND IN LEAD-BASE ALLOY WITH PYROCATECHOL VIOLET AND TRI-n-OCTYLAMINE

IWAO TSUKAHARA*, MASANAO SAKAKIBARA and MINORU TANAKA

The Furukawa Electric Co., Ltd., Central Research Laboratory, 2-9-15, Futaba, Shinagawa-ku, Tokyo (Japan)

(Received 7th January 1977)

SUMMARY

A sensitive spectrophotometric method is described for the determination of antimony in copper and lead metals and in lead-base alloy. Optimal conditions have been established for the extraction and determination of antimony. Antimony (III) is extracted from a potassium iodide—sulfuric acid or a hydrobromic—sulfuric acid medium with toluene and converted to an antimony—pyrocatechol violet (PV) complex. The complex is then extracted with tri-n-octylamine (TOA) and the absorbance of the resulting ternary Sb(III)—PV—TOA complex is measured at 555 nm. As little as 0.5 p.p.m. of antimony in copper metal and 0.2 p.p.m. of antimony in lead metal and lead-base alloy can be determined.

Traces of antimony in copper and lead metals have generally been determined by spectrophotometry with rhodamine B [1—5]. The methods usually require a prior separation of antimony to avoid matrix interferences. Separation by coprecipitation with manganese dioxide has been most frequently employed [1, 3, 4], but this is tedious and time-consuming. Lead has been removed as sulfate in the determination of traces of antimony in lead [5], and antimony has been extracted from a hydrochloric acid solution with isopropyl ether for the determination of antimony in copper metal [2] and tin-lead solder [6].

Bȳkhovtseva and Tserkovnitskaya [7] and Naruskevicius et al. [8] determined antimony spectrophotometrically with pyrocatechol violet (pyrocatechol sulfonphthalein, PV). Bailey et al. [9] investigated the ternary antimony—PV—cetyltrimethylammonium bromide complex and reported a sensitive spectrophotometric method for antimony. These studies suggested application of the spectrophotometric PV method to the above materials: a preliminary investigation showed that a sensitive determination of antimony was possible by extracting the antimony—PV complex with a toluene solution of tri-n-octylamine (TOA) and measuring the absorbance of the organic layer, but numerous elements interfered. Byrne [10] and Grimanis and Hadzistelios [11] investigated the extraction behaviour of antimony into toluene from potassium iodide—sulfuric acid systems, and into benzene from hydrobromic—sulfuric acid systems, respectively; they suggested the possibility of selective

separation of antimony from numerous elements. These previous investigations for the determination and separation of antimony indicated that a satisfactory routine method for metallurgical analyses could be developed.

The proposed method involves the extraction of antimony(III) with toluene from a potassium iodide—sulfuric acid or a hydrobromic—sulfuric acid medium, conversion of the extracted antimony iodide or bromide to the antimony—PV complex by shaking the organic layer with an aqueous PV solution, extraction of the resulting complex with a TOA—toluene solution, and measurement of the absorbance of the organic layer. The present paper describes the optimal conditions for the extraction and determination of traces of antimony in copper and lead metals and in lead-base alloy.

EXPERIMENTAL

Apparatus and reagents

A Hitachi 139 spectrophotometer with 1-cm cells and an Iwaki KM shaker were used.

PV solution A. Combine 200 ml of 1 M sodium acetate solution, 5 ml of saturated sodium sulfite solution and 12 ml of 0.1% (w/v) PV solution. Adjust to pH 4.5 with sulfuric acid (1 + 2) and make up to 500 ml with water. Prepare this solution just before use.

PV solution B. Prepare in the same way as solution A but use 15 ml of 0.1% (w/v) PV solution.

TOA solution. Dilute 22.5 ml of TOA (Wako Pure Chemical Industries, Ltd.) to 100 ml with toluene.

Wash solution A. Combine 250 ml of 6 M sulfuric acid, 5 ml of saturated sodium sulfite solution and 25 ml of 1 M potassium iodide solution, and make up to 500 ml with water. Prepare just before use.

Wash solution B. Combine 450 ml of 9 M sulfuric acid, 5 ml of saturated sodium sulfite solution and 25 ml of 0.2 M hydrobromic acid, and make up to 500 ml with water. Prepare just before use.

Standard antimony(III) solution. Dissolve 0.100 g of antimony in 160 ml of 9 M sulfuric acid (heat to assist dissolution), and make up to 500 ml with water. Before use, dilute the solution to an appropriate concentration with 3 M sulfuric acid.

General procedure A (Iodide extraction)

Transfer an aliquot (20 μg Sb) of the standard antimony solution to a 150-ml separatory funnel. Add 33 ml of 9 M sulfuric acid, 1 ml of saturated sodium sulfite solution and 5.0 ml of 1 M potassium iodide solution. Make up to 100 ml with water and extract antimony with 10.0 ml of toluene for 5 min. Discard the aqueous layer. Wash the organic layer with 50 ml of wash solution A for 5 min. Discard the aqueous layer. Shake the organic layer with 50.0 ml of the PV solution A for 5 min. Add 5.0 ml of the TOA solution to the separatory funnel containing both the organic and aqueous layers, and then shake for

5 min. Discard the aqueous layer. Measure the absorbance of the organic layer at 555 nm against the TOA solution or a reagent blank taken through the procedure.

General procedure B (bromide extraction)

Transfer an aliquot (20 μg Sb) of the standard antimony solution to a 150-ml separatory funnel. Add 45 ml of 18 M sulfuric acid, 1 ml of saturated sodium sulfite solution and 5.0 ml of 0.2 M hydrobromic acid. Make up to 100 ml with water and extract antimony with 10.0 ml of toluene for 5 min. Discard the aqueous layer. Wash the organic layer with 20 ml of wash solution B for 1 min. Discard the aqueous layer. Shake the organic layer with 50.0 ml of the PV solution B for 5 min, and then proceed as directed in the general procedure A.

Recommended procedures for the analysis of metal and alloy

Determination of antimony in lead metal and lead-base alloy. Decompose 0.1—5 g of sample with 10—50 ml of nitric acid (1+2); heat gently to assist the decomposition. Add 20 ml of 11 M hydrochloric acid and 75 ml of 9 M sulfuric acid. Evaporate gently just to fumes of sulfur trioxide and then heat strongly on a sand bath for 10 min (allow copious fumes to evolve). Transfer the solution together with lead sulfate precipitate to a 100-ml volumetric flask and dilute to the mark with water. Transfer a 50.0-ml aliquot of the supernatant solution to a 150-ml separatory funnel. Add 1 ml of saturated sodium sulfite solution and 5.0 ml of 1 M potassium iodide solution, and make up to 100 ml with water. Then proceed as directed in the general procedure A. Carry a reagent blank through the entire procedure.

Determination of antimony in copper metal. Decompose 0.1—2 g of sample with 10 ml of hydrochloric acid (1 + 1) and 10 ml of nitric acid (1 + 1); heat gently to assist the decomposition. Add 20 ml of sulfuric acid (1 + 1) and evaporate to dryness on a sand bath. Add 20 ml of 9 M sulfuric acid and 30 ml of water, and heat gently to dissolve the salt. Transfer the solution to a 150-ml separatory funnel. Add 35 ml of 18 M sulfuric acid and dilute to about 90 ml with water. Add 1 ml of saturated sodium sulfite solution and 5.0 ml of 0.2 M hydrobromic acid, and make up to 100 ml with water. Extract antimony twice with 5.0-ml portions of toluene for 5 min and discard the aqueous layer. Combine the organic layers and wash with 20 ml of wash solution B for 1 min. Then, proceed as directed in the general procedure B. Carry a reagent blank through the entire procedure.

Preparation of calibration curves

Transfer aliquots of the standard antimony solution (0—30 μg Sb) to 150-ml separatory funnels. To each solution and a blank (water), add 9 M or 18 M sulfuric acid, saturated sodium sulfite solution and 1 M potassium iodide solution or 0.2 M hydrobromic acid as directed in the general procedure A or B, and make up to 100 ml with water. Then, treat these solutions in par-

allel with samples as directed in the recommended procedure A or B, and measure the relationship between the absorbance and the amounts of antimony.

RESULTS AND DISCUSSION

Absorption spectra

Figure 1 shows the absorption spectra of the ternary Sb(III)—PV—TOA complex taken through general procedure A or B. The absorption maximum of the complex was at 555 nm. The absorbance measured against a reagent blank taken through procedure B was lower than that taken through procedure A. The cause of the difference in the absorbance is not clear, but the percentage extraction of antimony into toluene from the bromide medium is probably lower than that from the iodide medium.

Effects of experimental conditions

The optimal conditions for the extraction and determination of antimony were investigated under the conditions of the general procedures except for the condition varied.

In the iodide extraction, antimony could be best extracted with toluene from 4.5—6 M sulfuric acid at 0.01 M potassium iodide, and from 3—6 M sulfuric acid at 0.05 M potassium iodide (Fig. 2), or from 0.03—0.06 M potassium iodide at 3 or 4 M sulfuric acid (Fig. 3); the curves for 20 μg of antimony (Fig. 2) are in good agreement with the extraction curves for antimony reported by Byrne [10]. In the bromide extraction, antimony could be best extracted with toluene from 8—10 M sulfuric acid at 0.05

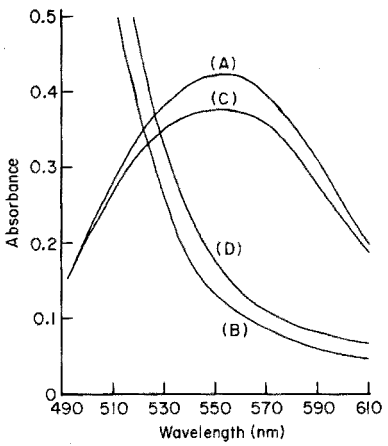

Fig. 1. Absorption spectra. (A, B) taken through the general procedure A. (C, D) taken through the general procedure B. (A, C) 20μg Sb, against reagent blank. (B, D) reagent blank, against the TOA solution.

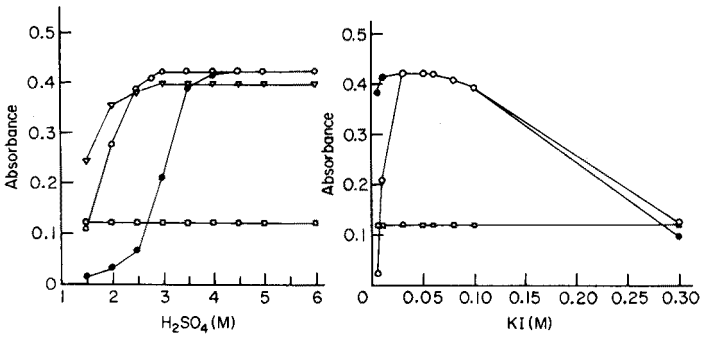

Fig. 2. Effects of potassium iodide and sulfuric acid concentrations on the extractability of antimony into toluene. KI concentration: (•) 0.01 M; (○) (□) 0.05 M; (▽) 0.1 M. (•) (○) (▽) 20 μg Sb, against reagent blank. (□) reagent blank, against the TOA solution.

Fig. 3. Effects of potassium iodide and sulfuric acid concentrations on the extractability of antimony into toluene. H_2SO_4 concentration: (○) (□) 3 M; (•) 4 M. (○) (•) 20 μg Sb, against reagent blank. (□) reagent blank, against the TOA solution.

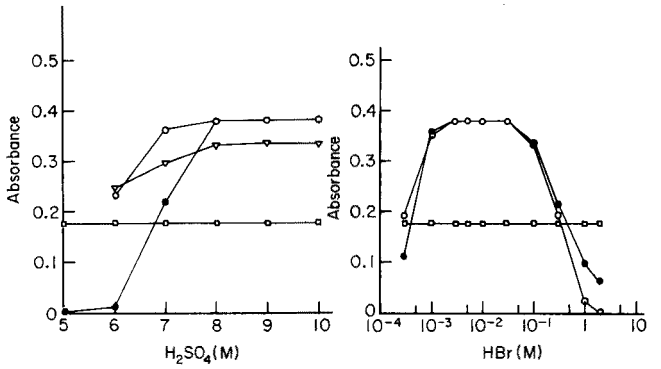

Fig. 4. Effects of hydrobromic and sulfuric acids concentrations on the extractability of antimony into toluene. HBr concentration: (•) 0.005 M; (○) (□) 0.03 M; (▽) 0.1 M. (•) (○) (▽) 20 μg Sb, against reagent blank. (□) reagent blank, against the TOA solution.

Fig. 5. Effects of hydrobromic and sulfuric acids concentrations on the extractability of antimony into toluene. H_2SO_4 concentration: (○) (□) 8 M; (•) 9 M. (○) (•) 20 μg Sb, against reagent blank. (□) reagent blank, against the TOA solution.

or 0.03 M hydrobromic acid (Fig. 4), or from 0.003—0.03 M hydrobromic acid at 8 or 9 M sulfuric acid (Fig. 5); the curve for 20 μg of antimony at 0.03 M hydrobromic acid (Fig. 4) is in good agreement with the extraction of antimony into benzene from a 0.03 M HBr—H_2SO_4 system reported earlier [11]. In the present work, the 0.05 M KI—3 M H_2SO_4 and 0.01 M HBr—8 M H_2SO_4 systems were selected; higher sulfuric acid concentrations are undesirable, because, in the iodide extraction, the percentage extraction of tin(IV) increases as sulfuric acid concentration increases [10], and in the bromide extraction, copper sulfate tended to precipitate in the determination of antimony in copper metal.

The shaking times for the extraction and for the washing of the organic layer were varied from 3 to 10 min and from 1 to 3 min, respectively; the absorbances were independent of the shaking time in both the iodide and bromide extractions. A 5-min extraction and a 1-min wash were selected.

When the concentration of PV in the PV solution was varied, the absorbance measured against a corresponding reagent blank increased rapidly as the PV concentration increased; maximal absorbances in the iodide and bromide extractions were obtained with 0.0024—0.0060 and 0.0030—0.0060 %(w/v) PV in the PV solution, respectively. The absorbance of the reagent blanks measured against the TOA solution increased linearly in both the iodide and bromide extractions as the PV concentration increased. A 0.0024 and a 0.0030% solution of PV were chosen in the iodide and bromide extractions, respectively.

The pH of the PV solution strongly affected the absorbance; the maximal absorbances in the iodide and bromide extractions were obtained in the pH range (at equilibrium) 4.2—4.7 and 3.9—4.4, respectively (Fig. 6). Since the pH of the PV solution was shifted to lower values by shaking with the organic layer, the pH of the PV solution had to be adjusted to a pH above the optimal equilibrium pH in each of the iodide and bromide extractions. PV solutions of pH 4.5 (equilibrium pH 4.4 in the iodide extraction and 4.2 in the bromide extraction) were therefore chosen.

When the concentration of TOA in the TOA solution was varied from 3 to 30%(v/v), the absorbance measured against a corresponding reagent blank increased rapidly up to 9%(v/v) TOA, then gradually over the range 9—30%(v/v) TOA, as the TOA concentration increased, in both the iodide and bromide extractions. The absorbance of reagent blanks measured against the TOA solution increased gradually with increase in the TOA concentration in the 3—30%(v/v) range. A 22.5% solution of TOA was selected.

The times of shaking for the organic layer with the PV solution and for the extraction of the resulting Sb(III)—PV complex with TOA in toluene were varied from 3 to 10 min; the absorbances were independent of the

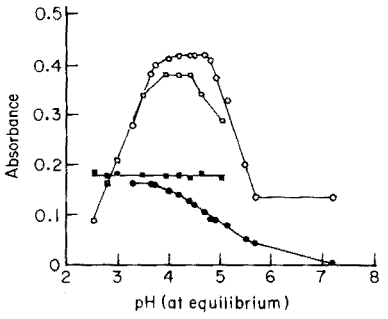

Fig. 6. Effect of pH of the PV solution. (○) (●) iodide extraction. (□) (■) bromide extraction. (○) (□) 20μg Sb, against reagent blank. (●) (■) reagent blank, against the TOA solution.

times, and a 5-min shake and a 5-min extraction were selected.

The color of the complex was stable for at least 1 h.

Effects of diverse acids

The effects of diverse acids on the determination of antimony were examined through the general procedures.

In the iodide extraction, up to 0.05 M hydrochloric acid and up to 0.01 M nitric acid did not interfere; hydrochloric acid above 0.1 M caused a negative error, and nitric acid above 0.05 M oxidized iodide to iodine, resulting in fluctuation of the absorbance on parallel and repeated runs.

In the bromide extraction, hydrochloric and nitric acids interfered strongly; both acids must be absent.

There was no interference from up to 0.5 M perchloric acid in either extraction system.

Effects of various elements

The effects of various elements on the determination of antimony were examined through the general procedures; most of the elements examined were added as sulfate or perchlorate.

In either extraction system, there was no interference from 10 mg of Bi^{3+}, Fe^{3+}, Ni^{2+}, Sn^{4+}; 1 mg of Al^{3+}, As(III), Be^{2+}, Ca^{2+}, Cd^{2+}, Co^{2+}, Cr^{3+}, In^{3+}, La^{3+}, Mg^{2+}, Mn^{2+}, Pb^{2+}, Ta^{5+}, Ti^{4+}, Tl^{+}, Tl^{3+}, V(V), Zn^{2+}; or 0.1 mg of Ag^{+}, Au^{3+}, Ga^{3+}, Ge(IV), Hg^{2+}, Mo(VI), Pt^{4+}, Se(IV), Te(VI) and Zr^{4+}. Since larger amounts of lead formed a lead sulfate precipitate and interfered with the extraction, lead was removed by precipitating it as sulfate, as in the recommended procedure for lead metal; antimony was recovered quantitatively through the procedure.

In the iodide extraction, up to 0.5 mg of copper did not interfere, but larger amounts caused a positive error.

In the bromide extraction, large amounts of copper diminished the absorbance; the absorbance was about 10% low in the presence of 1 g of copper. The interference of as much as 2 g of copper could be eliminated by extracting antimony bromide twice with 5-ml portions of toluene instead of once with 10 ml of toluene; this indicates that the decrease in the absorbance is due to a lowering of the percentage extraction of antimony in the presence of copper.

Analytical results

Antimony in copper and lead metals and in lead-base alloys was determined by the proposed method (Table 1); the precision of the method was good, and as little as 1 μg of antimony could be determined. Somewhat large fluctuations of the slope of the calibration curve on repeated runs were observed; it is therefore essential to prepare a calibration curve for each run.

TABLE 1

Analytical results for various samples

Sample	Sample taken (g)	Sb added[c] (μg)	Total Sb found (μg)	Sb content in the sample (p.p.m.)
Lead metal	5.0	0	<1	<0.2
	5.0	0	<1	
	5.0	20	20.6	
	5.0	40	38.6	
Lead-base alloy[a]	0.10	0	64.0	650
	0.10	0	66.0	
Lead-base alloy[b]	2.0	0	20.0	10
	2.0	0	23.0	
	2.0	20	40.5	
	2.0	20	40.0	
Copper metal (V.M.C.)	2.0	0	7.4	3.3
	2.0	0	7.0	
	2.0	10	16.0	
	2.0	10	15.8	
Copper metal (tough pitch)	2.0	0	7.3	4.1
	2.0	0	8.8	
Copper metal (electrolytic)	2.0	0	2.5	1.2
	2.0	0	1.9	
	2.0	10	13.5	
	2.0	10	11.7	
Anode copper	0.25	0	21.0	86
	0.25	0	21.8	

[a]Components other than lead and antimony: Sn 0.35%.
[b]Components other than lead and antimony: Sn 0.003, Cd 0.018, As 0.002 and Bi 0.008%.
[c]Antimony, in the form of aliquot portions of the standard antimony solution, was added to the solid samples before the decomposition.

REFERENCES

1 Japanese Industrial Standards, H 1101-1973.
2 C. M. Dozinel, Z. Anal. Chem., 157(1957) 401.
3 Japanese Industrial Standards, H 1121-1974.
4 C. L. Luke, Anal. Chem., 31(1959) 1680.
5 C. L. Luke, Anal. Chem., 25 (1953) 674.
6 W. C. Coppins and J. W. Price, Metallurgia, 80 (1956) 183.
7 T. T. Bŷkhovtseva and I. A. Tserkovnitskaya, Zavod. Lab., 30 (1964) 943; Anal. Abstr., 12 (1965) 6440.
8 L. Naruskevicius, R. Kazlauskas, J. Skadauskas and L. Vaskite, Referat. Zh., Khim., 19GD (1974) 4G94; Anal. Abstr., 28 (1975) 5B118.
9 B. W. Bailey, J. E. Chester, R. M. Dagnall and T. S. West, Talanta, 15 (1968) 1359.
10 A. R. Byrne, Anal. Chim. Acta, 59 (1972) 81.
11 A. Grimanis and I. Hadzistelios, Anal. Chim. Acta, 41 (1968) 15.

Analytica Chimica Acta, 92 (1977) 387—392

THE APPLICATION OF TIRON IN PHOTOMETRIC TITRATIONS

G. den BOEF*, W. OZINGA and G. J. van ROSSUM

Laboratory for Analytical Chemistry, University of Amsterdam, Nieuwe Achtergracht 166, Amsterdam (The Netherlands)

(Received 5th March 1977)

SUMMARY

Tiron is a suitable titrant for the direct, selective photometric titration of bismuth(III), iron(III) and thorium(IV) in acidic solutions. Metal ions such as lead(II), nickel(II) and copper(II) do not interfere; this is in contrast with titrations in which EDTA or a similar chelating agent is used as the titrant.

A disadvantage of ligands of the EDTA-type, forming 1:1 complexes with nearly all metal ions, is their lack of selectivity. Polyamines such as Trien are more selective because complexation is restricted to metal ions with a preference for nitrogen as the coordinating atom.

Ligands with oxygen as the only coordinating atom show selectivity towards another group of metal ions; those that form 1:1 complexes with metal ions have not been described extensively in the literature so that it was reasonable to examine whether or not ligands that have oxygen as the only coordinating atoms and show step-wise complex formation might be helpful in the selective titration of metal ions. In recent papers [1—3] it has been demonstrated that titrations of metal ions with ligands forming 1:2 complexes may be feasible when linear end-point indication is applied.

The first reagent studied was tiron, 1,2-dihydroxybenzene-3,5-disulphonic acid, H_4L, which forms complexes with a number of metal ions and has adequate light absorption properties for photometric indication of the end-point of a titration. The protonation constants mentioned in the literature for this ligand are: $\log K_1 = 12.5$ for $L + H \rightleftarrows LH$, and $\log K_2 = 7.5$ for $LH + H \rightleftarrows LH_2$. From these constants the side-reaction coefficient $\alpha_{L(H)}$ can be calculated as a function of pH, according to $\alpha_{L(H)} = 1 + 10^{12.5}\,[H^+] + 10^{20}\,[H^+]^2$. The values for $\log \alpha_{L(H)}$ for tiron at pH 1, 2, 3, 4, 5, 6 and 7 are 18.0, 16.0, 14.0, 12.0, 10.0, 8.0 and 6.1, respectively.

The literature data [4] for the stability constants of complexes of metal ions with tiron are very incomplete, but some general conclusions can be drawn. 1:1, 1:2 and 1:3 complex formation has been described. Generally $K_1 \gg K_2 \gg K_3$ which means that end-point determination is possible when the ligand has been added in a 1:1 ratio, provided that the end-point can be

indicated. The value of the first stability constant for a number of metal ions, e.g. iron(III), hafnium(IV) and zirconium(IV), is reported to be larger than 10^{20} which means that the conditional stability constant at pH 3, or even lower, is larger than 10^6 so that titrations of 10^{-4}—10^{-5} M solutions of these metal ions should be possible in fairly acidic solutions. Interferences by copper(II), lead(II) and nickel(II), which nearly always occur when EDTA is used as the titrant, are very unlikely as the conditional stability constants for the complexes of these metal ions with tiron are very low at pH 3. For aluminium(III) a log K_1 value of 17 has been reported which suggests that moderate amounts of aluminium(III) should not interfere. For uranium(VI) and vanadium(IV), log K_1 values of ca. 16 have been reported, suggesting the possibility of titrations of these metal ions at the 10^{-5} M level at pH 6.

Ternary complex formation of complexes of metal ions and tiron with other ligands has been frequently reported.

DETERMINATION OF THORIUM(IV)

To check the applicability of tiron as a titrant the photometric titration of thorium(IV) with tiron has been thoroughly investigated. Although complex formation constants of thorium(IV) with tiron are not in the literature, a behaviour not too different from hafnium(IV) and zirconium(IV) is to be expected. Special attention has been given to the influence of those metal ions which generally interfere in titrations of metal ions with EDTA in acidic solutions.

Experimental

Absorption spectra were recorded with a Beckman Acta M VI spectrophotometer. Photometric titrations were carried out with a Zeiss PMQ II spectrophotometer provided with a M4Q III monochromator. A microburette (Metrohm type E 457; 0.5 ml) was used. Titration curves were obtained either by manual operation or semiautomatically.

Analytical-grade reagents and deionized water were used. Metal ions were added as their nitrates. Tiron was standardized by potentiometric titration with sodium hydroxide (result: 100.5%). Solutions of tiron in water and in an acetic acid—acetate buffer solution are stable for at least one month.

In order to select a suitable wavelength for the photometric titration of thorium(IV) with tiron, the spectra of the ThL complex and H_2L^{2-}, the form in which the ligand is present in acidic solution, were recorded (Fig. 1). From these spectra, an obvious choice for the wavelength for the titration is 315 nm. The value of the molar absorptivity at this wavelength for ThL, about 6000 cm^{-1} mol^{-1} l, sets a lower limit of determination of 10^{-5} M thorium(IV) from the point of view of the indication method.

Preliminary titrations showed that, at this concentration level, suitable curves were possible only at ca. pH 3. Below this pH there was considerable curvature at the equivalence point, because the value of the conditional

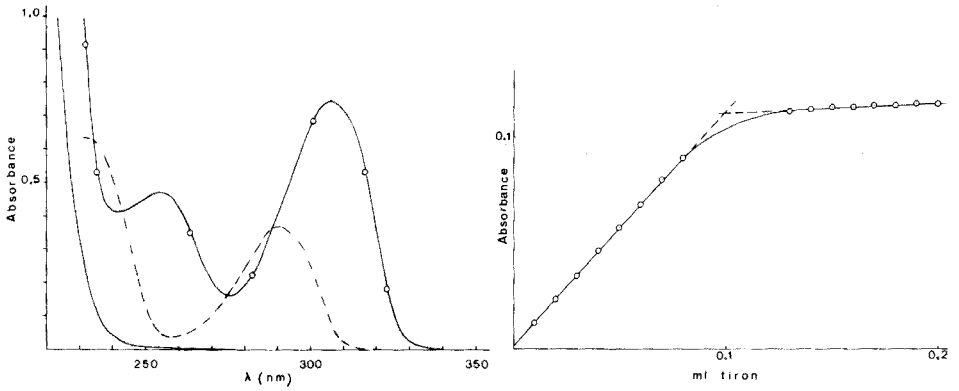

Fig. 1. Absorption spectra of 10^{-4} M $Th(NO_3)_4$ (——), 10^{-4} M tiron (-------) and 10^{-4} M $Th(NO_3)_4$ + 10^{-4} M tiron (—o—o—) all at pH 3.0 (perchloric acid).

Fig. 2. Photometric titration curve of the titration of 10 ml of 10^{-5} M $Th(NO_3)_4$ with 10^{-3} M tiron; 315 nm; pH 3.0 (perchloric acid).

stability constant of ThL is too low; pH values greater than 3 should be avoided because of possible hydrolysis of thorium(IV).

A curve for the titration of 10 ml of 10^{-5} M thorium nitrate (20 μg of thorium) in 10^{-3} M perchloric acid with 10^{-3} M tiron at 315 nm is given in Fig. 2; the value of the conditional stability constant for ThL estimated from this curve is 10^{21}—10^{22}.

Titration procedure. Transfer 8—10 ml of 10^{-5} M thorium(IV) (20 μg) solution in perchloric acid, pH 3, to the titration cell of the photometer (optical path length 2 cm). Titrate with 10^{-3} M tiron at 315 nm. The equivalence point is the point of intersection of the two straight branches in the curve.

High local pH values during the pretreatment of the titration solution may lead to low results because of the formation of hydroxo complexes of thorium(IV) that do not react with tiron. Therefore adjustment of the pH should be carried out with great care.

Results

The standard deviation for a single determination of 20 μg of thorium(IV) was about 1%. The results of determinations of 20 μg of thorium(IV) in the presence of some other ions (Table 1) agree with what could be expected. Sulphate interferes because it forms a complex with thorium(IV). The relatively large values of the standard deviation arise mainly from the fact that the determinations are carried out near the limit of determination. The possibility of small losses of thorium has been mentioned above.

The effects of bismuth(III), copper(II), iron(III), lead(II) and nickel(II) were also investigated. As expected, bismuth(III) and iron(III) interfere. The separation of these metal ions from thorium(IV) at a mercury pool cathode has been described previously [5]. Lead(II), nickel(II) and copper(II) in 100-fold

TABLE 1

Determination of 20 μg (10^{-5} M) thorium(IV) at pH 3 in the presence of other ions

Other ion(X)	[X]:[Th]	Error (%)	s_r (%)	No. of detns.
Al(III)	10	+1	1.0	3
	100	+3.5	2.3	3
	1000	No e.p.		
Zn(II), Co(II), Cd(II)	100 each	−0.1	1.8	3
Cr(III)	1	+2		
	100	+5	2.4	4
Ce(III), La(III)	100 each	+1.5	2.3	3
U(VI)	100	+4	0.4	3
Hg(II)[a]	10	+5	1.0	3
SO_4^{2-}	1	−2.5	3.0	4
	10	No e.p.		

[a]Titrations in the presence of mercury(II) were carried out at pH 2.7 to prevent the formation of a precipitate.

concentrations do not interfere even when present together (error, +2%; s_r, 1%). With much larger amounts of these ions, difficulties from different causes arise:

(1) the metal ions are added as their nitrates, and large concentrations of nitrate have a considerable absorbance at 315 nm, thus making end-point determination difficult. Moreover, even analytical-grade nitrates contain traces of iron which cause positive errors;

(2) the curvature of the titration curve at the equivalence point increases when very large amounts of other ions are present. This effect can be corrected by a small increase in the pH.

For these reasons some titrations of 10^{-5} M thorium(IV) were carried out at pH 3.5 in the presence of 1000-fold amounts of nickel(II), copper(II) and lead(II) perchlorate, prepared from the Specpure oxides. The reaction was slightly slower, but end-point determination was easily possible (error, +5%, s_r, 1.2%; $n = 3$).

The interference of iron(III) and bismuth(III) with the determination of thorium(IV) suggested the feasibility of the photometric titration of these ions with tiron as well.

DETERMINATION OF BISMUTH(III)

Values for the stability constants of complexes of bismuth(III) with tiron are not available in the literature. Preliminary photometric titration curves suggested a value for log K_1 much larger than 20. The absorption spectrum of BiL is nearly identical with that of ThL given in Fig. 1. Hence, the same wavelength was selected as for the determination of thorium(IV), i.e. 315 nm.

To prevent hydrolysis of bismuth(III), titrations were carried out below pH 3 only.

A pH of 2.8 was suitable for the determination of 10^{-5} M solutions of bismuth(III) (20 μg in 10 ml), whereas 10^{-4} M bismuth(III) (200 μg in 10 ml) could be titrated at pH 1.6, in both cases with a standard deviation of about 2%. At pH 2.8 the determination of bismuth(III) by titration of a solution containing 10^{-5} M bismuth(III), 10^{-2} M copper(II), 10^{-2} M lead(II) and 10^{-2} M nickel(II) was possible with the same precision. A 100-fold amount of aluminium(III) (molar ratio) also did not interfere, but with a 1000-fold amount of aluminium(III) the standard deviation was rather large (5%).

At pH 1.6, determinations of 10^{-4} M bismuth(III) in the presence of 1000-fold amounts of copper(II), lead(II) and nickel(II) (molar ratio) are also possible, but the precision is worse, probably because of the high ionic strength of the solutions to be titrated resulting in a decrease of the conditional stability constant of BiL. At pH 1.6 the presence of 100-fold amounts of thorium(IV) can be tolerated.

DETERMINATION OF IRON(III)

The literature values [4] for the stability constants of the complexes of iron(III) with tiron are $\log K_1 = 20.7$; $\log K_2 = 15.2$ and $\log K_3 = 11.0$. These values suggest the possibility of the determination of 10^{-4}—10^{-5} M iron(III) by photometric titration at pH 3. Absorption spectra for FeL, Fe(III) and H_4L are given in Fig. 3. Two wavelengths appear to be suitable

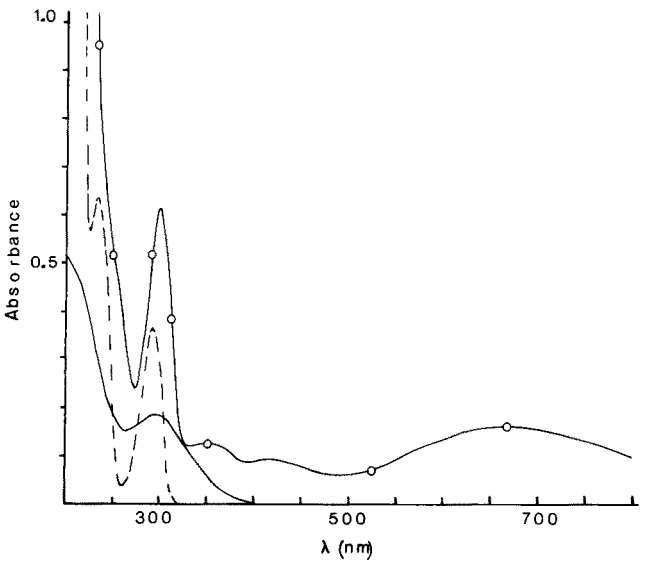

Fig. 3. Absorption spectra of $5 \cdot 10^{-5}$ M $Fe_2(SO_4)_3$ (——), 10^{-4} M tiron (------) and $5 \cdot 10^{-5}$ M $Fe_2(SO_4)_3$ + 10^{-4}M tiron (—○—○—) all at pH 3.0 (perchloric acid).

for the titration, viz. 305 nm and 675 nm. At 305 nm $\epsilon_{FeL} - \epsilon_{Fe}$ is about 4500 cm^{-1} mol^{-1} l; at 675 nm, only FeL absorbs with ϵ_{FeL} = 1700 cm^{-1} mol^{-1} l. Although the latter value is much lower than the former, titrations at 675 nm were also carried out with a Zeiss Elko II filter photometer. This apparatus operates according to the substitution principle and allows the accurate and precise determination of very small absorbance values; the 660-nm filter was used. The titration of 10 ml of 10^{-5} M iron(III) (about 5 μg of iron) with tiron at pH 3 (perchloric acid) was possible at 305 nm (s_r, 2%) and at 660 nm (s_r, 1%).

The investigation of the influence of other metal ions was restricted to copper(II), nickel(II) and lead(II). A solution containing 10^{-5} M iron(III), 10^{-2} M copper(II), 10^{-2} M nickel(II) and 10^{-2} M lead(II) was titrated with tiron; no significant error was observed. The standard deviation was 2.5% for titrations at 305 nm and 1% at 660 nm.

Titrations of uranium(VI) and vanadium(IV) at pH 6 and 7 were not successful.

REFERENCES

1 F. Freese, G. den Boef and G. J. van Rossum, Anal. Chim. Acta, 58 (1972) 429.
2 F. Freese and G. den Boef, Anal. Chim. Acta, 60 (1972) 131.
3 G. J. van Rossum and G. den Boef, Anal. Chim. Acta, 61 (1972) 144.
4 L. G. Sillen and A. E. Martell, Stability Constants, Chemical Society, London, 1964 and 1971.
5 F. Freese, R. Oostervink and G. den Boef, Talanta 18 (1971) 1064.

Analytica Chimica Acta, 92 (1977) 393—397

SPECTROPHOTOMETRIC DETERMINATION OF CARBON DISULPHIDE AS THE 1,2,3,4-THIATRIAZOL-5-THIOLATE ION

E. A. NEVES

Instituto de Química da U.S.P., C.P. 20780, São Paulo, S.P. (Brazil)

D. W. FRANCO and P. F. ROMANELLI

F.F.C.L.R.P., Depto. de Química, Av. dos Bandeirantes, s/n Ribeirão Preto, S.P. (Brazil)

(Received 26th October 1976)

SUMMARY

A simple, precise and selective procedure for the spectrophotometric determination of carbon disulphide in water is described. The method is based on the quantitative formation of the 1,2,3,4-thiatriazol-5-thiolate ion from carbon disulphide and azide. The specific rate for this reaction at ionic strength 4.0 (NaN_3) and 25°C is $8.4 \cdot 10^{-3}$ mol^{-1} s^{-} the kinetic parameters $\Delta H^{\ddagger}$ and $\Delta S^{\ddagger}$ are 16.7 kcal mol^{-1} and −14 cal mol^{-1} deg^{-1}, respectively. At the analytical wavelength of 313 nm, the molar absorptivity is $7.27 \cdot 10^{3}$ l mol^{-1} cm^{-1}. The system obeys Beer's law for 2.3—8.6 g ml^{-1} of carbon disulphide. The effects of foreign ions are discussed.

Browne and Currier [1] were the first to suggest the analytical use of the reaction between carbon disulphide and azide. This study dealt with the absorption of carbon disulphide vapor by solutions of sodium or potassium azide. Further work [2] led to a procedure for the determination of the product of reaction (I), the 1,2,3,4-thiatriazol-5-thiolate

(I)

Feigl and Chargav [3] employed the catalytic effect of carbon disulphide in the reaction between iodine and azide for the determination of azide. A procedure for the determination of carbon disulphide in waste waters has been suggested by Solenkiand and Wojciak [4] based on this work. Reaction (I) has also been used for the determination of CS_2 in human body fluids [5, 6].

This paper reports a procedure in which CS_2 is quantitatively converted to $CS_2N_3^{-}$, which is determined at 313 nm. The sensitivity and selectivity attained are higher than those reported earlier [1—6]. The kinetics of reaction (I) as well as the effects of several foreign ions were also investigated.

EXPERIMENTAL

Apparatus

Spectrophotometric and kinetic measurements were made in 1.00, 0.500 and 0.100-cm cells with Beckman DU and DB-G spectrophotometers.

A Metrohm E-485 multiburet provided with a 20.0-ml cylinder was used for the reproducibility studies. An Horizont thermostat regulated the temperature of the cell compartment within ±0.1°C for the kinetic measurements.

Reagents and solutions

All chemicals were of reagent grade. Sodium azide and carbon disulphide were purified as described previously [7].

Saturated aqueous carbon disulphide solution. Place 12 ml of CS_2 and enough distilled water to make up to 250 ml in a glass-stoppered Erlenmeyer flask. Protect the solution from light and maintain at 18—25°C for 8 h. Shake the flask occasionally. This solution contains around 2 mg CS_2 ml^{-1} [8]. From this solution samples can be taken and diluted with distilled water. To avoid losses of CS_2 by volatilization, the solution should be introduced slowly into a calibrated graduated pipet and carefully transferred to a volumetric flask. The upper quarter of the solution in the pipet should be discarded. The use of cold distilled water, 10—15°C, minimizes loss of carbon disulphide and so enhances reproducibility. The solutions of carbon disulphide were standardized as described by Hofman-Bang and Holten [9].

Sodium azide solution (5.0 M). This was standardized by West's procedure [10].

Sodium 1,2,3,4-thiatriazol-5-thiolate solution (0.1 M). A weighed amount of the solid $NaCS_2N_3$ was dissolved in cold distilled water in an amber volumetric flask and the solution protected from light [7]. The $NaCS_2N_3$ was prepared by the reaction of aqueous 4—5 M NaN_3 with CS_2, as reported earlier [7]. The $NaCS_2N_3$ solutions were standardized by Volhard's method [2]

Kinetic measurements

The spectrophotometric cells were almost filled with solutions of sodium azide and thermostated at the desired temperature. The carbon disulphide solutions were thermostated in separate flasks. Then a measured volume of CS_2 solution was added to the cell as quickly as possible, and the cell was closed immediately and shaken vigorously. The progress of the reaction was followed by the increase in absorbance at 313 nm. The reaction was observed for a period of time corresponding to at least 10 half-lives. The last absorbance measurement was used to calculate the initial carbon disulphide concentration. The data were plotted as log $(A_\infty - A)$ vs. time or log $([a]/[a-x])$ vs. time (where $[a]$ is the original carbon disulphide concentration, and $[a-x]$ is the concentration of carbon disulphide at time t) The psuedo first-order plots were linear for at least 9 half-lives. The second-

order rate constants were obtained by dividing the pseudo first-order rate constant by the azide concentration.

General analytical procedure

Place 8.0 ml of 5.0 M NaN_3 solution in a 10.0-ml volumetric flask and cool to 10—15°C. Add 0.5—2.0 ml of sample, close the flask, and put it upside down for 25—30 min in the dark at room temperature. After diluting to 10.0 ml with distilled water, measure the absorbance at 313 nm against a reagent blank solution prepared by placing 8.0 ml of 5.0 M NaN_3 solution in a 10.0-ml volumetric flask and diluting to 10.0 ml with distilled water.

Procedure in the presence of S^{2-}, SO_3^{2-}, NO_3^-, NO_2^-. Prepare two samples. With one, follow the general procedure. Bubble nitrogen through the other solution for 10—15 min to eliminate all CS_2. Then add 8.0 ml of 5.0 M NaN_3 solution and adjust the volume to 10.0 ml with distilled water. Use this solution as a comparison solution instead of the reagent blank.

Procedure in presence of Cu^{2+}. To a 10.0-ml volumetric flask, immersed in cold water, add 1.0 ml of 1.0 M NaCN solution followed by the sample; stir gently, and add 7—8 ml of 5.0 M NaN_3 solution. Close the flask and follow the procedure described above. Measure the absorbance against a blank solution which contains the same amount of sodium azide and cyanide as the sample.

Procedure in presence of cations in general. To a 10.0-ml volumetric flask, immersed in cold water, add first 1.0 ml of saturated Na_2CO_3 solution and then the sample; shake gently, add 7—8 ml of 5.0 M NaN_3 solution, and follow the general procedure. Centrifuge the solution before measuring the absorbance against a blank solution with the same concentrations of NaN_3 and Na_2CO_3. In the absence of Cr^{3+} and Fe^{3+} and when the concentration of Ni^{2+} or Co^{2+} does not exceed 10 times the concentration of CS_2, the Na_2CO_3 solution can be replaced by a saturated solution of the disodium salt of ethylenediaminetetraacetic acid. In this case no centrifugation is required.

RESULTS AND DISCUSSION

Kinetic study

To develop an analytical procedure based on reaction (I), a knowledge of its kinetics is helpful. Hofman-Bang and Holten [11] have studied this reaction under second-order conditions and at low ionic strength. From these data, the values of 22.2 kcal mol^{-1} and + 4.5 cal mol^{-1} deg^{-1} for $\Delta H^{\ddagger}$ and $\Delta S^{\ddagger}$ respectively [12] were calculated. For analytical purposes, however, it is desirable to work with a large excess of azide, to decrease the time for complete conversion of CS_2 to $CS_2N_3^-$. In the quite different conditions desirable for analytical purposes, changes in the activity coefficients of the ions, the carbon disulphide molecules, and the solvent are expected [12, 13]. These changes are reflected in the kinetic data

presented in Table 1. The temperature range employed is that of analytical interest, 8—25°C. Although temperatures above 25°C are desirable from a kinetic point of view, this would decrease the analytical accuracy because of errors from volatilization of carbon disulphide. At temperatures below 20°C, the loss of carbon disulphide by evaporation can be disregarded [14].

The data obtained (Table 1) show that 25 min is sufficient to ensure the complete conversion of CS_2 to $CS_2N_3^-$ in 3.5—4.0 M NaN_3, even at the lowest temperature, 8°C. More concentrated solutions of NaN_3 do not reduce the time substantially, and present the disadvantage of increasing the blank absorbance.

For the enthalpy and entropy of activation, the values of $\Delta H^{\ddagger} = 16.7$ kcal mol^{-1}, and $\Delta S^{\ddagger} = -14$ cal mol^{-1} deg^{-1} were calculated. The values reported here for the specific rate constants are higher than the earlier values [11]. The compensation of the change in $\Delta H^{\ddagger}$ and $\Delta S^{\ddagger}$ explains why the deviation from the earlier values is not greater.

The determination of carbon disulphide

The absorption spectra obtained for $CS_2N_3^-$ in an aqueous 4.0 M sodium azide solution is the same as that presented earlier [7]. However, because of a change in the ionic strength of the medium, the molar absorptivity at 313 nm becomes $7.27 \cdot 10^3$ l mol^{-1} cm^{-1}. Changes in the concentration of sodium azide solution in the range 3.5—4.0 M do not produce detectable changes in this molar absorptivity.

The calibration graphs are linear over the range $3.02 \cdot 10^{-5}$—$1.13 \cdot 10^{-4}$ M (2.3—8.6 μg ml^{-1}) carbon disulphide in the final solution. For practical purposes, the final solution should be 3.5—4.0 M in NaN_3, and the lowest concentration of CS_2 in the collected sample before the addition of the 7.0—8.0 ml of NaN_3 solution should be 11 μg ml^{-1}. Calibration plots were obtained by appropriate dilutions of solutions of $NaCS_2N_3$ and by generating the $CS_2N_3^-$ ion in situ by reacting a standardized carbon disulphide solution with excess of azide ion. The agreement between the two methods was better than 99%.

TABLE 1

Reaction of azide ion with carbon disulphide
($[N_3^-] = 4.00$ M)

Temp. (°C)	$t_{\frac{1}{2}}$ (s)[a]	10^3 K (mol^{-1} s^{-1})
25.0	20.6	8.40
20.0	36.5	4.75
15.0	60.3	2.87
11.0	82.5	2.10
8.0	120.0	1.44

[a]Each value is the mean of four independent determinations with an average deviation of less than 4%.

For a series of twenty independent samples, each containing originally 55.2 μg CS_2 ml^{-1}, the standard deviation was ± 0.6 μg ml^{-1}. At the 90% confidence limit based on a single analysis, a value of 55.2 ± 1.0 μg ml^{-1} can be estimated. The absorbances are stable for 3 h if the solutions are kept at room temperature in the dark.

Diverse ion study

A study of potentially interfering ions was made by adding various amounts of the different ions to 2.0 ml of aqueous carbon disulphide solution (10 μg ml^{-1}), before the addition of sodium azide. At the 1.0 mg ml^{-1} level urea and the following ions do not interfere: CNO^-, CN^-, F^-, SCN^-, I^-, Cl^-, Br^-, ClO_4^-, HCO_3^-, $H_2PO_4^-$, CH_3COO^-, $HCOO^-$, $C_6H_5O_7^-$, $C_4H_7O_6^-$, CO_3^{2-}, SO_4^{2-}, $S_2O_3^{2-}$, $C_2O_4^{2-}$, HPO_4^{2-}, PO_4^{3-}, K^+, NH_4^+. At the 0.5 mg ml^{-1} level, S^{2-}, SO_3^{2-}, NO_3^- and NO_2^- do not interfere. If the procedures recommended in the Experimental are used, the analyses may also be performed in the presence of 0.5 mg ml^{-1} of Mg^{2+}, Ca^{2+}, Sr^{2+}, Ba^{2+}, Fe^{2+}, Co^{2+}, Ni^{2+}, Mn^{2+}, Cu^{2+}, Pb^{2+}, Zn^{2+}, Al^{3+}, Cd^{2+}, Cr^{3+}, Fe^{3+}, and 1.0 mg ml^{-1} of S^{2-}, SO_3^{2-}, NO_3^- and NO_2^-.

This study indicates that with the modified experimental conditions, high selectivity can be obtained by the proposed method. Its characteristics make it more adaptable to the determination of carbon disulphide in waste water and human body fluids than procedures reported earlier [3—6].

Financial support through FAPESP Grant 74/135, and an FAPESP fellowship for P. F. Romanelli (73/461), are gratefully acknowledged.

REFERENCES

1 A. W. Browne and A. J. Currier, J. Am. Chem. Soc., 44 (1922) 2849.
2 A. W. Browne, L. F. Audrieth and G. B. L. Smith, J. Am. Chem. Soc., 49 (1927) 2129.
3 F. Feigl and F. Chargav, Z. Anal. Chem., 74 (1928) 376, 80.
4 R. Solenkiand and W. Wojciak, Chem. Anal., 12 (1967) 849; Chem. Abs., 68 (1968) 53080m.
5 T. Dutkiwicz and B. Baranowska, Ann. Acad. Med. Lodz, 175080 (1966); Chem. Abs., 70 (1969) 22713 g.
6 D. Djuric, L. Graovac and R. L. Jubica, Med. Radiolog. Prot., 19 (1968) 245; Chem. Abs., 70 (1969) 22711e.
7 E. A. Neves and D. W. Franco, J. Inorg. Nucl. Chem., 36 (1974) 3851.
8 H. Stephen and T. Stephen, Solubilities of Inorganic and Organic Compounds, Pergamon Press, Oxford, 1963, part 1 p. 369.
9 N. Hofman-Bang and W. Szybalski, Acta Chem. Scand., 3 (1949) 926.
10 C. A. West, J. Chem. Soc., 77 (1900) 705.
11 N. Hofman-Bang and B. Holten, Acta Chem. Scand., 5 (1951) 333.
12 J. F. Bunnet, From Kinetic Data to Reaction Mechanism, in the Techniques of Chemistry series, Vol. VI, Part I, E.S. Lewis (Ed.), Wiley-Interscience, New York, 1974, pp. 402—421.
13 A. A. Frost and R. G. Pearson, Kinetics and Mechanics, J. Wiley, New York, 2nd edn., 1961 , pp. 150—156.
14 N. Hofman-Bang, Acta Chem. Scand., 3 (1949) 1418.

Analytica Chimica Acta, 92 (1977) 399—403

Short Communication

CESIUM- AND THALLIUM(I)-SENSITIVE LIQUID MEMBRANE ELECTRODES BASED ON CESIUM- AND THALLIUM TETRAKIS(*m*-TRIFLUOROMETHYLPHENYL)BORATES

C. J. COETZEE and A. J. BASSON

Department of Chemistry, University of the Western Cape, Bellville (South Africa)

(Received 10th December 1976)

Previously reported [1—4] cesium- and thallium-sensitive electrodes based on heteropolyacid salts in an inert support were not selective and their calibration curves did not have Nernstian slope. The authors [5] reported the use of cesium tetraphenylborate dissolved in an appropriate solvent, as the membrane material, for a cesium-sensitive electrode.

The use of tetra-arylborates as precipitants for the gravimetric determination of cesium in the presence of rubidium or potassium has been reported [6]. Because of the high selectivity of the trifluoromethyl derivative for cesium and thallium, cesium- and thallium tetrakis(*m*-trifluoromethylphenyl)borates dissolved in an appropriate solvent were investigated as membrane materials for ion-selective electrodes.

Experimental

All chemicals used, except ethylnitrobenzene, which was redistilled under reduced pressure, and the tetra-arylborate salts, were of A.R. grade. Sodium tetrakis(*m*-trifluoromethylphenyl)borate was prepared by the method of Meisters et al. [6], as was the cesium salt. The thallium(I) salt was prepared analogously.

Electrode assemblies were as described previously [5]. The organic phase consisted of 0.2 g of salt dissolved in 4 ml of ethylnitrobenzene. As reported previously by Coetzee and Freiser [7], the concentration of active material in the membrane did not have a notable effect on the response characteristics of the electrodes, though below a 1% concentration the membrane resistance would become too high and membranes would not respond. The aqueous reference phases were 0.10 M cesium chloride and 0.10 M thallium nitrate saturated with thallium chloride, respectively. The lifetimes of the electrodes were more than 4 months. n-Decanol and nitrobenzene were also suitable for use as solvents for the active material, but these electrodes had a lifetime of only 3—4 weeks. After preparation, electrodes were conditioned for at least 1 h by immersion in 0.10 M metal nitrate solutions of the appropriate cations, after which they gave stable potential readings.

Electrodes were usually stored in this manner when not in use. A good response was also attained if the electrodes were blotted dry after use and stored in air.

Results and discussion

The electrodes gave linear calibration curves in pure nitrate solutions in the concentration range 10^{-1}—10^{-4} M. The calibration curves could be used to determine cesium(I) concentrations as low as 10^{-6} M and thallium(I) concentrations as low as 10^{-5} M. In the case of the cesium electrode, the slope of the calibration curve at 20°C was independent of the anion present in the test solution, the values being 57.0, 57.5 and 58.0 mV/pCs in sulphate, chloride and nitrate solutions, respectively. Because of the insolubility of certain thallium(I) salts, the slopes of the calibration curves were determined only in nitrate and sulphate solutions, being 58.3 and 57.0 mV/pTl at 20°C, respectively.

The pH-dependence of the electrodes was studied for the pH range 2—12. The pH of the test solutions was adjusted by addition of nitric acid and sodium hydroxide solutions having the same concentration of the cation in question as in the test solution. The results indicated a "working range" for both electrodes between pH 3 and 12. With thallium concentrations $\leqslant 10^{-3}$ M the working range was pH 3—9. Both electrodes were less sensitive to hydronium ions than the previously described cesium electrode [5].

The response times for e.m.f. measurements were not studied in detail. In 10^{-1}—10^{-3} M solutions, stable readings were obtained within 30 s; with more dilute solutions a 1—3-min period was required to obtain stable readings. Stability of measurements was better with slow than with fast stirring.

Selectivity. The effects of cations on the responses of the two electrodes were studied in two ways. First, calibration curves were prepared from potential measurements in solutions containing only the metal nitrate in question: the results are summarized in Table 1. Secondly, a systematic examination of the interferences of sodium, potassium, rubidium, cesium, ammonium, thallium(I), silver, magnesium, calcium, strontium and barium ions on electrode response was undertaken. Calibration curves for cesium or thallium ions in the presence of fixed concentrations of interfering ions were prepared.

The curves showed no interference from Na^+, K^+ and NH_4^+ ions at concentrations of these ions smaller than 10^{-2} M for the cesium electrode and concentrations smaller than 10^{-4} M for the thallium electrode. Concentrations of Mg^{2+}, Ca^{2+}, Sr^{2+} and Ba^{2+} ions up to 10^{-2} M had no influence on the thallium electrode response in $\geqslant 10^{-3}$ M thallium solutions. Selectivity coefficients K_{CM}, were calculated from these curves by means of the equation

$$K_{CM} = (10^{\Delta E/S} - 1)\, a_{C^+}/(a_{M^{z+}})^{\frac{1}{z}}$$

TABLE 1

Selectivity coefficients for the cesium and thallium electrodes, and slopes and ranges of calibration curves in metal solutions at 20°C

Cation	Cesium-sensitive electrode			Thallium-sensitive electrode		
	K_{CsM}[a]	Slope (mV/pM)	Linear range (pM)	K_{TlM}[b]	Slope (mV/pM)	Linear range (pM)
Cs^+	$1 \cdot 10^0$	57.5	1—4	$2.9 \cdot 10^0$	57.0	1—4
Tl^+	$5.8 \cdot 10^{-1}$			$1 \cdot 10^0$	58.3	1—4
Na^+	$7.5 \cdot 10^{-3}$	—	—	$2.3 \cdot 10^{-2}$	36.0	1—3
K^+	$7.4 \cdot 10^{-2}$	42.3	1—3	$2.55 \cdot 10^{-1}$	50.0	1—3, 5
Rb^+	$2.2 \cdot 10^{-1}$	47.3	1—3, 5	$8.65 \cdot 10^{-1}$	56.0	1—4
NH_4^+	$3.7 \cdot 10^{-2}$	49.0	1—3	$1.25 \cdot 10^{-1}$	44.5	1—3, 5
Ag^+	$9.6 \cdot 10^{-2}$			$1.9 \cdot 10^{-1}$		
Mg^{2+}	$1.8 \cdot 10^{-3}$			$5.1 \cdot 10^{-3}$		
Ca^{2+}	$3.0 \cdot 10^{-3}$			$1.3 \cdot 10^{-2}$		
Sr^{2+}	$3.3 \cdot 10^{-3}$			$1.3 \cdot 10^{-2}$		
Ba^{2+}	$3.6 \cdot 10^{-2}$			$5.6 \cdot 10^{-2}$		

[a] $a_{Cs^+}/a_{Mz^+} = 10^{-3}$, except for thallium and barium where the ratio was 10^{-2}.
[b] $a_{Tl^+}/a_{Mz^+} = 10^{-2}$, except for barium where the ratio was 10^{-1}.

where ΔE is the change in potential in the presence of the interfering ion, S is the slope of the calibration curve for the primary ion, and a_{C^+} and a_{Mz^+} the activities of Cs^+ or Tl^+ and the interfering ion, respectively. The results (Table 1) show that the cesium electrode has a higher degree of selectivity for cesium ion over the other alkali ions than the previously reported epoxy resin-membrane electrodes [3], but are of the same order as those reported for the liquid-membrane cesium tetraphenylborate electrode [5]. With both the cesium and thallium electrodes, the response decreases in the order: $Cs^+ > Tl^+ > Rb^+ > K^+ > Ag^+ > NH_4^+ > Na^+$.

Standard addition potentiometry [8]. This method was applied to test the performance of the electrodes as described previously [5]. Error-free results were obtained in all cases for 33.2 mg of cesium in 50-ml samples at constant ionic strength ($5 \cdot 10^{-1}$ M $NaNO_3$), and for 51 mg of thallium(I) in 50-ml samples at constant ionic strength (10^{-1} M $NaNO_3$).

The standard-addition method was also applied to determine the solubility of cesium and thallium tetrakis(*m*-trifluoromethylphenyl)borate in water at 25°C. Titrations were done in a jacketed titration vessel and the slopes of calibration curves at 25°C were used in the calculations. The results quoted are the mean of at least three determinations and are: cesium salt 0.131 g l^{-1} at pH 6.6 (literature value, 0.131 g l^{-1} [6]) and thallium salt 0.541 g l^{-1} at pH 6.3.

Titrations. When the thallium electrode was used, the following titrations gave satisfactory results: (i) Titration of 511 mg Tl^+ in 25 ml of water with 0.100 M K_2CrO_4 or Na_2CrO_4. (The end-points correspond to the precipitation of Tl_2CrO_4. A better shaped titration curve resulted with sodium chromate

as titrant because the electrode is less sensitive to sodium than potassium ions.) (ii) Titration of 204 mg Tl^+ in 30 ml of water with 0.100 M sodium tetraphenylborate solution; (iii) Titration of 20.4 mg Tl^+ in 30 ml of water with 0.0100 M sodium tetrakis(*m*-trifluoromethylphenyl)borate solution. Figure 1 (curve a) shows the titration of thallium(I) in the presence of some potassium(I) with $1.053 \cdot 10^{-2}$ M sodium tetrakis(*m*-trifluoromethylphenyl)borate solution; only thallium is titrated, curve (b) shows the titration of thallium(I) and cesium(I); in this case the total cation content is titrated.

When the cesium electrode was used the following titrations gave satisfactory results: (i) Titration of 33.2 mg Cs^+ in 25 ml of water with 0.0100 M sodium tetraphenylborate solution; (ii) Titration of 33.2 mg Cs^+ in 25 ml of water with $1.053 \cdot 10^{-2}$ M sodium tetrakis(*m*-trifluoromethylphenyl)borate solution; (iii) Titration of 13.3 mg Cs^+ and 3.9 mg K^+in 35 ml of water with the same titrant as in (ii), only the cesium ions being determined. Figure 1 (curve c) shows the titration of 13.3 mg Cs^+ and 8.6 mg Rb^+ in 35 ml of water with this titrant; again only the Cs^+ content is titrated. Figure 1 (curve d) shows the subsequent titration of the rubidium content of this sample with $1.048 \cdot 10^{-2}$ M sodium tetraphenylborate solution.

All the titration curves have the normal shape.

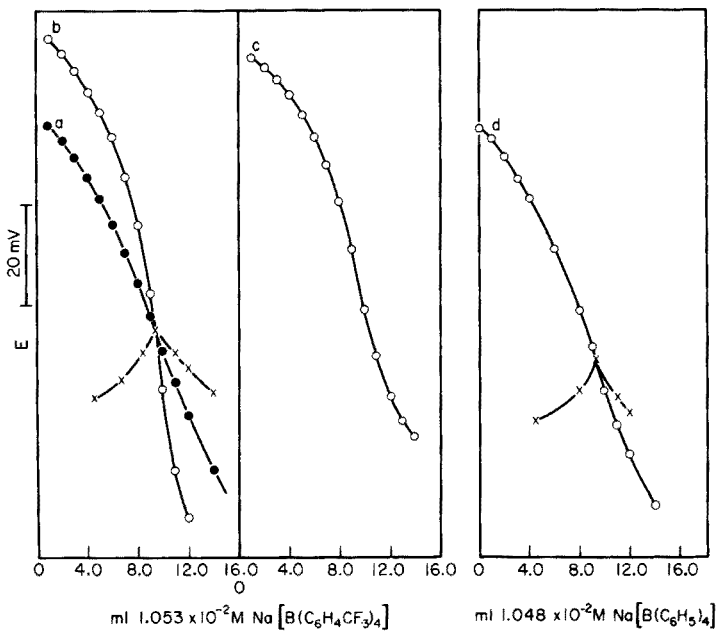

Fig. 1. Curve (a). The titration of 20.4 mg Tl^+ in the presence of 4 mg K^+ in 30 ml of water with $1.053 \cdot 10^{-2}$ M sodium tetrakis(*m*-trifluoromethylphenyl)borate solution. Curve (b). The titration of 10.2 mg Tl^+ and 6.7 mg Cs^+ in 30 ml of water with the same titrant. Curve (c). The titration of 13.3 mg Cs^+ and 8.6 mg Rb^+ in 35 ml of water with the same titrant. Curve (d). The subsequent titration of the rubidium content of the sample for curve (c) with $1.048 \cdot 10^{-2}$ M sodium tetraphenylborate solution. (X – X – X) indicate first derivative curves to establish endpoints.

The authors thank the South African CSIR for financial support.

REFERENCES

1 C. J. Coetzee and A. J. Basson, Anal. Chim. Acta, 56 (1971) 321; 57 (1971) 478.
2 C. J. Coetzee and A. J. Basson, J.S.A. Chem. Inst., 26 (1973) 39.
3 C. J. Coetzee and A. J. Basson, Tydskr. Natuurwetensk., 13 (1973) 20.
4 C. J. Coetzee and A. J. Basson, Anal. Chim. Acta, 64 (1973) 300.
5 C. J. Coetzee and A. J. Basson, Anal. Chim. Acta, 83 (1976) 361.
6 M. Meisters, C. E. Moore and F. P. Cassaretto, Anal. Chim. Acta, 44 (1969) 287.
7 C. J. Coetzee and H. Freiser, Anal. Chem., 41 (1969) 1128.
8 A. Liberti and M. Mascini, Anal. Chem., 41 (1969) 676.

Analytica Chimica Acta, 92 (1977) 405—407

Short Communication

A SOLVENT EXTRACTION—ATOMIC ABSORPTION SPECTROMETRIC METHOD FOR THE DETERMINATION OF IRON IN NON-FERROUS MATERIALS

P. R. SKIDMORE and K. TAYLOR*

The Ever Ready Co. (Holdings) Ltd., Central Laboratories, London N15 3TJ (England)

(Received 24th October 1976)

A rapid simple method was required for the determination of iron at the 0.001—0.01% level in a large number of non-ferrous alloy samples. Atomic absorption spectrometry is probably the simplest method of determining iron in a variety of matrices, but direct aspiration of sample solutions lacks sensitivity, because of the limited concentrations of dissolved solids which can be aspirated; severe interferences can also occur [1]. Specker and Doll [2] have shown that iron is quantitatively extracted from 5.5—7 M hydrochloric acid into 4-methylpentan-2-one and that this solvent is superior to either diethyl or di-isopropyl ether. Robinson [3] has shown that the aspiration of ketones produces a steady flame which enhances sensitivity for many elements.

Preliminary experiments showed that when the ketone extract from 6 M hydrochloric acid was aspirated directly, large irreproducible signals were caused by iron pick-up from corrosion of the burner support. It was therefore necessary to wash the dissolved acid out of the organic phase whilst retaining the iron. Ammonium pyrrolidinedithiocarbamate (APDC) was selected as being the most suitable reagent for retention of iron because of the stability of its metal complexes in acidic solution and its lack of sensitivity to pH changes [4]. The initial ketone/HCl extraction is still required because the APDC extraction is not selective.

Experimental

Apparatus and reagents. Measurements were made with a modified Unicam SP90 atomic absorption spectrophotometer fitted with a 10-cm triple-slot burner and a Juniper neon-filled hollow-cathode lamp operated at 15 mA.

Hydrochloric acid (36%) and ammonium pyrrolidinedithiocarbamate were of AAS grade. 4-Methylpentan-2-one (G.P.R. grade) was redistilled. Standard iron solutions were prepared from high-purity iron by dissolution in hydrochloric acid and suitable dilution.

Procedure. Transfer 20 ml of an aqueous solution containing 1—5 g of the sample as chloride, sulphate and/or phosphate to a 100-ml separating funnel. Add 30 ml of hydrochloric acid (36%) and 15 ml of 4-methylpentan-2-one. Shake for 30 s, allow the layers to separate and discard the aqueous phase. Shake the organic phase with 10 ml of 7 M hydrochloric acid and discard the aqueous phase. Add 40 ml of aqueous 0.25% (w/v) ammonium pyrrolidinedithiocarbamate solution and 5 ml of 7 M hydrochloric acid, shake for 30 s, and discard the aqueous phase.

Dry the stem of the funnel and insert a small plug of cotton wool. Filter the organic phase through the cotton wool, to remove entrained water droplets, into a 15-ml volumetric flask. Wash the filter with 4-methylpentan-2-one, collecting the washings in the flask, and dilute to volume. Aspirate this solution into a lean air—acetylene flame, and measure the absorbance at an appropriate resonance line, depending on the expected iron concentration.

Calibration curves. Transfer aliquots of the appropriate standard iron solution to 100-ml separating funnels. Dilute to 20 ml and follow the Procedure from "add 30 ml of hydrochloric acid".

Results and discussion

Synthetic 5% (w/v) alloy solutions were prepared, from either high-purity metals or AnalaR salts; compositions are shown in Table 1. Aliquots (20 ml) of each of these solutions were spiked with known amounts (100 μg or 3.0 mg), of iron, and were analysed by the recommended procedure. The recoveries of iron are shown in Table 1. The intrinsic iron content of the synthetic solutions was less than 10 p.p.m. The relative standard deviation was about 3% over a series of 30 determinations.

The effects of the various mineral acids, commonly used for sample dissolution, on the recovery of iron were investigated by dissolving 1 g of Cominco high-purity zinc (99.9999%) in 10 ml of the appropriate AnalaR concentrated acid, adding 100 μg of iron to the solution and following the recommended procedure. The results are shown in Table 2.

TABLE 1

The recovery of iron from synthetic alloy solutions

Alloy	Composition	Fe recovered[a] (μg)	Fe recovere (mg)
Astroloy	Ni 57%, Co 15%, Cr 15%, Mo 15%, Al 4%, Ti 4%	101, 101, 102	3.0, 3.0,
Gun metal	Cu 90%, Sn 10%	101, 100, 101	3.0, 3.0,
Leaded bronze	Cu 80%, Sn 10%, Pb 10%	100, 100, 101	3.0, 3.0,
Duralumin	Al 93%, Cu 5%, Mg 1%, Mn 1%	100, 99, 100	3.0, 2.9,
Zinc alloy B	Zn 95%, Al 4%, Cu 1%	98, 100, 99	3.0, 3.0,
Dolomite	Ca 22%, Mg 12%	100, 99, 98	3.0, 3.0,

[a]100 μg Fe added. [b]3.0 mg Fe added.

TABLE 2

Effect of different acids on the recovery of iron (100 μg) added to high-purity zinc

Acid	HCl	HNO_3	H_2SO_4	$HClO_4$	H_3PO_4[a]
Fe recovery (%)	100	14	100	52	103
	100	20	99	48	101
	99	17	99	42	101

[a] Very high blanks (of the order of 15 μg Fe per ml of acid) were obtained for AnalaR phosphoric acid.

The recovery of iron from the various alloys tested shows that no interference can be expected in the determination of iron in a wide range of non-ferrous materials. With samples containing a large proportion of copper or cobalt more than one acid wash of the ketone extract may be necessary, because significant amounts of these metals may be extracted. No loss of iron occurred in a series of six washes carried out on a leaded bronze solution.

Hydrochloric, sulphuric and phosphoric acids may be used for the initial dissolution of the sample without effect on the extraction efficiency. However, phosphoric acid normally contains up to 20 μg Fe ml^{-1}, so that if the use of phosphoric acid is unavoidable, care must be taken to ensure that identical volumes are used both for sample dissolution and in the blank. Mineral samples requiring hydrofluoric acid treatment, and organic samples requiring nitric acid treatment, must be fumed with sulphuric acid in the usual manner. Perchloric acid interferes and must be avoided.

The authors thank the Directors of The Ever Ready Co. (Holdings) Ltd. for permission to publish this work.

REFERENCES

1 J. M. Ottaway, D. T. Coker, W. R. Rowston and D. R. Bhattarai, Analyst, 95 (1970) 567.
2 H. Specker and W. Doll, Z. Anal. Chem., 152 (1956) 178.
3 J. W. Robinson, Anal. Chim. Acta, 23 (1960) 479.
4 C. A. Watson, Hopkins and Williams, Monograph No. 74, Hopkins and Williams Ltd., Chadwell Heath, Essex, U.K., 1969.

Analytica Chimica Acta, 92 (1977) 409—412

Short Communication

DETERMINATION OF MERCURY IN MANGANESE NODULES AND CRUSTS BY COLD-VAPOR ATOMIC ABSORPTION SPECTROMETRY

J. R. TOTH

School of Oceanography, Oregon State University, Corvallis, OR 97331

J. D. INGLE, Jr.*

Department of Chemistry, Oregon State University, Corvallis, OR 97331 (U.S.A.)

(Received 15th September 1976)

The concentration of mercury and other "volatile" elements (e.g. As, Pb, Cd) in manganese nodules and crusts is of interest to marine geologists [1]. Mercury(II) is readily adsorbed from solution by hydrous manganese oxides [2], so that the mercury concentration in manganese deposits is related to the mercury concentration in the sea water at the time of their formation. Mercury concentrations in oceanic waters are extremely low (2—40 ng l^{-1}) [3] which is reflected by the low mercury concentrations (<60 μg kg^{-1}) found in normal manganese nodules [4]. However, mercury concentrations in bottom waters over active spreading ridges are extremely variable, ranging up to 1100 ng l^{-1} [5, 6]. This and other evidence suggests that mercury is injected into the ocean as a result of submarine vulcanism [4, 7, 8], which should result in local manganese deposits of correspondingly high mercury content.

This communication is concerned with the problems associated with determination of mercury in these manganese deposits. The primary difficulties are related to the dissolution of the deposits without loss of mercury and to the low concentrations of mercury to be measured. After dissolution of the manganese deposits, the mercury concentration in solution is often less than 1 μg l^{-1}, which means that the analytical technique must possess a low detection limit and that blank problems from reagents may be severe. For analysis, the cold-vapor atomic absorption technique was employed.

Experimental

All measurements were made with a cold-vapor atomic absorption instrument designed [9] for maximum sensitivity, so that solution concentrations in the part-per-trillion range can be accurately measured. All the modifications described recently [10] were included. The injection procedure was identical to that previously described [9]; 1 ml of a mercury standard solution or mercury-containing sample solution was injected into the

reduction vessel after addition of 0.1 ml of 1% $SnCl_2$. Mercury standard solutions, the $SnCl_2$ solution, and glassware were prepared as previously described [9, 10].

Several digestion procedures were examined. Digestion procedures for geological and mineral samples which contain mercury have been reviewed [11—16]. In all cases, the sample was digested in a covered Teflon cup in a steel pressure bomb at 125°C; the sample was then diluted to 25 ml. Blanks were determined for each variation.

Digestion with HCl. Concentrated HCl (8 ml) was used to digest about 100 mg of sample; dissolution was complete except for a little silicate. Reproducibility was poor, partly because peaks were broader and shorter than those obtained with standards. Apparently, the large amount of chloride reduces the rate of atomization because of the formation of Hg—Cl complexes. Precipitation of some of the chloride with Ag^+, after digestion, did not improve matters. Dilution of the sample sharpened the peaks but also increased the detection limit. The depressive effect of chloride was significant above 1% (v/v) HCl. The mercury blank from HCl was high.

Digestion with HNO_3. Concentrated HNO_3 (8 ml) was used to digest about 100 mg of sample. After 24 h, only 50% of the sample had dissolved.

Digestion with HCl—HNO_3. Concentrated HNO_3 (2 ml) and concentrated HCl (0.5 ml) were used to digest 50 mg of sample. After heating for 4 h, the sample had completely dissolved except for some silicates. This digestion was unsuitable because of very poor reproducibility between runs of the same solutions, apparent loss of mercury during digestion, and still a high blank value.

Digestion with HCl—H_2O_2. Concentrated HCl (0.5 ml) and 2 ml of 30% H_2O_2 were used to digest about 50 mg of sample. After heating for 2 h, only silicates remained. This digestion appeared promising, but there were occasional reproducibility problems and a blank of about 0.1 p.p.b. Hydroxylammonium chloride was added to reduce the excess of peroxide.

Digestion with HF. This digestion was finally chosen because it provided the best reproducibility, the lowest blank values, and complete digestion of the sample. It is necessary to wet the sample with a little HNO_3 to prevent a brown precipitate (possibly MnO_2) from forming after addition of H_3BO_3. Initially aqua regia was used to wet the sample but blank values were then higher.

Procedure. Chip or scrape off a sample and grind in an agate mortar; mix the powder thoroughly (Spex Mixer) and dry it overnight in a desiccator. Add a portion (50 mg) of sample to the Teflon cup, which has previously been cleaned with fuming nitric acid; add 0.4 ml of HNO_3 to wet the sample, followed by 2 ml of 48% HF. Place the Teflon lid on the cup, place the cup in the pressure bomb, and tighten the screw top to 250 lb with a torque wrench. Heat for 1.5 h at 125°C in an oven. After the bombs have cooled, add 1.9 g of H_3BO_3 directly to the Teflon cup. Then transfer the solution to a 25-ml volumetric flask and dilute to volume with double-distilled water.

Blanks are run for each set of analyses by taking the reagents through the complete digestion procedure. The procedure involves only one transfer of the sample solution; this reduces contamination and improves precision.

Results and discussion

Manganese nodules from the equatorial and North Pacific, the East Pacific Rise, and the Bauer Deep in the Southeast Pacific, and manganese crusts from the Juan de Fuca Ridge, the East Pacific Rise, and the mid Atlantic Ridge, were analyzed with the HF digestion procedure and cold-vapor atomic absorption. Mercury concentrations were lowest in nodules from the stable, deep ocean basins of the Pacific (20—50 p.p.b.), relatively high in nodules and thin crusts from active spreading ridges (95—290 p.p.b.) and widely variable in thick, rapidly forming hydrothermal crusts [18, 19] from spreading centers (40—1300 p.p.b.). These values are consistent with the hypothesis [5, 20] of intermittent Hg-rich hydrothermal injections from active spreading centers. The above range gives final solution concentrations of 0.04—2 p.p.b. Hg.

The blank absorbances for reagent-grade HF and reagent-grade HF distilled in a Teflon still [21] were 0.082 ± 0.028 p.p.b. and 0.039 ± 0.017 p.p.b. respectively, where the second number is one standard deviation; the distilled HF was therefore used for all analyses.

The detection limit defined as the concentration which provides an absorbance signal one standard deviation above the blank absorbance, was 0.02 p.p.b. in the final solution or 10 p.p.b. in the manganese deposit. This detection limit is considerably above that obtained on the instrument for pure standards, and is totally limited by the reproducibility of the blank mercury contamination. The relative standard deviation for repeated total analyses including digestion on the same manganese deposit, was 5—10% for samples with greater than 300 p.p.b. Hg, and 10—15% for samples with mercury concentrations in the 50—300 p.p.b. range.

Some samples were spiked with mercury standards before digestion for the method of standard additions. The results were identical within experimental error to those obtained with a calibration curve made from measurements on pure standard mercury solutions.

REFERENCES

1 J. Korkisch, H. Hubner, I. Steffan, G. Arrhenius, M. Fisk and J. Fraser, Anal. Chim. Acta, 83 (1976) 83.
2 R. A. Lockwood and K. Y. Chen, Environ. Sci. Technol., 7 (1973) 1058.
3 D. E. Robertson, Pacific Northwest Laboratory Annual Report for 1973 to The USAEC Division of Biomedical and Environmental Research, Part 2, Ecological Sciences, U.S. Atomic Energy Commission, Washington D.C., 1974.
4 R. C. Harriss, Nature, 219 (1968) 54.
5 R. A. Carr, M. M. Jones, and E. R. Russ, Nature, 251 (1974) 489.
6 R. A. Carr, M. M. Jones, T. B. Warner, C. H. Cheek and E. R. Russ, Nature, 258 (1975) 588.
7 K. Bostrom and D. E. Fisher, Geochim. Cosmochim. Acta, 33 (1969) 743.

8 D. S. Cronan, Can. J. Earth Sci., 9 (1972) 319.
9 J. E. Hawley and J. D. Ingle, Jr., Anal. Chem., 47 (1975) 719.
10 D. R. Christmann and J. D. Ingle, Jr., Anal. Chim. Acta, 86 (1976) 285.
11 L. A. Branvold and S. J. Marson, At. Absorpt. Newsl., 13 (1974) 5.
12 B. Bernas, Anal. Chem., 40 (1968) 1682.
13 A. M. Ure, Anal. Chim. Acta, 76 (1975) 1.
14 F. N. Ward, U.S. Geol. Surv. Prof. Paper, 713 (1970) 46.
15 S. R. Aston and J. P. Riley, Anal. Chim. Acta, 59 (1972) 349.
16 P. C. Head and R. A. Nicholson, Analyst, 98 (1973) 53.
17 S. H. Omang and P. E. Paus, Anal. Chim. Acta, 56 (1971) 395.
18 M. R. Scott, R. B. Scott, P. A. Rona, L. W. Butler, and A. J. Nalwalk, Geophys. Res. Lett., 1 (1974) 355.
19 W. S. Moore and P. R. Vogt, Earth Planet. Sci. Lett., 29 (1976) 349.
20 H. Craig, W. Clarke and M. A. Beg, Earth Planet. Sci. Lett., 26 (1975) 125.
21 J. M. Mattinson, Anal. Chem., 44 (1972) 1715.

Analytica Chimica Acta, 92 (1977) 413—416

Short Communication

THE DETERMINATION OF ALUMINA IN A COPPER MATRIX BY ATOMIC ABSORPTION SPECTROMETRY

J. P. CELIS, J. A. HELSEN, P. HERMANS and J. R. ROOS

Departement Metaalkunde, Katholieke Universiteit Leuven de Croylaan 2, B-3030 Heverlee (Belgium)

(Received 10th January 1977)

Dispersion-hardened materials can be prepared by mixing metallic and non-metallic powders, by internal oxidation of alloys, or by electro-codeposition. The properties of such materials are determined mainly by the size, concentration and distribution of the particles in the matrix. In the electrolytic method, inert particles like alumina, titania and silicon carbide are suspended in an electrolyte and co-deposited with the metallic matrix; as the mechanism of such co-depositions is far from being well understood, it is difficult to obtain the optimal mechanical properties in such materials. A study of the mechanism of electro-codeposition of copper and alumina required a reliable analytical method.

The weight percentages of embedded particles are usually determined gravimetrically. Sautter [1] analysed electrolytic Ni—Al_2O_3 deposits (mean size of alumina particles, 0.1—0.3 μm) by dissolution of nickel in 50% nitric acid; alumina was then separated by centrifugation, washed, dried and weighed. Hoffmann and Mantell [2] analyzed electrolytic Cu—Al_2O_3 deposits (mean size of alumina particles, 0.02—0.7 μm) by dissolution of copper in nitric acid, adjustment to pH 7—8 with ammonia liquor, filtration and weighing. There are two objections to these procedures: first it is very difficult or even impossible to retain such fine alumina particles (0.02—0.1 μm) on a filter; secondly, it is assumed that alumina is insoluble in the chemicals used [1—3].

To check the partial solubility of alumina, the amount of aluminium dissolved from a suspension in 20% (v/v) nitric acid was determined by atomic absorption spectrometry of the supernatant liquid after centrifugation (Fig. 1). Two types of alumina were tested: α-Al_2O_3 with a hexagonal structure (mean size, 0.3 μm; Linde A; Buehler Ltd.) and γ-Al_2O_3 with a spinel-type cubic structure (mean size, 0.05 μm; Linde B; Buehler Ltd.). The partial solubility of alumina can be predicted from the amphoteric nature of aluminium; the solubility calculated from Fig. 1 is in good agreement with that determined by other authors [4]. Consequently, a new procedure for the more accurate determination of alumina in dispersion-

hardened $Cu—Al_2O_3$ alloys was developed. The total amount of aluminium present is determined by atomic absorption spectrometry (a.a.s.).

Experimental

The $Cu—Al_2O_3$ sample is digested in sulphuric acid, sufficient hydrogen peroxide (30%) being added to obtain complete dissolution of the copper matrix. Copper is removed from the solution by electrolysis on a mercury pool cathode at low current density with constant stirring. The solution is then transferred quantitatively to a platinum dish (60-mm diameter, 80-ml capacity) and evaporated to dryness. After addition of sodium carbonate (2 g), fusion at 850°C, dissolution of the melt with concentrated hydrochloric acid, and dilution to 100 ml in a volumetric flask, the aluminium content is determined by a.a.s. at 309.3 nm.

Solutions and standards (5—250 p.p.m. aluminium) are made up to contain the same final concentration of potassium nitrate (2000 p.p.m.) and sodium chloride (10000 p.p.m.).

Alumina can be determined with reasonable accuracy down to 0.02 wt% in copper for 1-g samples. The result is independent of particle size and of the solubility of the alumina used.

Merck analytical-grade reagents were used throughout.

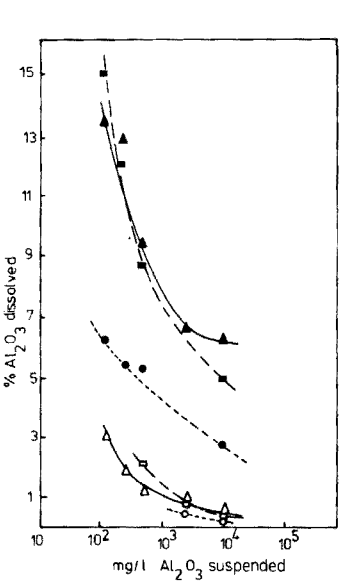

Fig. 1. Solubility of α-Al_2O_3 (open symbols) and γ-Al_2O_3 (closed symbols) in nitric acid after different contact times. ○ ●, 0.24 h; ■ □, 1 week; ▲ △, 2 weeks.

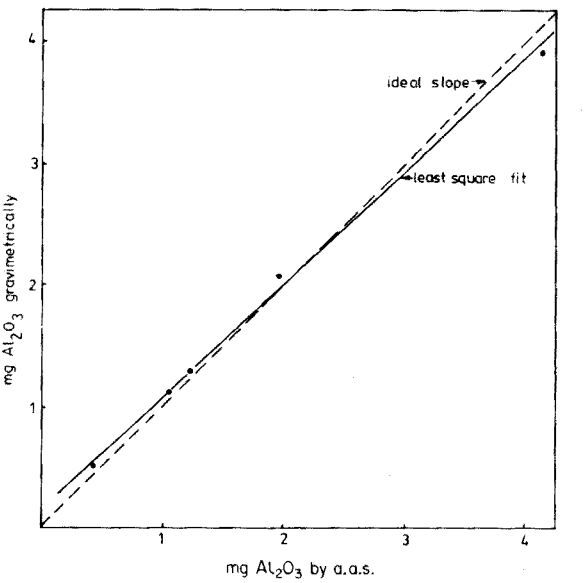

Fig. 2. Accuracy of the method. Alumina values obtained by the proposed method compared with the gravimetrically determined "exact" quantities.

Results

The proposed method was checked for weighed quantities of alumina and for synthetic suspensions of alumina in acidified copper sulphate solutions. The alumina powders used were α- and γ-Al_2O_3, referred to above. The reproducibility and accuracy of the fusion procedure were checked by weighing known quantities of α-Al_2O_3 (4.72, 6.98 and 9.44 mg) in platinum crucibles; after fusion and dissolution of the melt, 2000 p.p.m. of potassium nitrate was added to each final solution. If complete dissolution of alumina and no subsequent losses are assumed, the concentration of aluminium should be 25, 37 and 50 p.p.m., respectively. The same quantities of alumina were suspended in a copper sulphate solution (15 g l^{-1}) to which 5 ml of hydrogen peroxide (30%) and enough sulphuric acid to give a final pH of 0.3 were added. After electrolysis on a mercury pool, the recommended procedure was followed. The aluminium standard solutions were prepared from pure metal and were made up to the same matrix as the test solution. The results are compiled in Table 1; it can be concluded that the alumina dissolves completely and that there is no appreciable loss of aluminium during either electrolysis or manipulation.

In another series of experiments, the validity of the procedure was checked for very small quantities of alumina. Stock suspensions of alumina (200 and 750 mg l^{-1}) were prepared in distilled water; the required volumes were removed by pipette to obtain samples containing 4, 2, 1.25, 1 and 0.4 mg of alumina. After addition of 50 ml of copper sulphate solution (pH 0.3) the analyses were performed as proposed (Table 2). The results are compared

TABLE 1

Mean values and standard deviations of a.a.s. measurements of aluminium, calculated from four replicate experiments

Method	Absorption measured ($\cdot 10^{-3}$)		
	25 p.p.m. Al	37 p.p.m. Al	50 p.p.m. Al
Standard solution	95.0 ± 6.55	145.0 ± 1.00	190.0 ± 2.0
Weighed + fusion	95.33 ± 5.69	—	187.33 ± 4.04
Weighed + electrolysis + fusion	96.25 ± 9.50	140.25 ± 5.68	189.75 ± 2.06

TABLE 2

Average results (in mg of alumina) of the gravimetric determination and of the a.a.s. method proposed, for small quantities of alumina

Type	A.a.s.	Grav.	Type	A.a.s.	Grav.
α-Al_2O_3	4.12	3.90	γ-Al_2O_3	1.94	2.07
	1.23	1.30		1.05	1.15
				0.41	0.53

with the gravimetric results in Fig. 2. A small (systematic) error is present.

This method of analysis was used for the determination of alumina in electrolytic Cu—Al_2O_3 deposits. Deposits containing α- or γ-Al_2O_3 were prepared under the same conditions of electrolysis. Ten complete repetitions of the determination of α-Al_2O_3 resulted in a mean value of 1.101 wt% alumina with a standard deviation of 0.172. Five complete repetitions with γ-Al_2O_3 resulted in a mean value of 0.174 wt% alumina with a standard deviation of 0.032.

Conclusions

The proposed method for the determination of alumina in a copper matrix proved to be reliable. The advantages of this procedure can be summarized as follows: (a) the solubility of the alumina in the reagents used has no effect on the exactness of the results; (b) the method is independent of particle size; (c) the method can be used for the determination of very small weight percentages of alumina.

The method can be extended to the analysis of other composites containing inert particles in a metallic matrix. The most important restriction is that the method cannot differentiate between an element present in the inert compound and the same element present in the matrix.

REFERENCES

1 F. K. Sautter, J. Electrochem. Soc., 110 (1963) 557.
2 J. E. Hoffmann and C. L. Mantell, Trans. Metall. Soc. AIME, 236 (1966) 1015.
3 E. S. Chen, G. R. Lakshminarayanan and F. K. Sautter, Metall. Trans., 2 (1971) 937.
4 E. Deltombe, C. Vanleugenhaghe and M. Pourbaix, Tech. Report Cebelcor, 42 (1956).

Analytica Chimica Acta, 92 (1977) 417—421

Short Communication

A KINETIC FLUORIMETRIC DETERMINATION OF ALUMINUM

R. L. WILSON* and J. D. INGLE, JR.

Department of Chemistry, Oregon State University, Corvallis, Oregon 97331 (U.S.A.)

(Received 5th August 1976)

The advantages of kinetic analysis [1] and more specifically kinetic fluorimetric analysis of metal ions [2, 3] have been discussed. Fluorimetric reaction-rate analysis is based on the reaction of a metal ion with an organic reagent to form a fluorescence product. Under suitable conditions, the initial rate of the reaction, measured as a change in fluorescence signal per unit time, is linearly related to the initial metal ion concentration. In many cases, this approach is more selective, more sensitive, and faster than conventional techniques [2, 3].

Recent studies of the silver—oxine-5-sulfonic acid—persulfate system [2] for the determination of silver showed that aluminum(III) interferes at very low levels, reacting slowly with oxine sulfonic acid to form a fluorescent product even in the absence of persulfate. Hence, it was felt that this chemical system could be used for a new kinetic procedure for trace aluminum(III).

Experimental

Solution preparation. All glassware and Teflon bottles were cleaned with $KMnO_4$ and HNO_3 as previously described [3] and solutions were stored in Teflon bottles. All solutions were prepared with doubly distilled water and reagent grade chemicals. The stock aluminum solution (100 ppm) was prepared by dissolving 1.39 g of $Al(NO_3)_3 \cdot 9H_2O$ in 1 l of 10^{-3} M H_2SO_4. The blank solution was 10^{-3} M H_2SO_4. 8-Hydroxyquinoline-5-sulfonic acid solution (100 ppm) was prepared in water. Lower concentrations were prepared by serial dilution.

Instrumentation. The design and operation of a fluorescence instrument designed for kinetic measurements have been described [3]. After the reaction and ratemeter circuitry have been initiated, and a measurement time preselected, a number in counts, proportional to the initial rate, is printed on a digital printer. All fixed-wavelength measurements were made with the excitation monochromator set to 366 nm with a 17-nm bandpass and the emission monochromator set to 510 nm with a 22-nm bandpass. For all measurements, the sample cell was maintained at 25°C.

*Present address: Department of Chemistry, University of Wisconsin-Eau Claire, Eau Claire, Wisconsin 54701, U.S.A.

Since the Al^{3+}—oxinesulfonic acid system reaches equilibrium in about 30 min (longer for the lower concentrations), to ensure measurement of only the initial 2% of the reaction, the measurement, integration and delay timing periods [4] were set at 16, 8 and 16 s, respectively.

Sample introduction procedure. The general sample introduction and mixing procedures were as previously described [2, 3]; 2 ml of oxinesulfonic acid solution and 1 ml of the Al^{3+} solution or blank were added to the sample with automatic pipets.

Optimization studies. The dependence of the initial rate on H^+, oxinesulfonic acid and Al^{3+} concentrations were measured and log—log plots of initial rate vs. reagent concentration were made to determine the order with respect to each of the reactants. The optimum concentrations for H^+ and reagent were taken as the concentrations which yielded the smallest relative standard deviation (s_r) in the rate and the lowest absolute order with respect to the reagent. Five measurements were made for each concentration and each study was repeated three times.

Interference studies. Interference studies were done with 25 metal ions as specified earlier [2]. The potentially interfering metal ion solution and a 1:1 mixture of the test metal ion with 50 ppb Al^{3+} were both substituted for the 1 ml of Al^{3+} solution.

Results and discussion

Initial studies. A small background reaction was observed when oxine sulfonic acid (OxSA) and double-distilled water were mixed; the rate of the background reaction was essentially independent of reagent concentrations, and the nature of the reaction is not known. The uncorrected fluorescence emission spectrum is shown in Fig. 1. The maximum is at 510 nm. The reaction seems to be a simple complexation reaction between Al^{3+} and oxine-5-sulfonic acid.

Optimization. The plotted Al^{3+} rates have had the background reaction rate subtracted and the reported relative standard deviations are for the total rate (Al^{3+} plus background). The results for the pH optimization are summarized in Fig. 2(a); the pH was adjusted with H_2SO_4 and the reported pH is the final pH measured after mixing. Optimum conditions (i.e., lowest s_r) were found at pH 3.1—3.4. Unfortunately, in this region the initial rate depends on $[H^+]$ to the inverse 5/3 power, so that careful pH control is required. Over the pH range studied, the s_r range was 1.6—0.43%.

The results for the OxSA optimization are shown in Fig. 2(b). The rate is directly proportional to [OxSA] and the optimum concentration is 10 ppm; s_r ranged from 4.9 to 0.48%, with 10 ppm OxSA yielding 1.34%. An OxSA concentration of 30 ppm gave better precision than 10 ppm but did not provide linearity between the initial rate and $[Al^{3+}]$ at lower Al^{3+} concentrations.

The reaction is first order in Al^{3+} over the concentration range 0.4 ppb—10 ppm with a slope of about $3.1 \cdot 10^3$ counts/ppm. For 1—10 ppm Al^{3+},

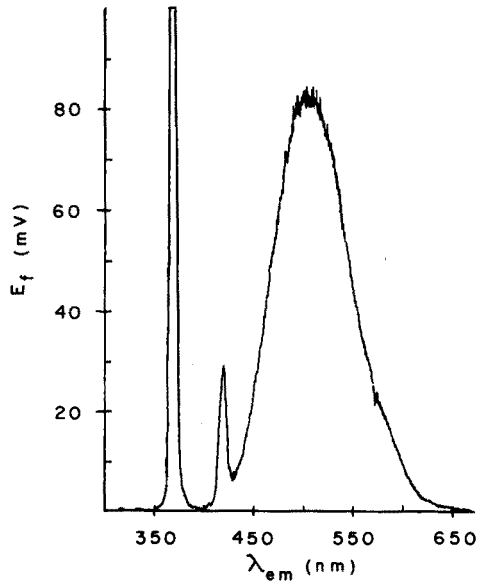

Fig. 1. Emission spectrum. $[Al^{3+}]$ = 1.0 ppm, (OxSA) = 10 ppm, $R_f = 10^7\ \Omega$, τ = 0.1 s, E_{PMT} = 800 V, λ_{ex} = 366 nm, scan rate = 100 nm min^{-1}, excitation slit = 2.0 mm, emission slit = 0.5 mm.

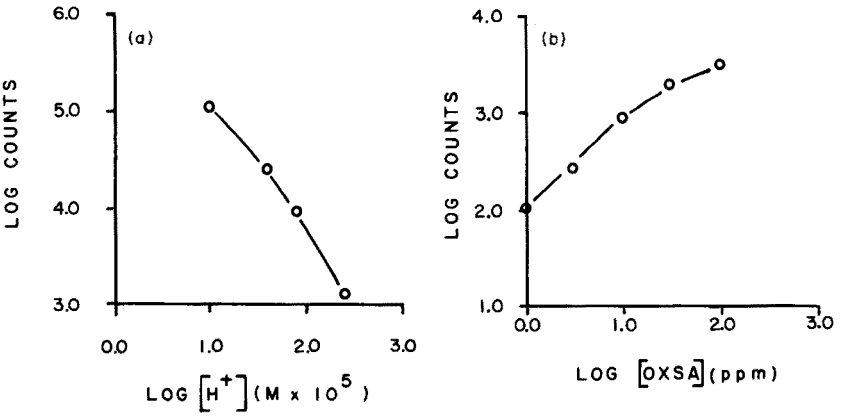

Fig. 2. (a) Log–log plot of $[H^+]$ vs. initial rate; $[Al^{3+}]$ = 1 ppm, [OxSA] = 10 ppm. (b) Log–log plot of [OxSA] vs. initial rate; $[Al^{3+}]$ = 0.1 ppm, pH 3.2. $R_f = 10^7\ \Omega$, τ = 1 s, E_{PMT} = 800 V.

the precision is 0.4%. As the Al^{3+} concentration is decreased, the s_r value in the Al^{3+} plus background rate increases to 2.1% at the detection limit. The detection limit, defined as the concentration which yields a net rate $(2)^{\frac{1}{2}}$ times the standard deviation of the background rate, is 0.4 ppb; *S/N* calculations were carried out as previously described [3]. These calculations indicate that measurements are limited by shot noise in the fluorescence signal

for concentrations below 1 ppm and by sampling and mixing reproducibility at higher concentrations. With this system, use of an emission interference filter instead of an emission monochromator increases the fluorescence signal incident on the PMT by about a factor of ten [3] and hence should improve the *S/N* at low concentrations.

The interference study was made as specified in the experimental section. All initial solutions were adjusted to a pH of 2.7. The results are shown in Table 1. The metal ions that interfered enhanced the initial rate, indicating that they probably formed complexes with the oxine sulfonic acid. The interfering metals affected the background and Al^{3+} reactions equally and the interference with Al^{3+} was additive. Clearly the technique is relatively selective.

Conclusions

Studies of the Al—OxSA system showed that the reaction is first order in both Al^{3+} and OxSA and inverse 5/3 order in $[H^+]$. From these studies, a new kinetic method for Al^{3+} was developed with a large dynamic linear range of 0.4 ppb—10 ppm and typical relative standard deviations of about 1%. Few metal ions interfere. The detection limit is considerably lower than that obtained with common techniques such as flame atomic absorption. About 25 analyses may be run per hour.

TABLE 1

Summary of interference study

Species	Conc.[a] (ppm)	Conc.[b] (ppm)
Zn(II)	10	100 (1.8)
Hf(IV)	0.5	6 (1.9)
Zr(IV)	0.5	1 (1.3)
Au(III)	50	100 (1.1)
Sn(IV)	1	5 (1.1)
Sn(II)	0.5	10 (1.5)

Metals giving no interference at 100 ppm were: Na(I), K(I), Mg(II), Ba(II), Sr(II), Ca(II), Pb(II), Hg(II), Cr(III), Co(II), Mn(II), Cd(II), Cu(II), Ni(II), Fe(III), Fe(II), Ti(II), V(IV), Pt(II). Of these, Cd(II) and Mg(II) underwent fast reactions but did not interfere with the initial rate measurements.

[a]Concentration that had no effect on the rate of the reaction of 25 ppb Al^{3+} and which could not be distinguished from the background reaction (i.e., within 1 σ). At higher concentrations, all these ions enhanced the initial rate.

[b]Concentration which yielded enhanced rate. Relative enhancement in rate compared to rate from 25 ppb Al^{3+} is given in parentheses.

Acknowledgement is made to the NSF (Grant Nos. MPS 75-05447 and CHE-76-16711) and Oregon State Research Council for partial support of this research.

REFERENCES

1 See, e.g. H. V. Malmstadt, C. J. Delaney and E. A. Cordos, CRC Crit. Rev. Anal. Chem., 2 (1972) 559; H. A. Mottola, CRC Crit. Rev. Anal. Chem., 5 (1975) 229; S. R. Crouch in J. S. Mattson, H. B. Mark, Jr. and H. C. MacDonald (Eds.), Computers in Chemistry and Instrumentation, Vol. 3, M. Dekker, New York, 1973, p. 107; and earlier references therein.
2 R. L. Wilson and J. D. Ingle, Jr., Anal. Chem., 49, No. 7 (1977) 000.
3 R. L. Wilson and J. D. Ingle, Jr., Anal. Chem., 49, No. 7 (1977) 000.
4 R. L. Wilson and J. D. Ingle, Jr., Anal. Chim. Acta, 83 (1976) 203.

Analytica Chimica Acta, 92 (1977) 423—427

Short Communication

SPECTROPHOTOMETRIC DETERMINATION OF NICKEL AND PALLADIUM BY EXTRACTION OF THEIR COMPLEXES WITH MOLTEN NAPHTHALENE

MASATADA SATAKE

Faculty of Engineering, Fukui University, Fukui 910 (Japan)

(Received 24th November 1976)

Spectrophotometric determination of metals after extraction of metal complexes with organic solvents is widely used for the determination of trace amounts of metals, but the method is not applicable when the solubility of the complexes in the solvent is small and the metal complexes are strongly hydrated.

A new method involving solid—liquid separation after liquid—liquid extraction has been successfully applied to the spectrophotometric determination of micro amounts of metals [1—4] by using a molten organic compound with appropriate melting point, e.g., naphthalene (m.p. 81°C) or biphenyl (m.p. 71°C). In this communication, determinations of nickel and palladium are reported. Nickel and palladium react with dimethylglyoxime, α-benzildioxime, α-furildioxime and 1,2-cyclohexanedionedioxime (nioxime) to form water-insoluble complexes. The dimethylglyoxime, α-benzildioxime and α-furildioxime complexes of nickel and palladium are easily extracted into both chloroform and molten naphthalene. The nioxime complexes of nickel and palladium are only slightly extracted into chloroform, but are easily extracted into molten naphthalene. After extraction, the mixture of solidified complex and naphthalene is dissolved in dimethylformamide or chloroform, and the absorbance of the solution is measured at a suitable wavelength. A characteristic of this method is that the equilibrium distribution in the two phases is attained rapidly, and the complexes are extracted merely by contact with molten naphthalene. The complexes are almost completely extracted and concentrated with only 0.5—3.0 g of naphthalene.

Experimental

Standard palladium solution. Dissolve 0.4433 g of palladium chloride in 20 ml of concentrated hydrochloric acid and dilute to 500 ml with water.

Standard nickel solution. Dissolve 1.4541 g of nickel nitrate in 500 ml of water.

Reagents. Use 0.5% dimethylglyoxime, 0.02% α-benzildioxime, 0.1 or 1.0% α-furildioxime, and 0.5% nioxime solutions in ethanol (all w/v).

The buffer solutions were acetate buffers for pH 3—6 and ammonia buffers for pH 8—11. All other reagents were reagent-grade and were not purified further. De-ionized water was used.

Apparatus. An Hitachi 200-20 spectrophotometer, with matched 10-mm glass cells, and a Toa Dempa HM-6A pH meter with a combined glass—calomel electrode were used.

Procedure. To 25 ml of nickel or palladium sample solution, in a tightly stoppered Erlenmeyer flask, add the complex-forming reagent and the buffer solution. Mix the solution well, and warm it on a water bath at around 60°C. Add 2.0 g of naphthalene and warm the mixture in the water bath at 90°C to melt the naphthalene completely. Shake vigorously till naphthalene solidifies, forming many fine crystals, and allow to cool to room temperature. Again warm to melt the very fine crystals slowly, and let them grow to give a coarser deposit. Cool to room temperature, collect the solidified deposit on a filter paper, wash with water, and remove the surplus water with a dry filter paper. Spread the crystals on a filter paper and allow to dry. Then dissolve them in the appropriate organic solvents and dilute to 10 ml. Measure the absorbance in 10-mm glass cells against a reagent blank prepared similarly. Calculate the amount of nickel or palladium from a calibration curve.

Results and discussion

The absorption spectra of dimethylglyoxime, α-benzildioxime, α-furildioxime, nioxime, and their nickel and palladium complexes are given in Fig. 1. The complexes have absorption maxima in the range 350—450 nm; the palladium complexes, except for α-furildioxime, also have shoulders in this range. The four reagents have similar spectra without absorption above 340 nm.

Effects of experimental variables. The effect of pH on the extraction of the nickel and palladium complexes is given in Fig. 2. The pH values of the aqueous solution after extraction were measured at room temperature. The results indicate that all the palladium complexes were extracted from more acidic solutions than the nickel complexes.

The ranges of reagent concentration giving quantitative extraction are summarized in Table 1. Variation in the volume of buffer solution in the range 0.5—5.0 ml, had no effect on the extraction. The nickel and palladium complexes in aqueous solution were quite stable above 81°C, and digestion times of 5—50 min did not affect the results. Several experiments showed that no digestion was necessary.

The amounts of naphthalene were varied from 0.5 to 3.0 g, the extraction being carried out by the recommended procedure; amounts exceeding 0.5 g did not improve the extraction. The volumes of chloroform and dimethylformamide required to dissolve 1.0 g of naphthalene were 2 ml and 3 ml,

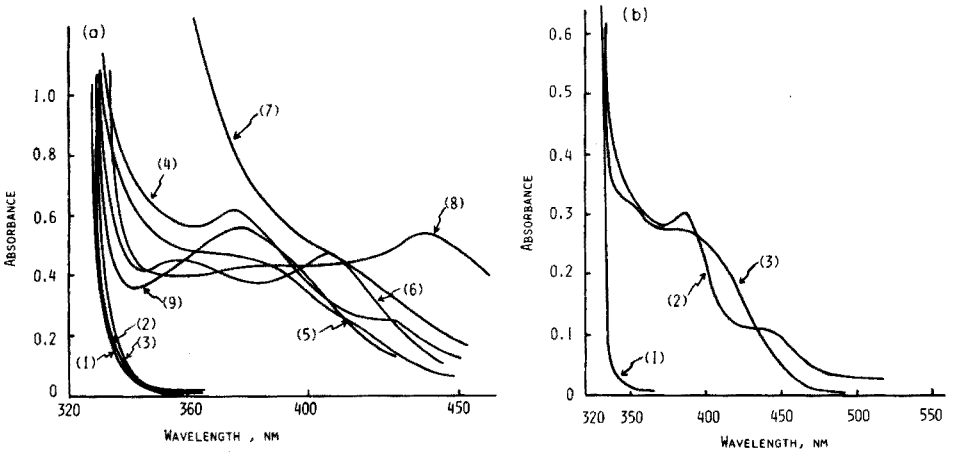

Fig. 1. Absorption spectra of reagents and metal complexes. (a) (1) 0.5% dimethylglyoxime, 0.5 ml; pH 8.6. (2) 0.02% α-benzildioxime, 3.0 ml; pH 9.5. (3) 1.0% α-furildioxime, 2.0 ml; pH 8.5. (4) Ni, 115 μg; 0.5% dimethylglyoxime, 0.5 ml; pH 8.6. (5) Pd, 266 μg; 0.5% dimethylglyoxime, 0.5 ml; pH 4.0. (6) Ni, 29 μg; 0.02% α-benzildioxime, 3.0 ml; pH 9.5. (7) Pd, 266 μg; 0.02% α-benzildioxime, 10 ml; pH 4.1. (8) Ni, 20 μg; 1% α-furildioxime, 2.0 ml; pH 8.5. (9) Pd, 27 μg, 0.1% α-furildioxime, 1.0 ml; pH 4.5. Reference: Water. (b) (1) 0.5% nioxime, 1.5 ml; pH 4.6. (2) Ni, 50 μg; 0.5% nioxime, 1.5 ml; pH 4.6. (3) Pd, 160 μg; 0.5% nioxime, 1.5 ml; pH 4.5. Reference: Water.

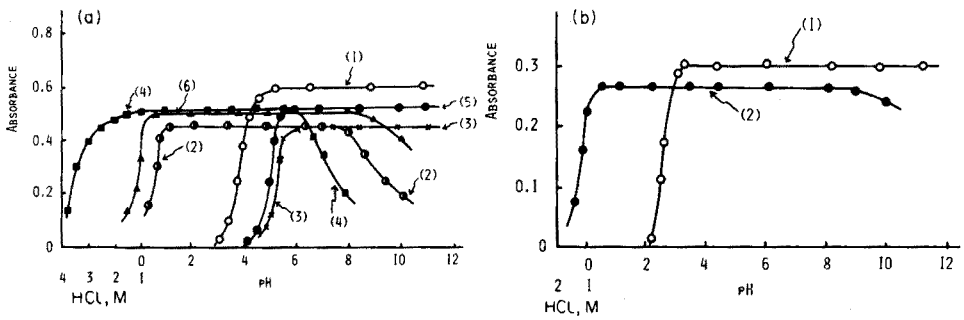

Fig. 2. Effect of pH on absorbance at the wavelengths recommended in Table 1. (a) (1) Ni, 115 μg; 0.5% dimethylglyoxime, 0.5 ml. (2) Pd, 266 μg; 0.5% dimethylglyoxime, 0.5 ml. (3) Ni, 29 μg; 0.02% α-benzyldioxime, 3.0 ml. (4) Pd, 266 μg; 0.02% α-benzildioxime, 10 ml. (5) Ni, 20 μg; 1% α-furildioxime, 2.0 ml; (6) Pd, 27 μg; 0.1% α-furildioxime, 1.0 ml. (b) (1) Ni, 50 μg; 0.5% nioxime, 1.5 ml. (2) Pd, 160 μg; 0.5% nioxime, 1.5 ml. Reference: Reagent blank.

respectively. Extraction of the complexes into molten naphthalene was very fast, owing to the high temperature; the complexes were easily extracted from aqueous solution merely by contact with molten naphthalene, or by two or three vigorous shakings. The absorbances of the complexes in naphthalene, naphthalene—chloroform or naphthalene—dimethylformamide solution were stable for some hours.

TABLE 1

Spectrophotometric determination of metals

Metal complex[a]	λ_{max} (nm)	Extraction pH	Amount of reagent (ml)[b]	Calibration curve (p.p.m.)[c]	ϵ (l mol^{-1} cm^{-1})	Sensitivity (μg cm^{-2})	s_r (%)
Ni—DMG	374	5.5—11.0	0.5% DMG, 0.2—1.0	1.0—23	$3.0 \cdot 10^3$	0.020	0.92
Pd—DMG	370	1.1—7.8	0.5% DMG, 0.3—3.0	3.0—53	$1.7 \cdot 10^3$	0.062	0.64
Ni—BD	406	6.0—11.0	0.02% BD, 1.5—7.0	0.4—6.0	$9.0 \cdot 10^3$	0.006	0.88
Pd—BD	400	0—6.0	0.02% BD, 5.0—15.0	2.7—53	$2.1 \cdot 10^3$	0.051	0.17
Ni—FD	438	6.0—11.0	1% FD, 1.5—4.5	0.2—3.6	$1.4 \cdot 10^4$	0.004	0.10
Pd—FD	378	0.4—8.0	0.1% FD, 0.3—5.0	0.3—5.0	$2.0 \cdot 10^4$	0.005	0.12
Ni—nioxime	384	3.2—11.0	0.5% nioxime, 0.1—5.0	0.8—7.0	$3.7 \cdot 10^3$	0.016	0.58
Pd—nioxime	385	0.5—8.0	0.5% nioxime, 0.1—5.0	2.8—32	$1.8 \cdot 10^3$	0.060	0.55

[a] DMG = dimethylglyoxime. BD = α-benzildioxime. FD = α-furildioxime.
[b] Naphthalene, 2.0 g. Solvent: chloroform for Pd—DMG, Pd—BD and PD—FD; dimethylformamide for Ni—DMG, Ni—BD and Ni—FD; chloroform for Ni—nioxime and Pd—nioxime at 65°C.
[c] Absorbance for minimum concn., 0.05; absorbance for maximum concn., 1.0, except for the nioxime complexes of nickel and palladium (0.5).

Choice of solvent. Dimethylformamide (DMF) and chloroform were found to be the most suitable solvents for the complexes after extraction into naphthalene. The dimethylglyoxime complex of nickel is soluble in DMF or $CHCl_3$; the palladium complex is insoluble in DMF even on heating, but soluble in $CHCl_3$. The α-benzildioxime complex of nickel is soluble in DMF or $CHCl_3$, whereas the palladium complex is insoluble in DMF at room temperature, but soluble in DMF at 50°C and soluble in $CHCl_3$. The nickel—α-furildioxime complex is soluble in DMF or $CHCl_3$; the palladium complex is unstable in DMF but stable in $CHCl_3$. The nioxime complexes of nickel and palladium are partially extractable with chloroform, but completely extractable with molten naphthalene. The naphthalene extracts are insoluble in dimethylformamide even on heating, but soluble in chloroform at 50°C.

Calibration curve, molar absorptivity, sensitivity and reproducibility. Under the optimum conditions described above, calibration curves for nickel and palladium determinations were established at the appropriate wavelengths against reagent blanks. The molar absorptivities, sensitivities and relative standard deviations on nickel and palladium were also calculated for ten determinations. The results obtained are summarized in Table 1. The molar absorptivities were of the order of 10^4 for the α-furildioxime complexes of nickel and palladium. The relative standard deviations were below 1%.

The author expresses his deep gratitude to Professor Taitiro Fujinaga, Faculty of Science, Kyoto University, for his kind advice.

REFERENCES

1 T. Fujinaga, T. Kuwamoto, E. Nakayama and M. Satake, Bunseki Kagaku, 18 (1969) 398.
2 T. Fujinaga, T. Kuwamoto, T. Yonekubo and M. Satake, Bunseki Kagaku, 18 (1969) 1113.
3 T. Fujinaga, M. Satake and T. Yonekubo, Bunseki Kagaku, 19 (1970) 216; 20 (1971) 1255; Bull. Chem. Soc. Jpn., 46 (1973) 2090; Talanta, 19 (1972) 689; Bull Chem. Soc. Jpn., 48 (1975) 899.
4 T. Fujinaga, M. Satake and M. Shimizu, Bunseki Kagaku, 25 (1976) 313.

Analytica Chimica Acta, 92 (1977) 429—431

Short Communication

DETERMINATION OF THIOLS IN NON-AQUEOUS SOLUTIONS

G. GABOR and A. VINCZE

Israel Institute for Biological Research, P.O. Box 19, Ness-Ziona (Israel)

(Received 28th January 1977)

The Ellman reaction for the determination of thiols in aqueous solutions [1, 2] is based on ionic scission of the disulfide bond [3]. The reaction mechanism involves nucleophilic attack on the —S—S— bond by a negative ion Y^-, i.e., RSSR + Y^- = RS^- + RSY. When R is an aryl group, RS^- has an intense absorption in the 420—490 nm range; thus Y^- can be determined.

The feasibility of applying this reaction to the determination of aliphatic thiols in organic solvents was investigated. The reagents were bis(2,4-dinitrophenyl)disulfide (RSSR) and 2-diethylaminoethanethiol (YH). The decreasing concentration of the thiol was monitored with a gas chromatograph equipped with a hydrogen-flame-ionization detector and a column of 5% SE-30 on chromosorb-W.

The efficiency and rate of the reaction depend [3] on the thiophilicity of the reagent (Y^-), the stability of the leaving group (RS^-), and on the dielectric constant of the solvent. The measurable absorption belongs to the negative ion (RS^-), whose existence requires ca. pH 8.5 in aqueous solutions.

The solvents used were: dimethylsulphoxide (DMSO), dimethylformamide (DMF), and dimethylacetamide (DMA).

The disulfide chosen was the symmetric bis(2,4-dinitrophenyl)disulfide (RSSR) for the following reasons: the 2,4-dinitrophenyl sulfide radical ion is highly electronegative and is the best leaving-group [3]; substitution of a nitro group (additional to the one in Ellman's original reagent) in an aromatic system gives an increased molar absorptivity and a large red shift on the π—π^* band (main absorption band).

As a result, the overlap between the main absorption bands of the reagent (RSSR) and the reduced product (RS^-) is decreased. The overlap of the absorptions of RSSR and RS^- and the relatively small absorbance of RS^- in the case of aqueous solutions of 5,5′-dithiobis-(2-nitrobenzoic acid), (DTNB), (Table 1), cause a considerable error, especially in the initial stages of the reaction, when the 410-nm band related to the RS^- ion is a mere shoulder on the broad, intense 320-nm band representing the RSSR molecule (Fig. 1).

TABLE 1

λ_{max} and molar absorptivity of various aryldisulfides (RSSR) and their conjugate ions (RS^-)

Solvent		RSSR		RS^-	
		λ_{max} (nm)	ϵ (l mol^{-1} cm^{-1})	λ_{max} (nm)	ϵ (l mol^{-1} cm^{-1})
Water, pH 8	DTNB	322	16000 [2]	410	13600 [2]
DMSO		320	10000	402	12000
DMSO	BDPS	350	12000	476	15400
DMA		350	12000	485	16000
DMFA		350	13000	476	20800

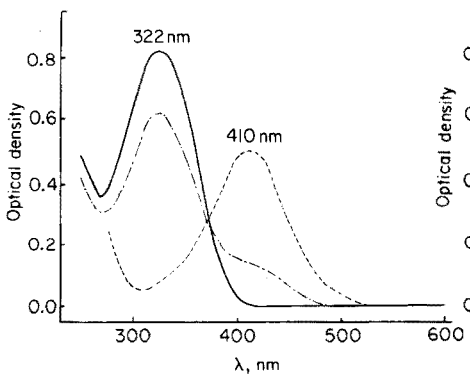

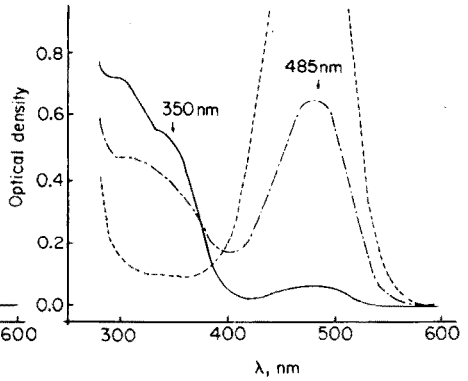

Fig. 1. Absorption spectra of aqueous solutions of DTNB ($5.44 \cdot 10^{-5}$ M) before (—) and after the addition of ca. 10^{-5} M YH (—·—·—·—) and $5.40 \cdot 10^{-5}$ M YH (--------).

Fig. 2. Absorption spectra of BDPS ($4.67 \cdot 10^{-5}$ M) in DMA before (—) and after the addition of $1.50 \cdot 10^{-5}$ M YH (—·—·—·—) and $4.60 \cdot 10^{-5}$ M YH (--------).

When bis(2,4-dinitrophenyl)disulfide (BDPS) is used in non-aqueous solutions, the error is reduced considerably (Fig. 2), even at the very beginning of the reaction, as the overlap of the absorption bands — at 350 nm for the molecular species and at ca. 480 nm for RS^- — is considerably smaller; in addition, the absorption of RS^- is larger (see Table 1).

In aqueous solutions, the reaction is instantaneous, but with BDPS reagent in polar organic solvents the reaction takes a finite time. By plotting $\{\ln([Y^-]_0[RSSR]/[Y^-][RSSR]_0)\}/([RSSR]_0 - [Y^-]_0)$ against time, a second-order rate constant, k_2, of 0.18 mol^{-1} min^{-1} was obtained. The initial concentrations [RSSR] and $[Y^-] = [RS^-]$ were obtained by measuring the respective absorptions at 350 and 485 nm (in DMA).

The production of the colored radical ion (RS^-) is completed in 2—10 min in DMSO; 20—30 min in DMA, and in ca. 100 min in DMF. (The long reaction time in DMF results, most probably, from its acidic proton, which might interact with the RS^- ion). The saturation value of RS^-, i.e. the concentration of the ion molecule when the reaction is completed, is a

linear function of the thiol (Y^-) added. The molar absorptivity of RS^- is 16000—21000 l mol^{-1} cm^{-1} and the limit of detection (D = 0.02) is 10^{-6} M thiol.

The authors are grateful to Dr. K. Bareli for helpful discussions. The technical assistance of Ms. T. Belogorotzky and Mr. L. Gefen is acknowledged.

REFERENCES

1 G. L. Ellman, Arch. Biochem. Biophys., 74 (1958) 443.
2 G. L. Ellman, Arch. Biochem. Biophys., 82 (1959) 70.
3 A. J. Parker and N. Kharasch, J. Am. Chem. Soc., 82 (1960) 3071.

Analytica Chimica Acta, 92 (1977) 433—436

Book Reviews

J. Bartos and M. Pesez, *Colorimetric and Fluorimetric Analysis of Steroids*, Academic Press, London, 1976, xii + 274 pp., price £9.80.

This is Volume 11 of an international series of monographs that describe the analysis of organic materials. The essential philosophy of the series is to bring together within each book a concise collection of analytical methods which, in the experience of the authors concerned, really do work.

This book is no exception. From the many thousands of papers that deal with the detection and characterization of steroids, the authors have selected working methods based on chemical reactions in solutions and yielding a fluorescence, or an exceptionally strong colour or absorption in the near u.v. Emphasis is placed upon natural or synthetic steroids of physiological interest.

After a preliminary chapter on nomenclature, the second chapter describes methods of steroid analysis by means of functional group determinations based mainly on the reactions given by the hydroxyl and keto groups, either isolated or conjugated with double bonds. Some reactions based on halochroism or halofluorism are gathered together in Chapter 3. These methods, which are based upon a colour or a fluorescence developed when a steroid is dissolved in a strong acid, are often highly sensitive but lack selectivity.

The remainder of the book comprises 10 chapters dealing with specific classes of steroids, e.g. sterols, bile acids, estrogens, gestogens, androgens, corticosteroids, steroid contraceptives, cardiac glycosides, saponins, and steroidal alkaloids. In most chapters selected procedures are described by way of illustration. Sufficient detail is given in each case so that the operator may work directly from the text.

This book will be essential reading for all active analysts of steroids. With over 850 references, it will also be a useful literature source for steroid chemists in general.

P. J. Sykes

R. P. W. Scott, *Contemporary Liquid Chromatography*, J. Wiley, New York, 1976, pp. viii + 326, price £15.25, U.S. $27.75.

This is Volume XI in the series "Techniques of Chemistry" edited by A. Weissberger. Unfortunately the production does not uphold the standard of technical excellence normally associated with this editor and publisher. The proof-readers involved should be dismissed on the spot; misprints are legion, and nothing is sacrosanct — the carelessness pervades sub-headings, headings to tables, captions to figures, and references. Many of the diagrams

are poor — they appear to be reproductions of hand-lettered efforts. The printers involved should suffer the same fate as the proof-readers; the text is marred by a pronounced unevenness of line and irregular spacing of the letters within words and the spaces between words. There is no doubt that Dr. Scott has been badly served by those responsible for the technical production of his text. When he puts in his next appearance at one of the annual international symposia on chromatography he is going to have to offer a large number of his friends something to drink in an effort to help expunge from their memories the mis-spelling of their names, the omission or mis-quotation of their initials, or the fact that some of their publications are ascribed to years that precede Tswett!

Fortunately, Ray Scott is so very well known and respected, and has a sufficiently sound reputation for the quality and originality of his achievements in chromatography, that his established reputation will not be seriously affected. The impact and credibility of his text have, however, been seriously undermined, and it is difficult to dismiss the general aura of carelessness when trying to reach a clear assessment of the real worth of the contents.

Basically, the text is what would probably have been widely anticipated from Dr. Scott — a highly original and stimulating account of wide areas of modern chromatography, with other areas completely ignored. Scott has never been afraid of mathematics nor of practical electronics and engineering principles; he is an all-or-nothing man endowed with technical brilliance and a touch of near-genius that brings him close, in some ways, to Martin; when that happens, and it is all too rare, allowances are easy to make for lesser failings. This book is particularly good on uncommon types of detector, on preparative scale chromatography, and on aspects of the combinations of liquid chromatography with spectroscopic techniques, particularly mass spectroscopy. It will probably be assessed overall as a stimulating and controversial book for the chromatographer but, with regret, it is not one for the general analytical chemist.

D. M. W. Anderson

E. A. Boudreaux and L. N. Mulay (Eds.), *Theory and Applications of Molecular Paramagnetism*, J. Wiley, London, 1976, pp. x + 510, price £25.00.

This excellent book gives a clear and comprehensive picture of an area of science which is of considerable importance to chemists, physicists, geo-scientists, materials scientists, and bio-scientists.

The text is divided into ten chapters, each written by an expert in the field. The last chapter is particularly useful because it discusses the definitions and units for magnetic terms, thus clarifying the jungle of confusion created in this area by the introduction of SI units.

An introduction by Professor Mulay surveys the types of magnetic behaviour and includes a short section on the relevance of magnetic research to societal needs. Chapters 1 and 2 by Dr. A. T. Casey contain highly mathematical accounts of the theoretical principles of paramagnetism and the theoretical basis for the magnetic behaviour of transition metal compounds respectively. My only criticism here is the small amount of space (5 pp.) devoted to the effects of covalent bonding on the equations which have been developed from an "ionic model", although in fairness to the author, several references to recent reviews on this topic are cited. However, for practical scientists who do not wish to struggle through the mathematics, Chapter 3 provides a comprehensive survey of the magnetic behaviour of magnetically-dilute transition metal complexes, based on the equations derived earlier. This chapter (120 pp.) contains many useful tables, figures and over 400 references to primary papers in this area.

An exciting innovation for books on magnetochemistry is a discussion of the magnetic behaviour (theoretical and experimental) of lanthanide and actinide compounds (Chapters 4—6). These include appendices that give recent results by Professor Boudreaux. An authoritative account of magnetically condensed compounds is given in Chapter 7 by W. E. Hatfield; additional information on this subject is given by the editors in Chapter 8.

This book, which is remarkably free of typing errors, will by an invaluable addition to the shelves of many scientific libraries although its high price will place it beyond the realm of most private bookshelves.

T. A. Stephenson

A. R. Butler and M. J. Perkins (Eds.), *Organic Reaction Mechanisms, 1975*, Interscience-Wiley, New York, 1977, 623 pp., price £27.50, $47.50.

The eleventh volume in this series arrives rather late. It is nonetheless welcome, although the latest literature quoted is now 15 months old and some is obviously over 2 years old. As with previous volumes, the important references are dealt with more fully than others, but as usual the literature coverage is good. Once again the largest chapter is on radical reactions and points the way to one of the more active areas.

The editors and contributors must be congratulated on keeping the volume within manageable proportions. Its production is up to the usual high standard.

E. J. Forbes

D. A. T. Southgate, *Determination of Food Carbohydrates*, Applied Science Publishers Ltd., Barking, 1976, pp. ix + 178, price U.S. $20.00.

It is widely accepted that the determination of carbohydrates has been one of the neglected areas of foodstuffs analysis. The field is a difficult one; many of the problems arise because of difficulties of chemical classification. Renewed interest in the analytical problems is being enforced, however, through the recent introduction of more rigorous requirements in the labelling of foodstuffs, and through the impending legislation in many countries regarding the declaration of additives and their nutritional aspects, and the elimination from formulations of substances that are not generally recognized as safe for human or animal consumption.

The author of this book has gained a wide experience of carbohydrate analysis at the Dunn Nutritional Laboratory in Cambridge; his decision in 1973 to write this book was a good one. Following a brief general introduction, chapters are devoted to : Carbohydrates in Foods; Measurement of Sugars; Measurement of Starch, its Degradation Products and Modified Starches; Measurement of Unavailable Carbohydrates, Structural Polysaccharides; Measurement of Unavailable Carbohydrates, Non-structural Polysaccharides; Analysis of Carbohydrates in Specific Groups of Foods; and Selected Methods of Analysis. There is an Appendix containing tables of Degrees Brix, Degrees Beaumé and factors for the Fehling, Munson and Walker, Lane-Eynon, etc. Methods: a short bibliography and reference to 136 original papers; and a Subject Index.

This book has been prepared carefully (misprints on pp. 22, 78 and 130 only were detected) and it presents a balanced and up-to-date, if somewhat superficial, survey of what must be regarded as a very wide and complex field. At the equivalent of almost £12 the price is higher than can reasonably be recommended as essential personal expenditure, but library copies of this book will be useful to the categories of workers for whom it was written, i.e., analysts, nutritional workers and food scientists.

ANALYTICA CHIMICA ACTA, VOL. 92 (1977)

AUTHOR INDEX

ANALYTICA CHIMICA ACTA, VOL. 92 (1977)

SUBJECT INDEX

(continued from page 4 of cover)

PRINTED IN THE NETHERLANDS

VOL. 92 NO. 2 ANALYTICA CHIMICA ACTA SEPTEMBER 1977

CONTENTS

(continued on inside page of the cover)